

A SUPPLEMENT TO ANALYSIS AND DESIGN OF FLIGHT VEHICLE STRUCTURES

William F. McCombs

TABLE OF CONTENTS

Article and Main Topic	Page	Article and Main Topic	Page
A5.23a Beam-Columns	1	C11.29a Tension Field Beam Holes	49
A5.24a Beam-Column Formulas	1	C11.24a Rivet Design	50
A5.25a Beam-Column Deflections	1	C11.31a Stringer Construction	51
A5.26a Beam-Column Formulas	1	C11.32a Diagonal Tension - Stringers	51
A5.27a Margins of Safety	1	C11.33a Stringer System Allowables	54
A5.28a Truss Analysis	1	C11.34a Stringer Construction Example	57
A5.29a Tangent Modulus	1	C11.35a Diagonal Tension - Longerons	60
A5.31a Multispan Beam-Columns	1	C11.36a Longeron System Analysis	61
A5.32 Approximate Buckling Formula	1	C11.37a Longeron Construction Example	63
A6.7a Plastic Torsion	1	C11.38a Diagonal Tension Summary	66
A7.1a Beam Deflections	1	C11.39a Problems for Part 2	67
A7.12a Numerical Analysis	1	C11.40a Problems for Part 1	67
A11.2a Moment Distribution	2	C8.1a Monocoque Shell Buckling Data	67
A11.5aa Stiffness/Carry Over Factors	2	C8.2a Shell Axial Comp. Buckling	67
A11.13a Moment Distribution Factors	2	C8.5a Effect of Internal Pressure	67
A11.15a Truss Analysis	2	C8.7a Shell Bending Buckling	67
A11.15b Truss Analysis	5	C8.8a Effect of Internal Pressure	67
A13.11a Curved Beams	6	C8.9a External Hydrostatic Pressure	67
A18.5a Column Analysis	7	C8.11a Shell Torsion Buckling	68
A18.8a Column Analysis	7	C8.12a Effect of Internal Pressure	68
A18.8b Torsional Buckling	7	C8.15a Combined Loads Buckling	68
A18.27a Column/Beam-Column Data	8	C8.19a Conical Shell Buckling	72
A18.28a Material Properties	8	C8.20 Buckling of Spherical Caps	73
A19.23 Rib Crushing Loads	8	D1.2a Fitting Design	74
C1.13a Margins of Safety	8	D1.3a Fitting Margins of Safety	74
C1.13b Dealing With Tolerances	11	D1.4a Factors of Safety	74
C1.6a Combined Stresses	11	D1.5a Bolts	74
C2.1a Column Curve Construction	12	D1.6a Nuts	74
C2.2a Free-Ended Columns	12	D1.8aa Bushings	74
C2.3a Shear Effect on Buckling	14	D1.12a Transversely Loaded Lugs	74
C2.3b Multispan Columns	14	D1.13a Obliquely Loaded Lugs	74
C2.6a Stepped Columns	16	D1.23a Riveted Splices	74
C2.6b Numerical Column Analysis	17	D1.27 Thread Design and Strength	75
C2.6c Initially Bent Columns	21	D3.5a Filler (Shim) Effects	76
C2.7a Column Design Data	23	D3.7a Curved Beam Data	77
C2.8a Column Elastic Supports	23	D3.3a Tension Clip Allowable Data	77
C2.10a Need for Successive Trials	23	D1.21a Flush Rivet Joints	77
C2.13a Column Elastic End Restraint	23	D1.22a Blind Rivet Joints	77
C2.16 Tangent and Effective Moduli	25	D1.7a Bolt Strengths	77
C2.17 Buckling Load Data	26		
C2.18 End Friction Effects	30	Design Check List	A1
- References for Chapter C2	30	Margins of Safety	A1
C3.4a Plastic Bending Data	31	Tension Clips	A1
C3.7a Plastic Bending Example	31	Preload Torque Factors for Bolts	A2
C3.10a Plastic Bending Procedure	31	Rockwell and Brinell Hardness Data	A2
C3.11a Complex Plastic Bending	31	Minimum I for Stiffeners	A3
C3.12a Shear Stresses in Plastic Range	32	Stress-Strain Curves	A3
C3.15 Yield Stress Bending Modulus	33	Sheet and Other Buckling Data	A4
C3.16 Residual Stress After Bending	33	Material Properties	A6
C3.18 Beam-Column Analyses	34	Fastener Joint Design Notes	A10
C4.20a Plastic Torsion	38	Fastener/Joint Allowable Data	A10
C4.23a Apparent Margins of Safety	39	Nut/Collar Tension Allowables	A21
C5.7a Flat Plate Shear Buckling	39	Bolt Allowable Bending Moments	A21
C5.8a Flat Plate Bending Buckling	40	Beam Formulas	A21
C7.10a Unequal Angle Leg Thicknesses	41	Additional References	A21
C7.30 Crippling Method Three	41	Bulkhead, Frame and Arch Analyses	B1
C7.31 Torsional Buckling	44	Column Elastic Support Design	B5
C9.13a Frame Stiffness Criteria	47	Operating Devices	B9
C10.15b Thick-Web Beam Analysis	47	Doubler and Splice Design	B10

PREFACE

The widely used and recommended college/industry textbook "Analysis and Design of Flight Vehicle Structures" by Dr. E.F. Bruhn has had only one revision since its inception in 1965.. That was the 1973 edition in which Chapter A23 was revised and expanded, Chapter C13 was completely rewritten by another author and a few minor changes were made in Chapter 11. Aside from these the book remains in its original form.

The purpose of this Supplement is to increase the scope and usefulness of the textbook in numerous specific areas of analysis. These include columns, beam-columns, bending strength, margins of safety, tension field analyses, fastener/joint data, arches, bulkheads and numerous others. The practical use of the Supplement is discussed in the Introduction. Only one or two applications of the Supplement's contents can be worth much more than its cost.

The Supplement may be expanded in some future year, so any suggestions for this, or for corrections or changes in its current text will be appreciated. Those readers who wish to be informed of any future revisions or who have suggestions can contact the author at P.O. Box 763576, Dallas, TX 75376-3576 (Tel. 214 337-5506).

The author is one of the coauthors of the textbook. His career includes over forty years of experience in structural analysis and design of numerous aircraft and missile projects in the aerospace industry. Also included are technical papers and the preparation and teaching of practical courses in structural design and analysis for engineers working in the aerospace and other industries.

William F. McCombs

FOREWORD

I am pleased to have the opportunity to recommend this Supplement to my late father's widely used college/industry textbook "Analysis and Design of Flight Vehicle Structures". I hope its practical applications will be a benefit to all who have the textbook. The additional data contained in this Supplement can be applied to both the study and the work of structural design and analysis. The Supplement should also be of interest to, and eventually benefit, those who may be considering purchasing the textbook.

Patricia Bruhn Beachler

INTRODUCTION

The purpose of this Supplement is to increase the scope and usefulness of the widely used and recommended college/industry textbook "Analysis and Design of Flight Vehicle Structures" by E.F.Bruhn. As such it is by no means a revision of that book. Rather, it is an expansion and clarification of numerous topics and data in the book, along with the introduction of additional topics and data.

For best coordination with the textbook the following has been done. Where an existing article such as, for example, Art. C1.13 has been expanded or otherwise changed or corrected, the Supplement includes it as Art. C1.13a, the letter indicating a change or addition. When a new topic is added to a chapter it is given an article number which is subsequent to the last article number in that chapter and includes no letter. For example, the last article in Chapter C3 is Art. C3.14. Two additional topics, "Yield Stress Bending Modulus" and "Residual Stresses Following Plastic Bending" have been added, so they have been given article numbers C3.15 and C3.16 respectively with no letters.

The same thing has been done with figure numbers and table numbers. Where a figure has been changed or added to, it retains the same figure number with an added letter. For example, Figure 2.27 has added information so it has the designation Fig.2.27a in the Supplement. When a new figure is added it is given a number which is subsequent to the last figure number in the chapter, so no letters are used with its number in the Supplement. This procedure also applies to tables.

Although the Supplement provides an Index, for most usefulness the textbook must be marked in such a manner as to guide the reader directly to revised, corrected and new topics, figures, tables and references in the Supplement. A highly recommended scheme for doing this is provided later.

Structural design and analyses are based on theory, empirical methods and data, various assumptions and individual judgement. The assembled structure is a result of various specific manufacturing methods and procedures. Because of these things and also the possibility of inadvertent calculation errors, it is always necessary to prove the adequacy and safety of the completed structure by means of a sufficient test program before it is put into use. Such tests must demonstrate the structure's adequacy as to ultimate and yield strength, fatigue life, fracture and stiffness. The test results must be properly evaluated since the test article's materials usually have properties in excess of the minimum required values.

Procuring agencies such as the military, the airlines and other government and private organizations usually specify the design and test requirements and other criteria which must be used or met.

Coordination of the Supplement and the Textbook*

In order to easily guide the reader from the textbook to the Supplement, the following marking of the textbook is recommended.

1. On the textbook's Table of Contents place an asterisk, in red ink, after "Contents" and add the following footnote at the bottom of the page:

* A red asterisk preceding any article or figure number in the textbook means that additional material is available in the same article or figure in the Supplement.

2. For each textbook article listed in the Supplement's Table of Contents, place a large asterisk, in red ink, just to the left of each corresponding article number in the textbook (e.g., *A11.2).
3. The 12 articles in the Supplement's Table of Contents not having a letter in the article number are new articles. (e.g., C3.18 Beam-Column Analyses). Their numbers and titles should be written in at the end of their chapters, with a red asterisk just to the left of their article numbers.
4. The following figures in the textbook should have an asterisk, in red ink, placed just to the left of their figure numbers, to indicate that a revision or additional data is in the Supplement:

A5.1	C2.17	C2.26	C5.14	C8.15	C8.28	C11.47
A18.8	C2.18	C2.27	C8.8a	C8.20	C8.29	C11.48
C1.8	C2.19	C3.27	C8.11	C8.25	C10.15	D1.15
C2.2	C2.20	C3.28	C8.13	C8.26	C11.43	
C2.16	C2.25	C5.11	C8.14	C8.27	C11.44	

5. The additional references shown on p. 30 (for Chapter C2) and on p. A21 (for Chapters C3, C4, C7 and C11) should be written in at the end of the list of references for these chapters.
 6. Put a black asterisk after "RINGS" on the title of p. A9.1 and, at the bottom of the right hand column add the footnote
* See Appendix B of the Supplement for alternative analyses of bulkheads, frames, arches and bents.
- * To increase the scope and usefulness of other such textbooks, put appropriate asterisks in their texts with footnotes saying which article to see in the Supplement.

A5.23a Introduction

Add the following at the end of Art. C5.23. For a discussion of all types of beam-columns, including non-uniform members, with numerous example problems see "Engineering Column Analysis" described in Art. A18.27a.

A5.24a Effects of Combined Axial and Lateral Loads

Add the following at the end of Art. C5.24. Formulas and example problems for beams in tension are available in the book described in Art. A18.27a.

A5.25a Equations for a Compressive Axially Loaded Strut with Uniformly Distributed Load

Add the following at the end of Art. A5.25. The deflection, y , at any beam station can be calculated as follows.*

$$M = M_Q + M_P = M_Q + Py$$

therefore

$$\begin{aligned} y &= -(M - M_Q)/P \\ &= (M_Q - M)/P \end{aligned}$$

The negative sign is introduced since a positive beam bending moment produces a negative (downward) deflection. M_Q is the moment due to the lateral loads only and M is the final moment.

To calculate the slope at any station calculate the deflection at a point very slightly to the left of the station and then very slightly to the right, the same amount, ΔL . The slope is then

$$\text{slope} = (y_R - y_L)/2\Delta L$$

A5.26a Formulas for Other Single Span Loadings**

Table A5.1a presents numerous additional cases of single span loadings.**

The case of a beam-column with a varying EI or a varying axial loading requires a numerical analysis, just as does a column of this nature. The numerical analysis procedure is presented in C3.18.

A5.27a Combinations of Load Systems, Margins of Safety and Accuracy of Calculations

For a beam-column the true margin of safety must be calculated as discussed in Art. C4.23a. The allowable stresses or bending moments are calculated as discussed in Art. C3.18.

A5.28a Example Problems

In Example Problem 2 member BD is considered to be pinned to ABC at joint B. This is why it does not pick up any of the 36,000 in lb bending moment at joint B.

A5.29a Stresses Above Proportional Limit Stress

If a column curve is not available

for the beam material, the axial stress, P/A , is calculated, $f_c/F_{0.7}$ is calculated Fig. C2.16 is entered with this value and E_t/E is obtained. Then $E_t = E(E_t/E)$. E' in Art. A5.29 is actually E_t .

A5.31a Beam-Columns in Continuous Structures

Multispan beam-columns require a moment distribution analysis to determine the end moments acting on each span. Once these are known the applicable single span formulas in Table A5.1 and A5.1a can be used to determine the bending moments at any station within a span. This is discussed in Art. C3.18.

A5.32 Approximate Formula for Beam-Columns

For preliminary sizing when there are no end moments the following formula can be used to determine the final bending moment at any station

$$M = M_Q/(1 - P/P_{cr})$$

where M_Q is the moment due to the transverse loads only and P_{cr} is the critical load as a column (Chapter 2). This is most accurate for a uniform lateral load and least accurate for a concentrated load. P_{cr} is calculated assuming the member has a stable cross-section even if this is not the case. For a beam in tension the negative sign in the formula is replaced with a positive sign (tension makes the bending moment smaller).

A6.7a Torsion of Solid Non-Circular Shapes

All of the previous formulas are based on the shear stresses being in the elastic range. With ductile materials failure (rupture) does not occur until the shear deformation has gone well into the plastic range (similar to the plastic bending case). The torsional moment at which rupture occurs can be predicted as discussed in Art. C4.20a.

For the special case of tubes having a circular cross-section the failing torque can be calculated as discussed in Art. C4.20 and its associated Figures C4.17 to C4.30 and in the example problems of Art. C4.21.

A7.1a Introduction

For practical purposes the deflection and slopes of beams are calculated as discussed in Art. A7.12a, standard formulas being used for uniform beams, and for varying section beams using tables such as Table C3.3 and the "End Fixity" discussion.

A7.12a Deflections and Angular Changes of Beams by Method of "Elastic Weights"

For beams of uniform section deflections and slopes are most easily cal-

* See footnote on p.37. L.H. column

** For other distributed loadings replace them with several statically equivalent concentrated loads and use superposition for these. For any case of one end fixed one simply supported not shown, use the both ends fixed case and then multiply the moment at the fixed end by $(1 + COP)$; M is zero at the other end. The exception to this is case 19 where $(1 - COP)$ must be used.

Table A5.1a Continuation of Table A5.1

$$M = C_1 \sin x/j + C_2 \cos x/j + f(w)$$

Case	LOADING	C_1	C_2	$f(w)$	MAX. MOMENT
9	Partial Uniformly Distributed Load	$x < a: -2w/j^2 \sin x/j \sin a/j$ $a < x < L-a: 2w/j^2 \sin x/j \sin a/j - wj^2 \sin b/j$ $b < x < L: 2w/j^2 \sin x/j \sin a/j$	0 $-wj^2 \cos a/j$ $-2w/j^2 \sin x/j \sin a/j$	0 wj^2 0	Determine by plotting
10	Symmetrical Partially Uniform Distrib. Load	$x < a: -w/j^2 \sin x/j \sec a/j$ $a < x < L-a: -w/j^2 \tan L/2 j \cos a/j$ $L-a < x < L: w/j^2 \sin x/j \sec L/2 j \cos L/j$	0 $-wj^2 \cos a/j$ $-2w/j^2 \sin x/j \sin L/2 j$	0 wj^2 0	$wj^2 \left[1 - \frac{\cos a/j}{\cos L/2 j} \right]$ At Midspan
11	Two Symmetrical Concentrated Loads	$x < a: -w/j \cos b/2$ $a < x < L-a: w/j \sin a/j \tan L/2 j$ $L-a < x < L: w/j \sin L/2 j \cos b/2$	0 $-wj \sin a/j$ $-wj \sin L/2 j \cos b/2$	0 0 0	$-wj \sin a/j$ At Midspan
12	Concentrated Moment	$x < a: -m \cos b/2$ $x > a: -m \cos a/j$	0 $m \cos a/j$	0 0	If $b < \pi/2$, M_{max} at $x=a$ If $b > \pi/2$, M_{max} at $L-\pi/2$
13	Fixed End Beam-Uniform Load	$x < L/2: -wL^2/2$	$-wL^2/2 \tan L/2 j$	wj^2	At $x=0$: $M_{max}^2 \left[1 - \frac{L/2}{\tan L/2 j} \right]$ At $x=L/2$: $M_{max}=w^2 j^2 \left[\frac{L/2}{\tan L/2 j} - 1 \right] / \sin L/2 j$
14	Fixed End Beam-Concentrated Load at Center	$x < L/2: -1/2 wj$ $x > L/2: 1/2 wj$ $1/2 wj \left[2 \cos L/2 j - 1 \right]$	$1/2 wj \left[\frac{1 - \cos L/2 j}{\sin L/2 j} \right]$ $1/2 wj \left[\frac{\cos L/2 - \cos L/2 j}{\sin L/2 j} \right]$	0 0	M_{max}^2 $1/2 wj \left[\frac{1 - \cos L/2 j}{\sin L/2 j} \right]$ At $x=0$: $(M_x=L/2) = M_{max}$
15	Fixed Simple Beam-Uniform Load	$x < L/2: -wL^2/2$ $x > L/2: -wL^2/2$ $-1 - \frac{1 - \cos L/2 j}{\sin L/2 j} wj^2$	$\left[\frac{\tan L/2 j - 1/2}{\tan L/2 j - L/2 j} \right] x$ $\left[\frac{\tan L/2 j - 1/2}{\tan L/2 j - L/2 j} \right] - wj^2$	wj^2	$M_{max} = wLj \left[\frac{\tan L/2 j - L/2 j}{\tan L/2 j - L} \right]$ $= (tan L/2 j) wj^2$ At $x=0$
16	Fixed Simple Beam-Concentrated Load	$x < L/2: -wL^2/2$ $x > L/2: -wL^2/2$ $wL^2/2 \left[\frac{L+2(\sin L/2 j - 2 \cos L/2 j)}{j \tan L/2 j - L} \right]$	$\frac{wL}{2} \left[\frac{1 - \cos L/2 j}{j \tan L/2 j - L} \right]$ $wL \left[\frac{1 - \cos L/2 j}{j \tan L/2 j - L} \right]$ $-2 \sin L/2 j$	0 0	$M_{max} = wLj \left[\frac{1 - \cos L/2 j}{j \tan L/2 j - L} \right]$ At $x=0$
17	Cantilever-Concentrated End Load	$x < a: -wL^2/2$ $x > a: -wL^2/2$	Or use case V with $L=2a$, $w=2W$ and $a=b=L$ there for same results	$M_{max} = wL \tan L/j$ $x \left(1 - \frac{\sin a/j}{\sin L/j} \right)$	
18	Cantilever-Uniform Load		Or use Case III	$M_{max} = wj \left[j(1 - \sec L/j) + L \tan L/j \right]$	
19	Fixed End Beam With Lateral Displacement	For C_1 use Case II with $M_2 = -M_1$	Or calculate $M_{max} = \frac{wP \tan L/2 j}{2 \left[\tan L/2 j - L/2 j \right]}$ $M = 6El_a/L^2 (2\theta - \alpha)$ See Art. 11.15a item 6, $(\theta = a/L)$ $C_2 = M_1$ (case II)	$M_{max} = \frac{wP \tan L/2 j}{2 \left[\tan L/2 j - L/2 j \right]}$ At $x=0$ And M_{max} At $x=L$	
20			$M_{max} = WL(b/j \cos L/j - \sin L/j + \sin a/j + \sin b/j - L/j \cos b/j + a/j)$ $(L/j)(2 - 2 \cos L/j - L/j \sin L/j)$	M_{max} as above but switching a and b	
21			$M_{max} = Wj \sin a/j [\cos b/j - \sin b/j (1 + \cos L/j) / \sin L/j]$ (Occurs under the loads W)	This is a superposition of Cases V	

Or use
Fig. A11.52

culated by using beam deflection and slope formulas widely available in the structural literature. These formulas are based on bending stresses only and are accurate unless the web is very thin or otherwise quite flexible due to holes etc., in which cases there may be significant additional deflection due to shear. For beam-columns the deflections and the slopes at any station can be calculated as discussed in Art. A5.25a.

For beams with a varying EI a numerical analysis is necessary to determine the deflections and slopes. This can be done as discussed and illustrated in Art. C3.18 where Table C3.3 shows the deflections due to the transverse loads only and Tables C3.4 and C3.5 show the additional deflections due to the axial loads, the final bending moments being in Table C3.6. The deflections are obtained using the data in the tables and the geometric series, p.35, as was done in Table C3.6 for moments. Tables for end fixity are discussed in Art. C3.18. With any elastic end restraint a moment distribution analysis is required to determine the end moments on the beam etc. as discussed in Ref. 3 (Art. A18.27a).

All.2a Definitions and Derivations of Terms

Add the following at the end of the article. In the moment distribution procedure, where adjacent spans "meet" (at a support) there is assumed to be a "joint" even though the member may be continuous across the joint. The sketch in Fig. All.92 shows the direction of (+) and (-) moments as they act upon the spans and also upon the joint. As seen there (+) moments act clockwise on the span and counterclockwise on the joint. This is different from conventional beam sign convention where a (+) moment produces compression in the "upper" surface.

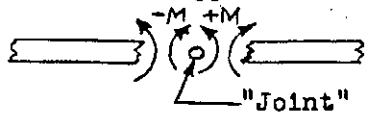


Fig. All.92 Sign Convention*

All.5aa Example Problems

The stiffness factor, K, as used in Art. All.5a and subsequently, is a "relative" factor rather than a true one. It has the value EI/L for the far end fixed and $.75 EI/L$ for the far end pinned. As such it applies only when there is no external elastic restraint, k (in-lbs per radian) at the ends or at any joint, and when there is no axial load in the spans. In such cases "correction factors" must be applied to it, as shown in Art. All.14 for example. In general, to avoid inad-

vertent calculation errors it is best to use the true value of the stiffness factor, SF, which is in in-lbs per radian and is

$$SF = 4SCEI/L$$

where SC is the stiffness coefficient and can be obtained from Fig. All.47 (as "C") or calculated per Art. All.13a. Doing this eliminates the need for introducing the correction factors otherwise needed. The carry over factor, COF, can be obtained from Fig. All.46 or calculated per Art. All.13a.

In doing moment distribution calculations, unless the "far end" of a span is pinned (or free) it is assumed to be fixed for determining the values of the stiffness and carry over factors.

All.13a Fixed End Moments, Stiffness and Carry Over Factors for Beam-Columns of Constant Cross-Section

Sometimes it is necessary to use the values of the SC and the COF (see Art. All.5aa) for larger values of L/j than are given in Fig. All.46, All.47 and All.56 (for $2\beta-\alpha$). Those values can be calculated as follows for compression members.*

$$\begin{aligned} SC \text{ (far end pinned)} &= 3/4\beta^2 \\ SC \text{ (far end fixed)} &= 3\beta/(4\beta^2 - \alpha) \\ COF &= \alpha/2\beta \end{aligned}$$

$$\text{where } \alpha = 6(L_j \cosec \frac{L}{j} - 1)/(L_j)^2$$

$$\beta = 3(1 - \frac{L}{j} \cot \frac{L}{j})/(L_j)^2$$

For members in tension the same formulas can be used, but the trigonometric functions are replaced with the hyperbolic functions, cosech and coth. Extensive tables of the SC and COF values (to 6 significant figures) from $L/j = 0$ to 2π for compression members and from 0 to 50 for tension members are in the book described in Art. A18.27a.**

All.15a Secondary Bending Moments in Trusses with Rigid Joints

Art. All.15 gives a procedure for determining the secondary bending moments in such trusses but no illustrative example is provided. The following illustrates the procedure except that in step one one finds the relative rotation of each member using the method of virtual work, step 2 is omitted and in step 3 "its relative rotation" is used in place of "these transverse displacements". That is, due to the applied loads the truss joints move, and therefore the members

*In Fig. All.56 $2\beta - \alpha$ can be calculated as follows:

$$2\beta - \alpha = \frac{6}{(L_j)^2} \left[2 - \frac{L}{j} \left(\frac{1 + \cos L/j}{\sin L/j} \right) \right]$$

**Also obtainable from P. B12 and B13

*Some books use an opposite sign convention.

SECONDARY BENDING MOMENTS IN TRUSSES

rotate relative to each other. These rotations generate fixed end moments at their ends (just as a beam with unequal-ly deflecting supports will undergo an angular rotation and develop fixed end moments). The following illustrates the procedure using the truss shown in Fig. All.92.

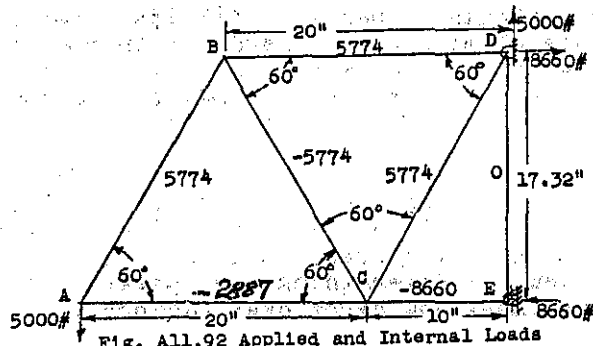


Fig. All.92 Applied and Internal Loads

- For the applied loads the resulting internal loads in the members are determined as shown in the figure.
- Member BC is arbitrarily selected as the "base member" from which the rotations of all other members are calculated.
- For each other member (one at a time) a clockwise 1 in-lb moment in the form of couple loads ($1/L$) at its ends is applied and reacted with a counter-clockwise couple at the ends of the base member BC. The resulting loads in the truss members are then determined. See Fig. All.93 and note that only a few (3 or 4) members are loaded in this procedure.
- Then for each loaded member the quantity $S_u L/AE$ is calculated and the results summed to obtain the relative rotation, θ , of the member to which the clockwise couple was applied.
- Steps (3) and (4) are repeated for each of the remaining members to get their relative rotations, θ . Table All.4 presents the basic data and Table All.5 summarizes the calculations.

Table All.5 Calculation of Relative Rotations, θ

Mem- ber	SL/AE	Couple at AB	Couple at AC	Couple at BD	Couple at CD	Couple at CE	
		u	uSL/AE	u	uSL/AE	u	uSL/AE
AB	.0205	-.0289	-593	-.0577	-1183	0	0
AC	-.0103	.0577	-594	.0289	-289	0	0
BC	-.0205	-.0289	593	.0289	-593	.0289	-592
BD	.0205	0	0	0	0	.0289	.592
CD	.0205	0	0	0	0	-.0577	1183
CE	-.0208	0	0	0	0	0	-.0289
DE	0	0	0	0	0	0	0
		$\theta_{AB} = -594$		$\theta_{AC} = -2065$		$\theta_{BD} = -1183$	
						$\theta_{CD} = 1183$	
						$\theta_{CE} = 591$	

Note: Multiply each θ by 10^6 . DE doesn't rotate since it is held by the supports.

See p.B11 for the critical (buckling) loading calculation and p.B12-13 for gusset plate data.

Table All.4 Basic Data

Member	S lbs	L in	A in ²	E $\times 10^6$	SL/AE	I in ⁴	i = in ² /S	L/J
AB	5774	20	.563	10	.0205	.0264	6.76	2.96
AC	-2887	20	.563	10	-.0103	.0264	9.56	2.09
BC	-5774	20	.563	10	-.0205	.0264	6.76	2.96
BD	5774	20	.563	10	.0205	.0264	6.76	2.96
CD	5774	20	.563	10	.0205	.0264	6.76	2.96
CE	-8660	10	.360	10	-.0208	.0108	3.53	2.83
DE	0	17.32	.250	10	0	.0053	∞	0

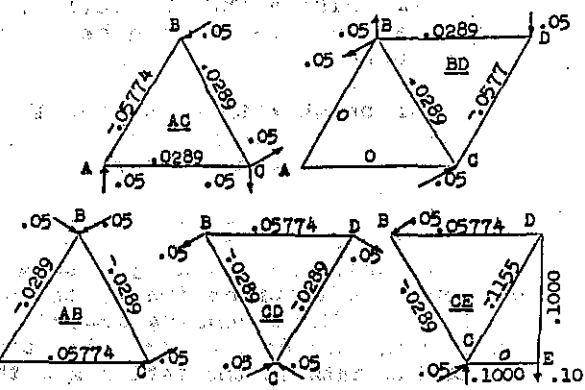


Fig. All.93 Relative Rotation Loads

For each of the above members the fixed end moments are calculated as

$$FEM = -6EI\theta / (2\beta - \alpha)$$

where $2G - \alpha$ is obtained from Fig. All.56 and accounts for the effect of the axial load, S , in the member. A positive (clockwise) relative rotation, θ , produces negative (counterclockwise) FEM's (per Example 2 sketch on p.All.2) hence the minus sign in the formula. If a member has one end pinned a fixed end moment occurs only at the other end and is calculated as

$$FEM = -6EI\theta(1 - COF)/L(2\beta - \alpha)$$

where COF is from the pinned end to the fixed end. Table All.5 summarizes the calculations for the values of θ .

- The fixed end moments at all truss joints are now known and the moment distribution procedure can be carried out as illustrated in Fig. All.43 to obtain the final moments at the ends of each member. Then see Art. A5.3a.

All.15b The Effects of Increased Internal Loads on Secondary Bending Moments

Although the secondary bending moments in the truss of Art. All.15a were relatively small, they can become quite large as the internal axial loads in the truss members increase. As the applied loading on the truss approaches the critical loading these moments will approach infinity. This is why the theoretical critical loading for a truss can never be attained; bending failure will precede it. The following example, using the simplest rigid joint truss illustrates this.

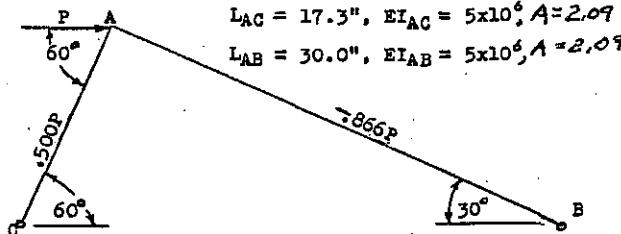


Fig. All.94 Rigid Joint Truss with Pinned Ends

A is a rigid joint and ends B and C are pinned. Assuming A to be a pinned joint only to determine the axial loads in AC and BC, they are as shown in the figure. With the axial loads known this simple truss can be analyzed for stability (buckling) as a two-span column with pinned ends, as is illustrated and discussed in Art. C2.3b, Example 2. By successive trial calculations, when $P = 101700$ lbs, $P_{AB} = 88072$ and $P_{AC} = 50850$.

$$(L/J)_{AB} = 30/\sqrt{5} \times 10^6 / 88072 = 3.9816$$

$$SC_{AB} = -1.5428$$

$$SF_{AB} = 4(-1.5428)(5 \times 10^6)/30$$

$$= \underline{1028500}$$

$$(L/J)_{AC} = 17.3/\sqrt{5} \times 10^6 / 50850 = 1.7446$$

$$SC_{AC} = .89059$$

$$SF_{AC} = 4(.89059)(5 \times 10^6)/17.3$$

$$= \underline{1029600}$$

Hence, at Joint A $\Sigma SF = 1029600 - 1028500 \approx 0$ so 101700 is the buckling (critical) load for the truss.* If A were assumed to be a pinned joint then an applied load of only 63315 would cause AB to buckle as a pinned-end column, since for pinned ends P_{CR} for AB is 54831 and $.866 \times 63315 = 54831$.

To illustrate the effects of applied loadings near the critical loading on secondary bending moments, assume that $P = 100000$ and find the resulting moments.

* When ΣSF at any joint $\neq 0$ there is no resistance to rotation so an infinitesimal moment will cause rotation and failure.

Let AC be the base member, apply a 1 in-lb couple on AB and react it with an opposite couple on AC as in Fig. All.95.

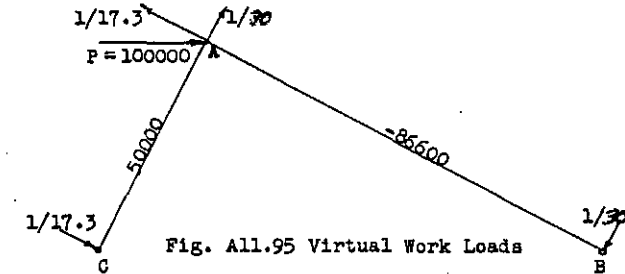


Fig. All.95 Virtual Work Loads

The relative rotation of member AB is then calculated as follows.

Member	$L/AE \times 10^6$	S	u	$Su/L/AE \times 10^6$
AC	.828	50000	1/30	1380
AB	1.435	-86600	1/17.3	-7183
			$\theta = \Sigma u = -5803$	

The only FEM is at A since end B is pinned (and AC has no relative rotation).

$$FEM_{AB} = -6(5 \times 10^6)(-5803 \times 10^{-6})(1 - 2.323)/30(1.44) \\ = -5331 \text{ in lbs}$$

Doing the moment distribution for the final moments at A

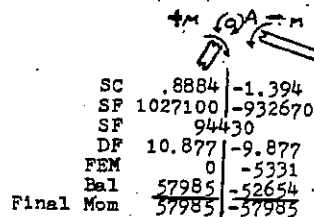


Fig. All.96 Moment Distribution

The extremely large final moments are, of course, unacceptable since bending failure would occur (if P were 101700 the moments would be infinite). Therefore, when the applied loading on a truss is near the critical loading bending failure will occur (and prevent the critical loading from being reached), due to the deflection of the truss joints under load.*

Repeating the above calculations for successively smaller values of the applied loading, P , results in the final moments shown in Table All.6. Note that as the applied loading decreases from near the critical loading the final moments decrease very rapidly at first. When the loading decreases to the value which is the critical value assuming pin joints

* The maximum bending in AB is 77,840 in-lbs, occurring 18.3" from A (using Case 2 in Table A5.1)

Table A11.6 Variation of Final Moments with Applied Loading

Applied Loading	% of Critical Loading	Final Moments At A
101700	100.0	∞
100000	98.4	-57985
99000	97.3	-24983
98000	96.4	-20522
95000	93.4	-8876
63315	62.3	0
40000	39.3	60

(63315) the final moments are relatively small. This is why an assumed pin joint analysis which ignores the secondary moments, a common procedure, is unlikely to result in strength failures. Fatigue life might be a concern for very light structures. If a truss member is subject to a lateral loading, that causes an additional type of secondary moment to occur and additional beam-column effects.

Although this illustrative example uses only the simplest type of rigid joint truss, the results would be similar for a conventional type of truss. The analysis would, of course, be more tedious. More about trusses is in the book mentioned in Art. A18.27a (and Fig. A11.43).

A13.11a Curved Beams

For compact cross-sections the beam is not subject to flange instability effects (Chapter 7). Therefore, with ductile materials, the ultimate bending strength can be calculated as discussed in Chapter C3, ignoring the curvature.

When the cross-section has relatively thin flanges, as with an I, channel, Z etc. there is another effect of curvature. It causes the flange to bend as shown in Fig. A13.22a, and therefore become less effective, resulting in higher bending stresses for the beam. It also generates bending stresses in the flanges in a direction normal to the plane of the web which are a maximum at the flange-to-web intersection.

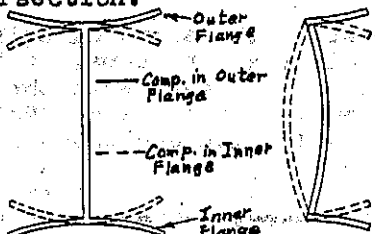


Fig. A13.22a Curved Beam Section Bending

For symmetrical cross-sections the circumferential bending stress at any point on the section can be calculated as

$$f_b = \frac{M}{AR} \left[1 + \frac{1}{Z} \left(\frac{y}{R+y} \right) \right]$$

where A = Area of cross-section
 R = Radius of curvature at the centroidal axis

M = Applied moment, positive for tension in the outer fibers and vice-versa

y = distance from centroidal axis, being + outward from this axis and - if inward

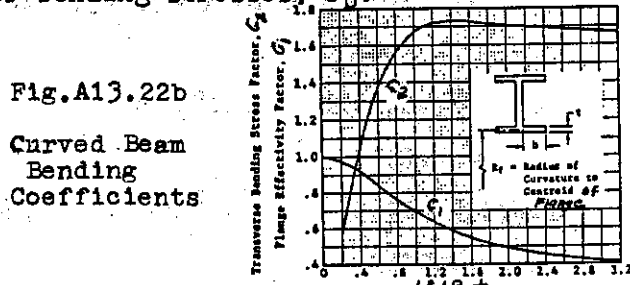
$$Z = - \frac{1}{A} \int \frac{ydA}{R+y} = - \frac{1}{A} \int \frac{wydy}{R+y}$$

where w = cross-sectional width at distance y

Table A13.4 presents formulas for Z for several cross-sections. Where a flange width is required, it is not the actual width, b , but rather an effective width, b_{eff} , due to the deflection shown in Fig. A13.22a. This can be calculated as

$$b_{eff} = C_1 b$$

where C_1 is obtained from Fig. A13.22b. b_{eff} is used for determining A and Z when flanges are present. Being less than the actual b , it results in higher bending stresses, f_b .



The transverse bending stress in the flange, f_{bt} , can be calculated as

$$f_{bt} = C_2 f_b$$

where C_2 is obtained from Fig. A13.22b and f_b is the stress calculated previously using C_1 . Again, this discussion applies only to symmetrical cross-sections as in Fig. A13.22a.

When weight is important and relatively thin flanges result in high stresses, the stresses can be reduced by using thin, closely spaced, machined in place "bulkheads" between the flanges, or beneath a T-member's flange. This reduces

the flange deflection and therefore reduces the beam bending stresses and the flange's transverse bending stress. Unfortunately, there is apparently no design criteria for this, so one must rely on judgement and tests as to, both, limit and ultimate load adequacy.

Unsymmetrical cross-sections should be avoided in fittings and hooks with large curvature since there are no formulas or data for predicting bending stress in such flanged members (tests required).

Finally, much curvature with flanged members can cause significant compressive ("crushing") stresses on the web and the thinner the web the worse the effect. These are generated as discussed for Fig. D3.28 and stiffeners are needed as illustrated to prevent crushing or buckling. The machined bulkheads also do this in the case discussed for machined items.

A18.5a Buckling Loads of Columns

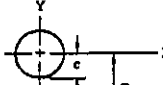
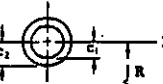
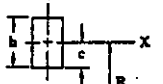
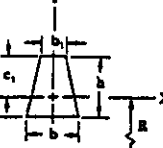
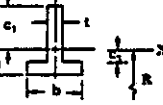
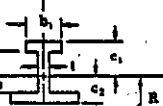
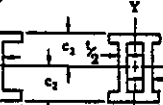
Equation 16(b) applies only when the axial stress is in the elastic range and when the cross-section of the column remains stable (i.e., no local buckling occurs before σ_{cr} is attained). When these conditions do not exist the critical load will be less than predicted by Eq. 16(b), as discussed in Art. A18.8a.

A18.8a Imperfect Columns. Tangent Modulus Theory

Add the following at the end of Art. A18.8. Since E_t (in Eq. 16b, 30 and 34) decreases as the compressive stress increases above the proportional limit (E_t being the slope of the stress-strain curve), a successive trials solution for σ_{cr} is indicated. That is, E_t must be the value corresponding to σ_{cr} . The successive trials can be avoided if a column curve is available as in Fig. A18.11, entering with L/r and reading σ_{cr} on the ordinate. If a column curve is not available the procedure illustrated in Art. C2.10 can be used.

Equations 16b, 30 and 34 also do not apply, nor does the column curve, if any part of the cross-section is thin enough to have a local buckling stress which is smaller than σ_{cr} as predicted by the above equations. In this case a special column curve which accounts for this local instability must be constructed and used as shown in Art. C7.26 and C2.16.

Table A13.4 Some Formulas for Z

	$Z = -1 + 2\left(\frac{R}{c}\right)^3 - 2\left(\frac{R}{c}\right)\sqrt{\left(\frac{R}{c}\right)^2 - 1}$
	$Z = -1 + \frac{2R}{c_1^2 - c_2^2} \left(\sqrt{R^2 - c_1^2} - \sqrt{R^2 - c_2^2} \right)$
	$Z = -1 + \frac{R}{h} \left[\log_e \left(\frac{R+c}{R-c} \right) \right]$
	$Z = -1 + \frac{2R}{(b+b_1)b} \left[\left(b_1 + \frac{b-b_1}{h} (R+c) \right) \log_e \left(\frac{R+c}{R-c_1} \right) - (b-b_1) \right]$
	$Z = -1 + \frac{R}{A} \left[t \log_e (R+c_1) + (b-t) \log_e (R-c_1) - b \log_e (R-c_1) \right]$
	$Z = -1 + \frac{R}{A} \left[b_1 \log_e (R+c_1) + (t-b_1) \log_e (R+c_1) + (b-t) \log_e (R-c_1) - b \log_e (R-c_1) \right]$
	$Z = -1 + \frac{R}{A} \left[b \log_e \left(\frac{R+c_1}{R-c_1} \right) + (t-b) \log_e \left(\frac{R+c_1}{R-c_1} \right) \right]$

A18.8b Torsional Buckling

The previous discussions are for the conventional form of general instability involving only a bent (buckled) shape, also referred to as bending buckling. There is another form of general instability which can result in smaller values of σ_{cr} . This form of buckling involves a twisting of the column (even though there is no applied twisting moment) and is called "torsional buckling". Depending upon the cross-sectional shape, the buckled shape may be either a pure twisting or a combination of twisting and bending about one or both axes. It occurs for open cross-sections having thin elements and is usually more critical than bending buckling in the short to medium range column range.* Torsional buckling is discussed further in Art. C7.3j and in detail in the book described in Art. A18.27a

* See Fig. C7.43

A18.27a Comprehensive Treatment of Column Strength

The broad coverage (180 pages) of column design referred to in Art. 18.27 as being in an originally planned "Volume 2" was not included when it was decided to publish only the current single volume rather than two volumes because of space requirements. However, this material is available in the book "Engineering Column Analysis" by W.F. McCombs, Datatec, P.O. Box 763576, Dallas, TX 75376-3576. Topics include columns, beam-columns, truss members, bents, arches, torsional buckling, local buckling, crippling, buckling of shells and members on elastic or otherwise sagging supports. Both, uniform and varying section members are included.

A18.28a Mechanical and Physical Properties of some Aircraft Materials

The last paragraphs of Art. A18.28 refer to a planned Volume 2 which was finally included as Parts B, C and D of the textbook. Therefore, it is Chapters B1 and B2 of the textbook to which the reference is made.*

A19.23 Crushing Loads on Ribs Due to Wing Bending

Chapter A19 provides methods for determining the stress in the flanges, shear webs, stringers and skin panels of the wing structure. Chapter A.21 discusses the shear loads and stresses in wing ribs. Neither of these chapters discusses the crushing loads on the rib webs at a rib-stringer joint which are caused by the bending of the wing or of any box beam having stringers supported by ribs. Since the ribs provide simple support for the stringers in compression, if a rib fails locally its simple support for the stringer will vanish and the stringer will fail as a column. When the rib web is thin with no local reinforcement and the crushing loads are large such failure can occur. The manner in which these crushing loads arise is as follows.

Fig.A19.44 shows a front view of a wing in its bent form (greatly exaggerated), the upper stringers being in compression, the lower ones being in tension and the load line from rib to rib shown by the broken line. Due to the bending radius of curvature, R , the angle θ will be $\theta = L/R$, a very small angle since R is very large in a practical wing structure. The load, P , in any stringer located at a rib will have components of load parallel to the rib which are re-

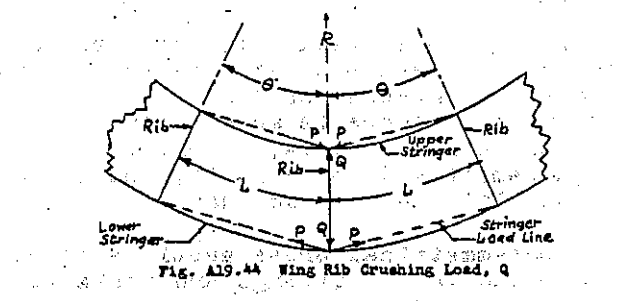


FIG. A19.44 Wing Rib crushing Load, Q

acted by the rib load, Q , in the amount

$$Q = 2P\sin(\theta/2) = P\theta$$

or, $Q = PL/R$

$$\text{Since } R = EI/M$$

$$Q = PLM/EI$$

If L_1 and L_2 are different rib spacings

$$Q = P(L_1 + L_2)M/2EI$$

Where Q is the crushing load on the rib web at the stringer, M is the bending moment on the wing at the rib station and EI is that of the wing at the rib station. Therefore, each stringer will need a clip to the rib (or its equivalent) which can pass the load Q into the rib web, and if the load is large enough to crush the rib the clip will also need to be extended and fastened so as to serve as a stiffener for the rib, to prevent crushing of the rib web.

C1.13a Factors of Safety and Margins of Safety

These items are discussed in articles A4.2 and in C1.13 through C1.15, but they do not provide specific associated numbers for factors of safety or methods for calculating the margin of safety for members under many combined load systems. The purpose of the following discussion is to do that.

Factors of Safety

Ultimate loads, also called design loads, are obtained by multiplying the limit loads (the actual or expected loads) by a factor of safety. For piloted aerospace vehicles the factor of safety is usually 1.5. For missiles, which are not piloted, the factor of safety is usually 1.25 except for any load condition where the safety of people is involved where it is 1.5 (e.g., for the ejection loads from a carrier airplane). Naval airplanes are designed for a very fast sinking speed, about 26 feet per second, so no safety factor is applied to

*Some such data are also on p.A6-A9

these loads. However, the landing gear must continue to function after such a landing and the major attach fittings (landing gear to wing or fuselage, wing to fuselage and major fuselage section splices) must show a margin of safety of .25 for this landing condition. In general, factors of safety are specified by the procuring agency.

Margins of Safety

The margin of safety for a structural member subject to a single load or stress is calculated as

$$M.S. = \frac{\text{Allowable Load (or Stress)}}{\text{Ultimate Load (or stress)}} - 1.0$$

and must be zero or more. However, in some cases it must have a specified positive value as mentioned for Naval airplanes and .15 for fittings. This margin is also required if additional fitting or casting factors have been specified. For shear joints a minimum margin of safety of .15 is required and for tension joints it is .50.* Also for these joints there must be no yielding at limit load. For shear joint attachments if the bearing yield strength is less than 2/3 of the ultimate bearing strength, the bearing allowable strength is taken as 1.5 times the bearing yield strength and the joint is said to be "yield critical". For riveted shear and tension joint allowable data see Chapter D1. Also see Appendix A.

The previous simple formula for the M.S. gives the decimal fraction by which the load may be increased and still have a M.S. of zero. For example, if M.S.=.20 the applied loads may be increased by a factor of 1.20. However, the simple formula applies only when all of the following conditions exist

1. The member is subject only to a single type of loading, not to several types such as shear plus compression etc.
2. The internal loads vary linearly with applied loads.
3. All applied loads are variable, i.e., none are fixed in magnitude such as a constant pressurization.

These conditions are discussed as follows.

1. For example a bolt may be subject to shear, bending and tension simultaneously. In such cases so-called "interaction equations", derived from

tests rather than theory, are used to show structural adequacy. A typical interaction equation is of the form

$$R_1^a + R_2^b + R_3^c + \dots + R_m^n = 1.0$$

Where $R_1 = f_1/F_1$, $R_2 = f_2/F_2$, $R_3 = f_3/F_3$ and $R_m = f_m/F_m$, f being the ultimate stress (or load) and F being the allowable stress (or load). R is called the "stress ratio". When the left side of the equation is 1.0 the M.S. is zero. When it is less than 1.0 the M.S. is positive but undefined and when it is more than 1.0 the M.S. is negative but undefined.

Example:

$$\begin{aligned} f_1 &= 10000 \text{ and } F_1 = 30000, \text{ so } R_1 = .333 \\ f_2 &= 40000 \text{ and } F_2 = 60000, \text{ so } R_2 = .667 \end{aligned}$$

$$\text{Interaction Equation: } R_1^a + R_2^b = 1.0$$

$$.333^a + .667^b = .778 (< 1.0)$$

Hence the M.S. is positive but undefined.

There are two cases for which the M.S. can be calculated directly using the interaction stress ratios, R , as follows.

- a) When all exponents (a, b, c, n) have values of 1.0 and/or 2.0. In this case

$$M.S. = \frac{2}{\sum R_i^2} - 1.0$$

- b) When all exponents have the same value, n , in which case

$$M.S. = \frac{1}{(R_1^n + R_2^n + \dots + R_m^n)^{1/n}} - 1.0$$

For all other cases the M.S. is found by using plots of the applicable interaction equation (discussed later) or by successive trial calculations. The latter is done by finding, by successive trials, by what common factor, A , all of the loads must be multiplied to satisfy the interaction equation. The M.S. is then $A - 1.0$. Or, when

$$(AR_1)^a + (AR_2)^b + (AR_3)^c + (AR_4)^d = 1.0$$

$$M.S. = A - 1.0$$

Example:

For the previous example

$$A \cdot .333^a + (A \cdot .667)^b = 1.0$$

* Also see p.A1, Margins of Safety

After several trials the equation is satisfied when $A = 1.171$, so

$$M.S. = A - 1.0 = 1.171 - 1.0 = .171$$

Since all exponents are 1.0 and/or 2.0 the M.S. can also be calculated by formula as

$$M.S. = \frac{2}{.333 + \sqrt{.333^2 + 4 \times .667^2}} - 1.0 = .171$$

When using this formula with other more lengthy interaction equations the parentheses around the term $\sum R_1$ must be noted and used. $\sum R_1$ is the sum of all stress ratios having the exponent 1.0 and $\sum R_2^2$ is the sum of those having the exponent 2.0.

When plots of interaction equations are available the M.S. can be determined by a graphical construction. This is illustrated in Art. C4.24a in the textbook using Fig. C4.36. However, graphical solutions are not needed when the prior formulas apply, and in many other cases the successive trials procedure may be easier with calculators or when the interaction curves are not available.

Listing of Interaction Equations

Numerous interaction equations appear in various parts of the book per the following listing.

Bending, Shear and Compression	C3.13
Bending and Shear	C3.12
Bending and Bending	C3.8
Beam-Column Bending & Axial Load	C4.22
<u>Tubing:</u>	
Bending and Compression	C4.22
Bending and Tension	C4.23a
Bending and Torsion	C4.24
Compression, Bending and Torsion	C4.24a
Bending and Shear	C4.25
Compression, Bending , Shear and Torsion	C4.26
Tension and Torsion	C4.27
<u>Flat Sheet</u>	
Bending and Compression	C5.9
Bending and Shear	C5.10
Shear and Tension or Compression	C5.11
Compression, Bending and Shear	C5.12

Monocoque Cylinder (Various) Table C8.1

<u>Curved Sheet</u>	C9.5
Compression or Tension and Shear	
<u>Stiffened Cylinder</u>	C9.11
Shear and Compression	
Torsion and Bending	C9.13
Shear and Bending	C9.13
<u>Shells in Diagonal Tension</u>	
Stringer Primary and Secondary Stresses	C11.33a
Ring (Frame) Primary and Secondary Stresses (for Stringer System)	C11.33a
Longeron Primary and Secondary Stresses	C11.36a
Ring (Frame) Primary and Secondary Stresses (for Longeron System)	C11.36a

2. There are cases where the internal loads in a member do not vary linearly with the applied loads. One example is the beam-column where the bending moment increases faster than does the applied loading. Another example is the axial stress in stringers due to tension field action. For such cases the M.S. as previously calculated would be an "apparent" M.S., not a true M.S. Whether the apparent M.S. is positive or negative, the true M.S. will always be closer to zero than the apparent M.S. The true M.S. must be calculated as follows.

By successive trials find the common factor, A, by which the applied loads (which produce the internal loads in the members) must all be multiplied to give a calculated M.S. of zero. The true M.S. is then $A - 1.0$. For a beam-column the applied loads are the axial load and the transverse loads. Multiplying these by any factor, F, will generate a bending moment in the beam-column which increases faster than the common factor, F. A is the value of F for which the calculated M.S. is zero, and then the true M.S. is $A - 1.0$. This procedure applies for any interaction equation that may be applicable. Note that this requires a greater effort than that in (1) previously. This is because increasing the applied loads requires another analysis to determine the internal loads, since they do not

vary linearly with the applied loads.

This is important because margins of safety are reported for structural members and are used to see if the members can withstand an increase in the applied loads. If the applied loads increased by a factor of, say, 1.20 and the report showed a M.S. of, say, 1.20 it would be judged to be acceptable as an increase. But if this happened to be an apparent M.S. the true M.S. would be smaller and the increase in applied loads would not be acceptable. Hence, the true values of the M.S. should be in the report. If not they should be "flagged" as being apparent ones so that a proper evaluation can be made when needed.

3. The internal loads in a member are due to the applied loads. Sometimes the applied loads consist of "fixed" loads which do not vary, such as, for example, constant pressurization loads. When such are present the internal loads or stresses in the member due to them should not be multiplied by the common factor, A, in (1) previously or by the factor, F, in (2) since they are constant. If such were done the calculated M.S. would be conservative (too small) if these loads were "additive" and vice-versa if they were "subtractive". This also applies when the M.S. is calculated by the formulas in (1a) and (1b), and when the M.S. is determined graphically, which makes these calculations not applicable for such cases. (the successive trials procedure is then needed).

Cl.15b Dealing with Tolerances

When calculating margins of safety for a structural member nominal (mean) dimensions are used to determine the stress in the member and its allowable load. Ideally, the M.S. is zero, generally. However, all drawings specify the manufacturing tolerance which accompanies each dimension such as, for example, $\pm .03"$ and these are considered as follows

In aerospace structures it is common practice to consider only the two worst tolerances affecting any dimension and to compute the reduced margin of safety based on the reduced dimensions. This will give a negative M.S. when the nominal M.S. is zero. Such negative margins are acceptable if they do not exceed $-.15$ for single load path members

or $-.25$ for redundant members. These are arbitrary limits, some companies allowing more negative values such as $-.19$ and $-.39$ respectively. Such negative margins caused by tolerances are acceptable since the probability is quite low that, simultaneously, the material will have minimum properties, the tolerances will be as large as allowed, the loading condition will be achieved and the internal loads in the members will be as large as predicted. If the M.S. had to be zero or more based on such minimum, rather than nominal, dimensions considerable weight would be added to the structure.

When dimensioning structural members care should be used to prevent the build-up of large tolerances affecting the final dimension. Unacceptable tolerance effects are most likely to occur when dimensioning small machined or cast protuberances or holes, where small internal corner radii are present and for thin machined or chem-milled parts.

However, the above should in no way be construed as sanctioning negative margins based on nominal dimensions or endorsing the salvage of parts having less strength than required per the drawing.

Cl.6a Combined Stress Equations

For practical calculation purposes the following summary and example problem are helpful. Fig. Cl.8a(a) shows the positive direction of known or given applied stresses. Fig. (b) shows the resulting stresses, σ_θ and τ_{xy} , on any plane θ (positive directions shown), which can be calculated as follows.

$$\sigma_\theta = \frac{1}{2}(\sigma_x + \sigma_y) + \frac{1}{2}(\sigma_x - \sigma_y)\cos 2\theta + \tau_{xy}\sin 2\theta$$

$$\tau_\theta = \frac{1}{2}(\sigma_x - \sigma_y)\sin 2\theta - \tau_{xy}\cos 2\theta$$

1. The principle stresses, σ_n , are calculated as follows.

$$\sigma_n = \frac{1}{2}(\sigma_x + \sigma_y) \pm \sqrt{\frac{1}{4}(\sigma_x - \sigma_y)^2 + \tau_{xy}^2}$$

2. The plane for the largest principle stress, Θ_p , is measured from the plane of the larger of σ_x or σ_y and is calculated as follows.

$$\Theta_p = \frac{1}{2}\arctan(2\tau_{xy}/(\sigma_x - \sigma_y))$$

The plane of the smaller principle stress is 90° away from this plane.

3. The maximum shear stress, τ_{max} , is calculated as follows.

$$\tau_{max} = \sqrt{\frac{1}{4}(\sigma_x - \sigma_y)^2 + \tau_{xy}^2}$$

4. The plane on which τ_{\max} is located is
 $\theta_r = \arctan((\sigma_x - \sigma_y)/-2\tau_{xy})$

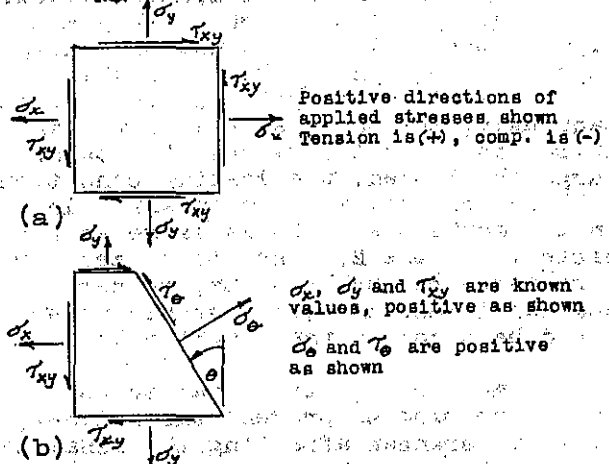
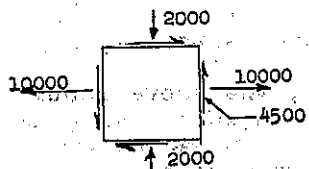


Fig. C1.8a Shear and Normal Stresses

Example Problem

For the stresses shown in the sketch above (note that σ_y is compressive, hence negative) what are σ and τ on a plane at $\theta = 60^\circ$? What are σ_n , θ_p , τ_{\max} and θ_r ?

$$\sigma_e = \frac{1}{2}(10000 - 2000) + \frac{1}{2}(10000 + 2000)\cos 120^\circ + 4500\sin 120^\circ = 4897$$

$$\tau_\theta = \frac{1}{2}(10000 + 2000)\sin 120^\circ - 4500\cos 120^\circ = 7446$$

$$\sigma_n = \frac{1}{2}(10000 - 2000) \pm \sqrt{\frac{1}{4}(10000+2000)^2 + 4500^2} = 11500 \text{ and } -3500$$

$$\theta_p = \frac{1}{2}\arctan(2 \times 4500 / (10000 + 2000)) = 18.43^\circ$$

$$\tau_{\max} = \sqrt{\frac{1}{4}(10000 + 2000)^2 + 4500^2} = 7500$$

$$\theta_r = \arctan(10000 + 2000 / -2(4500)) = -26.57^\circ$$

θ_r is always 45° away from θ_p .

If any of the above calculated values had been negative they would be acting or located in a direction opposite to that shown in Fig. C1.8a.

Usually one is interested only in deter-

FREE-ENDED COLUMNS

mining the value of the largest σ_n and of the largest τ_{\max} .

C2.1a Methods of Column Failure.
Column Equations

The last paragraph is extended to include the following. Predicting failure due to local instability requires that the column curve be reconstructed in the short to intermediate ranges. This reconstruction is discussed and illustrated in Art. C7.25 through C7.27.

C2.2a Free-Ended Columns **

Fig. C2.2 shows only a special case of the free-ended column, one end being fully fixed and the load remaining parallel to the axis of the member in its straight (unbuckled) form. In general, however, the load, P , may be directed either to or from a given point, "o", as shown in Fig. C2.2a.

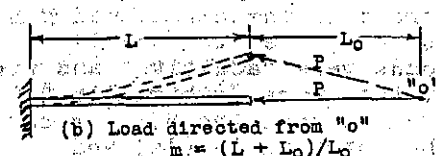
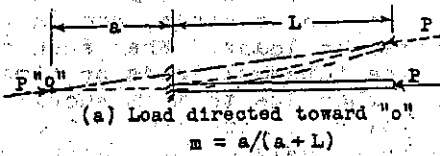


Fig. C2.2a Free-Ended Column, Fixed End

As shown in Ref. 4 (Art. A18.27a), the buckling load is defined by the transcendental equation

$$(L/j)ctnL/j = 1 - (1/m)^*$$

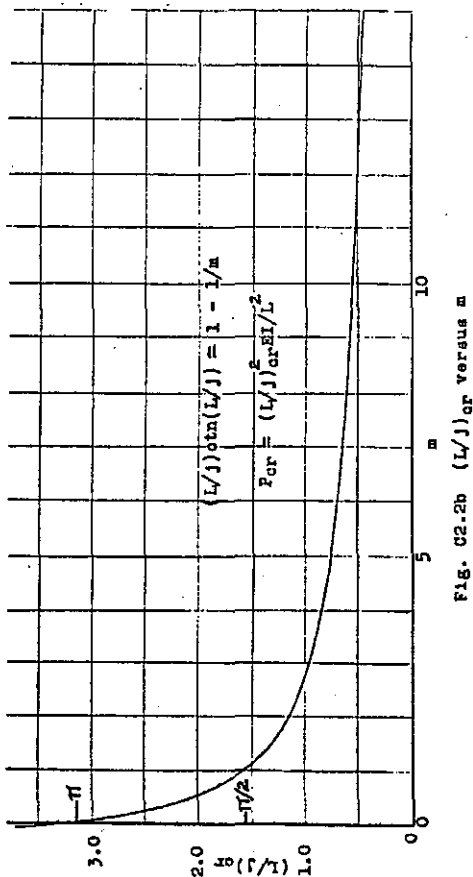
For any given value of m (Fig. C2.2a), P_{cr} is found by successive trials. That is, one assumes a value for P , calculates $j (= \sqrt{EI/P})$ and uses this in the equation. When $P = P_{cr}$ the equation will be satisfied. However, this effort can be greatly reduced by using Fig. C2.2b, entering the figure with m and obtaining $(L/j)_{cr}$. P_{cr} is then calculated as

$$P_{cr} = (L/j)_{cr}^2 (EI/L^2)$$

Note that when $a = 0$ or $L_o = \infty$, $m = 1.0$ and $P_{cr} = (\pi/2)^2 (EI/L^2)$; When $a = 0$, $m = 0$ and $P_{cr} = \pi^2 (EI/L^2)$; when $L_o = 0$, $m = \infty$ and $P_{cr} = 0$. That is, as a decreases P_{cr} increases, but as L_o decreases P_{cr} decreases.

* For Fig. (a) an alternate form is $\tan L/j = -a/j$
and for Fig. (b) $\tan L/j = (L+a)/j$

** For free-ended beam-columns see Art. A18.27a book



Elastically Restrained End

Instead of being fully fixed, the end may be elastically restrained as shown by the "torsion spring", k , in Fig. C2.2c, which has a value in in-lbs/radian. This results in a smaller buckling load than when fully fixed ($k = \infty$).

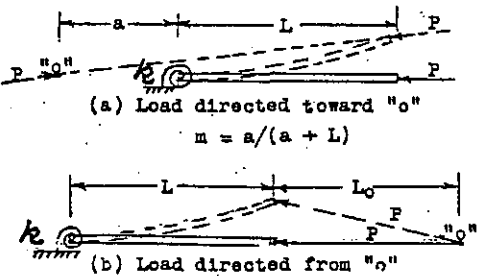


Fig. C2.2c Free-Ended Column Having an Elastically Restrained End

For this case, as shown in Ref. 4, the buckling load is given by the equation*

$$k - \frac{P_m L}{1 - m(1 - (L/J)ctnL/J)} = 0$$

P_{cr} is found by successive trial calcu-

* Derived by using the moment distribution procedure.

When $m = 1$ the equation becomes simply $k - P_j \tan L/J = 0$

lations as follows. For a given k and m one assumes a value of P , calculates j and uses these values in the equation. When $P = P_{cr}$ the equation is satisfied.

For the special case where a or L is infinity, so that $m = 1.0$, P_{cr} can be determined directly by entering Fig. C2.44 with kL/EI , obtaining the value of C and calculating P_{cr} as

$$P_{cr} = C\pi^2 EI/L^2$$

Note that when $k = \infty$ (fully fixed) $C = .25$ as given in Fig. C2.2.

It must be remembered that in all column calculations E is E_t , which decreases as the compressive stress exceeds the proportional limit. Also, when the column has an unstable (thin) cross-section E is an "effective" modulus.* To determine it one finds the buckling stress from the modified column curve (Art. 7.26) and then calculates it as

$$E_{eff} = F_{cr}(L/\rho)^2 / \pi^2$$

For free-ended columns Fig. C2.17 is applicable only when $m = 1.0$.

If the column has lateral loads or an initially bent shape it becomes a beam-column. Free-ended beam-columns are discussed in Ref. 4, also Table A5.1a, Case 17.

Example Problem 1

For a column as in Fig. C2.2a(a) assume that $a = 30"$, $L = 30"$, $E = 10.5 \times 10^6$ (7075-T6 Extrusion, p.B1.11), $I = .191$, $A = .50$ sq in and a stable cross-section. What is P_{cr} ?

$m = 30/(30 + 30) = .50$. Per Fig. C2.2b for $m = .5$, $(L/J)_{cr} = 2.03$. Therefore,

$$P_{cr} = 2.03^2 (10.5 \times 10^6) (.191) / 30^2 = 9183$$

$$F_{cr} = 9183/.50 = 18366$$

Since $F_{cr} < \text{Prop. Limit}$, $E_t = E$ as assumed.

Example Problem 2

Repeat Example 1 assuming the fixed end is replaced with an elastic restraint of $k = 50000$, as in Fig. C2.2c. This must be solved by successive trials.

Trial 1: Assume $P_{cr} = .8\pi^2 EI/4L^2 = 4399$
Then $j = \sqrt{EI/P} = \sqrt{10.5 \times 10^6 (.191) / 4399} = 21.35$ and $L/J = 1.405$

$$\text{Then } 50000 - \frac{4399(.50)(30)}{1 - .5(1 - 1.405 \operatorname{ctn} 1.405)} = -56849 \quad (\neq 0)$$

* See Art. C2.16

After several more trials it is found that when P is 2622 the equation is satisfied, so this is the critical load, as follows.

$$j = \sqrt{10.5 \times 10^6 (.191) / 2622} = 27.656$$

$$L/j = 30 / 27.656 = 1.0848$$

$$50000 = \frac{2622(.5)(30)}{1 - .5(1 - 1.0848ctn1.0848)}$$

$$= -4.7 \text{ which is essentially zero.}$$

So this particular elastic restraint has reduced the critical load from 9148 for a fully fixed end to only 2622 lbs.

C2.3a The Effect of Shear on Buckling Stress

Equations (1) and (2) of Art. C2.1 consider only the bending stiffness of columns. When a beam bends because of applied transverse loads and the resulting bending moments, the usual deflection formulas consider only the bending moment. There is, however, an additional deflection due to shear. For example, a simply supported beam of uniform EI having a load, Q , at mid-span will have a maximum deflection given by

$$y = QL^3 / 48EI + nQL^2 / 4AG$$

The first term is due to bending and the second term is due to shear, where n is a form factor which depends upon the shape of the cross-section. This is usually negligible, but as n increases due to a thin or perforated or otherwise more flexible web it can become significant.

For a column there is no applied transverse load, but a shear load is generated by the axial load as the column takes on a bent (buckled) shape, as shown in Fig. C2.2d

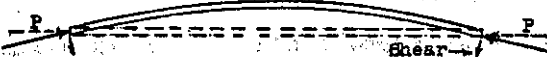


Fig. C2.2d Generation of Shear in a Column

At any station the bending moment is $M = Py$ and the shear in the member is

$$V = dM/dx = Pdy/dx$$

where dy/dx is the slope of the bent shape. Hence, for the uniform simply supported column the shear varies from a maximum at the ends to zero at the

middle where dy/dx , the slope, is zero. Consequently there is a shear in the member which, in effect, makes the column more flexible and thereby reduces the buckling load or stress.

As discussed in Ref.5, for uniform columns the buckling load, considering shear, is

$$P_{cr} = \frac{\sqrt{1 + 4n^2P_{cr}/AG} - 1.0}{2n/AG}$$

where P_{cr} is the buckling load ignoring shear, n is the form factor for the cross-section, A is the cross-sectional area and G is the shear modulus of elasticity ($G = E/2(1 + \mu)$) where μ is Poisson's ratio. The values of n for several cross-sections are shown in Table C2.2.

Table C2.2 Cross-Section Form Factors

Cross-Section	n
Rectangle	1.200
Solid Circle	1.100
Thin Round Tube	2.000
I-Beam or Rectangular Tube	Area/Web Area

n can be calculated for other cross-sections as

$$n = (A/I) \int_A Q dA/b$$

where A is cross-sectional area, Q is the static moment of area beyond dA about the neutral axis and b is the width at the neutral axis. For columns having latticed struts (trussed columns or "batten" plates) or having perforated webs see Ref. 5. It is when the web becomes thin or otherwise has less shear stiffness that the column buckling load is significantly reduced.*

C2.3b Multispan Columns

Unfortunately, this and most other textbooks do not discuss columns having more than one span. Such columns are easily checked for stability by applying a 1 in-lb couple at any "joint" (support) not having full fixity and carrying out the moment distribution procedure as discussed and illustrated in Art. A11.13 - A11.14 and its example problems. If the successive carry-over moments at all joints become smaller (converge) the column is stable. The larger the axial load the "slower" the convergence. If they diverge at any joint the column is unstable. The critical load is that for which they do neither, found only by successive trial analyses, varying the axial load used in each moment distribution.

* For varying EI columns the tables in Art. C2.6b can be amended to account for shear, see Ref.4.

There are some helpful techniques for doing this in Ref. 4, including some "quick checks" for detecting instability sometimes without the above procedure. Ref. 4 also contains numerous example problems for multispan columns including those on elastic or otherwise deflecting supports, those having free-ended members and those having varying loads and EI values within the spans.

The alternative to doing the moment distribution analysis is to conservatively assume that each span is simply supported and check each span individually. This is accurate only when all spans are identical, the two ends are simply supported and the axial load is constant.

"Quick Check" Instability Criteria

- 1) The following can be done when each span is uniform and the axial load does not vary along the span (j is constant). If any span has a value of L/j greater than shown in Table C2.3 the column is known to be unstable. If less than these values it may or may not be unstable, but a moment distribution analysis is required.

Table C2.3 Instability Criteria**

Type of End Support	$(L/j)_{\max}$
A. One end elastically restrained, one end free	$\pi/2$
B. Both ends simply supported	π
C. One end simply supported, one elastically restrained	4.49+
D. Both ends elastically restrained	2π

Elastic restraint is provided by an adjacent span in a multispan column or by a torsion spring as in Fig. C2.2c.

- 2) If at any joint the sum of the stiffness factors, ΣSF , is negative the column is unstable (see the footnote for Art. All.15b).

The Two-Span Column

The following applies not only to a two-span column but to any number of spans meeting at a common joint (support). If the outer ends of the members are either simply supported or fully fixed or free (no elastic supports) the column is known to be stable if at the common joint ΣSF is positive.* If it is negative the column is known to be unstable. No moment distribution is, therefore, required so the analysis is quite simple. The criti-

* and if criteria (1) above is met

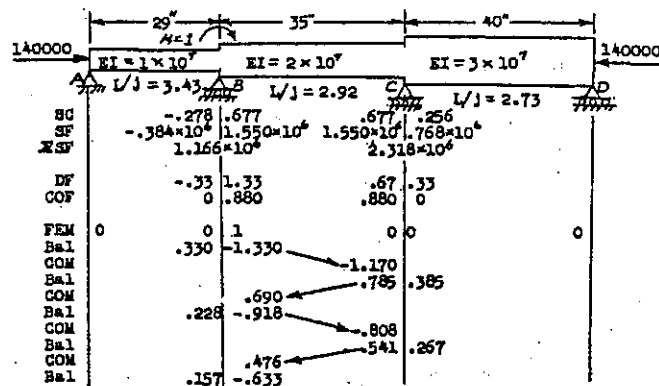
** The listed L/j values are for $P = P_{cr} = Cr^2 EI/L^2$

*** For any 3-span column, ABCD, having fixed and/or pinned ends (p.15) the stability can be checked as follows.
If $DF_{sc} COF_{sc} DF_{cs} COF_{cs} < 1.0$ the column is stable and vice versa.
If span BC is uniform then $COF_{sc} = COF_{cs}$

cal load is that for which $\Sigma SF = 0$, found by successive trial values of the axial load.*

Example Problem 1

Is the three-span column shown in the sketch below stable or unstable?

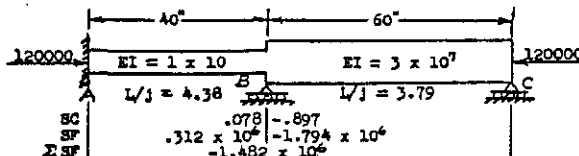


The analysis is carried out as shown, applying a 1 in-lb couple to the joint at B. Note that the SC, SF and COF are omitted at the ends, A and D, since they are simply supported and no initial moments (FEM's) are present there.* As the moment distribution process shows, the successive carry over moments (COM's) at all joints are decreasing. Therefore the column is known to be stable.***

Actually, one should always calculate the compressive stress, P/A , for each span and use the corresponding value of E_t (or E_{eff}) in calculating the value of j . Also, Ref. 4 contains extensive tables giving the values of SC and COF to six significant figures (better than Fig. All.46-47).

Example Problem 2

Is the two-span column shown in the sketch below stable or unstable?



Proceeding as discussed before for the two-span column, it is seen that ΣSF at the common joint, B, is negative. Therefore, the column is known to be unstable.

By successive trials it is found that when the axial load is 93040 lbs $\Sigma SF = 0$, so that is the buckling load.

If the axial load were 168750 to 219600

* For a free-ended column when $m = 1$ (Fig. C2.2a) the S.F. is $-Pjtam/L^2$

** If a end has elastic bending restraint (e.g., a torsion spring) use its k value as its J^2 and include this end as another joint in the moment distribution procedure (k being the spring constant)

ΣSF would be positive, indicating stability, but this would not be applicable because L/J for span BC would exceed the maximum (4.49+) allowed in Table C2.3. This is why the Table C2.3 criteria should always be checked first, before proceeding with any other analyses.

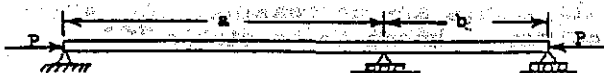
In summary, the moment distribution procedure can be used to check any multi-span column for stability. But before doing this instability can be detected quickly per the criteria of Table C2.3 and if at any joint ΣSF is negative. Then, for any two-span column if ΣSF is positive at the common joint the column is known to be stable if criteria (1) is met.

Uniform Two-Span Column Formula

For the special case of a uniform member on three simple supports an approximate formula for the buckling load is

$$P_{cr} = \pi^2 EI(2 - b/a)/a^2$$

where a is the longer span and b is the shorter span. When $a = b (=L/2)$ the formula is exact. When b becomes zero (i.e. as a becomes L) the error is only 2.44% and is conservative (one end becomes essentially fixed as a becomes L).



The formula can be verified numerically by calculations for a two-span column as previously illustrated, or theoretically as in the book "Theory of Limit Design" by J.A. Van Den Broek (J. Wiley and Sons).

C2.6a Stepped Columns

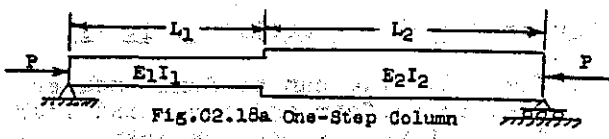
These are a special case for which formulas (buckling equations) are available as discussed in Ref. 7. Formulas are presented for the cases of simply supported members having one, two and three steps in EI. For more than three steps the formulas become too lengthy for practical usage, so a simple tabular calculation form is presented with an example problem shown.

Since the equations are transcendental in form, a successive trials procedure is necessary to determine the critical load. This consists of assuming a value for P (and Et), calculating any associated parameters and using these values in the equations. When the assumed P is P_{cr} the equation will be satisfied.

F_c ($= P_{cr}/A$) should be calculated for each step to be sure that the values used for E_t (Fig.C2.16) or E_{eff} (Art.C2.16) correspond to P_{cr} , which they must.*

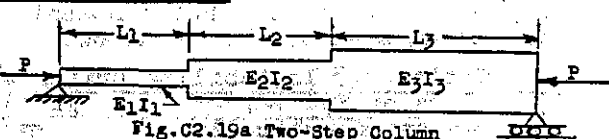
Since it is possible for more than one value of P to satisfy the equations (quite different values), it is best to use a length-weighted average EI , calculate a corresponding value for P_{cr} as $\pi^2 EI/L^2$ and use this as the initially assumed value for P . For the special cases of one-step and symmetrical two-step columns graphical plots are available in Fig. C2.21 and C2.22 for a direct determination of P_{cr} .

One-Step Column*



$$\frac{\tan L_1 \sqrt{P/E_1 I_1}}{\tan L_2 \sqrt{P/E_2 I_2}} = -\sqrt{E_2 I_2/E_1 I_1}$$

Two-Step Column



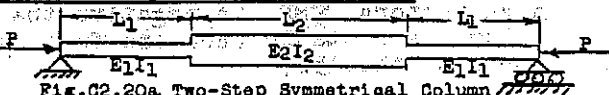
$$\sqrt{\frac{E_1 I_1}{E_3 I_3}} \tan \phi + \sqrt{\frac{E_2 I_2}{E_3 I_3}} \tan \sqrt{\frac{E_1 I_1 L_2}{E_2 I_2 L_1}} \phi$$

$$1 - \sqrt{\frac{E_1 I_1}{E_2 I_2}} \tan \phi \tan \sqrt{\frac{E_1 I_1 L_2}{E_2 I_2 L_1}} \phi$$

$$= -\tan \frac{L_3}{L_1} \sqrt{\frac{E_1 I_1}{E_3 I_3}} \phi$$

where $\phi = L_1 \sqrt{\frac{P}{E_1 I_1}}$

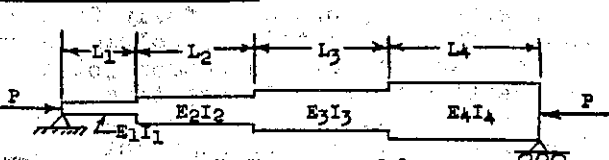
Two-Step Symmetrical Column



$$\tan(L_1 \sqrt{P/E_1 I_1}) \times \tan(L_2 \sqrt{P/E_2 I_2/2})$$

$$= \sqrt{E_2 I_2/E_1 I_1}$$

Three-Step Column



* These equations are easily programmed for rapid solution by computer or suitable calculators.

** An alternative helpful buckling equation is that for stability if $\cot \frac{L_1}{J_1} + \cot \frac{L_2}{J_2} > 0$

$$\frac{\tan\theta_1 + \tan\theta_2 + \tan\theta_3 - \beta_2 \tan\theta_1 \tan\theta_2 \tan\theta_3}{\beta_1 \beta_2 \beta_3} = -\frac{\tan\theta_4}{\beta_4}$$

where $\beta_n = \sqrt{P/E_n I_n}$ and $\theta_n = \beta_n L_n$

The equations are easily programmed for rapid evaluation using a suitable calculator (or computer). The derivation of the equations is available in Ref. 7.

Columns Having More than Three Steps

For these cases (and also for 2 or 3 steps) the following tabular numerical procedure can be used, as illustrated in Table C2.4. It, too, is a successive trials procedure (successive tables). One assumes a value for P (and E) as suggested later and carries out the tabular calculations as shown. When the assumed P is P_{cr} the value in Col. 6 for the last segment, N, will be equal to the value in Col. 8 for the segment N-1 multiplied by -1. Any number of segments can be used. The example below shows the last of several successive trials with different values for P, the last being 79200 lbs.

As discussed previously, to start with a reasonable value for P a length-weighted average EI should be used and P calculated as $\pi^2 EI/L^2$. When Col. 6_N is less than -Col. 8_{N-1} a larger value for P should be assumed for the next trial and vice-versa for 6_N > -8_{N-1}.

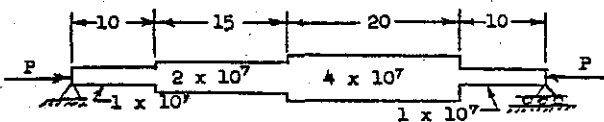


Fig.C2.20c Data for Table C2.4 Example Problem

Table C2.4 Stepped Column Analysis

①	②	③	④	⑤	⑥	⑦	⑧
Segment n	EI Data	$\frac{1}{L}$	$\tan(\frac{1}{L})$	$\tan(\frac{1}{L})/1$	$(\tan(\frac{1}{L})/1)/1$	$\beta_1 + \beta_2 + \beta_3 + \beta_4$	$1 - \beta_{n-1} - \beta_n$
1	1×10^7	11.237	10	1.2344	13.871	.10985	13.871
2	2×10^7	15.891	15	1.3866	21.938	.08688	-174.582
3	4×10^7	22.407	20	1.2321	27.719	.05476	-13.907
4	1×10^7	11.237	10	1.2344	13.871		

Since $\beta_4 \approx -\beta_3$, $P_{cr} = P = 79200$ lbs.

As discussed for the formulas in Art. C2.6a, the proper values of E must be used for each segment.*

C2.6b Numerical Column Analyses

Except for those cases discussed in Art. C2.1 through C2.3, Fig.C2.21 through

C2.27 or other similar type data, a numerical analysis is required to determine the critical load or stress. Art.C2.6a presented a numerical solution for the special case of stepped columns on simple supports. The following presents a procedure for any variation in shape and for simple and fixed supports.

These procedures are in tabular form, rather than as computer programs, since this gives a better understanding of what is being done. The procedures are, of course easily programmable for solution by computer. As before, the critical load is determined by successive trials, which means successive tables of calculations. Example problems illustrate the procedures.*

The basic procedure uses the method of discrete elastic weights (also called "Mohr's Method" and the "Conjugate Beam Method") to replace the M/EI diagram and calculate deflections and is due to Newmark, Ref. 6. The formulas for the elastic weights are discussed in Ref. 4.

Simply Supported Columns

Referring to Fig.C2.20d and Table C2.5, the procedure is as follows:

1. Divide the column into several equal length segments, S, at least five or six segments, but ten or more will give a more accurate value of P_{cr}.
2. Assume (sketch) an initial buckled (deflected) shape. Any initial shape will do (even two straight lines), but the more realistic it is the sooner the effort will be completed.
3. At the station in (2) above which has the largest deflection, y, let its deflection be taken as 1", and let the deflections at the other stations be proportional to this (per the sketch).
4. Let P be one lb. Then at any station, n, the bending moment will be M_n = P_{y_n} = y_n, so the values in (3) above are entered in Col. 2. Positive deflections are upward and positive bending moments produce compression in the upper surface, hence the minus sign used in the headings for Col. 2 and 4.
5. At each station enter the value of EI in Col. 3. If there is a "step" in EI an adjustment is made to EI at the station nearest to the step, discussed later, and its EI is "flagged" with an asterisk to indicate this adjustment.

* These (and other) tables are easily programmed for rapid solution by computer or suitable calculators.

* To check for stability under a given load, P, use that load. If 6_N < -6_{N-1} the column is stable, and vice-versa. A similar check can be made with the formulas.

Tapered portions can be subdivided into several stepped portions

6. The "equivalent concentrated elastic loads" ("elastic weights") are then calculated per the formulas below the table for each station and are entered in Col. 5. These formulas are discussed in Ref. 4.
7. The tabular operations are then carried out as shown, and a range of P_{cr} values is obtained in Col. 10. If the axial load is below this range the column is stable, and if above it the column is unstable. An average value for P_{cr} is calculated as shown: 44,150 lbs. Note that several checks are made to detect any errors made after the Col. 5 data are calculated. Column 9 (and 8) defines a new shape which will be different from that assumed in Col. 2.
8. Using the deflections in Col. 9 or in Col. 8, let the largest of these be one inch and get the others by dividing their deflections by the largest deflection. Enter these in a second table's Col. 2 and complete the table.
9. Repeat (8) as needed until the range of P_{cr} values is quite small, and P_{cr} can then be taken as the average of the values in Col. 10.

10. If at any station F_{cr} ($= P_{cr}/A$) is significantly above the proportional limit stress (or above any local buckling stress), the value of E_t (or E_{eff}) used in the term EI must correspond to F_{cr} (or to the local buckling stress), which can require more successive trial tabular calculations (Art. C2.16).

Tables C2.5 through C2.7 illustrate the procedure. Three or four tables are usually sufficient. For the example shown $P_{cr} = 45000$ lbs per Table C2.7, (actually between 44200 and 45900 lbs). If the applied load were less than 39300 the column would be known to be stable after only the first table. Or, if more than 47600 it would be known to be unstable, without further effort. Using ten segments instead of five results in a more accurate value of $P_{cr} = 44200$ lbs. The values of E_t and of E_{eff} at any stress level are obtained as discussed in Art. C2.16.

Adjustment for a Step in EI

Referring to Fig. C2.20e, this is done to keep the tabular operations simple.



Fig.C2.20e Adjustment for a Step Geometry

- Let the station nearest to the step be "n" and that on the other side of the step be "m".

2. Calculate

$$EI_{av} = 2 \left(\frac{E_n I_n \times E_m I_m}{E_n I_n + E_m I_m} \right)$$

3. Calculate

$$R = EI_{av} - E_n I_n$$

4. Calculate

$$(E_n I_n)_{eff} = E_n I_n + (1-2a/S)R$$

- Use $(E_n I_n)_{eff}$ in Column 3 for station n. Note that if the step is midway between n and m, $(E_n I_n)_{eff} = E_n I_n$ so no adjustment is necessary. If $a = 0$ then $(E_n I_n)_{eff} = EI_{av}$.

Example

For the column in Fig. C2.20d station 3 is nearest to the step, which is between stations 3 and 4, $a = 3.8$ " and $S = 9.4$ ". Therefore, EI at station 3 is adjusted as follows where $n = 3$ and $m = 4$ in the above formulas. $E = 10.5 \times 10^7$.

$$1. n = 3 \text{ and } m = 4$$

$$2. EI_{av} = 2 \left(\frac{1.5(10^7) \times .5(10^7)}{1.5(10^7) + .5(10^7)} \right) = .75 \times 10^7$$

$$3. R = .75(10^7) - 1.5(10^7) = -.75(10^7)$$

$$4. E_n I_{3,eff}$$

$$= 1.5(10^7) + (1-2 \times 3.8/9.4)(-.75)(10^7)$$

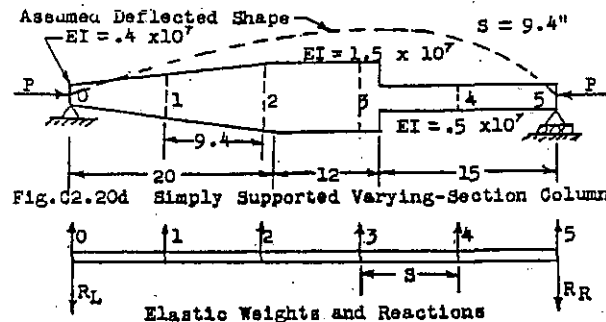
$$= \underline{\underline{1.36 \times 10^7}}$$

- Therefore 1.36×10^7 is entered in Table C2.5 for EI at station 3.

Column Fixed at the Left End

The following procedure is used for a column fully fixed at its left end. If the right end is fixed, rotate the column so that it becomes the left end. The procedure is the same as before except that a longer table is needed to account for the fixed end moments at the left end. The table is shown as Table C2.8.

The data in the table are for the member shown in Fig. C2.20d except that the left end is fully fixed. Therefore,



$$N = \text{No. of Segments} = 5$$

$$S = \text{Length of Segment} = 9.4$$

Table C2.5 Determination of PCR (First Trial)

$$\frac{S^3}{12} = 7.36$$

(1)	(2)	(3)	(4)	(5)	(6)	(7)	(8)	(9)	(10)
Sta.	M = -P _y	EI	-M _Q /EI	Eq. Conc.* El. Loads	Mom. of Loads	Unit Slope	Unit Def.	True Def.	PCR
n	Data	Data	- (2)/(3)	(4) in Eqs.	(5) x (1)	R _L - Σ (5) _n	Σ (7) _n	(8) x S ² /12	- (2)/(9)
	P = 1#	x 10 ⁻⁷	x 10 ⁻⁷	x 10 ⁻⁷	x 10 ⁻⁷	x 10 ⁻⁷	x 10 ⁻⁷	x 10 ⁻⁷	
0	0	.40	0	1.03	0		0	0	
1	-.40	.92	.435	4.91	4.91	15.17	15.17	101.7	39,300
2	-.80	1.43	.559	6.76	13.52	10.26	25.43	187	42,800
3	-1.00	1.36**	.736	9.59	28.77	3.50	28.93	213	46,900
4	-.80	.50	1.600	16.73	66.92	-6.09	22.84	168	47,600
5	0	.50	0	4.43	22.15	-22.82	.02	0	

*See formulas below

$$\Sigma = 43.45 \quad 136.27$$

$$4 | 176,600$$

**Adjusted for step

$$PCR_{AV} = 44,150$$

$$R_R = \frac{\Sigma (6)}{N} = \frac{136.27}{5} = 27.25$$

$$R_L = \Sigma (5) - R_R = 43.45 - 27.25 = 16.20$$

CHECKS:

$$(7)_{N-1} + (5)_N = R_R$$

$$(8)_N = 0$$

EQUIV. CONC. EL. LOADS OF COL. (5)

a) At Ends, Sta. 0 & N,

$$(5)_0 = 3.5 \times (4)_0 + 3.0 \times (4)_1 - .5 \times (4)_2$$

$$(5)_N = 3.5 \times (4)_N + 3.0 \times (4)_{N-1} - .5 \times (4)_{N-2}$$

b) At Other Stations, n,

$$(5)_n = (4)_{n-1} + 10 \times (4)_n + (4)_{n+1}$$

True slope = Unit slope x S/12

Slope at left end = R_L x S/12Slope at right end = R_R x S/12Beam Sign Convention

- (+) Loads act upward
- (+) Reactions act downward
- (+) Deflections are upward
- (+) Slope is up to the right
- (+) M puts top in compression
- (+) Axial load is compression

The development of the calculation tables is shown in Ref. 4

NUMERICAL COLUMN ANALYSIS

Table C2.6 Determination of P_{cr} (Second Trial)

$N = \text{No. of Segments} = 5$
 $S = \text{Length of Segment} = 9.4"$

(1)	(2)	(3)	(4)	(5)	(6)	(7)	(8)	(9)	(10)
Sta.	$M = -P_y$	EI	$\frac{M_Q}{EI}$	Eq. Conc.* EI , Loads	Mom. of Loads	Unit Slope	Unit Def.	True Def.	P_{CR}
n	Data	Data	$-(2)/(3)$	(4) in Eqs.	$(5) \times (1)$	$R_L - \sum (5)_n$	$\sum (7)_n$	$(8) \times S^3/12$	$-(2)/(9)$
	$P = 1#$	$\times 10^{-7}$	$\times 10^{-7}$	$\times 10^{-7}$	$\times 10^{-7}$	$\times 10^{-7}$	$\times 10^{-7}$	$\times 10^{-7}$	
0	0	.40	0	1.25	0		0	0	
1	-.478	.92	.519	5.80	5.80	16.14	16.41	121	39,500
2	-.879	1.43	.613	7.29	14.58	10.34	26.75	197	44,600
3	-1.000	1.36**	.736	9.55	28.65	3.05	29.80	219	45,700
4	-.790	.50	1.580	16.54	66.16	-6.50	23.30	171	45,200
5	0	.50	0	4.37	21.85	-23.04	26	0	

* Use applicable formula $\Sigma = 44.80$

** Adjusted for step

$$R_R = \frac{\Sigma (6)}{N} = \frac{137.04}{5} = 27.41$$

$$R_L = \Sigma (5) - R_R = 44.60 - 27.41 = 17.39$$

Table C2.7 Results of Third Table of Calculations

Station	0	1	2	3	4	5
P_y	0	-.553	-.900	-1.000	-.781	0
P_{cr}	-	44200	44700	45200	45900	-

when sketching the assumed initial buckled shape its slope at the left end should be zero, to be realistic. The unit values (due to the left end fixity) in

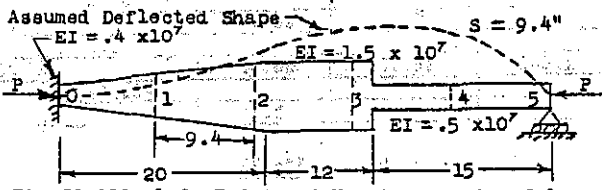
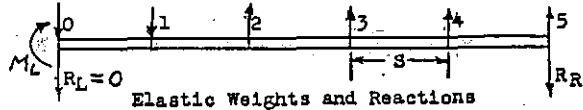


Fig. C2.20f Left End Fixed Varying-Section Column



Elastic Weights and Reactions

Table C2.8 Determination of P_{cr} (First Trial)

(1)	(2)	(3)	(4)	(5)	(6)	(7)	(8)	(9)	(10)	(11)	(12)	(13)	(14)	(15)	P_{CR}
Sta.	$M = -P_y$	M_ML	EI	$-M/EI$	$-M_L/EI$	Eq. Conc.* Loads	Eq. Conc. Loads	Mom. of (7)	Mom. of (8)	M_L Loads	Total Loads	Unit Slope	Unit Def.	True Def.	P_{CR}
n	Data	Unit	Data	$-(2)/(4)$	$-(3)/(4)$	(5) in Eqs.	(6) in Eqs.	(7) $[N-1]$	(8) $[N-1]$	(8) $\times M_L$	(7) + (11)	$-\Sigma (12)$	$\Sigma (13)$	$(14) \times S^3/12$	$-(2)/(15)$
				$\times 10^{-7}$	$\times 10^{-7}$	$\times 10^{-7}$	$\times 10^{-7}$	$\times 10^{-7}$	$\times 10^{-7}$	$\times 10^{-7}$	$\times 10^{-7}$	$\times 10^{-7}$	$\times 10^{-7}$		
0	0	1.0	.40	0	-2.30	.43	-11.15	2.17	55.75	-5.64	-5.20	5.20	0	0	
1	-.20	.8	.92	.218	-.87	2.60	-11.62	10.40	-46.48	-5.88	-3.28	5.20	38.3	52,100	
2	-.60	.6	1.43	.420	-.42	5.15	-5.36	15.45	-16.08	-2.71	2.44	6.48	101	59,300	
3	-1.00	.4	1.36**	.735	-.29	9.57	-3.72	19.14	-7.44	-1.88	7.69	6.04	19.72	145	69,000
4	-.90	.2	.50	1.800	-.40	18.74	-4.29	18.74	-4.29	-2.17	16.57	-1.65	18.07	133	67,600
5	0	0	.50	0	0	5.03	-1.04	0	0	-0.52	4.51	-0.15	0		

$$\Sigma = 41.52$$

$$65.90 \quad -130.04 \quad -18.80 \quad 22.73$$

$$4 | 248,000$$

$$ML = \frac{-\Sigma (9)}{\Sigma (10)} = \frac{-65.90}{-130.04} = 506$$

$$P_{CRAV} = 62,000$$

$$R_L = 0 \quad R_R = \sum (12)$$

$$\text{CHECKS: } \Sigma (7) + \Sigma (11) = \Sigma (12); (15) N-1 - (12) N = -\Sigma (12); (14) N = 0$$

$$41.52 - 18.80 = 22.73; -18.22 - 4.51 = -22.73; -.15 \approx 0$$

Note that Mom. of (7) (and (8)) is calculated differently for this case (about the right end),

Table C2.9 Determination of Pcr (Second Trial)

(1)	(2)	(3)	(4)	(5)	(6)	(7)	(8)	(9)	(10)	(11)	(12)	(13)	(14)	(15)	(16)
Sta.	M =	M_{ML}	EI	$-M/EI$	$-M_L/EI$	Eq. Conc. Loads	Eq. Conc. Loads	Mom. of (7)	Mom. of (9)	M_L Loads	Total Loads	Unit Slope	Unit Def.	True Def.	P _{CR}
				$\times 10^7$	$\times 10^7$	$\times 10^7$	$\times 10^7$	$\times 10^7$	$\times 10^7$	$\times 10^7$	$\times 10^7$	$\times 10^7$	$\times 10^7$	$\times 10^7$	
0	0	1.0	.40	0	-2.50	.60	-11.15	3.00	-55.75	-6.20	-5.60	0	5.60	0	
1	-.26	.8	.92	.28	-.87	3.29	-11.62	13.16	-46.78	-6.46	-3.17	5.60	41.2	63,100	
2	-.70	.6	1.43	.49	-.42	5.91	-5.36	17.73	-16.08	-2.98	2.93	8.77	14.37	105.7	66,200
3	-1.00	.4	1.36 ^{**}	.73	-.29	9.63	-3.72	19.26	-7.44	-2.07	7.56	5.84	20.21	148.7	67,200
4	-.92	.2	.50	1.84	-.40	19.13	-4.29	19.13	-4.29	-2.39	16.74	-1.72	18.49	136.1	67,600
5	0	0	.50	0	0	5.16	-1.04	0	0	-58	4.58	-18.46	.03	0	

* See Table C2.5

$$\Sigma = 43.72 \quad 72.28 \quad -130.04 \quad -20.68 \quad 23.04$$

$$** M_L = \frac{\Sigma (9)}{\Sigma (10)} = \frac{-72.28}{-130.04} = .556$$

Make same checks as before

$$P_{CRAV.} = \underline{\underline{66.025}}$$

Columns 3, 6, 8, and 10 do not change in successive tables. For any station, n, the entry in column 3 is $1 - n/N$ where N is the number of segments used. Hence, these decrease uniformly from 1.0 for station 0 to zero for station N. Columns 1 through 10 are completed, then M_L is calculated as shown and the rest of the table is completed. For the member in Fig. C2.20f using five segments P_{cr} is found to be 66025 after two tables are completed. A third table would reduce the spread in the Col. 16 values for P_{cr} .

Column Fixed at Each End

The procedure is the same as for the previous left end fixed case except that additional columns are needed to account for the fixed right end. The initial assumed buckled shape should be sketched in with zero slope at each end to be realistic. Table C2.10 shows the procedure.

The values entered in Col. 3, 4, 7, 8, 10, 11, 13 & 14 do not change in successive tables. For any station, n, the entry in Column 4 is n/N , where N is the number of segments used. Hence, these entries increase uniformly from zero at station 0 to 1.0 at station N. Columns 1 through 14 are completed; then M_L and M_R are calculated and the rest of the table is completed. Using five segments the buckling load, P_{cr} , is found to be 172250 lbs after two tables are completed. More tables would give more accuracy. The suggested checks should be made to detect any errors made after Column 11.

These tables, with a minor change, are also used to determine the bending moments in beam-columns with a varying EI as discussed in Art. C3.18. The value of P_{cr} for the member as a column can also be calculated as shown in Table C3.6*.

* See footnote on p.14.

Other Uses of the Tables

For a complete discussion of the tabular method development, the "equiv-concentrated elastic loads" and additional examples see Ref. 4 (described in Art. A18.27a) which also discusses the following applications.

1. Axial loads between the ends
2. A column consisting of two pieces connected by a torsion spring (which could also be a splice).
3. Multispan columns having one or more spans of a varying EI
4. Free-ended columns having a varying EI
5. The numerical determination of carry-over factors and stiffness factors
6. Multispan columns on elastic supports which may be present as either discrete isolated supports or another beam or column.

C2.6 Columns Having an Initial Bent Shape

When a column has an initially bent shape as in Fig. C2.40 the axial load will generate a bending moment along the column in the amount $M = Py$, where y is the deflection of the bent shape at any station. The column may be uniform or it may have a varying EI.

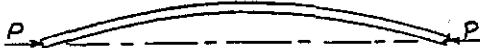


Fig.C2.40 Column With Initial Bent Shape

Therefore, the column is actually a beam-column, as discussed in Art. C3.18, Beam-Columns Having an Initially Bent Shape" except that there are no trans-

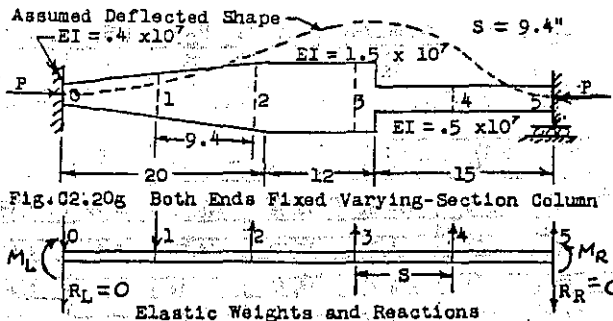


Table C2.10 Determination of P_{cr} (First Trial)

$$N = \text{No. of Segments} = 5$$

$$S = \text{Length of Segment} = 9.4^{\prime \prime}$$

①	②	③	④	⑤	⑥	⑦	⑧	⑨	⑩	⑪	⑫	⑬	⑭	⑮	⑯	⑰	⑱	⑲	⑳	㉑
Sta	Mo-Py	MML	MMR	EI	-M EI	-ML EI	-MR EI	Equiv. Conc. Loads	Equiv. Conc. Loads	Mom. of ⑨	Mom. of ⑩	Mom. of ⑪	⑩ x ML	⑪ x MR	Total Loads	Unit Slope	Unit Def.	True Def.	FCR	
n	Data	Unit	Unit	Data	- $\frac{2}{5}$	- $\frac{3}{5}$	- $\frac{4}{5}$	6 in Eqs.	7 in Eqs.	8 in Eqs.	9 x 1	10 x 1	11 x 1	10 x ML	11 x MR	$\frac{9+13}{16}$	- $\Sigma 17$	$\Sigma 18$	$19 \times S^2/12$	$(2)/20$
					$\times 10^7$	$\times 10^7$	$\times 10^7$	$\times 10^7$	$\times 10^7$	$\times 10^7$	$\times 10^7$	$\times 10^7$	$\times 10^7$	$\times 10^7$	$\times 10^7$	$\times 10^7$	$\times 10^7$	$\times 10^7$	$\times 10^7$	
0	0	1.0	0	:40	0	-2.50	0	.73	-11.15	.51	0	0	0	-3.20	.26	-2.73	0	0	-	
1	-.3	.8	.2	.92	.326	-.87	-.217	3.75	-11.62	2.45	3.75	-11.62	2.45	-3.33	-1.26	-.84	2.73	2.73	20.09	149,000
2	-.7	.6	.4	1.43	.489	-.42	-.279	3.95	5.35	-3.45	11.90	-10.70	-6.90	-1.54	-1.77	2.64	3.51	6.30	46.37	151,000
3	-1.0	.4	.6	1.36	.735	-.29	-.441	8.84	-3.76	6.29	26.52	-11.26	-18.87	-1.08	-3.23	4.51	7.23	53.21	128,000	
4	-.5	.2	.8	.50	1.000	-.40	-1.600	10.74	-4.29	-18.44	42.96	-17.16	-73.76	-1.23	-9.48	.03	3.63	26.72	122,000	
5	0	0	1.0	.50	0	0	-2.000	2.63	-1.05	-11.58	13.15	-5.25	-57.90	-.30	-5.95	-3.62	0	0	-	

$$\Sigma = 32.64 - 37.22 - 42.72 \cdot 98.28 - 56.01 - 159.88 - 10.68 - 21.95 - .01 \quad | 670.000$$

$$\Sigma(12) - \Sigma(9) \times \frac{\Sigma(14)}{\Sigma(11)} \quad \Sigma(12) - 2(9) \times \frac{\Sigma(13)}{\Sigma(10)} \quad \text{CHECKS: } 0 = L(9) + M_L \times \Sigma(10) + M_R \times \Sigma(11); \quad PCRAY. 157.500$$

$$M_L = \frac{\Sigma(10) \times \frac{\Sigma(11)}{\Sigma(10)} - L(13)}{L(10)} = .287 \quad M_R = \frac{\Sigma(11) \times \frac{\Sigma(13)}{\Sigma(10)} - L(14)}{\Sigma(10)} = .514 \quad 0 = \Sigma(9) + \Sigma(13) + \Sigma(16); \quad 0 = \Sigma(17); \quad 0 = 32.64 - (-10.68) + (-21.95); \quad 0 = -.01$$

$$0 = \frac{16}{15} N^{-1} - \frac{17}{15} N; \quad 0 = \frac{19}{15} N^{-1}; \quad 0 = \frac{18}{15} N^{-1} - \frac{17}{15} N; \quad 0 = \frac{19}{15} N^{-1}$$

$$0 = 1.62 - (-1.52); \quad 0 = 0$$

* See Table C2-5

*, ** See Table C2.5

Table C2.11 Determination of P_{cr} (Second Trial)

①	②	③	④	⑤	⑥	⑦	⑧	⑨	⑩	⑪	⑫	⑬	⑭	⑮	⑯	⑰	⑱	⑲	㉑	
n	Data	Unit	Unit	Data	- $\frac{2}{5}$	- $\frac{3}{5}$	- $\frac{4}{5}$	6 in Eqs.	7 in Eqs.	8 in Eqs.	9 x 1	10 x 1	11 x 1	10 x M _L	11 x M _R	9 + 15 - 16	12 + 17	13 + 18	14 + 19	15 + 20
0	0	1.0	0	.40	0	-2.50	0	.93	-11.15	-5.51	0	0	0	-3.94	-2.26	-3.27	3.21	0	0	
1	-.38	.8	.2	.92	.410	-.81	.217	4.72	-11.62	2.45	4.72	-11.62	2.45	-4.11	-1.26	-.55	3.27	24.04	118,000	
2	-.87	.6	.4	1.43	.610	-.42	.279	7.24	-5.35	3.45	14.98	-10.70	-6.90	-1.89	-1.71	3.58	7.19	52.90	165,000	
3	-1.00	.4	.6	1.33	.730	-.29	-.441	8.91	-3.76	6.29	26.73	-11.28	-18.87	-1.33	-3.23	4.23	7.53	55.40	180,000	
4	-.50	.2	.8	.50	1.000	-.40	-1.600	10.73	-4.29	-18.44	42.92	-17.16	-73.76	-1.52	-9.48	-.27	3.64	26.80	185,000	
5	0	0	1.0	.50	0	0	-2.000	2.84	-1.05	-11.58	13.30	-5.25	-57.90	-3.37	-5.95	-3.68	.02	0	—	

verse loads and their initial bending moments, Mo. Thus, the column would be analyzed as discussed there using an equivalent transverse loading such as that in Fig.C3.33 or thereabouts.

Actually, no column is perfectly straight although this is assumed in using the numerous buckling load formulas and data for P_{cr} . Because of this many analysts and designers maintain a small positive margin of safety when the mar-

gin is based on using Poco

Therefore, an alternative approach is to assume an initial bent shape having a "bow" of $L/800$ inches or thereabouts, or of what the drawing specifies such as "straight within X inches" where X is usually on the order of $L/800$ or so. X is actually a tolerance for deviation from straightness of $\pm X$ inches, so the mean would be $\mp X/2$ and this would be used to show a zero or positive margin of safety.

Then a check is made using X to be sure that there is not a negative margin of safety greater than $-.15$ or $-.25$ (per Art.C1.13b). Sometimes X , rather than $X/2$, is used to show a positive margin, which is a conservative procedure. In any case a beam-column analysis is made.

C2.7a Design Column Curves for Columns with Non-Uniform Cross-Sections

For columns with other steps the procedures in Art.C2.6a are used. For columns whose taper does not meet the requirements of Fig. C2.23 or C2.24 either a conservative assumption (adjustment) for the taper must be used or a numerical analysis as in Art. C2.6b is required.

C2.8a Column Fixity Coefficients C for Use with Columns with Elastic Side Restraints and Known End Bending Restraints

Fig.C2.25a and C2.26a provide the envelopes (for $q = \infty$) for Fig.C2.25 and C2.26.

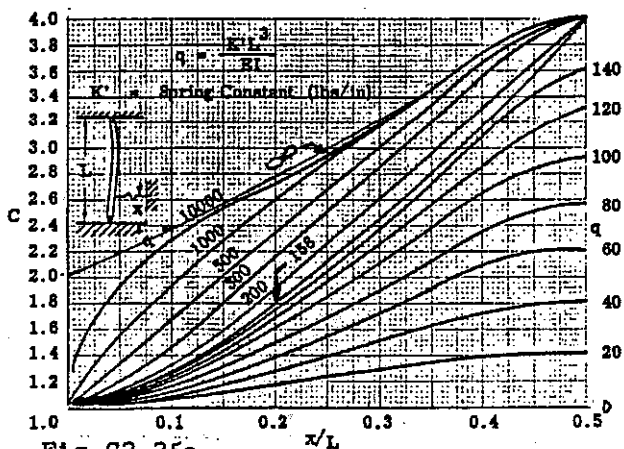


Fig.C2.25a

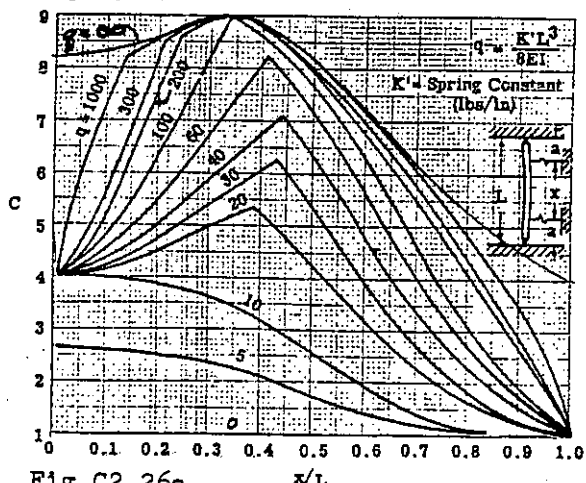


Fig.C2.26a

C2.10a Solution Without Using Column Curves

The inside scales for Fig. C2.17 are not shown in the textbook. Fig.C2.17a shows the inside scales for the ordinate and for the abscissa.

It must be understood that, like a column curve, Fig.C2.17 (and C2.17a) cannot be used when determining the critical load requires using a parameter which is also a function of E . This occurs, for example, with Fig.C2.25, C2.26, C2.27 (and C2.27a) where the parameter C is a function of E . This also occurs for other such data. In these cases a successive trials procedure must be used (as in Art.C2.12, Case 2 Inelastic Failure, Portion 2). That is, the value of E used in determining P_{cr} per the figures must also be the value of E corresponding to $F_{cr} = P_{cr}/A$ when the stress is in the plastic range (E is E_t) or when local instability is present (E is E_{eff}). E_t and E_{eff} are discussed in Art.C2.16.

C2.13a Column Strength With Known End Restraining Moments

Fig.C2.27a is much more useful than Fig.C2.27 since it provides curves for numerous values of k and k_1 , where the symbol "k" is "u" in Fig.C2.27 and in Art C2.12. The curves can be obtained by using the moment distribution procedure.

Referring to the example shown for Fig.C2.34, for each of the restraining members, AC, AE and AF the value of k is calculated as $k = 4SC(EI)/L$ where SC is obtained as C in Fig.All.47, conservatively using the "far end pinned" curves, for tension or compression in the member. The total restraint at end A of the member AB will then be

$$k_A = k_{AC} + k_{AE} + k_{AF}$$

The same thing would be done at end B for members BF, BG and BD to obtain k_B . Then having the values of k P_{cr} for member AB is obtained by using Fig.C2.27a. Note in Fig.All.47 when L/j exceeds π for compression members C becomes negative for the pinned end case.

This procedure is more accurate than that in Art.C2.13, but it is still an approximate one. For more exactness the procedure discussed in Art.All.15b should be used. Many trusses are designed assuming pinned joints which is generally conservative as discussed in All.15b.

NON-DIMENSIONAL DATA FOR COLUMNS

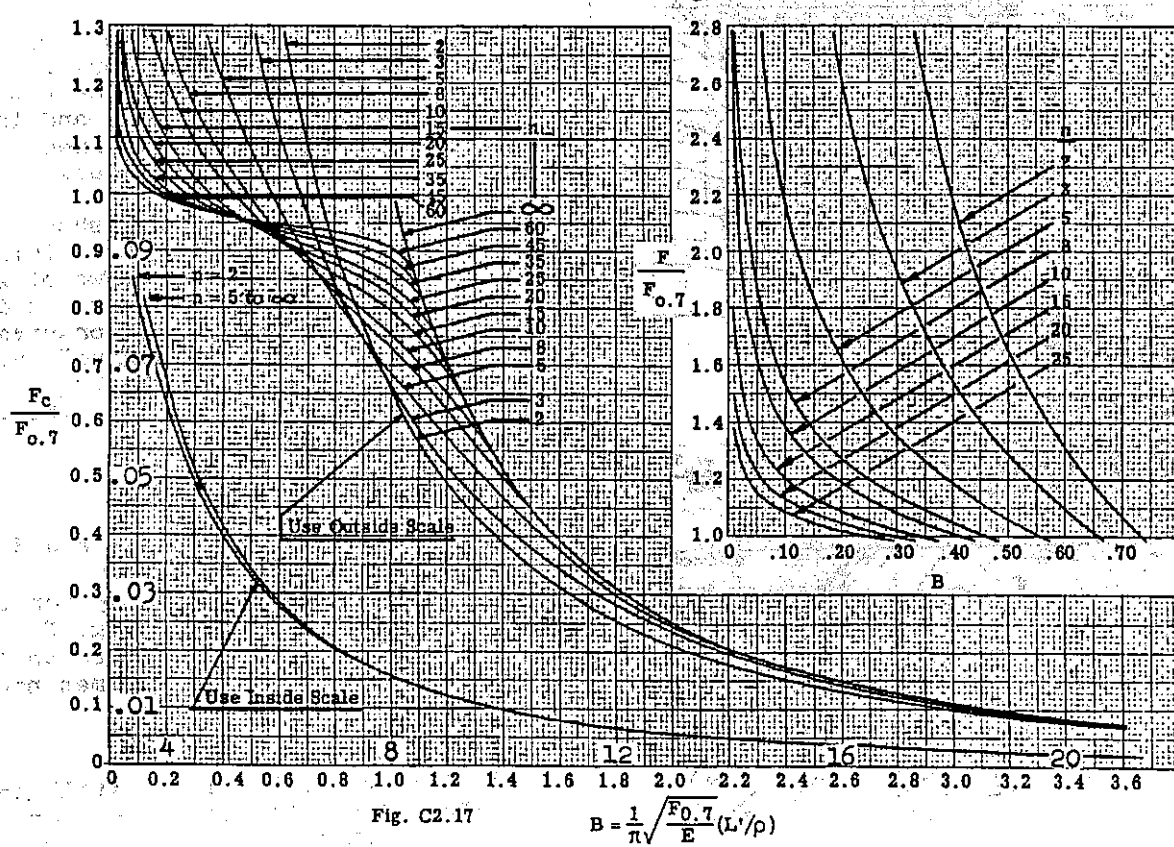
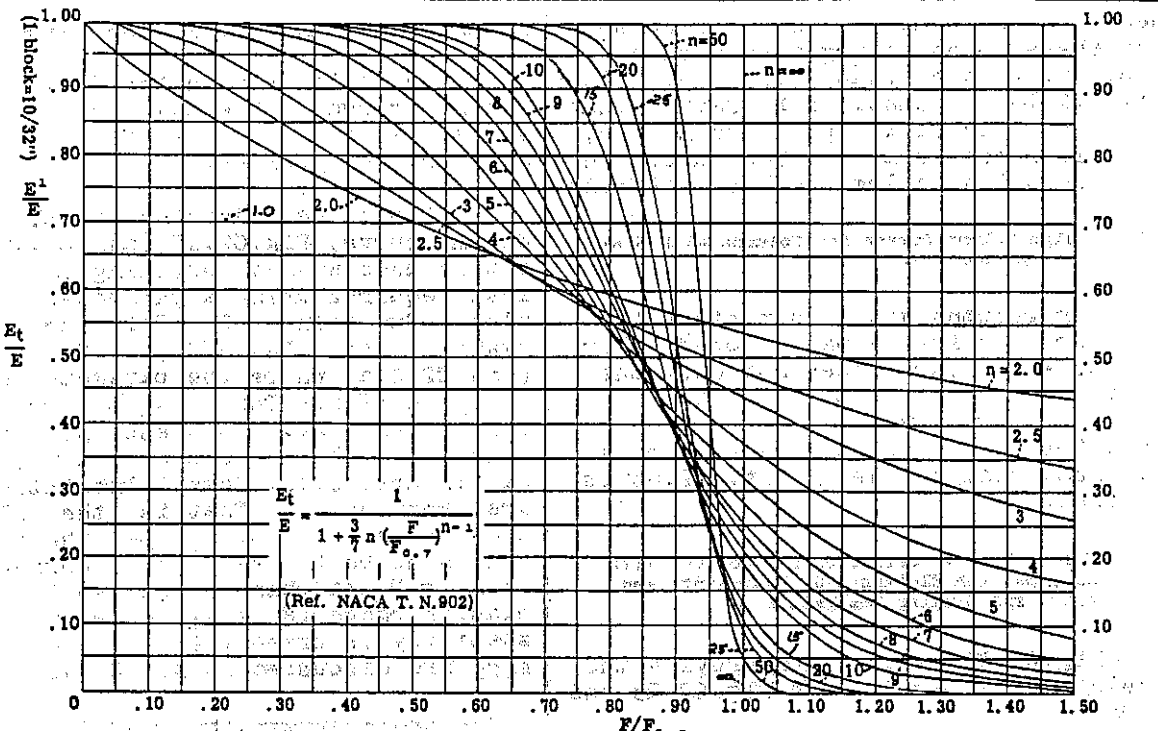


Fig. C2.17a Non-Dimensional Column Curves

B is also $\sqrt{F_{0.7}/F_{cr}}$ where $F_{cr} = \pi^2 E / (L/\rho)^2$, E being Youngs Modulus (not E_t)

Example Problem

Proceeding as discussed, recalculate F_{cr} for member AB of Fig.C2.34 assuming that the loads in the restraining members at ends A and B are due to an applied upward load of 3,000 lbs at joint D, reacted at A and B. The following table shows the calculations for k at ends A and B.

Table C2.12 Generation of Stiffness Factors, k

Member	Load	$EI \times 10^{-4}$	J	L	L/J	SG	$k = 4SCEI/L$
AC	9000C	1.121	11.16	30.0	2.69	.30	448,000)
AE	4243T	.805	13.77	42.4	3.08	1.13	858,000) $\Sigma=1,984,000$
AF	3000C	.697	15.24	30.0	1.97	.73	678,000) $=k_A$
BD	3000C	1.121	19.33	30.0	1.55	.62	927,000)
BF	4243T	.805	13.77	42.4	3.08	1.13	858,000) $\Sigma=2,463,000$
BG	3000C	.697	15.24	30.0	1.97	.73	678,000) $=k_B$

Using Fig.C2.27a, $k_1 = k_B$ (the larger k) and $k = k_A$.

$k_1 L/EI = 246300(30)/1,121,000 = 6.59$ so $k/k_1 = .80$ and C is obtained from Fig. C2.27a as 2.2.

For this member $D/t = 1.25/.058 = 21.6$ and per Fig.C4.9 its crushing (crippling) strength is quite high, 67500 psi. Therefore, the column curve of Fig.C2.3 for RT can be used without modification. For member AB

$$\begin{aligned} L' &= L/\sqrt{C} = 30/\sqrt{2.2} = 20.2 \\ L/\rho &= 20.2/.422 = 47.9 \end{aligned}$$

Then, per the column curve, for member AB $F_{cr} = 53,000$. This is slightly less than obtained per the Art.C2.13 procedure.

If pinned ends were assumed for all joints then $C = 1.0$, $L/\rho = 30/.422 = 71.1$ and $F_{cr} = 43,000$ (too small), but words about bending failure in Art.A11.15b also applies here. If the truss has members subject to local instability see Art. C2.16. Also if the members' b/t were large, say 9 or more, and of open section, torsional buckling might be critical (Art.C7.31).

C2.16 The Use of E_t and E_{eff} The Tangent Modulus, E_t

As the axial stress in a column becomes increasingly greater than the proportional limit stress, the tangent modulus which is the slope of the stress-strain curve becomes successively smaller. This reduction in E_t is shown in Fig.B1.5 (the curves on the right being E_t) and also in the following sketch,

As discussed in Art.A18.8, Shanley

has shown and experimental data has verified (Fig.A18.11 and A18.12) that the use of E_t is justified for determining the buckling stress of columns. It is also used for beam-columns having significant axial stresses. Hence, the use of E_t in Art.C2.1 and subsequent articles is understood.

However it must be understood that E_t is applicable only for columns of stable cross-sections (reasonably thick flanges etc.). That is, there must be no flange having a local buckling stress smaller than the column's buckling stress

If there is then E_t does not apply and an "effective" modulus, E_{eff} , must be used instead. It is smaller than E_t at any L/ρ value.

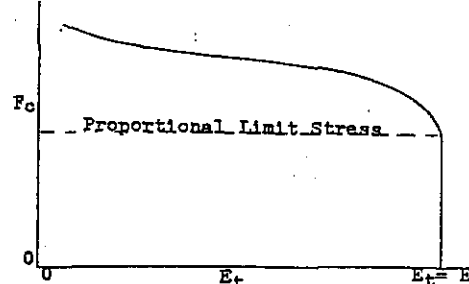
The Effective Modulus, E_{eff}

When any flange has a local buckling stress smaller than F_{cr} for the column, assuming a stable cross-section, an "effective" value for E, E_{eff} , must be used. E_{eff} is obtained as follows.

A column curve is constructed as discussed in Art.C7.25 and illustrated in Art.C7.26. Method 1 there is the most frequently used, followed by Method 2. Having this adjusted column curve which accounts for the reducing effect of local instability, F_{cr} can be obtained for any value of L/ρ .

However, when the buckling stress is determined for other than the above simple case it is necessary to use E_{eff} which can be gotten as follows. For any value of F_{cr} the value of L/ρ is obtained from the column curve and E_{eff} is calculated as

$$E_{eff} = F_{cr}(L/\rho)^2/\pi^2$$



It is for cases where F_{cr} is determined using a "constant" which is a function of E that E_{eff} must be determined and used. Examples of such cases are Fig.C2.25, C2.26, C2.27, C2.41 etc. In these cases a successive trials procedure is needed

(just as would be if E_t were applicable). That is, one assumes a value for E_{eff} , determines F_{cr} and then determines the value of E_{eff} corresponding to this F_{cr} per the above formula. If it is not the same (essentially) as the assumed E_{eff} another value for E_{eff} is assumed and the procedure is repeated. This is repeated as necessary until the assumed value is essentially the value corresponding to F_{cr} . This procedure is similar to that required when using E_t as discussed in Art.C2.10a. E_{eff} is not used with beam-columns (only E_t is) since the beam-column allowable stress considers any local buckling effect when Method 2 therein is used. However, with Method 1 E_{eff} would be used when local instability is present. see Art.C3.18.

c2.17 Additional Buckling Load Data

This article provides additional buckling load data for various types of columns. It is generally self-explanatory.

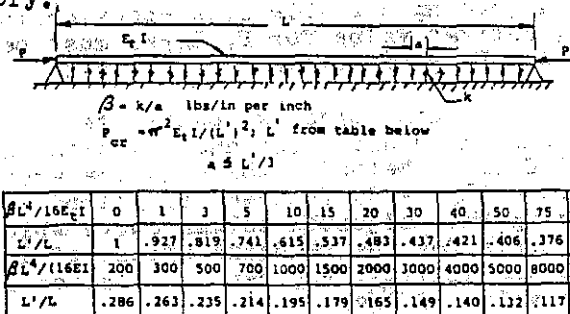


Fig.C2.41 Column On Elastic Foundation

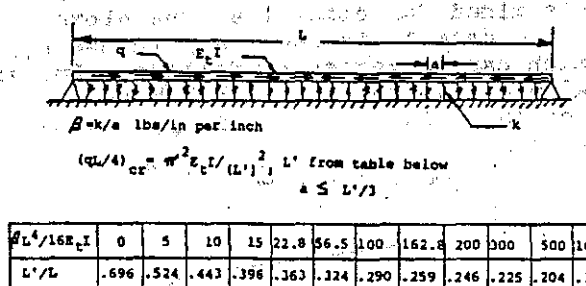


Fig.C2.42 Column On Elastic Foundation With a Distributed Axial Load



Fig. C2.43 Column With Intermediate Load

Note that the intermediate load, P_2 , in Fig.C2.43 must be located at the step, if one exists.* The buckling equation is

* See "Formulas for Stress and Strain", Roark and Young, 5th Edition, for rapid solution for numerous cases and end conditions.

$$\frac{k_4^2}{k_1^2} - \frac{k_1^2 L + k_4^2 L_1}{k_1^2 \tan k_1 L_1} = \frac{k_2^2}{k_3^2} + \frac{k_3^2 L - k_2^2 L_2}{k_3^2 \tan k_3 L_2}$$

where $k_1^2 = \frac{P_1}{EI_1}$ $k_2^2 = \frac{P_2}{EI_2}$ $k_3^2 = \frac{P_1 + P_2}{EI_2}$ $k_4^2 = \frac{P_2}{EI_1}$

The critical load combination, called P_1 and P_2 must be in the same ratio as the applied loads P_1 and P_2 and are found as follows. For the given loads calculate $a = P_1/P_2$. Assume P_2 is P_2 and per the formulas find by successive trials the value of P_1 which satisfies

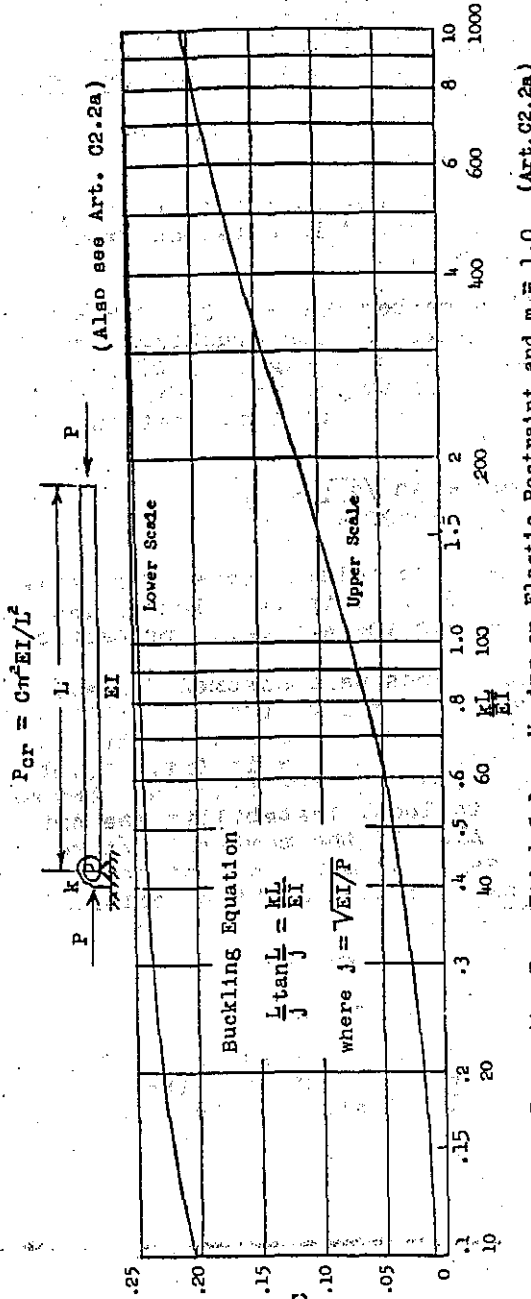


Fig.C2.44 Free-Ended Column Having an Elastic Restraint and $m = 1.0$ (Art.C2.2a)

the equation and then calculate $a' = P_1'/P_2'$. If $a' \neq a$ assume a different value of P_2' , calling it P_2'' , and repeat. Repeat as necessary until $a' = a$. P_1' and P_2' are then the critical load combination.** The margin of safety is then

$$M.S. = P_1'/P_1 - 1.0 \quad (\text{or } P_2'/P_2 - 1.0)$$

If F_{cr} is in the plastic range for either

$$P_{cr} = C\pi^2 EI/L^2$$

portion then the value of E_t must be used, and the value of E_t corresponding to F_{cr} must be the same, essentially, as the value used in calculating it. (successive trials). If local instability is present E_{eff} would be used instead of E_t . The procedure is, of course, much simpler for the special case where there is no step ($EI_1 = EI_2$), or when $P_2 = 0$.

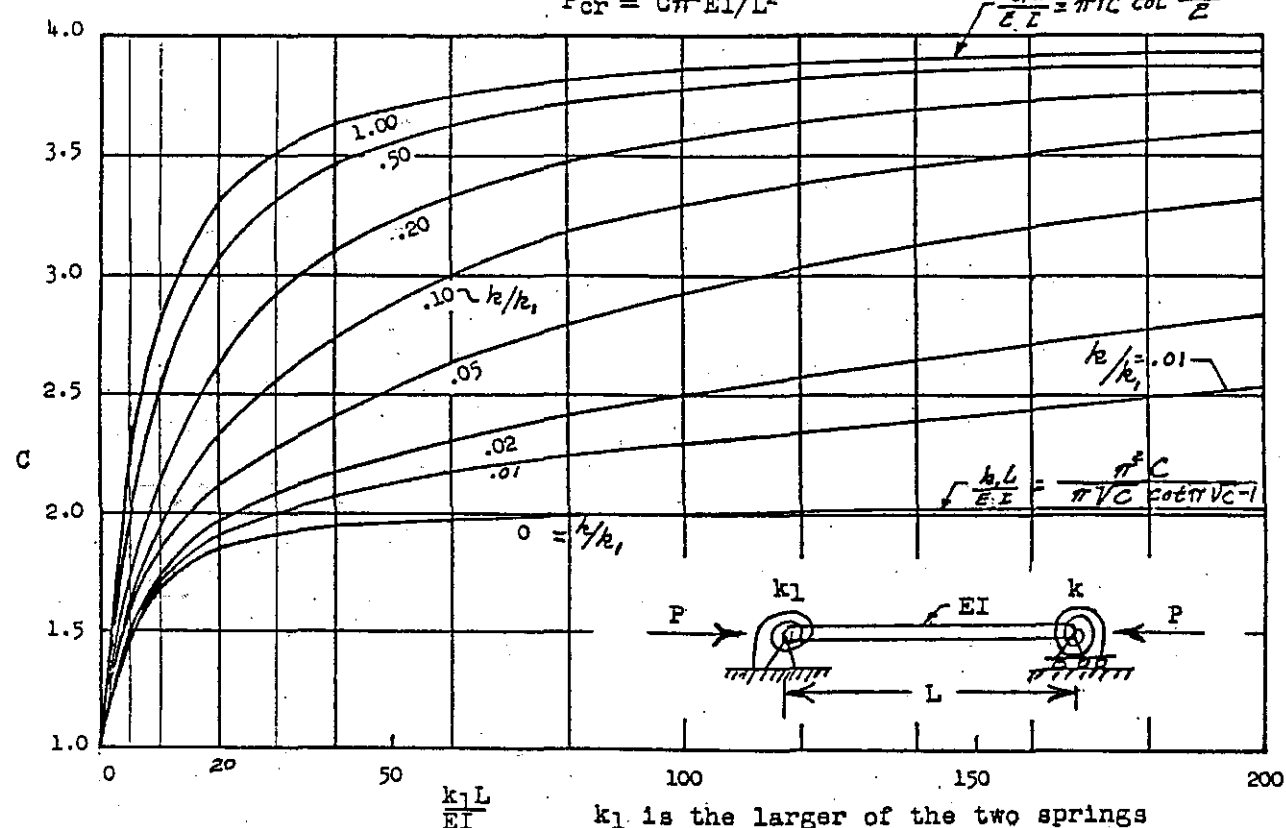


Fig. C2.27a Constant Section Column Having Elastically Restrained Ends

Note that interpolation for C "between the lines" is non-linear. For an exact value here, or for $k_1 L/EI > 200$, P_{cr} can be found by successive trials, as follows.

1. Use the figure to get an approximate value of C and calculate P_{cr} .
2. Get the corresponding values of j , L/J COF and SF ($= 4SCEI/L$).
3. Enter the values in the following buckling equation (see Ref. 4 for derivation of the equation).*

$$SF^2 (COF)^2 / ((k_1 + SF)(k + SF)) = 1.0$$

4. If the left side of the equation

is < 1.0 assume a slightly larger value for P_{cr} and repeat steps (2)-(4); if > 1.0 assume a smaller value.

5. Repeat steps (2)-(4) until the equation is satisfied and P_{cr} is as assumed.

The value used for E must correspond to E_t for F_{cr} when F_{cr} is in the plastic range, or to E_{eff} .

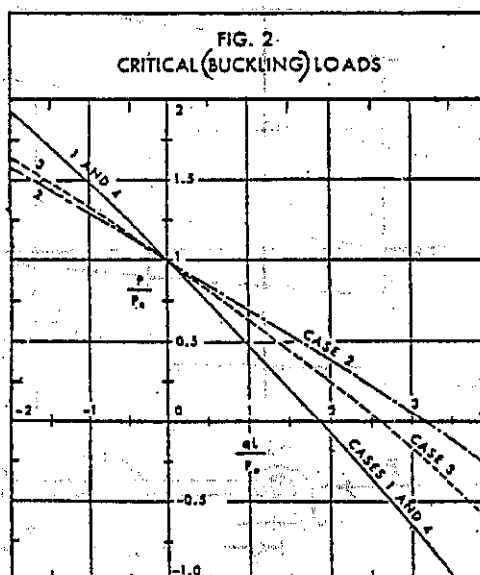
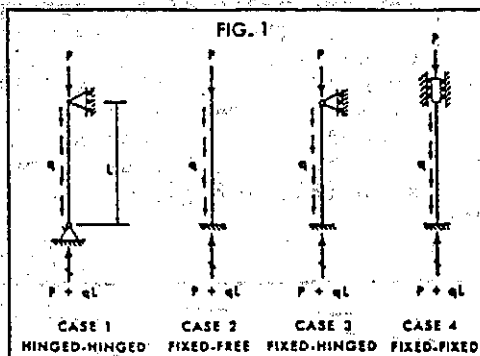
To check a column's adequacy under a given load enter its values of SF and COF in the equation. If the left side is < 1.0 it is stable; if > 1.0 it is unstable. See AII.13a for SC and COF values. The k/k_1 curves in the above figure were generated using the buckling equation.

* If $k_1 = \infty$ (fully fixed) the buckling equation is $SF + k = 0$, so for stability $L/J < 27$ and $SF + k > 0$

** or directly with an error of $< 1\%$ for the special case where $E_1 = E_2 = E$ and $L_1 = L_2$ with $n = I_2/I_1$ and $m = (P_1 + P_2)/P_1$ (Ref. 5, p.100)

$$P_1 + P_2 = \frac{(m^2 EI_2/L^2)(m+1)}{m + \frac{m(m-1)^2}{6} - \frac{8(m-1)}{\pi^2} + n \left[\frac{1}{n} + \frac{n(n-1)^2}{6} + \frac{8(n-1)}{\pi^2} \right]}$$

Table C2.13 Uniform Column with Distributed Load and End Load*

TABLE I
CRITICAL(BUCKLING) LOADS

$\frac{qL}{P_e}$	$\frac{P}{P_e}$			
	CASE 1	CASE 2	CASE 3	CASE 4
-4	2.743	2.113	2.204	2.766
-3	2.352	1.848	1.932	2.365
-2	1.933	1.373	1.643	1.937
-1.5	1.712	1.435	1.491	1.715
-1.0	1.483	1.292	1.333	1.484
-0.5	1.246	1.147	1.170	1.246
0	1	1	1	1
0.25	0.874	0.925	0.913	0.874
0.50	0.746	0.830	0.824	0.746
0.75	0.618	0.774	0.733	0.616
1.0	0.483	0.697	0.649	0.484
1.5	0.212	0.542	0.449	0.215
2	-0.067	0.384	0.250	-0.061
3	-0.445	0.059	-0.173	-0.435
4	-1.257	-0.277	-0.629	-1.234
5	-1.872	-0.629	-1.117	-1.835
6	-2.542	-0.992	-1.435	-2.496
8	-3.914	-1.740	-2.748	-3.825
10	-5.337	-2.384	-3.940	-5.204
$P_e = \frac{\pi^2 EI}{L^2}$				
$\frac{P_e}{EI/L^2}$				
$\frac{(qL)}{P_e} = \frac{1.641}{P_e}$				
for $P=0$				

The above data are used as follows: For a given P_e , the critical value of q is found. Or, for a given value of q the critical value of P is found. Positive values for the loads act as shown; negative values act in the opposite direction. If $P > P_e$ then q_{cr} will be negative. If $q > q_{cr}$ (for $P=0$) then P_{cr} will be negative.

For a given q P_{cr} is found as follows.

1. Compute P_e using the equation in Table 1 (20th row)
2. Compute qL/P_e observing the proper sign for q
3. Obtain P/P_e from either Table 1 (interpolating) or Fig. 1
4. Compute $P_{cr} = P_e(P/P_e)$

For a given P q_{cr} (the maximum allowable value of q) is found as above, but using P/P_e in step (2), qL/P_e in step (3), and computing $q_{cr} = P_e/L \times (qL/P_e)^{1/2}$ in step (4).

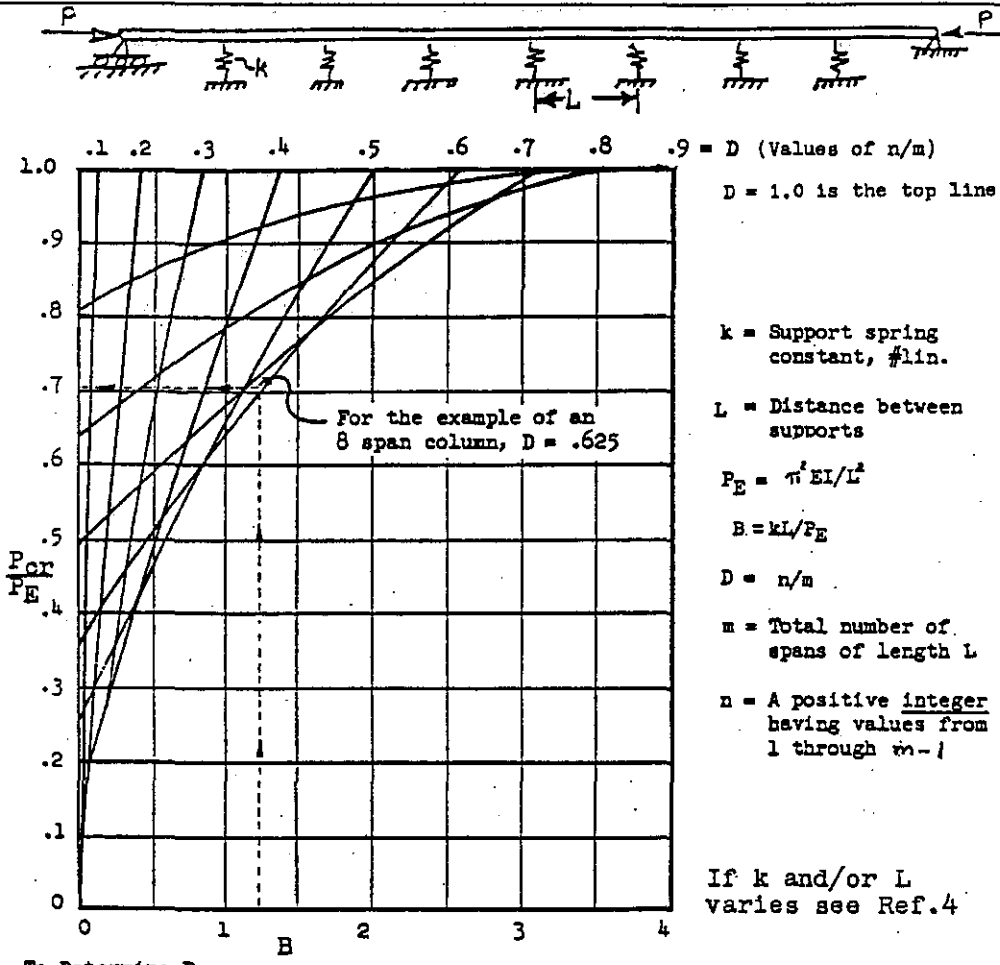
Example 1 (For all cases $L=50$, $EI=10$)
 $P=50000$, Case 3. What is q_{cr} ? $P_e=2.04$
 $(\pi^2 EI/L^2) = 80773$, $P/P_e=.619$. Per Fig. 2
 $qL/P_e=1.05$. So $q_{cr}=1.05(80773)/50=1696$

Example 3
 $q=1000$, Case 1. What is P_{cr} ?
 $P_e=39478$, $qL/P_e=1.64$. Per Fig. 1
 $P/P_e=.34$. So $P_{cr}=.34(39478)=13423$

Example 2
 $P=-30000$, Case 1. What is q_{cr} ?
 $P_e=\pi^2 EI/L^2 = 39478$, $P/P_e=-.76$. Per Table 1
 $qL/P_e=3.17$. So $q_{cr}=3.17(39478)/50=2503$

Example 4
 $P=133000$, Case 3. What is q_{cr} ?
 $P_e=80773$, $P/P_e=1.65$. Per Table 1
 $qL/P_e=-2.02$. $q_{cr}=-2.02(80773)/50=3263$

* For many cases of a varying q see Roark (p.26, footnote).



To Determine P_{cr} :

1. Compute value of B .
2. Compute all possible values of D .
3. Interpolating between the above plotted values of D with the actual values of D in (2) and the value of B , find the smallest value of P_{cr}/P_E .
4. Compute $P_{cr} = (P_{cr}/P_E)_{\min}(P_E)$

NOTE: In doing step (3) above it is easiest to first simply find which one of the plotted values of D give the smallest P_{cr}/P_E . Then consider only the 2 actual values of D that are closest to this for interpolating.

A quick conservative estimate can be obtained by only using B and the lower "envelope" of the plotted D values.

Fig.C2.45 Uniform Column on Equally Spaced Elastic Supports Having Simply Supported Ends

Example

For an eight span column having $L = 20"$, $EI = 10^6$, $k = 1510 \text{ lbs/in}$ what is the buckling load? Proceeding as outlined;

$$P_E = \pi^2 (10)^6 / 20^2 = 24674$$

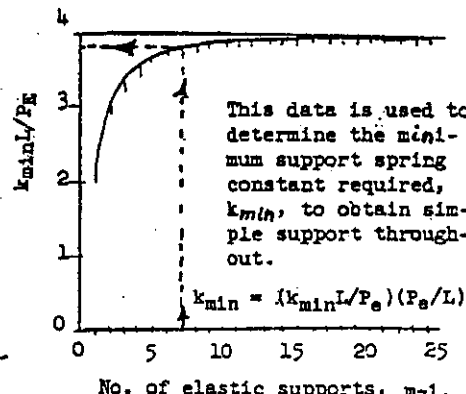
$$B = 1510(20)/24674 = 1.22$$

$$m=8, \text{ so } D=1/8, 2/8, 3/8, \dots \dots \dots 7/8.$$

$$\text{Per the above figure, } P_{cr}/P_E = .705$$

$$\text{Therefore, } P_{cr} = 24674(.705) = 17395$$

$$\begin{aligned} \text{To obtain simple support throughout } k_{\min} \\ = 3.82(24674)/20 = 4713 \quad (\text{then } P_{cr} = P_E). \end{aligned}$$



C2.18 End Friction Effects

For pin-ended columns the presence of end fixity due to friction will affect the axial load carrying ability in two different ways. One is to increase it and the other is to decrease it. Such columns typically have an end fitting which includes either a plain (or spherical) bearing or a roller (or ball) bearing with a connecting bolt or pin. With plain or spherical bearings the end friction can be quite significant, whereas with ball or roller bearings it is essentially negligible.

The effect depends upon the manner in which the column functions. If it is a stationary column with no end rotation relative to its supporting structure (such as a column in a testing machine) the effect is to increase the buckling load. If it is part of a mechanism or structure where such a relative rotation at the ends occurs the effect is to generate a bending moment which reduces the axial load carrying ability.

Stationary Columns

For these the effect is to oppose any rotation at the ends (which occurs when a column buckles). Therefore, the buckling load increases, but this cannot be used in design or analysis since it is not reliable.

Moving Columns (End Rotation)

These cases must consider the end friction since it causes end moments which reduce its strength. Fig.C2.46 illustrates the two possibilities here.

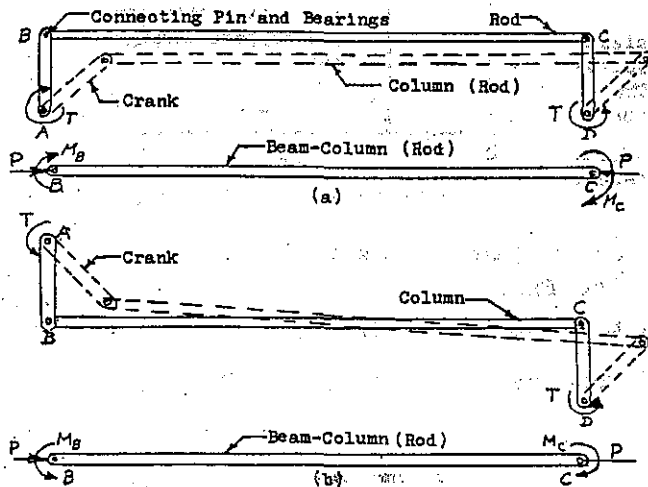


Fig.C2.46 Column as Part of a Mechanism

The two cranks and the rod, BC, are a mechanism which moves as shown by the broken lines. For each case, (a) and (b) the "input" torque, T , on crank AB causes the mechanism to move to the right and is reacted by the "output" torque at D. This puts rod BC in compression. The broken lines show the relative rotation between the rod and the cranks. The axial load, P , and the end moments, M , due to friction are shown for each case. Note that case (b) is more severe than is case (a). The magnitude of the moments are calculated as

$$M = P(uD/2)$$

$uD/2$ is the radius of the "friction circle" where

u = coefficient of friction between the pin and the bearing

D = Diameter of the connecting pin

For most cases $u \approx .20$ but can be much higher if high-friction materials are used. The axial load, P , actually acts tangent to the radius of the friction circle as shown in Fig.C2.47 for the above two cases.

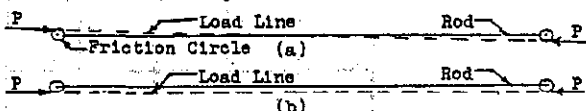


Fig. C2.47 Load Line Tangent to Friction Circle

Hence, the rod BC is a beam-column, due to the friction end moments, and therefore will fail before its buckling load, P_{cr} can be attained. The bending moment along the rod can be gotten per Case I (or II) in Table A5.1, and the stress analysis made per Art.C3.18. If the friction effects are ignored there will be a bad "surprise" when an earlier than predicted failure occurs, particularly when P approaches P_{cr} .

References: (Add to those on p.C2.18)

- 4) Engineering Column Analysis, (see Art.A18.27a)
- 5) Theory of Elastic Stability, Timoshenko, S.P. and Gere, J.M., McGraw Hill Co.
- 6) Numerical Procedure for Computing Deflections, Moments and Buckling Loads, Newmark, N.W., Trans. ASCE, Vol.108, 1943
- 7) "Critical Loads of Columns of Varying Cross Section," Thompson, W.T., Journ. of App. Mechanics, June, 1950

C3.4a The Cozzzone Simplified Procedure

The following presents a correction and an addition to Fig.C3.8.

1. The value of K for the tube in the figure should be 1.27 to 1.7.
2. The first two sentences of the final paragraph are revised as follows.

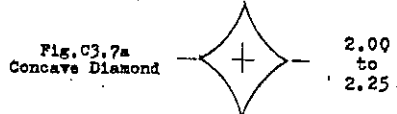
If the calculated value of K is greater than the ranges shown or greater than, say, 2.0 for combinations an error has been made. For the concave diamond shown in Fig.C3.7a, if the shape is given as $y = tax^n$ (for the left side) then $K = (9n + 3)(4n + 2)$. For example, if $n = 1$ (a diamond) then $K = 2.0$; if $n = 1.2$ (a slight concavity) then $K = 2.03$; if $n = 2$ (a large concavity) then $K = 2.1$; if $n = \infty$ (the maximum, but impractical, concavity) then $K = 2.25$, the maximum value. A four-pointed star would have similar values. The Fig.C3.7a data should be added below the diamond in Fig.C3.7.

C3.7a Example Problems in Finding Bending Strength

The following should be added after the end of Solution 1 of Example Problem No. 3.

32,750 in-lbs not the predicted bending strength of the member. It is the first approximation. This is because the compression and tension loads (due to the compression and tension stress distributions) are not equal. They must be equal since no applied axial loads are present (see Art.C3.3, second paragraph, second sentence). In this case the stress distributions produce a compression load of 32,780 lbs on the portion above the N.A., but a tension load of only 23,350 lbs on the portion below the N.A. Therefore more calculations are needed assuming the N.A. is farther up from the section's centroid which was assumed to be the N.A. After additional trials, it is found that when the N.A. is assumed to be .42" down from the top, the compression and tension loads are essentially equal, and the allowable bending moment is 31,080 in-lbs.

This applies to all allowable bending moment determinations when the cross-section is not symmetrical (or when the tension and compression stress-strain curves are not assumed to be identical). This discussion also applies to the solution of Example Problems 3 and 4.



In doing the plastic bending analyses the allowable compressive unit strain is $\epsilon = F_{cc}/E$, and this is at the mean line of the compression flange.

However, a more realistic and larger prediction of the bending strength for members like the above cases is presented in Art.C10.15b. It is based upon experimental data and does not base failure only on the flange allowable stress.

C3.10a Unsymmetrical Section With No Axis of Symmetry

If the procedure in Art C3.10 does not give a positive margin of safety, the more exact procedure outlined in Art. C3.11a should be tried.

C3.11a Alternate More Exact Method for Complex Bending

The steps used in carrying out the more exact procedure suggested in Art. C3.11 are as follows (for an unsymmetrical section with no axis of symmetry) as shown in Fig.C3.27a. Referring to Fig. C3.27a, xx is the axis about which the applied bending moment is given.

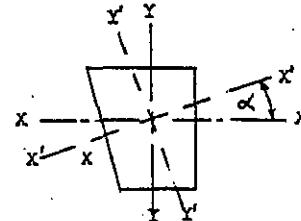


Fig.C3.27a Unsymmetrical Section

1. Assume a neutral axis position, α .
2. Find the allowable plastic bending moment about axis $x'x'$. This will require several iterations, moving $x'x'$ parallel to itself until the tension and compression loads on the cross-section are essentially equal, as in Art.C3.7a. This gives the allowable bending moment about $x'x'$, $M_{all\,x'x'}$.
3. Find the moment of the stresses in (2) about axis $y'y'$. This gives the corresponding allowable moment about $y'y'$, $M_{all\,y'y'}$.
4. Resolve the moments $M_{all\,x'x'}$ and $M_{all\,y'y'}$ into moments about axes xx and yy to get $M_{all\,xx}$ and $M_{all\,yy}$.

$$M_{all\,xx} = M_{all\,x'x'} \cos \alpha + M_{all\,y'y'} \sin \alpha$$

$$M_{all\,yy} = M_{all\,x'x'} \sin \alpha + M_{all\,y'y'} \cos \alpha$$

- The left hand rule, shown in Fig.C2.27b, is used for any set of axes.
5. Plot the point M_{allxx} , M_{allyy} as shown in Fig.C2.27b.
 6. Repeat steps (1) - (5) for several other assumed values of α (one of which can be $\alpha = 0$) to establish an allowable curve of M_{allxx} vs. M_{allyy} as in Fig.C2.27b. It is only necessary to obtain that portion of the curve (the solid line) wherein the applied moments are acting, as shown by the point m_x and m_y in the figure.
 7. Using this plot, for any applied moments, m_{xx} and m_{yy} , the margin of safety can be determined as

$$M.S. = \frac{ob}{oa} - 1.0$$

or,

$$M.S. = \frac{ob'}{oa'} - 1.0$$

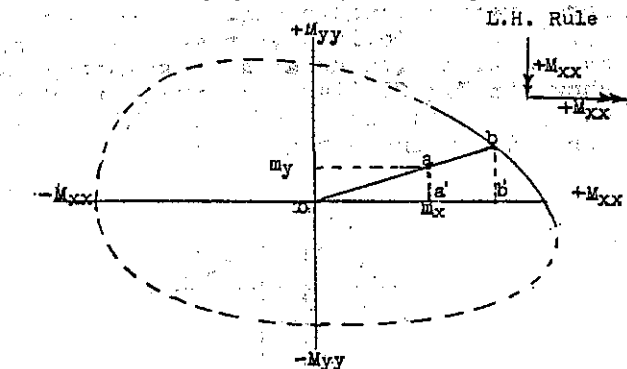


Fig. C3.27b M.S. for Unsymmetrical Sections.

C3.12a Flexural Shear Stress in the Plastic Range

In Art.C3.2 it was stated that in the plastic range the equation for the shear stress is CVQ/It . In the elastic region $C = 1.0$, but with plastic bending it is larger than 1.0 in the neutral axis region and less than 1.0 near the outer fibers. The procedure in Art.C3.12 for calculating C is an approximate one. This is because flexural shear is $\Delta M/\Delta X$, and when M changes in the plastic region, f_m and f_o also change, which the Art.C3.12 procedure does not consider. Following is the more exact procedure.

For a given bending moment at a given beam station one determines the corresponding values of f_m and f_o by successive trials as previously shown (f_b is calculated as Mc/I). Or, for a symmetrical section one calculates $f_b = Mc/I$ and then assumes a strain, ϵ , obtains f_m and

f_o and calculates $f_b = f_m + (K - 1)f_o$. This is repeated until the value of f_b equals that calculated as Mc/I . The proper values of f_m , f_o , f_b and ϵ are then known for the applied bending moment, M .

Then, at the point f_m and ϵ on the f_m curve one draws a straight line which is tangent to the curve and which intersects the ordinate f_o , calling the value of f_m at the ordinate f_m' . This is repeated using f_o and the f_o curve calling the value of f_o at the ordinate f_o' . This procedure is illustrated in Fig.C3.28c.

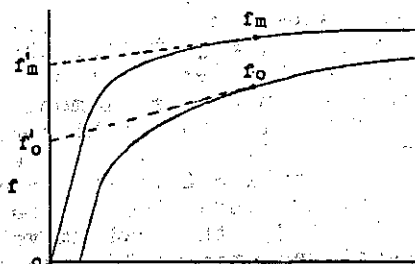


Fig. C3.28c Determining f_m' and f_o' . The corresponding value of f_b is then calculated using f_m' and f_o' in the previous formula. One then calculates

$$\Delta f_m = f_m - f_m', \Delta f_o = f_o - f_o' \text{ and } \Delta f_b = f_b - f_b'$$

Fig.C3.28d illustrates all of the above stresses (along with Fig.C3.28e).

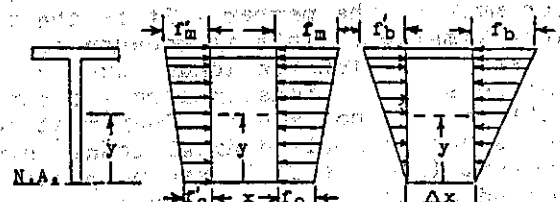


Fig. C3.28d Plastic and Linear Stresses

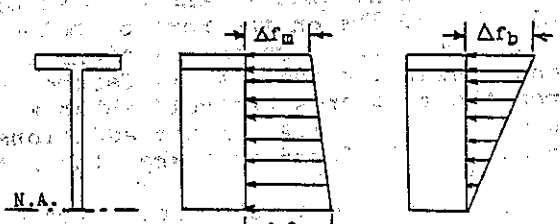


Fig. C3.28e Net Plastic and Linear Stresses

One then calculates the axial load on the section (on one side of the N.A.) due to the Δf_m and Δf_o stress distributions, calling this load P_a and repeats this using the Δf_b and $\Delta f_b'$ stress distribution, calling this load P_b . C is then calculated as

$$C = P_a/P_b$$

Example Problem

Using the data from Example Problem 2 on p.C3.10 and its associated curves in Fig.C3.19, calculate the shear stress at the N.A. given in Fig.C3.28 and also at the intersection of the web and flange.

Per the example $f_m = 35,800$, $f_o = 19700$ and $\epsilon = .0222$. Constructing the straight lines tangent to the f_m and f_o curves at $\epsilon = .0222$, these intersect the ordinate at $f'_m = 23,000$ and $f'_o = 13,000$, $f_b = 39150$ (p. C3.10) and

$$f'_b = 23000 + (1.17 - 1)(13000) = 25,210$$

Using the above stresses as previously discussed,

$$\Delta f_m = 35,800 - 23,000 = 12,800$$

$$\Delta f_o = 19,700 - 13,000 = 6,700$$

$$\Delta f_b = 39,150 - 25,210 = 13,940$$

These are used as in Fig.C3.28d to calculate the axial loads. At the N.A.,

$$P_a = 1.375(.125)(12,800 + 11,930)/2 + .875(.125)(11,930 + 6,700)/2 = 3,143$$

$$P_b = 1.375(.125)(13,940 + 12,198)/2 + .875(.125)(12,198 + 0)/2 = 2,913$$

$$\text{Therefore, } C = 3,143/2,913 = \underline{1.08}$$

This is slightly smaller than the 1.09 value obtained using the approximate procedure (p.C3.11). However, for other sections and other materials C is frequently much larger than when the approximate procedure is used.

At the web to flange intersection,

$$P_a = 1.375(.125)(12,800 + 11,930) = 2,125$$

$$P_b = 1.375(.125)(13,940 + 12,198) = 2,246$$

$$\text{Therefore, } C = 2,125/2,246 = \underline{.946}$$

C3.15 Yield Stress Bending Modulus

At limit load there must be no detrimental yielding (Art.C1.14) which generally means limiting the applied stress to the yield stress, F_{ty} or F_{cy} , determined as shown in Fig.B1.1. This allows the use of a yield bending modulus, F_{by} , which will be slightly larger than the yield stress. For the materials listed in Table C3.2 F_{by} can be calculated as

$$F_{by} = f_m + f_o(K - 1)$$

where f_m and f_o are the values listed in the table under "Yield". These are the values at the unit strain, ϵ , corresponding to the yield stress on a f_m and f_o vs ϵ plot.

For a material not included in Table C3.2 (or not in any other similar available tables) the basic f_m and f_o vs ϵ curves are needed. F_{by} can then be determined by locating the values of F_{ty} or F_{cy} on the f_m curve and dropping vertically from this point to obtain the corresponding value of f_o on the f_o curve. F_{by} is then calculated as previously shown using these f_m and f_o values (f_m here is the yield stress, F_{ty} or F_{cy}).

C3.16 Residual Stresses Following Plastic Bending

When a beam is loaded so that the bending stresses are in the plastic range and the applied loads are then removed, there will remain a residual stress and a residual strain in the beam. This will be largest at the extreme fibers. Those fibers which were loaded in compression will have a tensile residual stress, and vice-versa for those which were loaded in tension. The residual stresses can be of importance when doing fatigue or fracture analyses and can be determined as follows

It is necessary to have a "K-curve" where K is the shape factor ($2Qc/I$) for the cross-section being analyzed. For such a curve see Fig.C2.19 where the curve for $K = 1.17$ is shown. It is also necessary to have the f_m (stress-strain) and f_o curves. The K-curve is generated as follows for any selected value of K .

1. Select a unit strain value, ϵ .
2. Obtain the f_m and f_o values at the selected ϵ .
3. For the selected K value calculate the bending modulus at this strain as

$$F_b = f_m + f_o(K - 1)$$

4. Repeat steps (1) - (3) for each of several values of ϵ .
5. Plot the points F_b, ϵ , draw a curve through them and label it $K = (\text{selected value})$. This is shown in Fig.C.29 (the f_m curve is for $K = 1.0$).

For this K-curve the residual stress and strain in the outer fibers can then be determined as follows.

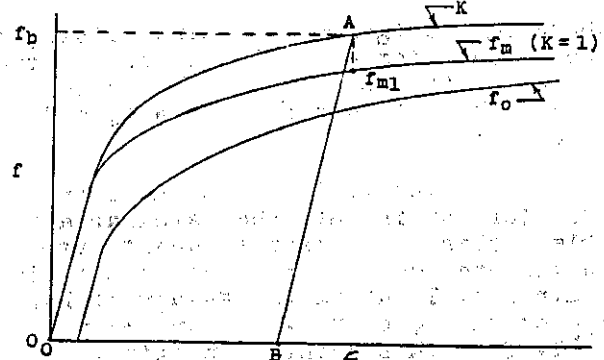


Fig.C3.29 Determination of Residual Stress

Symmetrical Cross-Sections

Referring to Fig.C3.29, calculate the bending stress $f_b = Mc/I$; enter the figure with f_b , and go across to the K-curve establishing the point A. Draw the straight line AB parallel to the linear portion of the stress-strain curve and establish the point B. Then go down from point A to establish f_{m1} on the stress-strain curve. The residual stress is

$$f_{res} = f_{m1} - f_b$$

The residual strain, ϵ_{res} , is that at point B. These are the outer fiber values, the largest values. The same procedure would establish the smaller values at any inner fiber.

Unsymmetrical Cross-Sections

Referring to Fig.(b) of Art.C3.7, more effort is required since the neutral axis is not the centroidal axis, and a successive trials procedure is therefore needed, as follows.

1. Assume an outer fiber strain, ϵ_1 , for the portion with the most depth from the centroid, y . ϵ_2 is then known for the other portion as shown in the Fig.
2. Proceed as discussed for Example Problem 3 in Art.C3.7 and also in Art.C3.7a to determine $M = m_1 + m_2$ (finding the correct neutral axis). This requires successive trials.
3. Repeat steps (1) and (2) for each of several other assumed values of ϵ_1 so that a curve of M vs ϵ_1 can be drawn.
4. Enter this curve with the applied moment and obtain the corresponding value of ϵ_1 . ϵ_2 will then also be known (step 1).
5. Enter the appropriate plastic bending curve with ϵ_1 , go vertically to intersect the applicable K-curve to estab-

lish point A. Then, in the same manner as for the symmetrical section, draw the line AB and determine the residual outer fiber stress and strain for portion 1 of the cross-section. Then repeat step (5) using ϵ_2 for portion 2 of the cross-section.

C3.18 Beam-Column Analyses

This article presents the procedure for doing the stress analyses for uniform and also varying section members.

Uniform Single-Span Members

For uniform single-span members numerous formulas for the bending moments along the span are presented in Tables A5.1 and A5.1a. For any case not available there (or by superposition of those cases), the bending moments can always be calculated by using the tabular procedure presented later for beam-columns of non-uniform spans. Allowable stresses and margins of safety are discussed later.

Multispan Members of Uniform Spans

For multispan members where the spans are uniform but EI may vary from span to span, the moment distribution procedure with axial load is used, as illustrated in Art.A11.14, to obtain the bending moments at the ends of each continuous span. The bending moments within any span are then obtained by using these bending moments as applied loads (e.g., Case II, Table A5.10) together with any applicable load case (e.g., Case III, V etc.), using superposition of the results (for the same axial load).

Varying-Section Single-Span Members

When EI varies along the span the formulas for uniform members in Table A5.1 and A5.1a cannot be used. In such cases a numerical procedure is required to determine the moments within the span. This is done by using the same tables of calculation as for varying-section columns in Art.C2.6b (Tables C2.5, C2.8, and C2.10), except that the bending moments, M , along the span due to the applied loads are used in Col.(2) of the first table of calculations. At this point the reader should review Art.2.6b as to how the tables and data are used there.

For the beam-column the difference is that instead of using an assumed shape for the first table one enters in Col.(2) the bending moment at each station due to the applied lateral loads and any end mo-

ments. These bending moments are determined assuming simply supported ends even though end fixity may actually be present. The procedure is as follows and applies for each type of table.

1. Calculate the bending moment at each station assuming simply supported ends and enter these moments in Col. (2) of the first table, calling them M_Q since they are for the applied lateral loads
2. Complete the table (as discussed in Art.C2.6b) but eliminate the last column for P_{cr} .
3. Multiply the true deflection at each station by the axial load, P , and enter this moment in Col. (2) of the next table, Table I, reversing the sign (because of the sign convention)
4. Carry out another table of calculations, Table II, as in (2) and (3).
5. Repeat again, Table III, etc.

After several tables are completed the final bending moment at each station, n , can be computed as*

$$M_n = M_Q + M_I + M_{II} + \dots + M_N / (1 - M_{N+1}/M_N)$$

This is a geometric series where the subscripts refer to the calculated table, Q being the first and N being the last. The value of M is taken from Col. (2) of each table, and M_{N+1} is obtained by multiplying the true deflection in the last calculated table, N, by the axial load. Usually three or four tables are adequate. Unless the axial load is quite large the deflections decrease fairly rapidly in the successive tables (if P is greater than P_{cr} the deflections will increase and are meaningless). If the axial stress, P/A , on any segment is greater than the proportional limit stress the tangent modulus, E_t (not E_{eff}) must be used. The geometric series converges only if $P < P_{cr}$ as a column.

The procedure is illustrated for a simply supported member in the following example. For members with end fixity the procedure is the same except that the table will be longer.**

Example Problem

The member in Fig.C3.32 is a beam-column subject to the applied loads as shown.

* See footnote on p.14.

** Can also be used for final deflections and slopes.

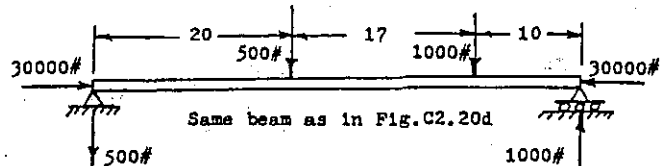


Fig.C3.32 Beam-Column

The bending moments at the six beam stations, 0 - 5, are, from statics

$$M_0 = 0 \quad M_2 = 9,400 \quad M_4 = 9,400$$

$$M_1 = 4,700 \quad M_3 = 10,000 \quad M_5 = 0$$

These values are entered in Col. (2) of Table C3.3 and the table is completed as shown. Note that this table is of the same form as Table C2.5 (Art.C2.6b) except that the above moments are in Col. (2) and Col. (10) is eliminated. The deflections in Col.(9) are then multiplied by the axial load, 30,000 lbs, and these moments are entered in Col.(2) of Table C3.4, reversing the sign, and that table is completed as shown.

Table C3.3 Beam-Column Numerical Analysis, First Table

①	②	③	④	⑤	⑥	⑦	⑧	⑨
Sta	M_Q	EI	M EI	Eq. Conc. El. Loads	Mom of Loads	Unit Slope	Unit Defl.	True Defl., $\times 10^3$
n	Data	Data	-2/ EI	(1) in Eqs. EI	(5) $\times 10^3$	$EI \times 10^3$	ΣEI	$\Sigma EI \times 10^3$
	$\times 10^3$	$\times 10^3$		$\times 10^3$	$\times 10^3$	$\times 10^3$	$\times 10^3$	$\times 10^3$
0	0	.40	0	-1.21	0	-17.17	0	0
1	4700	.92	-.511	-5.77	-5.77	-11.40	-17.17	-.126
2	9400	1.43	-.657	-7.82	-15.64	-3.58	-28.57	-.210
3	10000	1.36	-.735	-9.89	-29.67	6.31	-32.15	-.237
4	9400	.50	-1.880	-19.54	-78.16	25.85	-25.84	-.190
5	0	.50	0	-5.27	-26.35	0	0	0

See Table C2.5 for calculation notes and procedures (Art.C2.6b)

Table C3.4 Beam-Column Numerical Analysis, Second Table

①	②	③	④	⑤	⑥	⑦	⑧	⑨
Sta	M_P	EI	M EI	Eq. Conc. El. Loads	Mom of Loads	Unit Slope	Unit Defl.	True Defl., $\times 10^3$
n	- P/EI	Data	-2/ EI	(1) in Eqs. EI	(5) $\times 10^3$	$EI \times 10^3$	ΣEI	$\Sigma EI \times 10^3$
	$\times 10^3$	$\times 10^3$		$\times 10^3$	$\times 10^3$	$\times 10^3$	$\times 10^3$	$\times 10^3$
0	0	.40	0	-1.01	0	-11.95	0	0
1	3750	.92	-.411	-4.55	-4.55	-7.40	-11.95	-.088
2	6300	1.43	-.441	-5.34	-10.68	-2.06	-19.35	-.142
3	7110	1.36	-.523	-6.81	-20.43	4.75	-21.41	-.158
4	5700	.50	-1.140	-11.92	-47.68	16.67	-16.66	-.123
5	0	.50	0	-3.16	-15.80	0	0	0

See Table C2.5 for calculation notes and procedures (Art.C2.6b)

Two more tables were completed and the results for all four tables are summarized in Table C3.5, showing only the values of M and true deflection for each station.

Table C3.5 Results of Tabular Calculations

Sta	Table Q	Table I	Table II	Table III				
	M _Q	Defl.	M _I	Defl.	M _{II}	Defl.	M _{III}	Defl.
0	0	0	0	0	0	0	0	0
1	4700	.126	3780	-.088	2640	-.059	1770	-.040
2	9400	.210	6300	-.142	4260	-.095	2850	-.063
3	10000	.237	7110	-.158	4740	-.105	3150	-.070
4	9400	.190	5700	-.123	3690	-.081	2430	-.053
5	0	0	0	0	0	0	0	0

The final bending moments at each station are calculated using the geometric series, as shown in Table C3.6. Col.(10) shows the calculation of P_{cr} , discussed later.

Table C3.6 Determination of Final Moments and P_{cr}

Sta	M _Q	M _I	M _{II}	M _{III}	M _{IV} *	M _{final} **	$P_{cr} = P(M_{III}/M_{IV})$
0	0	0	0	0	0	0	
1	4700	3780	2640	1770	1200	16617	44300
2	9400	6300	4260	2850	1890	28417	45300
3	10000	7110	4740	3150	2100	31309	45000
4	9400	5700	3690	2430	1590	25875	45700
5	0	0	0	0	0	0	

* See text ** See text Average $P_{cr} = 45075$

End Fixity

If one or both ends are fixed the same procedure is used with the longer calculation tables, like Table C2.8 and C2.10.

Critical Axial Load

The critical axial load for a beam-column is the same load as if it were a column (no bending moments). The maximum allowable axial load for a beam-column is less than the critical load since earlier failure will occur by bending due to the applied lateral loads or moments. The critical load for the above member is 45000 lbs and the axial load is 30000. If it were larger the bending moments would increase, and as it approached the critical load the moments would approach infinity. Of course, bending failure would occur before this could occur.

Calculating P_{cr} from Beam-Column Data

The data in the beam-column calculation tables can also be used to easily and quickly calculate P_{cr} as follows. At any station

$$P_{cr} = P(M_N/M_{N+1})$$

where N is from the last calculation Table and M_{N+1} is as discussed before. For the above example P_{cr} is calculated in the last column of Table C3.6 and is, for example, at station 2

$$P_{cr} = 30,000(2850/1890) = 45,300 \text{ lbs}$$

Note that the small range in P_{cr} values is similar to that in Table C2.7. The formula for P_{cr} is discussed in Ref.3 (Art.A18.27a) and applies only when all segments of the member have the same value of E (i.e., in the elastic range), for P/A .

Salvaging Tabular Calculations for Changes in the Applied Loads

The results of the tabular calculations can be used for changes in applied loads as long as two conditions are met.

1. E is the same for all segments (P/A is in the elastic range).

2. All lateral loads change by the same factor.

This can save much effort by not having to repeat the tabular calculations. The procedure is as follows.

1. Let the final moments from the tabular calculations be

$$M_Q, M_I, M_{II}, \dots, M_N$$

2. Let the factor for the change in (all) lateral loads be L

3. Let the factor for the change in the axial load be K

4. The new bending moments along the span at each station will then be

$$\begin{aligned} M'_Q &= LM_Q & M'_{II} &= LK^2 M_{II} & M'_{IV} &= LK^4 M_{IV} \\ M'_I &= LKM_I & M'_{III} &= LK^3 M_{III} \end{aligned}$$

Or, for any Table, n, starting with Q as $n = 0$

$$M'_n = LK^{M_n}$$

These are used to determine the new final bending moments (i.e., by replacing the values in Table C3.6).

Example Problem

Repeat the previous example problem if P is increased to be 39,000 lbs and the lateral loads are increased by a factor of 1.2. For this case L = 1.2 and $K = 39000/30000 = 1.3$.

Applying these factors in the specified manner to the bending moments in Table C3.6, the new final bending moments become the much larger values shown in Table C3.7. Note that although the applied loads have been increased by an

* Which can also be used to calculate the SF, COP and FEM's as illustrated in the book of Art.A18.27a

Sta	M_Q	M_I	M_{II}	M_{III}	M_{IV}	M_{final}	F_{cr}
0	0	0	0	0	0	0	
1	5640	5897	5354	4666	4113	25670	Same
2	11280	9828	8639	7514	6478	43739	as in
3	12000	11092	9613	8305	7197	48207	Table C3.6
4	11280	8892	7483	6406	5449	39510	
5	0	0	0	0	0	0	-

average factor of only 1.25, the bending moments for those four stations affected by the axial loads have increased by a much larger average factor of 1.61.

Beam-Columns Having an Initial Bent Shape

Sometimes for various reasons a beam-column may not be "straight" even before any loads are applied. For uniform members, for which various formulas apply as in Table A5.1 and A5.1a, the member should simply be considered to be straight and a lateral loading applied which produces the same bending moment along the span (assuming simple supported ends) as does the axial load times the bent shape deflections at the stations. This is in addition to any actual lateral loading. Proper signs must be observed in doing this. That is, downward (-) deflections result in a positive bending moment. Fig. C3.33 illustrates the procedure. A single bend is shown in (a), a reversed bending in (b) and a smooth continuous bend in (c). The "equivalent" loads for a straight beam are shown beneath each of these. That in (c) is a good approximation. Thus, the loads consist of the equivalent loads and the applied loads, and the formulas of Tables A5.1 and A5.1a apply.*

For the case of a varying section member it is best to complete the first table (for the lateral applied loads). Then the bent shape deflections at each station are added (+ or -) to the true deflections calculated and their totals are multiplied by P to obtain the bending moments for Col.(2) of the second table. This is done only once, for the second table. Additional tables are completed in the routine manner.

Approximate Formula for Bending Moments

When there are no end moments the following formula can be used to estimate the bending moments along the span for a uniform, simply supported beam-column. At any station

$$M_{final} = M_Q / (1 + P/P_{cr})$$

P_{cr} is the critical load if the member were a column. If F_{cr} ($=P_{cr}/A$) is in the

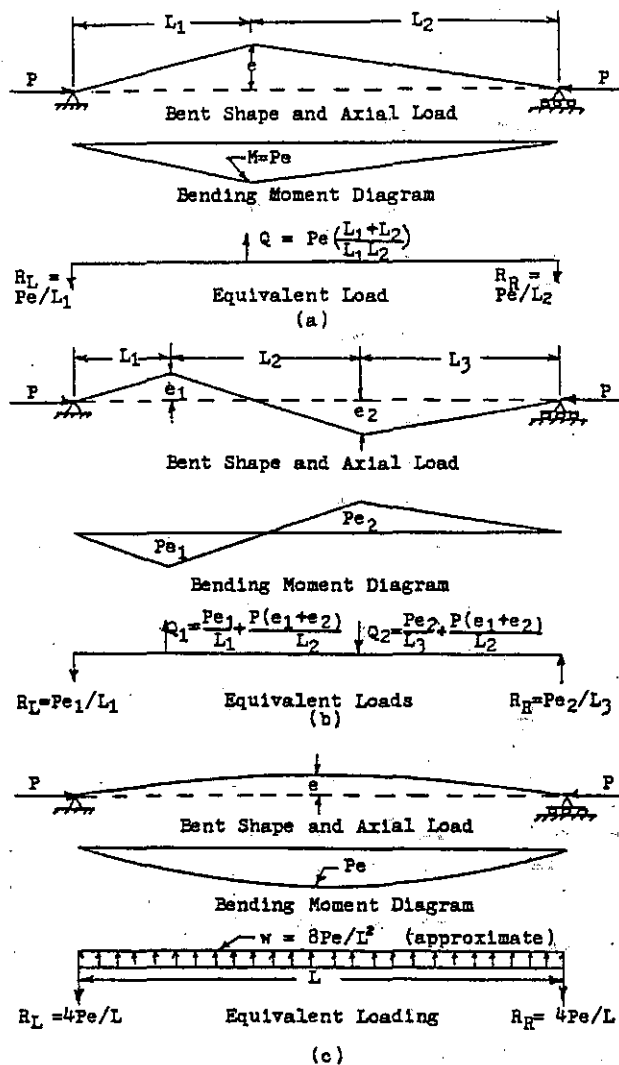


Fig.C3.33 Bent Shapes and Equivalent Loads

plastic range E_t is applicable (but not E_{eff}), hence a column curve can be used, but not one having any crippling adjustment. M_Q is the moment due to the lateral loads only. The formula is most accurate for a uniformly distributed load and least accurate* for a concentrated load.

The formula can also be used when the axial load is tension, adjusted as shown.

$$M_{final} = M_Q / (1 + P/P_{cr})$$

A tensile axial load reduces the moments.

Other Beam-Column Considerations

There are numerous other considerations which affect the bending moments generated in a beam-column. These are discussed in detail with example problems in Ref.3 (Art.A18.27a) and include the following topics.

* Since there is no actual transverse loading $M_Q = 0$, so $y_{final} = -M_{final}/P$ at any station.

* But conservative

1. Axial loads within a span
2. Elastic (rotational) end fixity
3. Members with internal (flexible) splices
4. Multispan beam-columns with ends spliced together, affecting fixed end moments, carry over and stiffness factors
5. Multispan beam-columns having varying EI spans require numerical evaluation of fixed end moments, carry over and stiffness factors
6. Multispan beam-columns on elastic supports and on sagging supports
7. Free-ended beam-columns
8. Beams in tension having a varying EI; the tabular procedure can be used but requires modifications

Allowable Loads or Stresses and Margins of Safety

Following are two different procedures for calculating the margin of safety for a beam-column. For a given case the larger of the two should be used.

1. The following interaction equation (from tests of circular tubes) is

$$P/P_{cr} + M/M_{ult} = 1.0$$

where P is the axial load, P_{cr} is the buckling load as a column, M is the final beam-column bending moment and M_{ult} is the allowable bending moment per Art.C4.17, C3.4 or C10.15b. The apparent M.S. (Art.C1.13a) is then

$$M.S. = 1/(P/P_{cr} + M/M_{ult}) - 1.0$$

2. An alternate procedure is

$$M.S. = F_c/(P/A + M_c/I) - 1.0$$

where P and M are as above, F_c is the outer fiber allowable compressive stress, determined as follows, and A is the cross-sectional area

- a) If the beam section shape factor, K , is 1.1 or less then F_c is the proportional limit stress* or that in (d) if smaller.

- b) If K is 1.5 or more then F_c is F_{cy}

- c) If K is between 1.1 and 1.5 then F_c

*The prop. limit stress can be found as where $P_c/P_{0.7}$ for the n curve is tangent to the n-curve in Fig.C2.17a

TORSIONAL MODULUS OF RUPTURE

is determined by interpolating linearly between (a) and (b) above.

- d) If the section has a local buckling stress (Art.C5.4, C5.5 and C6.4) less than in (a) - (c) then F_c is the outer fiber stress corresponding to the local buckling stress at the flange's meanline, and see p.46 footnote
- e) For cases where no permanent set is allowed at some particular load level, such as at proof load for actuators, F_c is the proportional limit stress. Method 1 above is not applicable for this case.

The margins of safety as calculated above are apparent ones. The true M.S. is calculated per Art.C4.23a and C1.13a.

C4.20a Torsional Modulus of Rupture Curves

Art.C4.20 discussed torsion stresses for only the case of circular cross-sections. For other cross-sections plastic torsion and a torsional modulus of rupture also occur for ductile materials. Following are methods for determining the ultimate strength in torsion for such members. The formulas, data and discussions in Art.A6.4 through A6.7 and in Table A6.3 apply only when the shear stress is in the elastic range.

Torsion in the plastic range is discussed in Ref.4 and 5. For non-circular cross-sections the ultimate torsional strength is proportional to the volume of dry sand (or table salt) that can be heaped upon the cross-section. If the cross-section has holes a special technique is required, as discussed later.

This volume of sand can be calculated for only three types of cross-sections, a rectangle, a circle and a triangle, as shown in Fig.C4.31.

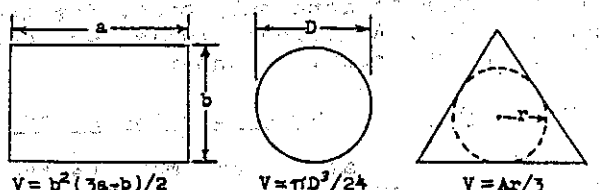


Fig. C4.31 Plastic Torsion Data

The equation for calculating the ultimate torsional strength, T_{ult} , when no local buckling can occur, as with very thin tubes etc, is

$$T_{ult} = 2VF_{rs}$$

where F_{rs} is a reference stress which can be taken as F_{su} for the material or calculated per Table C4.9. V is the sand heap volume in cu. in.

For other cross-sections without holes a cardboard template of the actual cross-section is made and sand is slowly poured onto the template until any additional sand runs off. The sand is then weighed and the volume is calculated as $V = \text{weight}/\text{weight per cu in of the sand}$. Having V , T_{ult} can then be calculated per the formula.

If the cross-section has holes the following is done to determine V . Snug fitting thin right cylinders made from thin paper are inserted in the holes, long enough to project above the volume of sand that can be piled on. The sand is then poured on as above, and the paper cylinders slowly pulled downward until their edges become contour lines at the max. elevation. (a bit of practice is helpful here). That is, none of the side area of the paper cylinders will be exposed. The weight of the heaped sand is then determined. To this weight of sand must be added the weight of sand required to fill the cylinders from the template up to their tips. The sand volume can then be calculated as discussed previously and T_{ult} is then calculated. It is generally unconservative to determine V simply by deducting from the strength of the cross-section without its holes the strength of solid sections having the cross-section of the holes, but this is sometimes done for rough preliminary estimates.

Instead of using F_{su} for F_{rs} in calculating T_{ult} , F_{rs} can be determined as follows. For the alloys in Fig.C4.17 through C4.30 the torsional modulus of rupture, F_{st} for solid circular cross-sections can be obtained at $D/t = 2$. Then, since $T_{ult} = 2VF_{rs}$, $F_{st} = T_{ult}R/J$, $J = \pi R^4/2$ and $V = \pi D^3/24$ one can solve for F_{rs} as a function of F_{st} . By algebraic manipulation

$$F_{rs} = .75F_{st}$$

Table C4.9 shows the values of F_{st} , F_{rs} , and F_{su} for several alloys from the Figures shown. F_{su} is from MIL-HDBK-5.

Table C4.4 Comparison of F_{rs} and F_{su}

Figure	Alloy	F_{st}	$F_{rs} = .75F_{st}$	F_{su}
C4.17	95 ksi Steel	71.4	53.5	55.0
C4.20	180 ksi Steel	142.5	106.9	109.0
C4.30	7075-T6 Forging	58.7	44.0	45.0
C4.28	6061-T6 Tubing	34.8	26.1	27.0
C4.27	2024-T4 Tubing	49.3	37.0	37.0

The values of F_{st} were obtained from Art. C4.20. They could also be gotten by doing torsion failure tests of rods having a circular cross-section.

C4.23a Illustrative Problems Involving Combined Bending and Compression

In Art.C4.22 Equation C4.14 does not give the true margin, but rather an apparent one (see Art.1.13a). Therefore, in Art.C4.23 the calculated M.S. of .09 is not the true margin which will be closer to zero (but not negative). To find the true M.S. one must find, by successive trials, the common factor by which all applied loads must be multiplied so that the calculated M.S. is zero. Calling this factor F , the true margin is $F - 1.0$. This applies to any beam-column, or to any other case where the internal loads or stresses do not vary linearly with the applied loads.

C5.7a Buckling of Flat Rectangular Plates Under Shear Loads

Add the following to Art.C5.7.

The use of the secant modulus for shear buckling stresses in the plastic range has no theoretical basis; it simply happens to match experimental results.

It is helpful to redefine the shear buckling coefficient as $K_s = k_s \pi^2/12(1-\nu^2)$. Then Eq.(5) becomes

$$T_{cr} = K_s E(t/b)^2 \text{ or } T_{cr} = E/(b/t K_s)^2$$

The abscissa in Fig.C5.13 will then be either of the above divided by $F_{0.7}$.

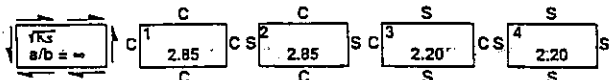
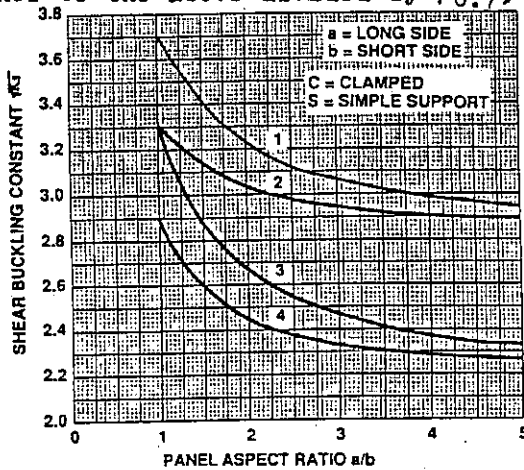


Fig.C5.11a Shear Buckling Coef., $\sqrt{K_s}$

The value of $\sqrt{K_s}$ is given in Fig. C5.11a. Fig. A11 gives F_{scr} ($=\tau_{cr}$) for several common materials and includes the effect of plasticity. Note that "cut-off" lines are used. These are at shear stresses of approximately $.5F_{0.7}$ (or $\approx .5F_{cy}$). This is a fairly common conservative practice.

For other materials Fig. C5.13 can be used entering with $K_s E(t/b)^2/F_{0.7}$ or with $E/(b/t/K_s)^2/F_{0.7}$, obtaining $F_{scr}/F_{0.7}$ and calculating $F_{scr} = F_{0.7}(F_{scr}/F_{0.7})$. Since n and $F_{0.7}$ are needed to do this they are obtained from Table B1.1, or for other materials n can be calculated per Art. B1.1 or read from Fig. B1.13 (obtaining $F_{0.7}$ and $F_{0.85}$ from the material's stress strain curve per Fig. B1.12).

5.8a Buckling of Flat Rectangular Plates Under Bending Loads

Useful data for two cases of plates subject to bending stresses are shown in Fig. 5.14a and Fig. 5.14b. That in (a) is for all edges simply supported with K_B being the value $k\pi^2 E_c / 12(1-\nu^2)$. The buckling stress is calculated as $F_{Bcr} = K_B E_c (t/b)^2$, where E_c is the compressive value of Young's Modulus. If F_{Bcr} is in the plastic range one calculates

$$F_{Bcr}/F_{0.7}$$

enters Fig. C5.8 with this and obtains $F_{cr}/F_{0.7}$. The corrected value of F_{Bcr} is then calculated as $F_{0.7}(F_{cr}/F_{0.7})$. For a/b values less than .30, K_B can be calculated as

$$K_B = \frac{(1+a^2/b^2)(1+4a^2/b^2)(1+9a^2/b^2)(b^2/a^2)}{.0576(1+a^2/b^2)^2 + .04938(1+9a^2/b^2)^2}$$

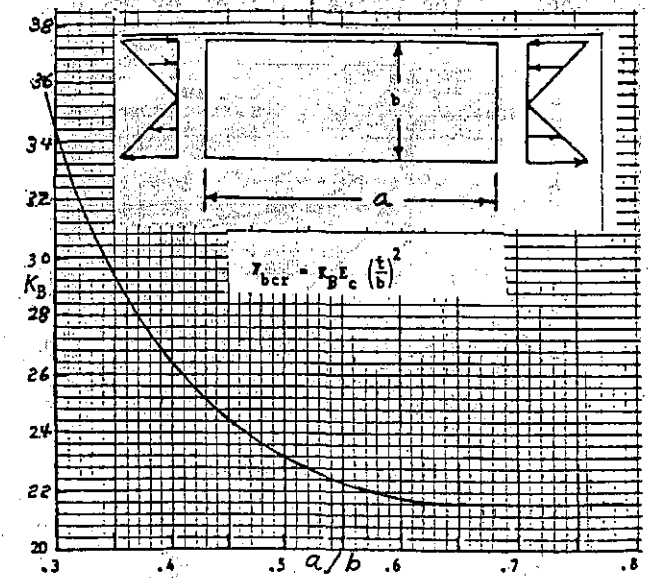


Fig. C5.14a Flat Plate Compression-Bending Buckling Coefficient, K_B

Fig. 5.14b is for a plate in bending and compression (not tension), with the compression (upper) edge free and the other three edges simply supported. This can also be useful, for example, in estimating the buckling stress for the up-standing free edge of a T-beam in bending with the upper edge in compression. The buckling stress is calculated as

$$F_{scr} = [k\pi^2 E_c / 12(1-\nu^2)](t/b)^2$$

If F_{cr} is in the plastic range it is corrected as discussed for the previous case. Note that the figure shows cases ranging from pure bending to pure compression ($b/h = 2$ to $b/h = 0$). For tension and bending $b/h > 2$ and is not covered by the data in the figure. h is the distance from the free edge to the line of zero stress

It should be noted that for this case the compressive buckling stress depends upon h , or the location of the line of zero stress. Therefore, it depends upon the relative magnitudes of the bending stress and the compressive stress, or upon M and P . So for a given case one must determine f_b and f_c and then find the value of h and b/h in order to enter the figure and obtain k . This is unlike other plate buckling stress which are for only a single stress f_s , f_b or f_c . Two examples will illustrate the procedure.

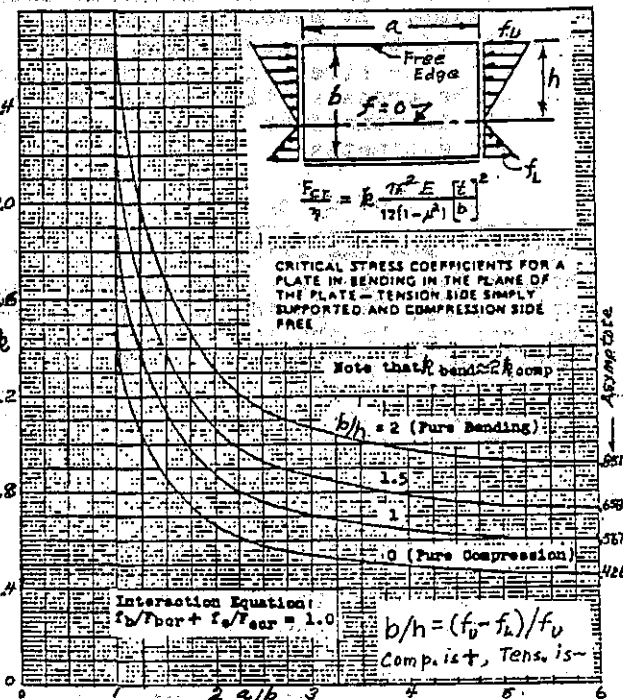
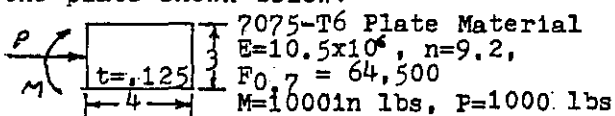


Fig. C5.14b Flat Plate Compression-Bending Buckling Coefficient, k

What is the buckling margin of safety for the plate shown below?



$$A = 3(.125) = .375, I = .125(3)/12 = .281$$

$$f_b = 1000(1.5)/.281 = 5338;$$

$$f_c = 1000/.375 = 2667$$

$$f_u = 5338 + 2667 = 8005 \text{ (comp.)}$$

$$f_L = 5338 - 2667 = 2671 \text{ (tens.)}$$

$$b/h = (8005 + 2671)/8005 = 1.334$$

$$a/b = 1.333; \text{ Per Fig. C5.14b } k = 1.4$$

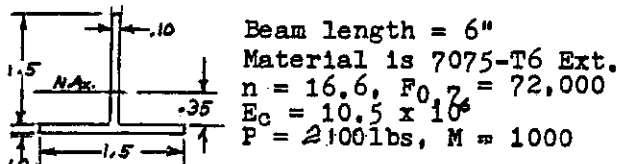
$$F_{cr} = 1.4(\pi)^2 (10.5 \times 10^6) (.125/3)^2 / 12(.89)$$

$$= 23,584 \text{ (not in plastic range)}$$

$$\text{Buckling M.S.} = 23,584/8005 - 1 = 1.95^*$$

Example Problem 2

What is the buckling margin of safety for the upstanding leg of the T-Beam below?



$$A = .30 \text{ in.}, I = .0763 \text{ in.}^3, c_u = 1.15 \text{ in.}$$

$$c_L = .35 \text{ (to bottom of upper leg)}$$

$$f_{bu} = 1000(1.15)/.0763 = 15072 \text{ (comp.)}$$

$$f_{bL} = 1000(.35)/.0763 = 4587 \text{ (tens.)}$$

$$f_c = 2100/.30 = 7000 \text{ (comp.)}$$

$$f_u = 22072 \text{ (comp.), } f_L = 2413 \text{ (comp.)}$$

$$b/h = (22072 - 2413)/22072 = .89 \text{ (Fig. C5.14b)}$$

$$a/b = 6/1.5 = 4$$

Per Fig. C5.14b $k = .62$

$$F_{cr} = 1.4(\pi)^2 (10.5 \times 10^6) (.1/1.5)^2 / 12(.89)$$

$$= 26,738 \text{ (not in plastic range)}$$

$$\text{Buckling M.S.} = 26738/22072 - 1 = .21^*$$

Had F_{cr} been in the plastic range for this case, Fig. C5.7 would be used.

C7.10a Illustrative Problems in Calculating Crippling Stresses

The previous Methods 1 and 2 show only a uniform thickness for the cross-section and do not discuss how to account for different element thicknesses. One approximate way to do this where angle units are involved is as follows. First, assume the two elements to have the thickness of the thinner leg and compute F_{cc} . Then assume them to have the larger thickness and compute F_{cc} . Then calculate the average of these and con-

sider this to be F_{cc} . However, a recommended Method 3 is provided in Art. C7.30.

C7.30 METHOD 3. For Crippling Stress Calculations

The following Method 3 for predicting crippling stresses is recommended, since it is more representative of what is used in the aerospace industry. It consists of calculating F_{cc} for each element of the cross-section and obtaining the weighted average of these as the crippling stress for the cross-section. The crippling load, P_{cc} , is then calculated as this average F_{cc} times the actual area of the cross-section. This is done in a tabular manner as discussed later.

Crippling Stress of Elements*

For any ductile alloy at any temperature the crippling stress for each element of the cross-section is calculated as follows.

a) For one edge free elements

$$F_{cc} = .566 F_{cy}^{.60} E^{.40} / (b/t)^{.80}$$

b) For no edge free elements

$$F_{cc} = 1.425 F_{cy}^{.60} E^{.40} / (b/t)^{.80}$$

The manner in which b is obtained is shown in Fig. C7.37. For clad material the bare thickness and the secondary modulus are used. Also see "cut-off" stress discussion.

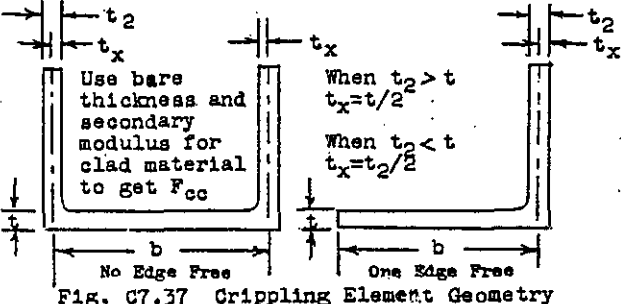


Table C7.2 shows the calculation procedure. The example in the table is for the zee section shown in Fig. C7.38. For this case, 7075-T6 Alc. the applicable properties and other data are shown in

Table C7.2 Crippling Stress and Load Calculations

Element	b	t	b/t	Free Edges	F_{cc}	bt	btF_{cc}
1	.50	.046	13.0	1	34026	.0276	939
2	1.25	.046	27.2	0	47457	.0576	2729
3	.70	.046	15.2	0	62000	.0322	1996
4	.28	.046	6.1	1	62000	.0129	800
						$\Sigma = .1303$	6464

$$F_{cc} = 6464/.1303 = 49609 \text{ psi}$$

$$F_{cc} = 49609(.123) = 6102 \text{ lbs}$$

* The crippling strength of built-up (attached) members is more than that of the separate members, see Ref. 14

* For ultimate bending (only) strength see p.48, "U-Sections"

the figure.*

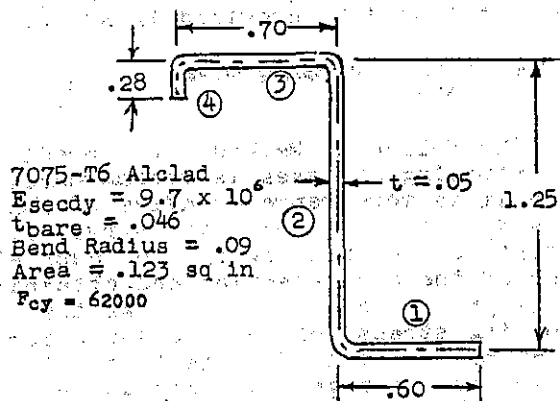


Fig. C7.38 Crippling Example Geometry

There are other considerations which may be present. These concern the ability of an element to be able to provide simple support for its adjacent element. There are three cases here, as follow.

Bulb Supporting Element

This case is discussed in Art.C7.9, in Fig.C7.10 and in Fig.C7.12, and in Example 10 on p.C7.9. If the bulb is not large enough to do this, a reduced crippling stress can be estimated as illustrated for a short flange (lip), using D_{bulb} instead of b_f , A_{bulb} instead of $b_1 t_1$, F_{cc} for F_{cc} and $(D/D_{min})^3$ instead of $(b_f/b_f^{min})^3$.

Effect of Short Outstanding Flanges (Lips)

As an outstanding flange is made progressively shorter, it will eventually be unable to provide simple support for its adjacent element. This flange length, b_f , can be determined as follows, referring to Fig.C7.39. The minimum flange length for providing simple support is that which satisfies the following equation.

$$.91(b_f/t_w)^3 - b_f/t_w = 5b_w/t_f$$

where b_w , t_f and t_w are known and b_f can be found by successive trials. Fig.C7.11 applies only when $t_f = t_w$.

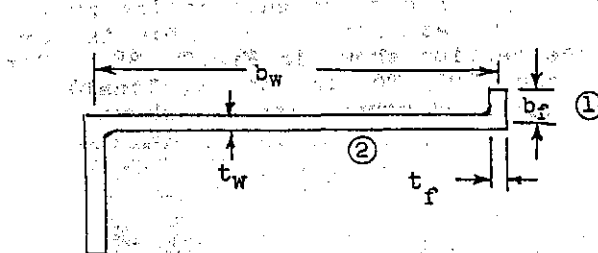


Fig. C7.39 Minimum Flange Geometry

* For jogged flanges see Fig.C.45(p.B1).

Example Problem

In Fig.C7.39 let $b_w = 1.25$, $t_w = .046$, $t_f = .046$. What is the smallest value of b_f which will provide simple support for element 2?

After several trials when $b_f = .247$ the above equation is satisfied, as

$$140.88 - 5.37 \approx 135.87$$

Hence, .247 is the least value for b_f that will provide simple support for b_w .

Reduction in F_{cc} for Short Flanges

When a flange is too short to provide simple support for its adjacent element, a reduced value for F_{cc} for the two elements (1 and 2 in Fig.C7.39) can be determined as follows.

- 1) Assume that b_f has the minimum value required and calculate an average F_{cc} for the two elements as follows.

$$F_{cc1} = F_{cc2} = (b_1 t_1 F_{cc1} + b_2 t_2 F_{cc2}) / (b_1 t_1 + b_2 t_2)$$

- 2) Calculate an F_{cc} for element 2 assuming it has one edge free.

- 3) Using the actual value of b_f , interpolate "cubically" between the F_{cc} values in (1) and (2) above to get the final value for F_{cc1} and F_{cc2} , that is,

$$F_{cc1} = F_{cc2} = (b_f/b_f^{min})^3 (F_{cc}(1) - F_{cc}(2)) + F_{cc}(2)$$

- 4) Use F_{cc} in (3) for elements 1 and 2 in the table for crippling calculations (i.e., in Table C7.2).

Example Problem

What is the crippling stress and the crippling load for the member in Fig.C7.38 if the length of element 4 is only .15"?

As illustrated previously, the minimum length of element 4 which will provide simple support for element 3 is found to be $b_3 = .205"$. Proceeding as outlined and using F_{cc} data from Table C7.2,

$$1) F_{cc3} = F_{cc4} = (800 + 1996) / (.0129 + .0322) = 62000$$

$$2) F_{cc3} (\text{for one edge free}) = 30026$$

$$3) F_{cc3} = F_{cc4} = (.15/.205)^3 (62000 - 30026) + 30026 = 42552$$

4) Using 42552 for elements 3 and 4 in Table C7.2 and .15 for b_4 , the reduced values for F_{cc} and P_{cc} are

$$F_{cc} = 42896 \quad P_{cc} = 5019$$

Outstanding Flanges not Perpendicular to Adjacent Elements*

On occasion a supporting flange must be inclined from the perpendicular direction, as shown in Fig. C7.40.

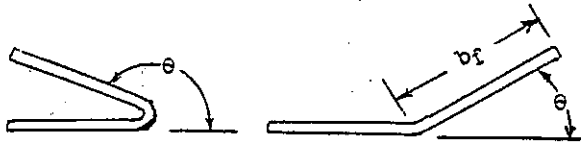


Fig. C7.40 Flanges at Small Angles*

In such cases the "effective" values, b_{eff} and t_{eff} , must be used when checking to see if it has adequate supporting length for its adjacent element, as discussed previously. These are calculated as follows.

$$b_{eff} = b \sin \theta \quad t_{eff} = t / \sin \theta$$

t_{eff} is then used for t_f in the cubic equation to determine the minimum flange length. If b_{eff} is less than this then b_{eff} is used in step (3) in place of b_f . The actual flange length, b_f , and thickness, t_f , are used to calculate F_{cc} for the two elements in step (1). It is recommended that θ be kept within the range of 20° to 160° . If θ is either quite small or large, the least will be quite small for an angle section and this will, of course, result in a small buckling load for the member as a column.

Example Problem

Repeat the Table C7.2 example problem assuming that element 4 is at an angle of 25° rather than at 90° .

$$b_{eff} = .28 \sin 25^\circ = .118$$

$$t_{eff} = .046 / \sin 25^\circ = .109$$

using .109 for t_f in the cubic equation, after several trials, when b_f is .156 the equation is (essentially) satisfied. Therefore, b_{eff} is not large enough to provide simple support for element 3. Using .118 for b_f in the previous step (3) and the value of .156 for b_{min} gives

$$F_{cc3} = F_{cc4} = (.118/.156)^3 (62000 - 30026) + 30026 = 43864$$

This results in $F_{cc} = 43277$ and $P_{cc} = 5323$ for the cross-section.

Large Curved Elements

The previous crippling calculation methods do not include data for cross-sections with large curved elements as in Fig. C7.41.

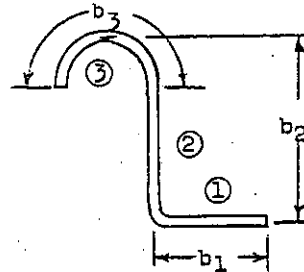
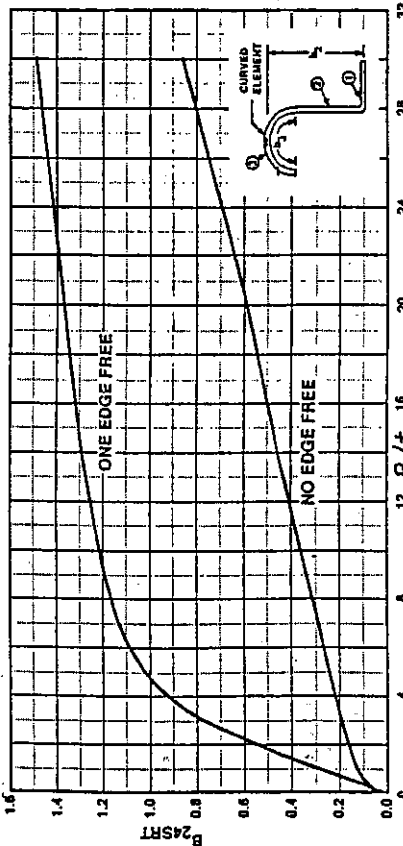


Fig. C7.41 Large Curved Element

Fig. C7.42 provides such data for one edge free and no edge free curved elements. The procedure would be the same as in Table C7.2, but with the following restriction. No elements in the cross-section are allowed to have a crippling stress greater than that of the curved element. That is, the curved element's



To determine F_{cc3} :

1. Enter figure with R/t and obtain $B24SRT$
2. Calculate $B = B24SRT \sqrt{F_0.7 / 0.0475E_c}$
3. Enter Fig. C2.17 with B and obtain $F_c/F_0.7$
4. Calculate $F_{cc3} = F_0.7 (F_c/F_0.7)$

Fig. C7.42 Calculating F_{cc} for Curved Elements

* Per NACA WRL 28 (1944) such angles can be considered to be 90° for calculating P_{cc} , so the following procedure is conservative and not necessary for calculating F_{cc} .

crippling stress is also a "cut-off", or maximum, crippling stress for all other elements. The reason for this is that tests show that when the large curved element buckles failure of the section will follow almost immediately.

Crippling "Cut-Off" (Maximum) Stresses

In using the formulas for crippling stresses, when b/t is very small the value for F_{cc} becomes unrealistically large exceeding F_{tu} ($=F_{cu}$) for the material. Therefore, it is necessary to use a realistic maximum or "cut-off" value for F_{cc} . There are three main ways that this has been done in the aerospace industry over the years.

$$1. F_{cc\max} = F_{cy}$$

$$2. F_{cc\max} = F_{co} \text{ (per Art.C4.4 and Tables C4.3 and C4.2)}$$

$$3. F_{cc\max} = F_{tu}$$

Using F_{cy} (item 1) is the most conservative, but has probably been used by most aerospace companies and is used in the examples of this Supplement.

These cut-off values are also used for F_{cmax} for columns not subject to crippling or local buckling (stable cross-sections), and also for columns subject to torsional buckling, discussed below.

C7.31 Torsional Buckling

Conventional (bending) buckling is a type of general instability which assumes that the buckled shape is due to bending only, as in Fig.C2.2. The buckling stress or load for a uniform column is as defined in equations (3), (5) and (6) of Art.C2.2 for stable cross-section shapes.

There is another type of general instability called "torsional" buckling for which the buckled shape involves twisting although there is no applied twisting moment. Torsional buckling is likely to be critical for members having open type cross-sections with relatively thin walls. In addition, it is usually most likely to be critical when the column is relatively short, that is, short and intermediate length column range. It is not a problem for closed cross-sections such as tubes, because of their high resistance to twisting deflections. It is not likely to be critical when the b/t (thinness) of no member of the cross-section is more than about 8.0 (see Fig.C7.43). Examples

of such cross-sections are zees, channels angles, tees, I-sections etc. The buckled shape is either a pure twisting or a combination of twisting and bending about one or two axes, as follows.

1. For a cross-section having two axes of symmetry or point symmetry it is a pure twisting only.
2. For one axis of symmetry it is a combination of twisting and of bending about the axis of symmetry.
3. For no axis of symmetry it is a combination of twisting and of bending about each principal axis.

For case (1) one computes the torsional buckling load and the conventional buckling load about the minor principal axis. The smaller of these is the critical load. For case (2) it is the smaller of the torsional buckling load and the conventional buckling load about the axis of non-symmetry. For case (3) the torsional buckling load is always critical. As the column length increases it will approach the conventional buckling load as calculated about the minor principal axis. Fig.C7.43 and C7.44 show for the cases of an equal leg angle and a channel section how torsional buckling can become critical. Note that as t decreases (and b/t increases) the loss in strength due to torsional buckling can become very large. For "thick" sections it will not be critical (b/t about 8 or less).

The previous discussion is for "free" struts. For restrained struts such as stringers attached to skin (as for wing structures) torsional buckling involves both twisting and bending, and may be less than the conventional buckling load.

Practical methods for calculating the torsional buckling stress of free struts and restrained struts are presented in Ref.14 (see Art.A18.27a).

Ref. 15,16 and 17 also discuss torsional buckling. Ref.15 shows a comparison with test results for the channel shown in Fig.C7.44, case (a). Ref.16 also shows some test results. Ref.17 has data for stringers attached to skins.*

Note:

Chapter C8 articles are located after Chapter C11 articles.

* References are on p.A21.

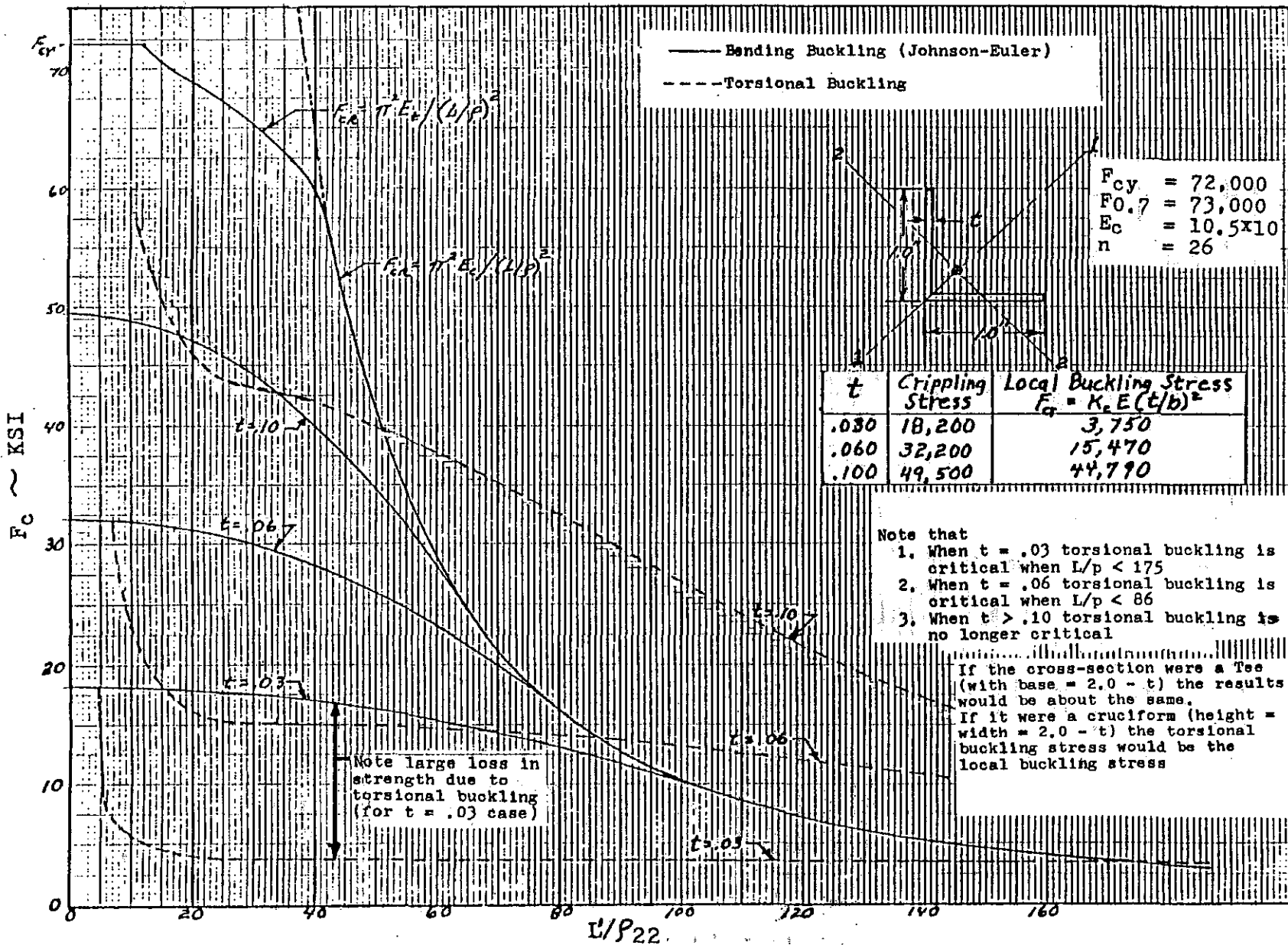
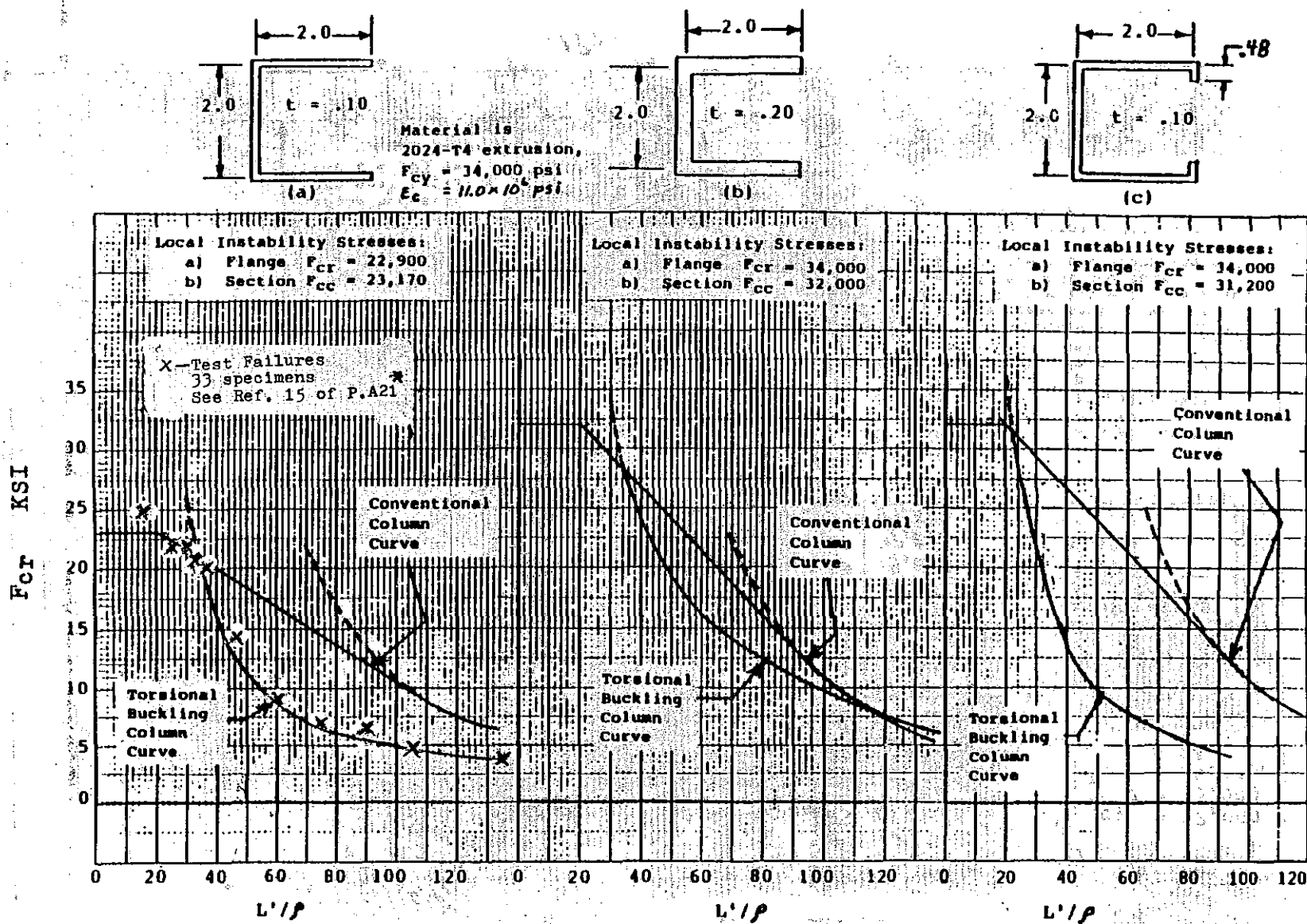


Figure C7.43 Buckling of an Equal Leg Angle Column



* "Airplane Structures", Vol. 2, 1943
Niles and Newell, John Wiley & Sons,
or NACA TN 733

Figure C7.44 Buckling of Channel Struts

C9.13a Calculation of General Instability

Art.C9.13 presents an equation (C9.7) for the required EI of light circular frames so that they will provide simple support for the stringers without collapsing (as illustrated in Fig.C9.7b), called "Shanley's Criteria" which is apparently greatly based upon work by N.J. Hoff. For elliptical frames it is suggested that for preliminary sizing purposes or checks the following be done. For a bending moment about the x-axis, M_x , let D in equation C9.7 be $2b$. For bending about the y-axis, M_y , let D be $2b^2/a$, referring to Fig.C9.9.

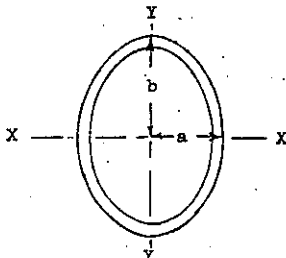


Fig.C9.9 Elliptical Frame

The frames must also have enough stiffness so that there will be no instability due to the shear in the skin panels, per Fig.C11.39.

Shanley's criteria applies only for a bending moment acting on a shell of stringer construction. When there is tension field action due to shear loads this will generate additional compression loads in the stringers. (Art.C11.31-.32). To account for the effect of this additional stringer loading it is recommended that the right side of equation C9.7 be multiplied by the factor $(P_c + P_{DT})/P_c$ where P_c is the most highly stressed stringer load due to M , and P_{DT} is the largest of the diagonal tension loads in this stringer and in the stringers on each side of it (3 stringers). The diagonal tension load in a stringer is calculated as

$$P_{DT} = .5(kf_{sh}htcota)_a + .5(kf_{sh}htcota)_b$$

as discussed in Art.C11.32, item 3. a and b are the panels on each side of the stringer being considered.

C10.15b Analysis of Thick-Web Beams

This textbook and others do not discuss the strength prediction for thick-web, shear resistant beams. These are quite commonly used in areas other than in the primary structure, such as for supporting numerous types of equipment.

There are two types of beams, thin-web and thick-web.

Thin-Web Beams

Thin web beams are shown in Fig. C10.1, C10.2 and C10.3. For these the web thickness is much smaller than that of the flanges. Thin-web beams may have either a non-buckling ("shear resistant") web, as in Chapter C10 or a buckling web ("semi-tension field") as in Chapter C11, Fig.C11.3 and C11.4. In general the deeper the beam relative to its length the more likely it is that the tension field type will be the lightest. Although a trade study is really needed to determine which is lightest, Wagner proposed that the following rough criteria for this be used. When the "index" $K = \sqrt{V/h}$ is more than even the shear resistant type is probably lightest, and when the index is less than seven the semi-tension field type is probably the lightest. In the index V is the shear in lbs and h is the beam depth between the flange centroids in inches.

The shear resistant type is usually the simplest from a manufacturing consideration, particularly if the web needs cut-outs or holes to allow wire bundles, rods etc. to pass through it (Fig.C10.19, C10.22 and D3.27). For thin-web beams the crippling strength of the compression flange is used in calculating the margin of safety, Art.C10.3, C10.5 and C10.15 on p.C10.13 (but too conservative for thick-web types as discussed later). However, if the beam's deflection (stiffness) is of importance, the initial buckling stress of the flange's outstanding legs should be used at limit load. This is because when such buckling occurs the beam's I will be become much smaller as to additional loads, so much stiffness will be lost. See Art. C6.1-C6.4 for initial buckling.

Thick-Web Beams

Thick-web beams have webs which are of about the same thickness as that of the flanges. Examples of thick-web beam cross-sections are shown in Fig.C10.15a.



Fig. C10.15a Some Thick-Web Beam Cross-Sections

In general, thick web beams are of one piece and are shaped by forming sheet metal, by extruding or by machining.

When subjected to bending the allowable compressive stress for strength calculations is frequently taken as the crippling stress of the flange, but this usually gives a quite conservative estimate, as bending tests of such members show. When deflection or stiffness is important, the flange's initial buckling stress (and limit load) should be used as discussed for the thin-web beam. For the cases of cee, zee, and U sections the ultimate bending strength can be more accurately determined by using the following empirical formulas. These are based upon bending strength tests made by the Curtiss-Wright Co. and reported in their Report R-162. In these the thickness was uniform, the two flanges had the same width and the zee section was prevented from deflecting laterally.*

Cee and Laterally Restrained Zee Beams

These are shown in Fig. C10.15b below.

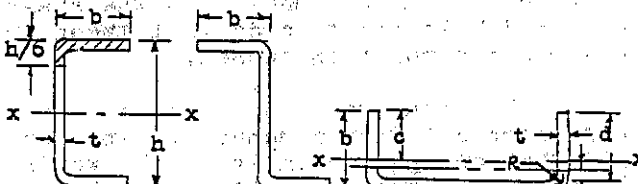


Fig.C10.15b Channel and Zee Beam Data

For aluminum alloy having $F_{cy} = 39,000$ and $E_{co} = 10.7 \times 10^6$

$$F_{bu} = 450,000(b/h)^{27} / (b/t)^{79}$$

so,

$$M_{all} = F_{bu} I/c$$

For other alloys, F_{bu} is multiplied by a factor of $(F_{cy}/E_c)^{50} / .0604$ where the prime marks refer to the other alloy's properties. Unsupported compression flanges must also be checked for lateral buckling, assuming a web height of $h/6$ to be integral with them when doing this.

U-Section Beams (Also for T-Sections)

For the same alloy as above

$$F_{bu} = 730,000/(b/t)^{17}$$

where b is the smaller of c and d . The formula is for compression in the outstanding flange. If it is in tension then $F_{bu} = F_{tu}$. For other alloys the same correction factor as for cees and zees is used. The formulas can be used also for extruded and machined shapes if they have a uniform thickness and the flanges of cees and zees are of the same widths.

* When a compressive load is also present these are beam-columns with M.S. per p.38 but do not use Method 2d for U or T-Sections. Use Fig. C5.14b to obtain F_c .

Cee and Zee Members Attached to a Skin in Tension

For these cases the following formulas can be used to calculate the allowable bending moments for any materials and at any temperature if $h \leq 8"$ and the beam spacing is 5" or more. The skin thickness, t , does not appear since the skin is assumed to take all of the tension load. The bending moment therefore is calculated about the base of the beam. The skin is in tension and the free flange of the beam is in compression.

For $h/t \leq 79$:

$$M_{all} = \left[684t^2 h(b/t)^{25} (F_{cy}E_c)^{50} \right] x \\ \left[-0.00303(h/t) + 1.20 \right]$$

For $h/t \geq 79$:

$$M_{all} = \left[684t^2 h(b/t)^{25} (F_{cy}E_c)^{50} \right] x \\ \left[-0.0005(h/t) + 1.00 \right]$$

where $b/t = (b + 0.7h)/2t$. Attachment to a skin provides lateral restraint for the beam.

Cee and Zee Members Attached to a Skin in Compression

For these cases the following formula can be used for any temperature and material if $8 \leq b/t \leq 20$ and the beam and skin are of the same material. If they are different materials the skin thickness, t , must be converted into an effective thickness, t_{ts} , using the beam's material. The equation is valid for $.50 \leq t/t_s \leq 2.0$.

$$M_{all} = \left[h t_s^2 (F_{cy}E_c)^{50} / b/t \right]^{278} x \\ \left[.816(E_c/F_{cy})^{25} + .462(b/t)^{723} \right] \\ \left[(t/t_s)^2 \right]$$

Unequal Flange Widths

When one flange is shorter than the other, use the shorter width for b (and d) in the previous formula.

Other Flanged Beams Symmetrical About the X-X Axis

With extruded or machined members the flanges might be thicker than the webs, and with an I-beam there is a flange portion on each side of the web. Although not covered by tests, the following procedure is suggested for an

approximate value for the allowable moment, M_{all} .

1. Determine the crippling load for each compression element outboard of the web and sum these to get P_{cc} .
2. Calculate the allowable bending moment carried by the flanges as

$$M_{flange} = P_{cc}(h - t_{flange})$$

3. Calculate the bending buckling strength of the web as

$$F_{bcr} = K_b E t_{web}^2 / (h - t_{flange})^2$$

4. Calculate the allowable moment due to the web as

$$\begin{aligned} M_{web} &= 1.45 F_{bcr} I_{web} / (h/2) \\ &= 1.45 f_{bcr} t_{web} h^2 / 6 \end{aligned}$$

5. Finally, calculate the beam's allowable bending moment as

$$M_{all} = M_{flange} + M_{web}$$

Fig. C5.14a can be used for obtaining K_b in (3) above. For most thick-web beams $a/b > 1.0$, so $K_b = 21.7$ (web stiffeners could result in smaller values of a/b).*

Other Flanged Beams Unsymmetrical About the X-X Axis

1. If the compression flange area is equal to or smaller than the tension flange area proceed as above (for symmetrical sections).

2. If the compression flange area is larger than the tension flange area proceed as in Art.C3.7, Example Problem 4 (but also see Art.C3.4a). Then assume it to have the same area as the tension flange and proceed as for the symmetrical section above (for different thicknesses). Use the larger of the allowable moments calculated. If the beam is also unsymmetrical about the Y-Y axis, supports will be needed to prevent lateral movement, just as for a zee.

Interaction Effects of Shear and Bending

If shear is present it will promote earlier failure because of web buckling and the ensuing tension field action.

$$M.S. = 1/\sqrt{(f_s/F_{scr})^2 + (M/M_{all})^2} - 1.0$$

The previous formulas do not apply when the web has significant holes,

since the tests did not include such. Holes will reduce the strength but no test data are available. In such cases unless the holes are quite small and near the beam centerline, it is probably best to base the strength upon the crippling stress of the flange, as for thin-web beams.

C11.29a Circular Holes in Flat Tension Field Beams

According to "Stress Analysis Manual", AD-759199, AFFDL-TR-69-42, a single unreinforced, unflanged centrally located circular hole in a web will reduce the strength of the tension field beam's components as follows.

1. The reduced allowable web strength is

$$F'_s = F_s(tD(d-D) + A_{ue}DC_4)/C_5td^2$$

where F_s is the allowable with no hole, C_4 and C_5 are per Fig.C10.17 and .18, D is the hole diameter, d is the upright spacing and A_{ue} is per Art.C11.19, equation (58). The parameter limitations based upon test data are

$$\begin{array}{ll} .02 \leq t \leq .132 & 7.0 \leq d \leq 18.0 \\ .04 \leq t_u \leq .079 & 2.375 \leq D \leq 5.875 \\ 7.4 \leq h \leq 19.4 & \end{array}$$

where h is the web height between flange centroids and t_u is the thickness of the upright.

Some aerospace company data indicate that a "small" hole without a doubler results in a reduced web strength of

$$F'_s = F_s(1 - 1.33D/d)$$

with the limitations that $D \leq .75$, $D/d \leq .15$, hole center is located $2.5D$ away from any fastener line, hole is not in a panel next to an upright introducing a significant load into the beam and the material is either 2000 or 7000 series aluminum or Ti-6Al-4V sheet.

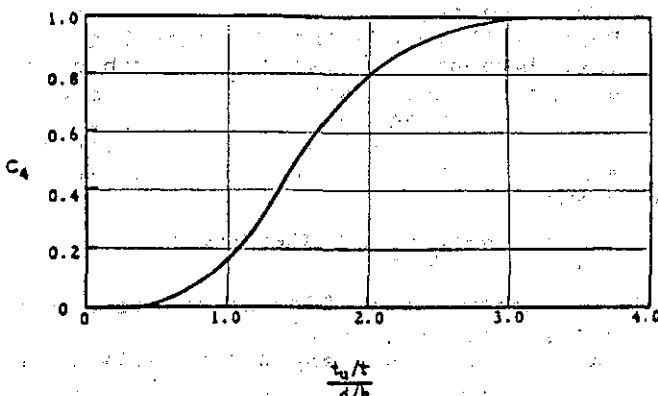
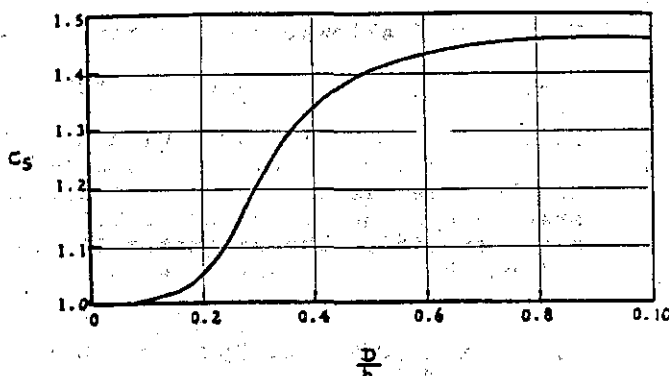
2. The reduced allowable upright (adjacent to the hole) forced crippling stress is

$$F'_u = F_u(1 + D/d)$$

3. The tension loads in the web-to-upright fasteners due to prying action of the buckled web (Art.C11.24, equation 66) should be multiplied by a factor of $1 + D/d$.

The strength of the web (and other compo-

* For I-beam type members (flanges on each side of web) of constant thickness a more realistic procedure is as follows:
 1) Using the web and 2 flanges (a Cee-section) calculate M_{all} .
 2) For the other flange calculate the crippling load, P_{cc} , and then $M_{flange} = P_{cc}(h-t)$.
 3) The total moment is then $M_{all} = M_{(1)} + M_{(2)}$.

Fig.C10.17 Reduced Web Strength Factor, C_4 Fig.C10.18 Reduced Web Strength Factor, C_5

Components can be maintained by installing a ring doubler which meets the requirements of Fig.C10.19 and the following limitations.

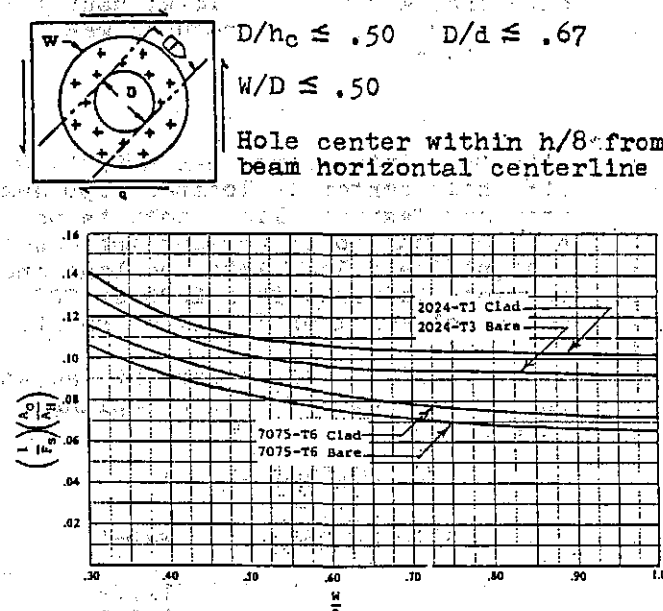


Fig.C10.19 Circular Hole Doubler Data

The rivet pattern is to be uniform and to

provide a running load strength per inch of $2F_{st} \times 10$ between tangent lines on each side of the hole. In the figure

t_r = reinforcing ring thickness

t = web thickness

F_s = Allowable web stress in ksi

A_0 = Cross-sectional area of the reinforcing ring = $2Wt_r$ sq in.

A_H = Cross-sectional area of the web removed by hole = Dt sq in

Using the figure, for a given (required) F_s and hole diameter, D , one can determine by successive trials the required size of the reinforcing ring and the required fasteners. Or, for a given hole, fastener pattern and reinforcing ring one can determine directly the value of F_s . Instead of being a separate piece, the reinforcing ring could be integral with the web (chem-milled or machined).

C11.24a Rivet Design

With a shear resistant (non-buckling) web the skin (or web) does not pry on the rivets and put them in tension. The only tension in the rivets then is that due to the "clamp-up" force, Q , as shown in Fig. D1.43c. When the web or skin buckles, the resulting "folds" try to go across the restraining upright or frame, and this puts the rivets in tension. The more severe the tension field (i.e., the larger the factor k), the larger is the tension in the rivets.

Equations (65) and (66)* specify the rivet joint tension strength required to prevent the folds in the buckled web or skin from lifting off of the upright or frame. This criteria was suggested by P. Kuhn in NACA TN 2661. The criteria does not involve the web stress or k , so it must be adequate for a very highly developed tension field, a large value of k . Hence, it will be quite conservative for a lesser tension field effect, a smaller k , and for a k of zero the required rivet tension strength (for this effect) would be zero. In view of this, some analysts assume that the above criteria for rivet strength applies down to a k of .50 or so, and then decreases linearly with k for lesser values of k , becoming zero for $k = 0$ (no web buckling). No further such data was published by the NACA, although some companies have run tests (unpublished) for smaller k values.

* of Art.C11.24

C11.31a General Discussion

On p.C11.30, item 5, at the end of the last sentence add the following: putting the rivets in tension

On p.C11.30, item 2, add: (e) the stringer bending moment (item 3) will increase.

On p.C11.31, R.H.Col., after the end of the 18th line down, add: For the case of stringers a more direct alternative method is in Ref.9, discussed later.

On p.C11.31 revise the "Floating rings sentence to be as follows: "Floating" rings support only the stringers and are therefore not attached to the skin, so they do not determine the spacing, d .

On p.C11.31, text line 26 down, put an * after A20 and add the footnote: * However, the effective skin area (per Art. A20.3) should be reduced per Eq. (83) as given later in Art.C11.32a.

On p.C11.32, R.H.Col., 4th line up, replace "before" with "assuming no"; put an * after "center" and add the footnote: * or better, at a point 70% of the way up from the lowest stressed edge (stringer) to the highest stressed edge (stringer), see Example Problem 1. Then at the end of the last line add "panel's".

C11.32a Stringer Systems in Diagonal Tension
Remainder of Part 2, Curved Web Systems

Beginning with the first line on p. C11.33, the remainder of Part 2 has been completely rewritten as follows.

compression stress increases more slowly. Thus one can write

$$f_c/f_s = B \\ \text{or} \\ f_c = B f_s \quad \dots \dots \dots \quad (73)$$

Substituting these formulas for F_{scr} and f_c back into the interaction formula, (71), one obtains

$$B f_s / A f_{scr} + (f_s / F_{scr})^2 = 1.0$$

Solving this quadratic for f_s

$$f_s = F_{scr} \left[-\frac{B}{A} + \sqrt{\frac{(B/A)^2}{A} + 4} \right] \quad \dots \dots \quad (74)$$

where f_s is the actual shear stress at which the panel buckles due to the presence of compression stresses. Calling this stress F_{scr} and calling the expression in the brackets R_c

$$F_{scr} = F_{scr} R_c \quad \dots \dots \dots \quad (75)$$

where

$$R_c = \frac{-B/A + \sqrt{(B/A)^2 + 4}}{2} \quad \dots \dots \quad (76)$$

R_c is always less than 1.0 when compression stresses are present. R_c is calculated for each panel.

Next, consider a panel subject to a shear stress and a tension stress, f_t . For this case it has been experimentally shown, Ref.6, that the interaction formula for buckling is

$$f_s / F_{scr} - f_t / 2F_{scr} = 1.0 \quad \dots \dots \quad (77)$$

The shear stress, f_s , at which the panel will buckle when tension is present is obtained from Eq.(77) as

$$f_{scr}' / F_{scr} = 1.0 + f_t / 2F_{scr}$$

or

$$f_{scr}' = (1.0 + f_t / 2F_{scr}) F_{scr} \quad \dots \dots \quad (78)$$

Calling the expression in parenthesis in Eq.(78) R_T and calling f_{scr}' F_{scr}'

$$F_{scr}' = F_{scr}' R_T \quad \dots \dots \quad (79)$$

where

$$R_T = (1 + f_t / 2F_{scr}) F_{scr} \quad \dots \dots \quad (80)$$

Since R_T is greater than 1.0 the actual shear buckling stress will always be greater than F_{scr} when tension is present and when the tension stress is large enough there will be no buckling.

Just as the compression stress reduces the panel's shear buckling stress, the shear stress also reduces the compressive buckling stress. Therefore, a factor, R'_c , is applied to the panel's effective area (items (1) and (2), p.A20.3) to obtain a reduced effective area (like having a smaller thickness). That is, the reduced compressive buckling stress is

$$f_{scr}' = R'_c F_{scr} \quad \dots \dots \quad (81)$$

where

$$R'_c = R_c (B/A) \quad \dots \dots \quad (82)$$

so,

$$A_{eskin} = A_{eskin} R'_c \quad \dots \dots \quad (83)$$

and A_{eskin} is used in all section property calculations and wherever effective skin areas are used (A_{eskin} is per Art.A20.3, items (1) and (2)).

2. Diagonal Tension Factor, k

The next step for each panel is the determination of the diagonal tension factor, k . This is a function of f_s / F_{scr}' where , as discussed above,

$$F_{scr}' = F_{scr} R_c \quad \text{or} \quad F_{scr}' = F_{scr} R_T$$

depending upon whether compression or tension stresses are present.

For a curved panel the formula for k as determined from many tests, Ref.3, is the empirical relationship

$$k = \tanh \left[(.5 + 300 \frac{td}{Rn}) \log_{10} \frac{f_s}{f_{scr}} \right] \quad (84)$$

with the auxiliary rules that

- a) if $d/h > 2$ use only 2
- b) if $h > d$ (longeron system) replace d/h with h/d and if $h/d > 2$ use only 2

k can also be found directly from Fig. C11.19.

3. Stringer Loads, Stresses and Strains

As in the case of the plane web system, the total stringer load will consist of the primary axial loads, P_p , due to the applied bending moments and/or axial loads, plus the diagonal tension induced loads, $P_{D.T.}$.

$$P_{STR} = P_p - P_{D.T.} \quad (85)$$

If P_p is tensile it would be a positive number in the above equation. P_p can be determined as in Chapter A20.2 - A20. $P_{D.T.}$ is calculated as follows, referring to Fig.C11.35a

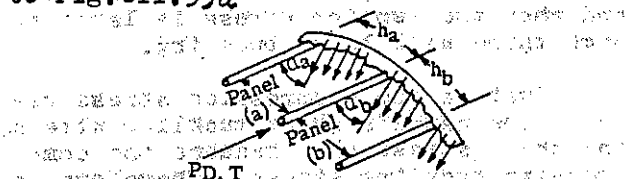


Fig.C11.35a Stringer Diagonal Tension Load

$P_{D.T.}$ is the diagonal tension load in a stringer bounded by panel "a" on one side and by panel "b" on the other. Let the width of panel a be h_a and that of b be h_b (for equally spaced stringers $h_a = h_b$). Let the shear flow in panel a be q_a and that in b be q_b . Then

$$P_{D.T.} = \frac{k_a q_a h_a \cot \alpha}{2} + \frac{k_b q_b h_b \cot \alpha}{2} \quad (86)$$

Ref.3 shows that a panel's effective area (at each stringer bordering it) for the diagonal tension load, $P_{D.T.}$, is

$$A_{D.T.} = .5ht(1-k)R_c/2$$

Therefore, the stringer stress is

$$f_{str} = f_p - f_{D.T.}$$

where f_p is negative when P is compressive and positive when P is tensile. So,

$$f_{str} = f_p - \frac{(kf \sin \alpha \cot \alpha)_a}{2A_{str} + .5(ht(1-k)R_c)_a} + \frac{(kf \sin \alpha \cot \alpha)_b}{.5(ht(1-k)R_c)_b} \quad (87)$$

If each panel has identical parameters or if their average values are assumed to be present in each panel Eq.(87) becomes

$$f_{str} = f_p - \frac{k f \sin \alpha \cot \alpha}{A_{str}/ht + .5(1-k)R_c} \quad (88)$$

The two panels can have identical parameters only when part of a circular shell subject only to torsion and compression, not to shear or bending which cause varying stresses, k and R_c values. However, for closely spaced stringers using average values and Eq.(88) is reasonable. The stringer strain, needed to determine α later, is

$$\epsilon_{str} = f_{str}/E_{str} \quad (89)$$

All terms in Eq.(87) and (88) are known except α , which is discussed later.

Per Art.C11.31, item 3, the diagonal tension generates bending of the stringers, bowing them inward. Per Ref.3 the result is a peak bending moment at the center of the stringer and at the ends (at the rings) in the amount

$$M_{str} = f_s h t d^2 k \tan \alpha / 24 R \quad (90)$$

where R is the radius of curvature

This produces tension on the inner surface of the stringer at its middle and compression on the inner surface at the rings. This bending is due to the diagonal tension and is increased when primary compression loads are also present (but not in defined amount, i.e., a beam-column effect).

Per Ref.3 $f_{D.T.}$ is an average stress. There is also a peak or maximum stress, $f_{D.T. MAX}$, calculated as

$$f_{D.T. MAX} = f_{D.T.} (f_{D.T. MAX}/f_{D.T.}) \quad (91)$$

where $f_{D.T. MAX}/f_{D.T.}$ is obtained from Fig.C11.21. $f_{D.T.}$ is the last term in Eq.(88). $f_{D.T. MAX}$ is used for a local strength check (see Example Problem).

4. Stresses and Strains in Rings

There are two types of rings. Conventional rings intersect the stringers and are notched to let them pass through, and are attached to the skin. So-called "floating" rings are located inside of the stringers and are not attached to the

skin. The resulting stresses in these two types of rings are therefore different.

Conventional Rings

Just as the tension field produces a compressive stress, $f_{D.T.}$, in the stringers it also produces a compressive stress f_{rg} in the rings. For circular shells this is, per Ref.3, for conventional rings

$$f_{rg} = \frac{k f_s \tan \alpha}{A g / d t + .5(1-k)} \quad (92)$$

Just as for stringers, Eq.(88), this assumes that the panels on each side of the ring have the same parameters (k , f_s , d , t , α). If not, Eq.(92) would be of a form similar to the last term in Eq.(87). However, as for stringers, average values can be used in Eq.(92) when the values are slightly different. The axial strain in the rings will be

$$\epsilon_{rg} = f_{rg} / E_{rg} \quad (93)$$

The strain is used to determine α .

Rings can also have a maximum or peak stress, like stringers (Eq.91), using f_{rg} in place of $f_{D.T.}$ in that equation. However, per Fig.C11.21, $f_{rg}/f_{rg\text{MAX}}$ will be 1.0 for typical stringer construction where $d/h > 1.0$, so there is then no peaking of the stress.

"Floating" Rings

For "floating" rings concentrated radial loads pushing inward on the rings are generated at the stringer locations, Fig.C11.30e. This produces a hoop compression in the circular ring and also a bending moment, since the radial loads are concentrated, not distributed. The axial compression in a floating ring is

$$f_{rg} = \frac{k f_s \tan \alpha}{A g / d t} \quad (94)$$

Note that there is no "effective" area term for this case. The axial strain in the ring, due to f_{rg} , is

$$\epsilon_{rg} = f_{rg} / E_{rg} \quad (95)$$

The maximum bending moment generated in the ring is

$$M_{rg} = k f_s t h^2 d \tan \alpha / 12R \quad (96)$$

It occurs at the ring-stringer junction, producing compression in the outer flange of the ring. There is a secondary bending moment, half as large, midway between the stringers. There is no "peak" stress for floating rings. As for conventional rings, Eq.(94) and (96) assume that the panels on each side of the ring have the same parameters.

Ring Stiffness (EI) Requirements

Since the rings support the stringers against general instability, see Fig.C9.7b, they must have an adequate EI. This value is affected by the diagonal tension loads in the stringers and is discussed in detail in Art.9.13a.

5. Strains in the Skin Panels

The strain in the skin panels is given in Ref.3 as

$$\epsilon_{sk} = \frac{f_s}{E} \left[\frac{2k}{\sin 2\alpha} + \sin 2\alpha (1-k)(1+\mu) \right] \quad (97)$$

where μ = Poisson's ratio (.33) and all terms are known except α . Fig.C11.36 is of help, giving the value of the bracketed term

6. Determination of α

For the stringer system ($d > h$) Ref.3 shows that α is related to the stringer strain, the ring strain and the web or skin strain by the formula

$$\tan^2 \alpha = \frac{\epsilon_{sk} - \epsilon_{str}}{\epsilon_{sk} - \epsilon_{rg} + h^2 / 24R^2} \quad (98)$$

where ϵ_{sk} is a tension (+) strain and ϵ_{rg} and ϵ_{str} are compression (-).

α is determined by successive approximation as follows. The strain equations are (for conventional rings)

$$\epsilon_{rg} = \frac{1}{E_c} \left[\frac{-k f_s \tan \alpha}{A g / d t + .5(1-k)} \right] \quad (93)$$

$$\epsilon_{str} = \frac{1}{E_c} \left[f_p - \frac{k f_s \cot \alpha}{A_{str} / h t + .5(1-k) R_c} \right] \quad (89)$$

$$\epsilon_{sk} = \frac{f_s}{E} \left[\frac{2k}{\sin 2\alpha} + (1-k)(1+\mu) \sin 2\alpha \right] \quad (97)$$

f_p is negative when in compression. To determine α for any panel use the values of k , f_s , R_c , t and d for that particular panel in the above strain equations. Also, for ϵ_{str} use the stringer bordering the panel which has the larger compressive value of f_p .

Assume a value for α , say 30° to 35° to start, and compute the values of the three strains. Then enter these into Eq.(98) and compute α . Compare with α assumed. Repeat as necessary until the calculated value of α is essentially the same as that assumed, and α is then known. Note that ϵ_{rg} and ϵ_{str} are negative, being in compression. For "floating" rings Eq.(94) is used in place of Eq.(93). Once α is known all of the stresses

and effects involving it are known.

7. Loads on the Attachments

The only remaining loads to be calculated are those on the attachments. These are of two types; those in the plane of the skins and those normal to the skins which are "prying" forces trying to "pop off" the rivet heads or to pull the skin upward around the rivets. These normal loads are most likely to be critical when countersunk rivets are present and are of small diameter.

The rivet loads due to the applied loads are called "primary" loads and those due to tension field action are "secondary" loads.

a) The secondary rivet shear loads must be considered whenever a shear-buckled skin is spliced or ends along an opening or "cut-out", such as along a stringer or a ring. At a splice or opening along a stringer the load per inch is

$$\text{Lbs/in} = f_{st} \left[1 + k \left(\frac{1}{\cos \alpha} - 1 \right) \right] \quad -(99)$$

Along a ring (a vertical direction) the loading is

$$\text{Lbs/in} = f_{st} \left[1 + k \left(\frac{1}{\sin \alpha} - 1 \right) \right] \quad -(100)$$

f_s is the total panel shear load and includes any redistribution effects due to a cut-out, as in Fig. D3.21. If the panel is non buckling then $k = 0$.

b) The normal or "prying" loads are not determinable by any formula from theory, but based on test data Ref. 3 recommends the following as the loading on the rivets.

When the skin is continuous across a ring or stringer

$$\text{Lbs/in} = .22tF_{tu} \quad - - - - - \quad (101)$$

When the skin stops along a ring or stringer (due to a cut-out)

$$\text{Lbs/in} = .15tF_{tu} \quad - - - - - \quad (102)$$

where t is the skin thickness and F_{tu} is the skin ultimate tensile strength.

These criteria are no doubt conservative and are discussed further in Art. C11.24a. Some data for the strength of rivet-skin combinations in the normal direction are in Fig. C11.37a, C11.37b and Art. D1.26. Flush heads are most likely to be critical.

C11.33a Allowable Stresses (and Interaction)

1. Stringers

Three methods of stringer analysis are presented:

- A "Quick Method" for preliminary sizing and quick checks.
- The N.A.C.A. Method which is quite tedious and therefore not recommended
- The Melcone-Ensrud Method which is the recommended one

The Quick Method

Two analyses are made, one for local strength and one for buckling. The local strength analysis uses the interaction equation

$$f_p/F_{cc} + (f_{D.T.} \text{Max}/F_{ST})^{0.5} = 1.0 \quad - - - (103)$$

where $f_p = M_y/I$, F_{cc} is the "natural" crippling stress, Art. C7.2, C7.4 or, better, Art. C7.30. $f_{D.T.} \text{Max}$ is per Eq. (91) and F_{ST} is per Fig. C11.38.

The buckling analysis uses the interaction equation

$$f_p/F_{cr} + f_{D.T.}/F_{D.T.} \text{cr} = 1.0 \quad - - - (104)$$

where F_{cr} = stringer buckling stress (Art. C7.26) using A_{eskin} in computing P_{str} and $L' = d$. However, torsional buckling is sometimes critical, Art. C7.31.

$F_{D.T.} \text{cr}$ = buckling stress due to diagonal tension load using an effective skin area of $.5ht(1-k)B_0$ in calculating P_{str} and $L = L/\sqrt{2}$ when stringer is continuous at both ends or $L' = L/\sqrt{1.5}$ when it is continuous at only one end.

However, in either case an effective skin area is not used in calculating P if this results in a larger P than for the stringer alone. This is because buckled skin has an undefined reduction effect on the stringer's buckling strength. (Fig. C7.36).

The N.A.C.A. Method

This is discussed only briefly since Method C, next, is recommended. Ref. 3 suggests the following analysis.

a) Local Strength Check

Consider the structure to be subject

only to its axial (or bending) applied loads, not to any shear, and calculate f_p and F_{cc} for the stringers. Then consider the structure to be subject only to its shear and torsion loads (no axial or bending loads) so that for all stringers $f_p = 0$. For any stringer the average shear in the two panels bordering it is f_s . Then using the last term (f_p) in Eq. (88) find by successive trials what value of f_s results in

$$f_{D.T. \text{ Max}} = F_{ST}$$

This is a very considerable effort, since for each assumed value of f_s one must determine numerous parameters k , ϵ 's, α etc. Then let this value of f_s be called F_{so} . The margin of safety is then found from the interaction equation

$$f_p/F_{cc} + (f_s/F_{so})^{.5} = 1.0 \quad \dots \quad (105)$$

by using Fig. C4.34 with R_b and R_t there being replaced with f_p/F_{cc} and f_s/F_{so} respectively. In Eq. (105) f_s is the actual (average) shear stress in the two panels bordering the stringer.

b) Buckling Check

The same approach as used in (a) applies, except that the allowable stress terms are F_{cr} instead of F_{cc} and F'_{so} instead of F_{so} and are determined as follows.

F_{cr} is determined in the same manner as for Eq. (104). As in (a), by successive trials find what value of f_s results in

$$f_{D.T.} = F_{D.T. \text{ cr}}$$

where $F_{D.T. \text{ cr}}$ is as defined for Eq. (104) in (a). Again, this is a very considerable effort as mentioned in (a). Then, let this value of f_s be called F_{so} and the margin of safety is determined from the interaction equation

$$f_c/F_{cr} + (f_s/F_{so})^{.5} = 1.0 \quad \dots \quad (106)$$

and can be found as suggested for Eq. (105).

The Melcone-Ensrud Method

This method is recommended since it is much more direct than method (b) and also considers the torsional stiffness of the stringer. As shown in Ref. 9, the stringer margin of safety is calculated as

$$\text{M.S.} = \frac{1}{[(f_p/F_{cr})^{.25} + ((f'_c + f''_c)/F'_c)^{.25}]^{.80}} - 1.0 \quad \dots \quad (107)$$

where

f_p = compressive stress in stringer due to the primary shell loads ($M_y/I + P/A$), bending and axial, as present.

F_{cr} = stringer critical load as a column calculated as discussed for Eq. (104).

F'_c = buckling strength of the stringer itself, considering crippling, and using a fixity of 2 when the stringer is continuous across rings at each end and 1.5 when continuous at only one end.

f'_c = See Table C11.1

f''_c = See Table C11.1

Table C11.1 involves five parameters which are defined as follows

$$v = 1 + (d/R) [(I_{str}/J_{str})(t/h)]^{.25}$$

where J_{str} = torsional stiffness factor

$$= A_{str} t_{str}^{.25} / 3 \text{ for open sections}$$

$$= 4A^2 t_{str} / p \text{ for closed sections}$$

where A = enclosed area

p = perimeter

$$\lambda = 1/(1 + f_{cg}/f_s)^{.25}$$

where f_{cg} = applied primary compressive stress based on stringer area plus total skin area (fully effective). When $f_{cg} = 0$, $\lambda = 1.0$ (no applied compressive loads). That is, $f_{cg} = M_y/I_{gross} + P/A_{gross}$.

$$F'_s = (\pi/4S^{.25})(Et/R)$$

where $S = d^2/8t$

$$F''_s = 5.25E(t/h)^2$$

$$F_{scr} = F'_s + F''_s$$

Table C11.1 Determination of f'_c and f''_c

$$f'_c = 0 \text{ when } f_s < \lambda F_{scr} \text{ (no buckling)}$$

$$f'_c = \frac{v(f_s - \lambda F_{scr})ht}{A_{str}} \text{ when } f_s \geq \lambda F_{scr}$$

$$f''_c = 0 \text{ when } f_s < \lambda F'_s$$

(Continued)

Table C11.1 (Con'd)

$$f_c'' = \frac{(f_s - \lambda F_s)(\lambda F_s dt)}{F_s' Astr} \left(\frac{.053h}{d} \right)^{3/3}$$

when $\lambda F_s \leq f_s < F_{scr}$

$$f_c'' = \frac{\lambda F_s dt}{Astr} \left(\frac{.053h}{d} \right)^{3/3} \quad \text{when } f_s \geq F_{scr}$$

When the value of f_s varies in the panels above and below the stringer use the average, or more conservatively use the larger. If h or t varies use the average.

The following is applicable to all three methods. If a stringer has a negative margin of safety it does not mean failure if the other stringers can carry enough of the shell's applied bending moment to prevent this (see Art.A19.11). However, each stringer must carry its own diagonal tension load, P.D.T..

Also, since diagonal tension loads do not vary linearly with the applied loads, the margins of safety as calculated are actually apparent ones rather than true ones (see Art.C1.13a, item 2), but this is not always considered. This also applies to other parts loaded by the tension field action.

It is, of course, best to determine F_{cr} from compression tests of a segment of the shell having four or five stringers, but this is expensive to do although it eliminates uncertainties.

2. Rings

Rings have allowable stresses similar to those for stringers. For conventional rings the margin of safety is obtained using the equation:

$$M.S. = \frac{1}{f_p/F_{cr} + f_{rgMax}/F_{rg}} - 1.0 \quad \text{--- (108)}$$

where f_p is the largest compressive stress in a flange due to any primary loading on the ring (bending and compression) if any, and F_{cr} is the crippling stress for that flange.

f_{rgMax} is f_{rg} (no peaking here for the stringer system), Eq.(92).

F_{rg} is the allowable forced crippling stress for the ring, per Fig.C11.38.

Since conventional rings are notched to let the stringers pass through, it is important to use an adequate clip at the notch to prevent local buckling of the ring's notched web.

Floating rings are not subject to any forced crippling, only to any axial stresses or bending stresses caused by primary loads, if any, and to the axial stress of Eq.(94) and to M_{rg} of Eq.(96). The margin of safety is calculated for the flange critical for these loads as

$$M.S. = \frac{F_{cc}}{f_c + f_b + f_{rg} + f_{Mrg}} - 1.0 \quad \text{--- (109)}$$

3. General Instability

A general instability check for the shell can be made using the empirical criteria presented in Fig.C11.39. This is obtained from test data and recommendations of Ref.7 and Ref.3. The allowables are based upon pure torsion tests. The margin of safety is calculated as

$$M.S. = \frac{F_{sInst}}{f_s} - 1.0 \quad \text{--- (110)}$$

4. Margin of Safety for the Skin

The allowable skin stress can simply be read from Fig.C11.42 as F_s . The margin of safety is calculated as

$$M.S. = F_s/f_s - 1.0 \quad \text{--- (111)}$$

f_s is the gross skin stress (ignoring rivet holes). The net shear stress (between rivet holes) can be carried up to F_{su} , the ultimate shear stress for the skin material.

5. Margin of Safety for Attachments

For any attachment (rivet) the margin of safety is calculated as

$$M.S. = \frac{\text{Joint Allowable Load}}{\text{Attachment Spacing (Load/in)}} - 1.0 \quad \text{--- (112)}$$

where the Load/in is as follows

a) At a splice or edge along a stringer (horizontal) Eq.(99) applies.

b) At a splice or edge along a ring (vertical) Eq.(100) applies

c) For a change in stress, or shear flow, across a ring or stringer (no edge or splice) Δf_s is used instead of f_s in Eq.(99) or (100).

Eq.(112) applies for, both, in-plane and normal loads. The joint allowable load is the allowable load per rivet.

The following Example Problem illustrates the analysis procedure.

C11.34a Example Problems

Determine the following margins of safety for the structure shown in Fig. C11.43a. All loads are ultimate.

- Skin rupture for panels a, b and c
- General instability in shear based on the shear in panel b
- Interrivet buckling of skin along stringer 2 in bay AB
- Stringer 2 between panels a and b
- The fasteners along stringer 1, assuming the skin is spliced there
- The ring between panels a and c and stringers 1 and 2
- The fasteners along the ring at A in panel b assuming the skin is spliced
- The fasteners in panel b along ring B

Internal Loads

The first step is to determine the internal loads in the structure due to the applied (external) loads. This can be done as discussed in Chapter A.20, or it may be done by finite element analysis. For tension field analysis purposes, it is necessary to do this for two structural conditions, first assuming the skin

does not buckle and then with the skin in the buckled condition. For the latter condition this is a successive trials procedure, since buckled panels have effective widths which depend upon the panels stress, and the stresses depend upon the amount of effective skin area.

It is assumed here that the internal loads have been determined for the shell and its applied loads, which are a shear, a torsion and a bending moment. The following table summarizes those internal loads and the geometry needed for the required analyses. All loads are ultimate.

Table C11.2 Internal Loads and Geometry

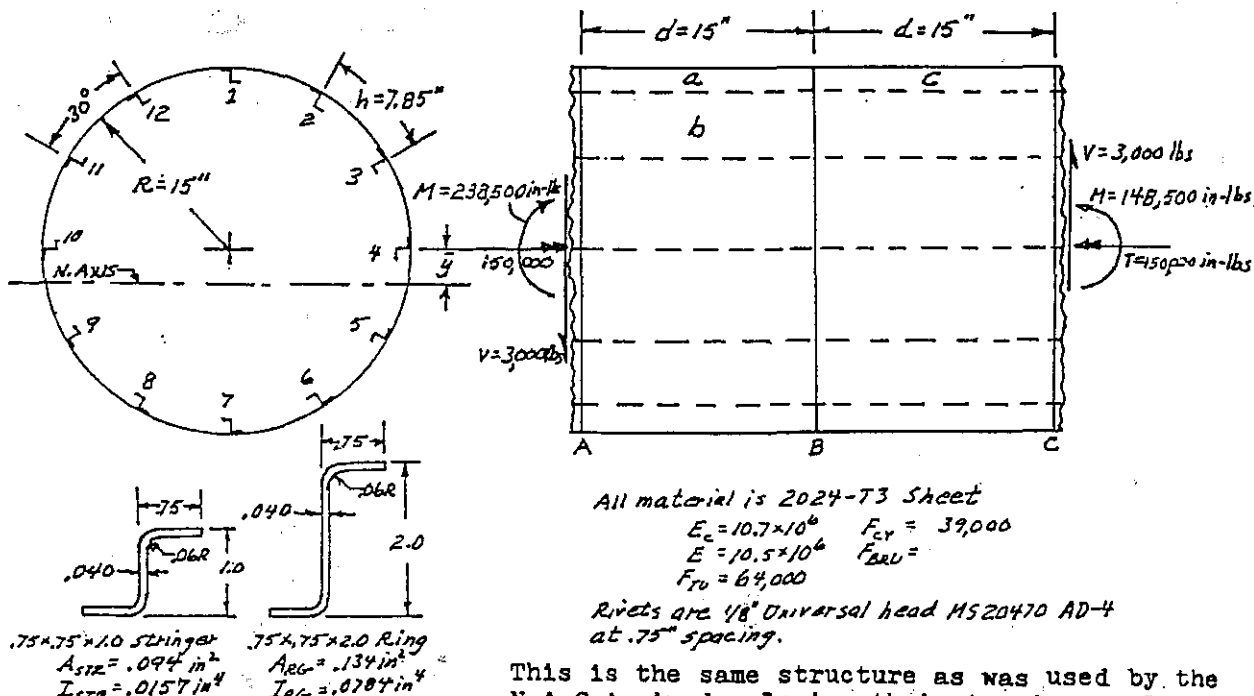
Condition of Skin	q_a lb/in ⁵	q_b lb/in ⁵	q_c lb/in ⁵	y^1 in	y_a in	y_b in	y_c in
No Buckling	111	121	111	0	14.40	11.34	14.40
Buckled	116	125	116	2.71	17.11	14.05	17.11

Table C11.2 (Continued)

Condition of Skin	y_{str1} in	y_{str2} in	MBC ³ in-lbs	MAB ³ in-lbs	I ⁴ in ⁴
No Buckling	14.61	12.65	171,000	216,000	382
Buckled	17.32	15.36	171,000	216,000	276

Notes

- For panels y is measured from the shell's neutral axis to a point 70% of the distance from the lower edge to the upper edge (rather than to the midpoint).
- For stringers y is to the stringer + effective skin centroid.



This is the same structure as was used by the N.A.C.A. in developing their tension field criteria, except that t_{str} was .080 there.

Fig.C11.43a Shell with Stringer Construction for Example Problem

3. M_{AB} and M_{BC} are bending moments at the middle of bay AB and BC respectively.

4. The same I is used for bay AB and BC although I_{AB} would be slightly smaller since the larger bending moment would result in less effective skin area.

5. $q = f_{st}$ (the formulas use f_{st})

Skin Panel Analyses

The analysis is illustrated for panel a only. The results of similar analyses for panels b and c are presented.

$$a/b = 15/7.85 = 1.91; Z = \frac{15^2(1-.33^2)^{.5}}{15(.025)} = 155; k_s = 32 (\text{Fig. C9.4}); k_c = .56 (\text{Fig. C9.1})$$

$$F_{scr} = 32\pi^2(10.7 \times 10^6)(.025)^2 / 12(1-.33^2) \\ (7.85)^2 = 3,205 (\text{Fig. C9.4})$$

$$F_{ccr} = \frac{56\pi^2(10.7 \times 10^6)(.025)^2}{(7.85)^2} / 12(1-.33^2) = 5,609 (\text{Fig. C9.4})$$

$$A = F_{ccr}/F_{scr} = 5609/3205 = 1.75 (\text{Eq. 72})$$

For the non-buckled skin (to determine R_c , F_{scr} and R_c)

$$f_c = My/I = 216,000(14.4)/383 = 8,121$$

$$f_s = q/t = 111/.025 = 4,440$$

$$B = f_c/f_s = 8121/4440 = 1.83 (\text{Eq. 73})$$

$$B/A = 1.83/1.75 = 1.05$$

$$R_c = (-1.05 + \sqrt{1.05^2 + 4})/2 = .60 (\text{Eq. 76})$$

$$R'_c = R_c(B/A) = .63 (\text{Eq. 82})$$

$$F'_{scr} = 3,205(.60) = 1,923 (\text{Eq. 75})$$

For the skin in the buckled condition

$$f_s = q/t = 116/.025 = 4,640$$

$$f_s/F'_{scr} = 4,640/1,923 = 2.41$$

$$300td/Rh = 300(.025)(15)/15(7.85) = .955$$

$$k = .51 (\text{Fig. C11.19})$$

$$F_s = 23,000 (\text{Fig. C11.42})$$

$$M.S.\text{ rupture} = 23000/4640 - 1.0 = \underline{\text{High}}$$

$$\epsilon_{sk} = f_s [2x.51/\sin 2\alpha + .652 \sin 2\alpha] / E \\ = .000442(1.02/\sin 2\alpha + .652 \sin 2\alpha) \\ - - - (\text{Eq. 97})$$

$$\alpha = 25.4^\circ (\text{see "Determination of } \alpha \text{"})$$

Proceeding similarly for panels b and c

$$R_{cb} = .69, k_b = .46, F_{sb} = 23,500, \\ f_{sb} = 5,000, R_{cb} = .52, \alpha_b = 24.8^\circ, \\ M.S.b = \underline{\text{High}}$$

$$R_{cc} = .67, k_c = .45, F_{sc} = 23,000, \\ f_{sc} = 4,640, R_{cc} = .56, \alpha_c = 24.0^\circ, \\ M.S.c = \underline{\text{High}}$$

Interrievet buckling along stringer 2 in bay AB

$$F_{ir} = \frac{\pi^2 \times 10.7 \times 10}{(.75/.58 \times .025)^2} = 39,473 (\text{Eq. C7.22})$$

$$f_c = f_{ccr} + f_{D.T. \text{ Max}} = \frac{216,000 \times 15.7}{276 + 9,761} (\text{see "Stringer"}) = 22,048$$

$$M.S. = 39473/22048 - 1.0 = .79$$

General Instability

The following is based upon panel 2 (it is more critical for panels at the neutral axis where panel shear stress is larger). Per Fig. C11.39 and its notes

$$\frac{F_{str} \rho_{rg} \times 10^3}{(dh)^2 R^{.75}} = \frac{409 \times .765 \times 10^3}{(15 \times .785)^2 \times 15^{.75}} = 44.8$$

$$F_{sInst}/E_c > 3,000$$

$$F_{sInst} > 3,000 \times 10.7 \times 10 > 32,000$$

$$f_s = 5,000$$

$$M.S. > 32,000/5,000 - 1.0 = \underline{\text{High}}$$

Stringer 2 (between panels a and b)

This will be checked using the three methods discussed and using an average of the values for data in panels a and b

$$f_{str} = f_p - f_{D.T.}$$

$$= \frac{My}{I} - \frac{k f_{sc} \cot \alpha}{A_{str}/ht + .5(1-k)R_c} (\text{Eq. 88})$$

$$= \frac{-216000(15.36)}{276} - \frac{.485(4820) \times}{.094/7.85 \times .025 +}$$

$$\frac{\cot(24.8^\circ)}{.5(1 - .485)(.645)}$$

$$= -12,021 - 7,736 = -19,757$$

$$f_{D.T. \text{ Max}} = -7,986(f_{D.T. \text{ Max}}/f_{D.T.}) (\text{Eq. 91})$$

$$= -7,936(1.23) = -9,761$$

$$F_{st} = N \times C = 21,800(.883) = 19,249 (\text{Fig. C11.38})$$

$$f_{str \text{ only}} = .409 \quad F_{cc} = 28,600$$

The three types of analyses follow.

Quick Analysis

Local Strength

$$12,021/28,600 + (9761/19,249)^{.5} = .776 \quad (\text{Eq.103})$$

M.S. = .23 (Fig.C4.34)

Buckling Strength

Per Eq.(104) and its discussion

$$F_{cr} = 28600 - 28600^2 (15/.409)^2 / 4\pi^2 \times 10.7 \times 10^6$$

$$= 25,995 \quad (\text{Eq.C7.31})$$

$$F_{DT,cr} = 28,600 - 28,600^2 (15/\sqrt{2} \times .348)^2 /$$

$$4\pi^2 \times 10.7 \times 10^6 = 26,801 \quad (\text{Eq.C7.31})$$

$$\text{M.S.} = \frac{1}{12021/25995 + 7736/26801} - 1.0$$

$$= \underline{.32} \quad (\text{Eq.104})$$

N.A.C.A. Method

Local Strength

For an applied torque loading only it is found after several successive trials that when f_s is 10,600 psi the resulting value of $F_{DT,MAX}$ is equal to F_{ST} (Fig.C11.38). Then, per Eq.(105) with $F_{so} = f_s = 10,600$

$$12021/28600 + (4820/10600)^{.5} = .727 \quad (\text{Eq.105})$$

M.S. = .30 (Fig.C4.34)

Buckling Strength

As above, it is found that when f_s is 13,400 psi the resulting values of F_{DT} and $F_{DT,cr}$ are equal. Then, per Eq.(106 with $F_{so} = f_s = 13,400$)

$$12021/25995 + (4820/12400)^{.5} = .678 \quad (\text{Eq.106})$$

M.S. = .39 (Fig.C4.34)

Melcone-Ensrud Method

$$f_c = 12,021, \quad F_c = 25,995,$$

$$F_c = 27,300, \quad f_s = 4,820$$

$$I_{str} = .0157, J_{str} = 094(.040)^2/3 = .000050$$

$$\tau = 1 + (15/15) \left[(.0157/.00005)(.025/7.85) \right]^{.25}$$

$$= 2.0$$

$$f_{cg} = My/I_{gross} = 21600(12.55)/383$$

$$= 7,078$$

$$\lambda = 1/(1 + 7078/4820)^{.25} = .798$$

$$S = 15^2/15(.025) = 600$$

$$F_s = \pi/4(600)^{.25} (10.7 \times 10^6 \times .025)/15 = 2,777$$

$$F_s'' = 5.25 \times 10.7 \times 10^6 (.025/7.85) = 559$$

$$F_{scr} = 2777 + 559 = 3,336$$

$$\lambda F_{scr} = .798(3336) = 2,662$$

$$f_c' = 2.0(4820 - 2662)(7.85)(.025/.094)$$

$$= 9,011$$

$$f_c'' = .798(559)(15)(.025)(.053 \times 7.85/15)/.094$$

$$= 539$$

$$\text{M.S.} = \frac{1}{\left[\frac{(12021)^{.25}}{25995} + \frac{(9011 + 539)}{27300} \right]^{.25} \times .80} - 1.0$$

$$= \underline{.37}$$

Summary of M.S. Results for Stringer 2

Item M.S.	Quick Analysis	N.A.C.A.	Melcone Ensrud
Local Strength	<u>.23</u>	<u>.30</u>	<u>.37</u>
Buckling	<u>.32</u>	<u>.39</u>	

Ring B (Between Stringers 1 and 2)

$$frg = \frac{fp}{F_{cc}} - \frac{k_f \tan}{Arg/dt + .5(1-k)} \quad (\text{Eq.92})$$

This adds the fp ratio not shown in the Eq.(92) previously but which applies when any primary loads are present on the ring. Using average values of the two panels (a and c) on each side of the ring, (fp and F_{cc} would be for the critical flange)

$$frg = -\frac{.48(4640)\tan 24.7^\circ}{.134/15 \times .025 + .5(1-.48)} = -7,844$$

$$frg_{Max} = 1.0, \quad frg_{Max} = 7,844 \quad (\text{Fig.C11.21})$$

$$Frg = NxG = 14000 \times .883 = 12,362 \quad (\text{Fig.C11.38})$$

$$\text{M.S.} = 12362/7844 - 1.0 = \underline{.58}$$

Attachments

Assuming a splice in the skin along stringer 1, the load/in is larger for panel a

$$\text{Load/in} = 4640 \times .025 \cdot 1 \cdot .51(1/\cos 25.4 - 1)$$

$$= 122 \quad (\text{Eq.99})$$

$$\text{Load/attachment} = 122(.75) = 92 \text{ lbs}$$

$$\text{Pall/attachment} = 356 \text{ lbs} \quad (\text{joint data})$$

$$\text{M.S.} = 356/92 - 1.0 = \text{High}$$

There is also the normal loading/in of

$$\text{Load/in} = .22(.025)(64000) = .352 \text{ lbs/in}$$

(Ea.102)

$$\text{Load/atm't} = 352(.75) = 264 \text{ lbs}$$

$$\text{Pall/atm't} = 197 \text{ lbs (Art.D1.26, Table A)}$$

$$\text{M.S.} = 197/264 - 1.0 = -.25$$

For the required M.S. of .15 the rivet spacing would have to be reduced to about .48 in.

For a splice along Ring B in the region of panel b

$$\text{Load/in} = 5000x.025[1+.46(1/\sin 24.8^\circ - 1)]$$

$$= 205 \text{ lbs/in} \quad (\text{Eq.100})$$

$$\text{Load/rivet} = 205(.75) = 154 \text{ lbs}$$

$$\text{M.S.} = 356/154 - 1.0 = 1.31$$

The tension M.S. here is the same as for the longitudinal splice above (-.25) and would also require the above .48 spacing

Determination of α in the Panels

$$\text{Panel a: } k = .51, f_s = 4640$$

$$R_c = .60, M = 216,000$$

$$\epsilon_{rg} = -\frac{1}{10.7 \times 10^6} \left[\frac{.51(4640) \tan \alpha}{.134/15 \times .025 + .5(1-.51)} \right]$$

$$= -.000367 \tan \alpha \quad (\text{Eq.93})$$

$$\epsilon_{str} = \frac{1}{10.7 \times 10^6} \left[\frac{216,000(17.32)}{276} - \frac{.51(4640) \cot \alpha}{.094/7.85 \times .025 + .5(1-.51)(.60)} \right]$$

$$= -.001267 - .000353 \tan \alpha \quad (\text{Eq.89})$$

$$\epsilon_{sk} = \frac{4640}{10.5 \times 10^6} \left[\frac{2(.51)}{\sin 2\alpha} + (1-.51)(1 + .33) \right] \times \sin 2\alpha$$

$$= .000451/\sin 2\alpha + .000288 \sin 2\alpha \quad (\text{Eq.97})$$

$$\tan^2 \alpha = \frac{\epsilon_{sk} - \epsilon_{str}}{\epsilon_{sk} - \epsilon_{rg} - (7.85/15)^2 / 24}$$

$$= \frac{\epsilon_{sk} - \epsilon_{str}}{\epsilon_{sk} - \epsilon_{rg} - .011412} \quad (\text{Eq.98})$$

After several trials it is found that when $\alpha = 25.4^\circ$ is used in the strain equations the resulting value of α from Eq.(98) is also 25.4° , hence $\alpha = 25.4^\circ$ for panel a

$$\text{Panel b: } k = .46, f_s = 5,000$$

$$R_c = .69, M = 216,000$$

and

$$\epsilon_{rg} = -.000342 \tan \alpha$$

$$\epsilon_{str} = -.001123 - .000323 \cot \alpha$$

$$\epsilon_{sk} = .000438/\sin 2\alpha + .000342 \sin 2\alpha$$

Proceeding as for panel a, $\alpha_b = 24.5^\circ$

$$\text{Panel c: } k = .45, f_s = 4,640$$

$$R_c = .69, M = 171,000$$

Proceeding as for panel a, $\alpha_c = 24.0^\circ$

These values of α were used in the previous calculations of stresses due to diagonal tension action.

Final Note

To illustrate the analyses, only the region in the upper portion of the shell has been considered, where the stringers are more critical. The shear is higher in the panels near the neutral axis, so the panels, rings and splice attachments will be more critical there.

LONGERON SYSTEM

C11.35a Longeron System in Diagonal Tension

The longeron structural system is somewhat simpler from a total analysis standpoint. This is because there are fewer members carrying the axial loads and not as many shear panels with varying shear loads. This type of structure may, or may not, be the optimum arrangement from a weight and manufacturing cost consideration for a particular airplane; that requires an optimization study. The methods of analysis presented here would, however, have a place in calculations for such a study.

Some typical types of longeron structural systems cross-sections for a fuselage are shown in Fig.C11.44a. and C11.47a.

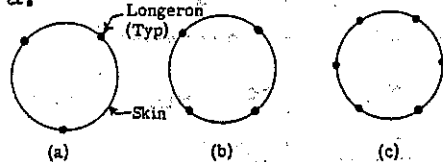


Fig.C11.44a Longeron System Structures

Fig.(a) shows the minimum arrangement as to the number of longerons, since at least three axial members are needed for equilibrium when bending moments in more than one plane are present. However, this does not provide a "fail-safe" design, since failure of any one member will not leave a structure capable of withstanding some arbitrary required percentage (usually 60-67%) of the design ultimate loads. The system

shown in Fig. 44b is capable of doing this and is the minimum type acceptable from the fail-safe standpoint (four longerons). Four to eight longerons are normally used depending upon other design and manufacturing factors.

The longeron system, however, requires more closely spaced rings than does the stringer system. The spacing is set after trade-off studies are made and is usually four to eight in., depending upon the size of the fuselage. The rings support the skin, dividing it into smaller panels. They also support the longerons in the same manner that "uprights" support the flanges in a plane web beam, but not in a radial direction. There are no "floating" rings in the longeron system.

After buckling the skin has tension folds which, rather than being "flat" as in the stringer system, lie on a hyperboloid of revolution. That is, they flatten diagonally between the closely spaced rings (see Ref. 3 and 7). In this system $d < h$, see Fig. C11.34.

C11.36a Analysis of Longeron System in Diagonal Tension

The engineering procedure for calculating the stresses and allowables for the longeron system is similar to that for the stringer system. The reader will note the differences.

1. First, at any bay being checked one determines the primary internal loads distribution in the longerons and shear panels, due to the primary applied loads, using engineering bending theory or a finite element analysis. Effective skin per Eq.(83) is used with the longerons in compression.

2. Next, one determines the shear buckling stresses in the skin panels. Since compression stresses are often present, pure shear buckling does not occur. Thus, as discussed for stringers, some rational interaction is used to obtain a "reduced" shear buckling stress. This can be done, for example, by using some "average" compression in the panel, weighted toward the high side for conservatism. Thereby the interaction method of Art. C11.32 can be used where

$$R_c = \frac{-B + \sqrt{(B^2) + 4}}{A}, \text{ as in Eq.(76)}$$

and A is determined for a curved panel of length "d" between rings and height "h" between longerons measured along the circumference, as in Fig. C11.34. B is the ratio f_c/f_s for the particular loading

condition being investigated. The compression stress is calculated for no skin buckled. Then, as in Eq.(75), the reduced shear buckling stress is

$$F_{scr}' = R_c F_{scr}$$

The effective skin areas are reduced by the shear stresses, per Eq.(83)

When tension strains are present with the shear then, as in Eq.(77)

$$R_T = 1.0 + ft/2F_{cr}$$

and

$$F_{scr}' = R_T F_{scr}, \text{ as in Eq.(79)}$$

3. Next, the loading ratio, f_s/F_{scr}' , can be calculated using F_{scr}' as determined in 2 above.

4. The diagonal tension factor, k, is obtained from Fig. C11.19.

5. The total axial stress in the longeron can be written as follows

$$f_L = f_P - f_{D.T.}$$

$$= f_P - \frac{k f_{sht} \cot \alpha_a}{2A_L + (.5ht(1-k)R_c)_a} + \frac{k f_{sht} \cot \alpha_b}{2A_L + (.5ht(1-k)R_c)_b} \quad (113)$$

where

f_P = primary stress from step (1), (+) if tension and (-) if comp.

A_L = Longeron Area

and

k, f_s , $\cot \alpha$, R_c , R_T , h, and t are as previously defined. One set, subscript (a), is for the panel above the longeron, and the other, (b), for the panel below it.

6. The average stress in the supporting ring (or frame) due to diagonal tension is given by the following formula (and note that this is different from that in the stringer system)

$$f_{rg} = - \frac{k f_s \tan \alpha}{\frac{Arg_e}{dt} + .5(1-k)} \quad (114)$$

where (as in Eq.(58))

$$Arg_e = Arg/(1 + (e/\rho)^2)$$

This formula is similar to that for the effective area of a single upright in a plane web system, Art. C11.20) where

e = distance from ring c.g. to the skin meanline

ρ = radius of gyration of the ring

cross-section about an axis parallel to the skin.

Equation (114) assumes that k , f_s , d , t , etc. are the same for the panels on each side of the ring. If not, then the average value should be used, otherwise, f_{rg} must be written as the sum of two effects, as was done for the longeron in Eq. (112).

If the ring (or frame) also has internal loads due to the primary applied loads, then a term f_p should be included in Eq. (114), as discussed for Eq. (108). This is most likely to be significant for the larger "frames" rather than for rings

The maximum stress, f_{rgMax} , in the ring will be

$$f_{rgMax} = f_{rg} \left(\frac{f_{rgMax}}{f_{rg}} \right) - - - (115)$$

where f_{rgMax}/f_{rg} is from Fig. C11.21.

7. The diagonal tension angle, α , for each panel (needed for the various equations) can be calculated in two ways for the longeron system. The quickest method, for preliminary sizing particularly, is to determine α directly from Fig. C11.45. The more accurate, but more tedious, is similar to that shown for the stringer system, as follows

$$\epsilon_{rg} = \frac{1}{E_c} \left[\frac{k f_s \cot \alpha}{A_{rg}/dt + .5(1-k)} \right] - - - (116)$$

$$\epsilon_L = \frac{1}{E_c} \left[f_p - \frac{k f_s \cot \alpha}{A_L/ht + .5(1-k)R_c} \right] - - - (117)$$

$$\epsilon_{sk} = \frac{f_s}{E} \left[\frac{2k}{\sin 2\alpha} + (1-k)(1+\mu) \sin 2\alpha \right] - - - (118)$$

where f_p , due to primary loads, is negative when in compression.

The equation for α is slightly different from the stringer system:

$$\tan^2 \alpha = \frac{\epsilon_{sk} - \epsilon_L}{\epsilon_{sk} - \epsilon_{rg} + (d/R)^2 (\tan^2 \alpha / 8)} - - - (119)$$

α is determined by successive trials as discussed for the stringer system. For the initial trial a value for α of 30° - 35° is reasonable, or use the value from Fig. C11.45.

8. Strength checks can then be made as follows

Longerons

The longeron acts as either a column or a beam-column, supported by the major frames (not by the rings) which have some spacing, L (which is much larger than d).

If the longeron is "straight" between the frames and has no radial loads from any ring, it can be analyzed as a column. If it has curvature between frames or radial loads from any ring it is a beam-column. In either case, although it may be continuous across supporting frames, it is usually conservatively assumed to be pin ended and of length L .

Column Analysis

$$P_{long} = P_p - P.D.T.$$

$$= f_p (A_L + A_{esk}) - \left[(k f_s h t \cot \alpha)_a / 2 + (k f_s h t \cot \alpha)_b / 2 \right]$$

$$P_{cr} = F_{cr} (A_L + A_{esk}) - - - (121) - - - (120)$$

where f_p = primary axial compression (-) stress, A_{esk} is per Eq. (83), F_{cr} is per Eq. (C7.31) or Fig. C7.33, with $F_{es} = F_{cc}$ per Art. C7.30, with L distance between major frames and f_p calculated with A_{esk} . Then,

$$M.S. = P_{cr} / P_{long} = 1.0$$

Beam-Column Analysis

If the longeron is a beam-column as described above, local failure must be checked for the critical compression flange stress which is

$$f = f_c + f_{D.T.} + M/I - - - (122)$$

where f_c is the primary compression (-) stress, and M is the bending moment due to beam-column action including A_{esk} . M will cause tension (+) in one flange and compression (-) in the other. Then

$$M.S. = 1 / (R_c + R_{D.T.} + R_{bend}) = 1.0$$

where R_c and R_{bend} are per Art. C3.18, Method 1 and $R_{D.T.} = f_{D.T.} / F_L$ where F_L is from Fig. C11.38.

Or, since R_c is per Art. C3.18, Method 2,

$$M.S. = \frac{f_c + M_c / I}{F_c} + \frac{f_{D.T.}}{F_L} = 1.0$$

where F_c is per Art. C3.18, Method 2. The larger of the above M.S. is used.

$f_{D.T.}$ is defined in Eq. (113). For a longeron fully supported (in two directions), as in Fig. C11.47a, there is no column or beam-column action since $M = 0$. Therefore

$$M.S. = 1 / (f_c / F_c + f_{D.T.} / F_L) = 1.0 - - - (123)$$

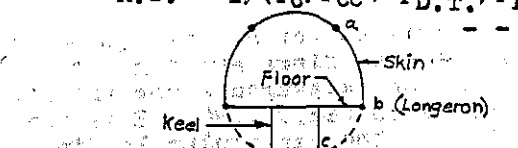


Fig.C11.47a Fully Supported Longeron (b)

Rings

$$M.S. = \frac{F_{rg}}{f_{rgMax}} - 1.0$$

Where F_{rg} is per Fig.C11.38

If the rings have stresses, f_p , due to any primary loads then

$$M.S. = 1/(f_p/F_{cc} + f_{rgMax}/F_{rg}) - 1.0$$

Skins

Strength check for skin rupture

$$M.S. = \frac{F_s}{f_s} - 1.0$$

where F_s is per Fig.C11.42

Permanent Buckling

Usually no permanent buckling is allowed at limit load.

$$M.S. = \frac{F_{sp,B.}}{f_s} - 1.0$$

where $F_{sp,B.}$ is per Fig.C11.46

General Instability

$$M.S. = \frac{F_{sInst}}{f_s} - 1.0$$

where F_{sInst} is per Fig.C11.39. Note that no effective skin is used and that f_{long} is limited to .34 at most. A M.S. of at least .15 is recommended.

Attachments

The margins of safety for the attachments are calculated in the same manner as discussed for the stringer system.

C11.37a Example Problem

Determine the following margins of safety for the structure in Fig.C11.48a and its ultimate applied loads.

- a) Skin rupture for panels a and b
- b) Skin permanent buckling
- c) Interrivet buckling along longeron 1
- d) General instability based on panel b
- e) Longeron 1
- f) Ring at A between longerons 1 and 2
- g) Fasteners along longeron 1 assuming skin is spliced there
- h) Fasteners along ring A, assuming skin is spliced there
- i) Same as (g) assuming no splice there.

As for Example Problem 1, the primary loads are determined for, both, the condition of no skin buckling and then for the skin buckled. The following table presents those internal loads and geometry needed for the above analyses.

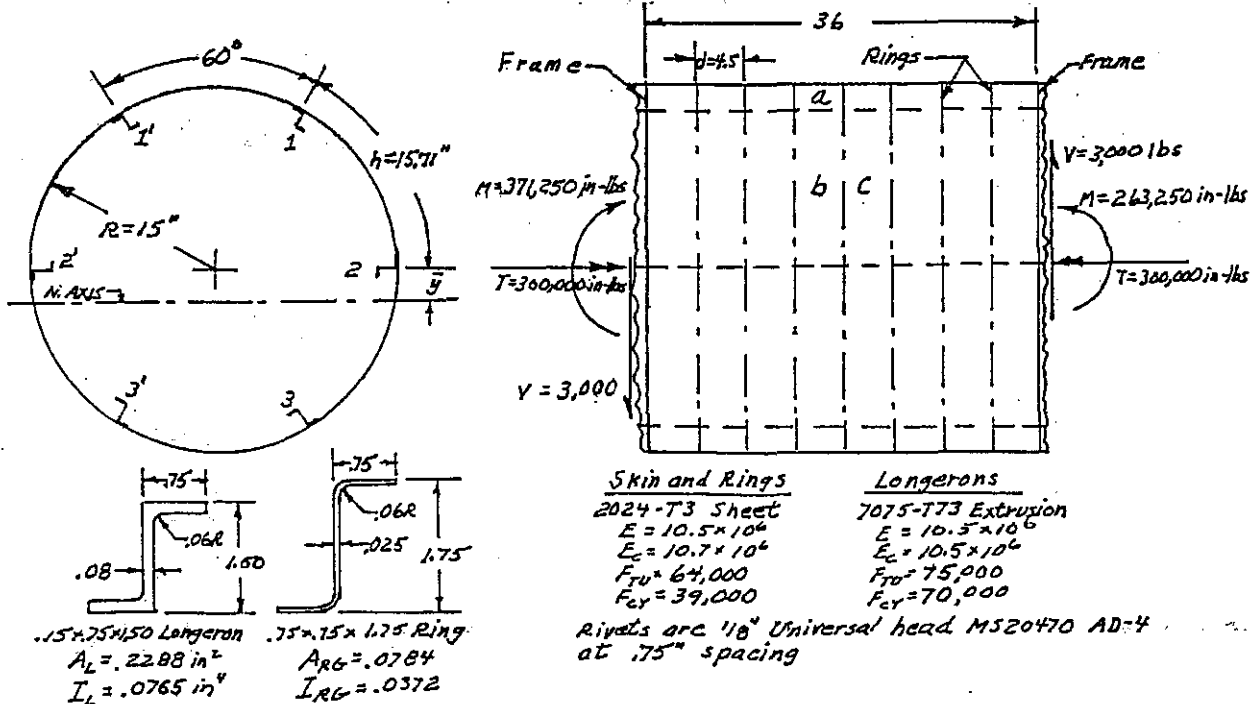


Fig.C11.48a Shell with Longeron Construction for Example Problem

Table C11.3 Internal Loads and Geometry

Condition of Skin	q_a lb/in	q_b lb/in	q_c lb/in	y_a in	y_b in	y_b in	y_c in
No Buckling	212	263	263	0	14.39	9.09	9.09
Buckled	212	264	264	3.30	17.70	12.39	12.39

Table C11.3 Internal Loads and Geometry (Continued)							
Condition of Skin	y_{Long1} in	y_{Long2} in	M_a, b in-lbs	M_c in-lbs	I_a, b in ⁴	I_c in ⁴	I_c in ⁴
No Buckling	12.33	0	324,000	310,500	402		
Buckled	15.63	3.30	324,000	310,500	261		

Notes: (Same as for Table C11.2)

Skin Panel Analyses

The analysis is illustrated only for panel a, but results of a similar analysis for panel b are presented later on.

Panel a

$$Z = b^2(1-\mu^2)^{1/2}/Rt = 4.5(1-.33^2)^{1/2}/15(.025) = 3.49; k_s = 17.51; 51; a/b = 15.71/4.5 = 3.49; k_s = 17.51; 51; Fscr = 17.5\pi^2 \times 10^6 / (0.025/4.5)^2 / 12(1-.33^2) = 5,334 \text{ psi} \quad (\text{Fig. C9.5})$$

$$K_c = 19.5; \quad (\text{Fig. C9.1});$$

$$Fccr = 19.5\pi^2 \times 10^6 / 10.7 \times 10^6 / (.025/4.5)^2 / 12(1-.33^2) = 5,944 \text{ psi}$$

For the non-buckled skin condition (to obtain E_c , k and R_c)

$$f_c = M_a y_a / I_a = 317,250(14.39)/402 = 11,356$$

$$f_s = q_a/t = 212/.025 = 8,480$$

$$A = Fccr/fscr = 1.112$$

$$B = f_c/f_s = 1356/8480 = 1.339$$

$$B/A = 1.20$$

$$R_c = (-1.20 + \sqrt{1.20^2 + 4})/2 = .57$$

$$R_c = .57(1.20) = .68$$

$$Fscr = R_c Fscr = 3,040$$

For the buckled skin condition,

$$f_s = q_a/t = 212/.025 = 8,480$$

$$f_s/Fscr = 8,480/3,040 = 2.79$$

$$300\text{th}/Rd = 300(.025)(2.0)/15 = 1.0$$

$$k = .59 \quad (\text{Fig. C11.19})$$

Skin Rupture

$$f_s = 8480; \quad F_s = 21,100 \quad (\text{Fig. C11.42})$$

$$\text{M.S.} = 21,100/8,480 - 1.0$$

$$= 1.49$$

Permanent Buckling (At Limit Load)

$$f_sLimit = f_sUlf/1.5 = 8,480/1.5 = 5,653$$

$$4Fscr \times 10^6 / E_c F_cy = 4 \times 5334 \times 10^8 / 10.7 \times 10^6 \times 39,000 = 5.11$$

$$Fsp.B./Fscr = 1.3 \quad (\text{Fig. C11.46})$$

$$Fsp.B. = 1.3(5,334) = 6,934$$

$$\text{M.S.} = 6,934/5,653 - 1.0 = .23$$

Interrivet Buckling, Along Longeron 1,a/b

$$Fir = \pi^2 \times 10.7 \times 10^6 / (1.75/.58 \times .024)^2 = 39,473 \quad (\text{Eq. C7.22})$$

$$f_c = f_{csk} + Fp.T. = 317,250(16.29)/261 + 10,445 \quad (\text{see "Longeron"}) = 30,246$$

$$\text{M.S.} = 39,473/30,246 - 1.0 = .31$$

General Instability, Based upon Panel b

Proceeding per Fig. C11.39 notes and data;

$$\frac{P_L P_{rg}^{1/2} \times 10^4}{(dh)^2 B} = \frac{.34 \times .689 \times 10^4}{(4.5 \times 15.71)^2 / 115} = 43.83$$

$$F_{sInst} \times 10^3 / E_c > 3$$

$$\text{Hence, } F_{sInst} > 3 \times 10.7 \times 10^6 / 10^3 > 32,000 \text{ psi}$$

$$f_s = 10,560$$

$$\text{M.S.} = 32,000/10560 - 1.0 = \underline{\text{High}}$$

Ring (Between Panels b and c)

$$Arg = .0784; \quad I_{rg} = .0372; \quad P_{rg} = .689$$

$$e = .875(.0125) = .888$$

$$Arge = .0784 / (1 + (.888/.689)^2) = .0295 \quad (\text{Eq. 55})$$

$$f_{rg} = \frac{.555(10560) \tan 36.05^\circ}{.0295/4.5 \times .025 + .5(1-.555)} = 8,801 \quad (\text{Eq. 114})$$

$$frgMax/f_{rg} = 1.30 \quad (\text{Fig. C11.21 for } k_{av} = .555)$$

$$frgMax = 1.30(8801) = 11,441$$

$$\text{M.S.} = 11,743/11,441 - 1.0 = .03$$

Longeron 1

The longeron is supported by the major frames, 36 in apart. This is the only support in the radial direction. Per Eq. (113) and data for panels a and b,

$$f_L = F_p - F_{D.T.}$$

$$= \frac{-317250(15.63)}{261} - \left[\frac{.59(8480)(15.71)}{2(.2288) + .5(15.71)} \right]$$

$$\frac{(.025) \cot 35.8^\circ + .56(10560)(15.71)}{(.025)(1-.59)(.56) + .5(15.71)(.025)}$$

$$\frac{(.025) \cot 36.1^\circ}{(1-.56)(.73)} = -18999 - 10445 \\ (f_p) (f_{D.T.}) \\ = -29,444 \text{ psi}$$

If Longeron 1 were supported in two directions (which it isn't) like the one (b) in Fig. 11.47a, then Eq. (123) would apply with $f_p = 371,250(15.63)/261 = 22,232$ (at the left end). Then

$$M.S. = \frac{1}{22232 + \frac{10445}{62690}} - 1.0 = .34$$

Buckling Check

This uses Eq. (120) and (121). For a longeron the effective skin width is (Eq. 1, p.A19.12)

$$2w = 1.9t\sqrt{E_c/f_c}$$

$$= 1.9 \times 0.025 \sqrt{10.5 \times 10^6 / 29444} = .89 \text{ in} \\ \text{so}$$

$$A_{esk} = .89(.025) = .0223 \text{ in}^2$$

and using Fig.C7.26,

$$\rho_{long} = 1.04(.51) = .59 \text{ and } L/\rho = 61.0$$

For the Longeron $F_{cc} = 62,690$ (Art.C7.30)

$$\text{So, } F_{cr} = \frac{62690 - 62690^2 (61)^2 / 4\pi^2 \times 10.5 \times 10^6}{27412}$$

Since this is $< F_{cc}/2$, use

$$F_{cr} = \pi^2 \times 10.5 \times 10^6 / 61^2 = 27850$$

$$P_{cr} = 27850(.2288 + .0243) = 6,993 \text{ lbs (Eq. 12)}$$

$$P_{long} = -18999 (.2288 + .0243) - [.59(8480)$$

$$(15.71)(.025)(1.387)/2 +$$

$$.56(10560)(15.71)(.025)(1.371)/2$$

$$= -7736 \text{ lbs (comp.)}$$

$$\text{So } M.S. = 6993/7736 - 1.0 = -.10$$

So, the longeron would need to be made larger (more thickness).

Beam-Column Check

The Example Problem does not have any beam-column loadings. If it did, the M.S. would be much less than the -.10 for buckling (beam-column margins are always less than for the column). To find the M.S. for this particular case (where $P > P_{cr}$) one must find the common factor, A , by which all of the shell applied loads must be multiplied to give a M.S.

of zero (and A will be < 1.0). The M.S. will then be $A-1.0$ (Art.C3.18).

However, to illustrate the general procedure assume that only the applied bending moments on the shell are reduced 30% to be 184,275 and 259,875, and that the data in Table C11.3 still applies (some of it will change slightly). Then, proceeding as before

$$f_L = -245025(15.63)/261 - 104455$$

$$= -14673 - 10445 = 25118$$

$$2w = 1.9(.025)\sqrt{10.5 \times 10^6 / 25118} = .97 \text{ in}$$

$$A_{esk} = .97(.025) = .0243 \text{ sq in}$$

$$P_{long} = -14673(.2288 + .0243) + 2965 = 6679$$

$$\text{and Buckling M.S.} = 7049/6679 - 1.0 = .06$$

For the beam-column check assume that the longeron has a slightly curved installed shape, as in Fig.C3.33c with $e = .10 \text{ in}$. Then, per the "approximate formula"

$$M' = 6679(.10)/(1 - 6679/7049) = 12724 \text{ "#}$$

Per Fig.C10.15b formula

$$\text{Mult} = \left[\frac{45000(.75 \times 1.5)^{27}}{(.75/.08)^{79}} \right] \\ (70000/10.5 \times 10^6)^{.50} / .0604 = 10717$$

Then, per Method 1 of Art.C3.18,

$$M.S. = \frac{1}{\frac{6679}{7049} + \frac{12724}{10717}} - 1.0 = -.53$$

Using Method 2, Art.C3.18

$$K = 1.19 \text{ (Fig.C3.8)}$$

$$F_c = 50000^* + \left[\frac{1.19 - 1.1}{1.50 - 1.1} \right] (70000 - 50000^*) \\ = 54500$$

$$f = P/A + Mc/I = \frac{6679}{2531} + \frac{14273(.75)}{.0765} \\ = 166320 \text{ psi (comp)}$$

$$\text{So } M.S. = \frac{54500}{166320} - 1.0 = -.67$$

Per Art.C3.18, the "better" M.S. of Method 1, -.53, would be used. Thus the longeron must be made larger (more thickness). Note the large negative margin caused by beam-column action, whereas the buckling margin was a small positive one.

* This is the prop. limit stress; see page 38 footnote.

Shear Panel b Calculated Data

The following data for panel b were calculated as was illustrated for panel a

$$\begin{aligned} f_s &= 10,560; F_{scr} = 5,994; F_{sc} = 5,334; \\ A &= 1.112; f_c = 317250(9.09)/402 = 7174; \\ B &= .68; R_c = .74; R_b = .45; F_{scr} = 3947 \\ k &= .56; M.S.Rupt. = 1.01; \\ M.S.P.B. &= .02; M.S.ir = .29 \end{aligned}$$

Attachments

The allowable load/rivet is the same as for the stringer system calculations.

a) For an assumed splice along Longeron 1 between panels a and b, the largest shear flow is 263 lbs/in

$$\begin{aligned} \text{Load/in} &= 264(1+.56(1/\cos 36.1^\circ - 1)) = 299 \\ \text{Load/rivet} &= 299(.75) = 224 \end{aligned}$$

$$\text{M.S.} = 356/224 - 1.0 = .59$$

Due to tension field prying action

$$\begin{aligned} \text{Load/in} &= .15(.025)(64000) = 240 \\ \text{Load/rivet} &= 240(.75) = 180 \end{aligned}$$

$$\text{M.S.} = 197/180 - 1.0 = .09$$

b) Along Ring, assuming panels b and c are spliced there

$$\begin{aligned} \text{Load/in} &= 264(1+.56(1/\sin 36.1^\circ - 1)) = 367 \\ \text{Load/rivet} &= 367(.75) = 275 \end{aligned}$$

$$\text{M.S.} = 197/275 - 1.0 = -.28$$

c.) Along Ring for no splice there is no shear transfer, only a prying load

$$\begin{aligned} \text{Load/in} &= .22(.025)(64000) = 352 \\ \text{Load/rivet} &= 352(.75) = 264 \end{aligned}$$

$$\text{M.S.} = 264/352 - 1.0 = -.25$$

Hence, for (b) and (c) a smaller rivet spacing is needed, about .60 in.

Diagonal Tension Angle,Panel a:

$$\begin{aligned} \epsilon_{rg} &= \frac{1}{10.7 \times 10^4} \left[\frac{-59(8480) \tan \alpha}{.0295/45 \times .025 + .5(1-.59)} \right] \\ &= -.001001 \tan \alpha \end{aligned}$$

$$\epsilon_L = \frac{1}{10.5 \times 10^4} \left[\frac{-317250(15.63)}{261} - \frac{.59(8480)}{.2288} \right]$$

$$\cot \alpha$$

$$15.71 \times .025 + .5(1-.59)(.56)$$

$$= -.00181 - .000683 \cot \alpha$$

$$\epsilon_{sk} = \frac{8480}{10.7 \times 10^4} \left[\frac{2(.59)}{\sin 2\alpha} + (1-.59)(1+.33) \sin 2\alpha \right]$$

$$= .000935/\sin 2\alpha + .000431 \sin 2\alpha$$

$$\tan^2 \alpha = \frac{\epsilon_{sk} - \epsilon_L}{\epsilon_{rg} + (4.5/15)^2 \tan^2 \alpha / 8}$$

$$\epsilon_{sr} = \epsilon_L \\ = \epsilon_{sk} - \epsilon_{rg} - .011250 \tan^2 \alpha$$

After several successive trials it is found that when $\alpha = 35.8^\circ$ is used in the three strain equations, the resulting value of α per the last equation is 35.8° , hence $\alpha = 35.8^\circ$

Panel b:

Proceeding as for panel a, the following data are obtained

$$k=.56; f_s=10560; R_c=.73 \text{ which result in}$$

$$\epsilon_{rg} = -.001134 \tan \alpha$$

$$\epsilon_L = -.001809 - .000758 \cot \alpha$$

$$\epsilon_{sk} = .001105/\sin 2\alpha + .000578 \sin 2\alpha$$

Proceeding as for panel a, $\alpha_b = 36.1^\circ$.

Panel c:

$$k=.55; f_s=10560; R_c=.744; M=310,500$$

Proceeding as for panel a, $\alpha_c = 36.0^\circ$.

C11.38a Summary

The effect of diagonal tension is to generate additional compressive stresses in the stringers, longerons and rings or frames, which if not accounted for will cause early failure.* The effect of compression stresses along with the shear stresses increases these effects, while tension stresses will reduce them.

The exact magnitude of the various diagonal tension effects throughout a network of skin panels defies simple evaluation, particularly when both shear and axial stresses vary from panel to panel. However, some rational approach is necessary to complete the design, or specimens for test programs, and the approaches given in this chapter represent one such procedure. Where margins are small, element tests are in order.

The stringer system is usually found, for example, in fuselage and wing structures where there are relatively few large "cutouts" to disrupt the stringer continuity. This is more likely for transport, bomber and other cargo carrying aircraft. The longeron system is more efficient and

* And also increased skin panel and fastener loads

suitable where a large number of "quick access" panels and doors or other "cut-outs" are needed to service various systems rapidly. These would "chop up" a stringer system very severely, making it inefficient and also more expensive from both a weight and manufacturing stand-point. Therefore, longeron systems are usually found in fighter and attack type aircraft, and in others having such features. There are, of course, other factors influencing the choice of structural arrangement.

Some further notes concerning this general subject are included in Chapter D3. These include "beef-up" of panels and axial members bordering cut-outs and non-structural doors, which is also related to "end bay" effects discussed in Art.C11.29.

Although tension field analysis has been discussed only for primary structure it can also significantly effect secondary structure such as flaps, ailerons and other control surfaces. For example, such surfaces usually have a relatively light trailing edge. Significant buckling of their skin can generate additional compressive loads in the trailing edge promoting buckling or local failure. A normal loading which bends the edge member inwards and generates additional loads in the supporting ribs is also present. Hence attention is needed here.

C11.39a Problems for Part 2

1. Recalculate the margins of safety for the stringer example problem assuming that the torsion on the shell is increased from 150,000 to 300,000 in-lbs. For the stringer analyses use only the "Quick" and Melcone-Ensrud methods.
2. Recalculate the margins of safety for the longeron example problem assuming that the torsion on the shell is increased from 300,000 to 450,000 in-lbs. Use only Fig.C11.45 for determining α .

C11.40a Problems for Part 1

The problems for Part 1 remain the same as in the textbook (p.C11.48).

The reader is encouraged to consult the references (p.C11.49), particularly (3), (4) and (9) for a broader understanding of the subject.

C8.1a Introduction

NASA CR-912, "Shell Analysis Manual" presents a large amount of data and discussions for the buckling of monocoque

shells. Some of the more helpful data are presented in the following articles and figures. The reader is encouraged to consult CR-912 for a broader understanding of the subject.

C8.2a Buckling of Monocoque Cylinders Under Axial Compression

σ_{cr}/η is calculated per Fig.C8.8aa. Then F_{cr} is found by entering Fig.C8.9 with $(\sigma_{cr}/\eta)/F_0.7$, obtaining $F_c/F_0.7$ and then calculating $F_{ccr} = F_0.7(F_c/F_0.7)$. The shell is then capable of withstanding an axial load of

$$P_{cr} = 2\pi R F_{ccr} t$$

C8.5a Buckling of Circular Cylinders Under Axial Load and Internal Pressure

When there is an internal (burst) pressure, p , along with an axial compressive load, the internal pressure increases C_c by an amount ΔC_c per Fig.C8.11a which increases σ_{cr}/η . F_{ccr} is then obtained as in Art.C8.2a above. P_{cr} becomes

$$P_{cr} = 2\pi R F_{ccr} t + \pi R^2 p$$

C8.7a Available Design Curves for Bending Based on Experimental Results

σ_{cr}/η is calculated per Fig.C8.13aa. F_{bcr} is then found by entering Fig.C8.9 with $(\sigma_{cr}/\eta)/F_0.7$, obtaining $F_c/F_0.7$ and then calculating $F_{bcr} = F_0.7(F_c/F_0.7)$. The shell can then withstand a bending moment of

$$M_{cr} = \pi R^2 F_{bcr} t$$

C8.8a Buckling Strength of Circular Cylinders in Bending with Internal Pressure

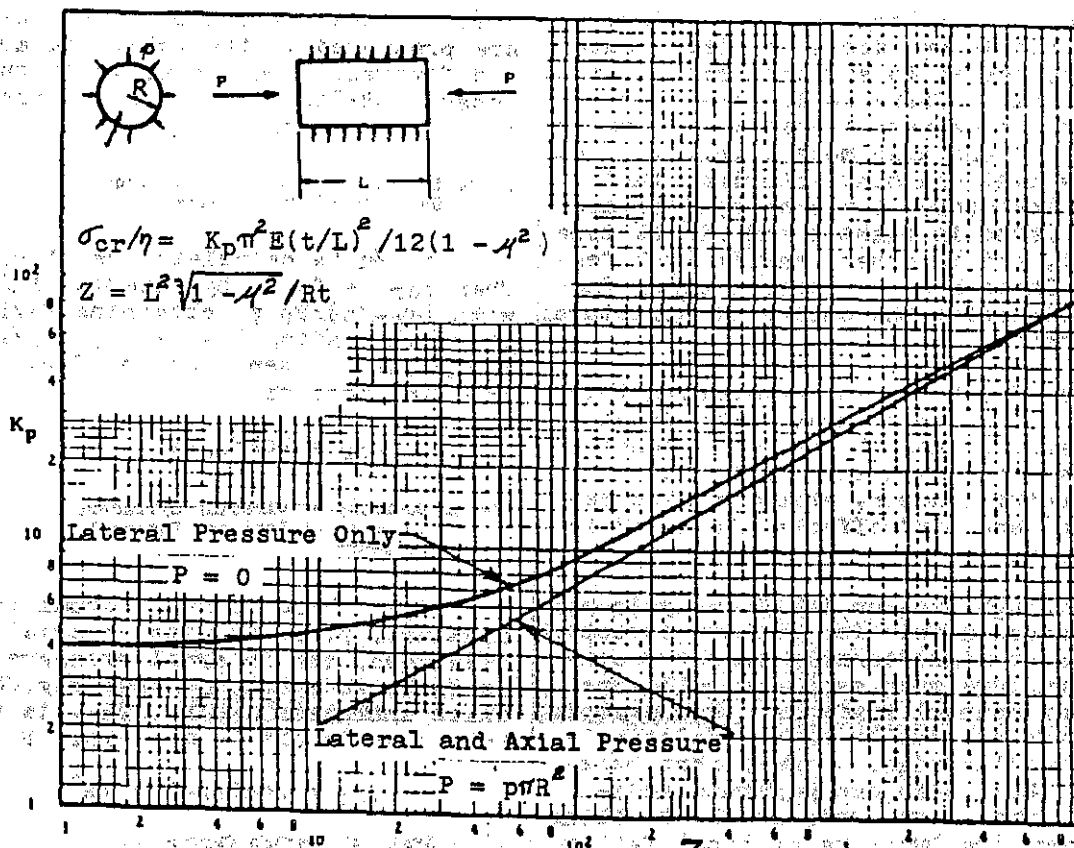
When there is an internal (burst) pressure, p , along with bending stresses the internal pressure increases C_b by an amount ΔC_b per Fig.C8.14a, which increases σ_{cr}/η . F_{bcr} is then obtained as in Art.C8.7a above. The shell is therefore capable of withstanding a bending moment of

$$M_{cr} = \pi R^2 F_{bcr} t + \pi p R^3 / 2$$

C8.9a External Hydrostatic Pressure

When there is a hydrostatic (collapse) pressure, p , σ_{cr}/η is calculated per Fig.C8.15a (the lateral plus axial pressure curve). F_{ccr} is then found by entering Fig.C8.9 with $(\sigma_{cr}/\eta)/F_0.7$, obtaining $F_c/F_0.7$ and then calculating $F_{ccr} = F_0.7(F_c/F_0.7)$. The axial stress is one-half of the circumferential stress. F_{ccr} is in the circumferential direction so

$$P_{cr} = F_{ccr} t / R$$

Fig.C8.15a Buckling Due to Hydrostatic (Collapse) Pressure, p_{cr}

When there is a radial (lateral) collapse pressure, p , only σ_{cr}/η is calculated per Fig.C8.15a using the upper curve. F_{scr} is then obtained in the same manner as in Art.C8.9a above. F_{scr} is in the circumferential direction, so

$$P_{cr} = F_{scr} r / R$$

C8.11a Buckling of Circular Cylinders Under Pure Torsion

For this case τ_{cr}/η is calculated per Fig.C8.20a. F_{scr} is found by entering Fig.C8.19a with $(\tau_{cr}/\eta)/0.7$, obtaining $F_s/F_0.7$ and then calculating $F_{scr} = F_0.7(F_{scr}/F_0.7)$. The allowable torsion is then

$$\tau_{cr} = F_{scr} 2\pi R^2 t$$

C8.13a Buckling of Circular Cylinders Under Pure Torsion With Internal Pressure

When there is an internal (burst) pressure, p , along with the torsion C_s is increased by an amount ΔC_s per Fig.C8.20b. This increases τ_{cr}/η and F_{scr} is obtained in the same manner as in Art.C8.11a above, as is P_{cr} .

C8.12a Buckling Under Transverse Shear

For the case of transverse shear, V , one proceeds as follows. Determine F_{scr} for torsion, as in Art.C8.11a or C8.13a and multiply it by 1.25 to determine F_{scr} for shear. Since $F_s = VQ/I_t$ one can solve this for V , for F_{scr} in place of F_s . For a cylinder this gives

$$V_{cr} = F_{scr} \sqrt{R t}$$

C8.15a Buckling of Circular Cylinders Under Combined Load Systems

The following interaction curve applies for the general case, and can be used to determine the margin of safety by successive trials (Art.C1.13a).

$$R_c + R_p + R_{st} + \alpha(R_s + R_b)^{3/3} = 1.0$$

The subscripts c, p, st, s, and b refer to compression, collapse pressure, torsion, transverse shear and bending respectively. Including R_p to only the first power is probably conservative, but collapse pressure is seldom present with the others.

For certain cases, where some of the loadings are absent, the margin of safety

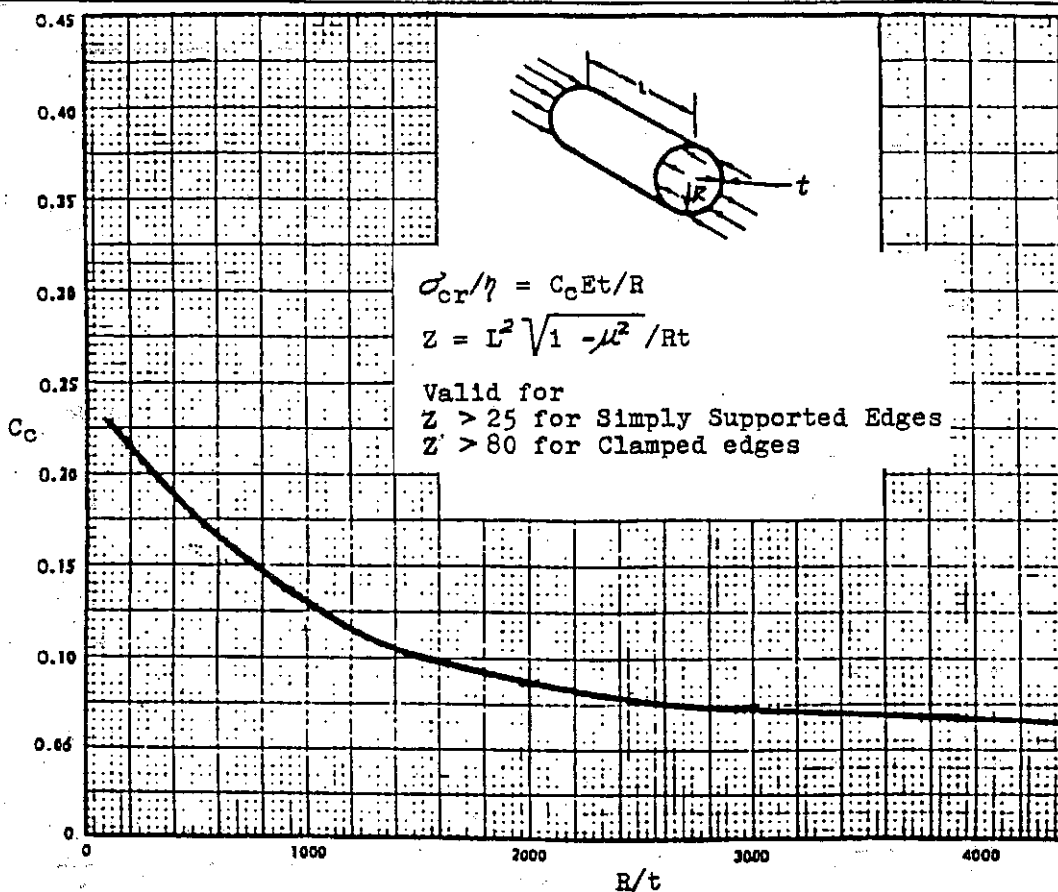
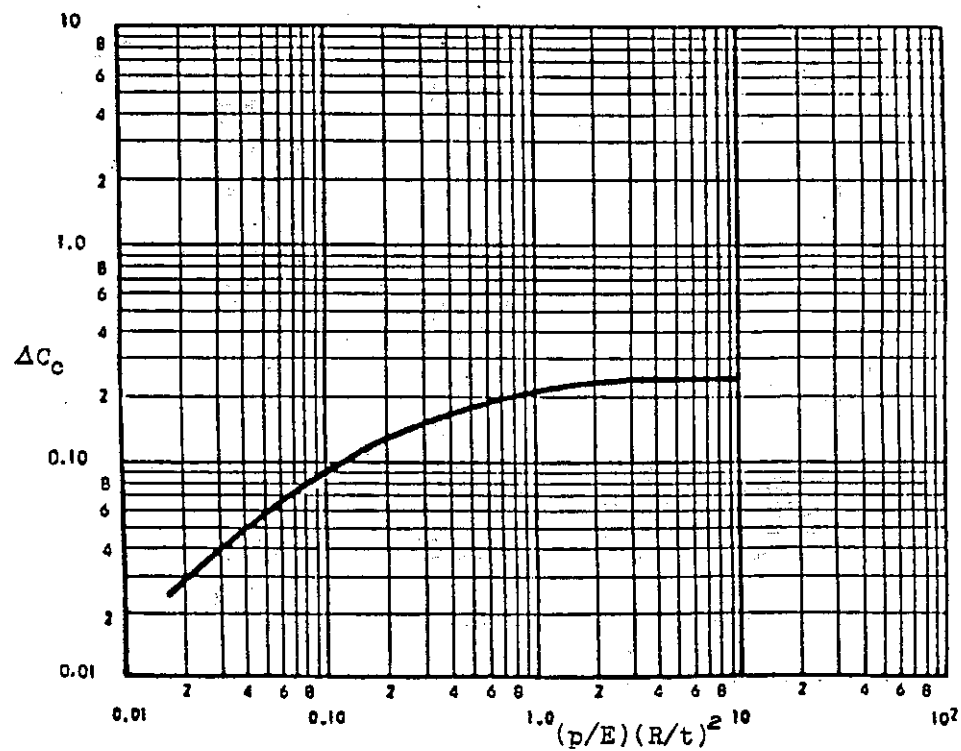


Fig.C8.8aa. Buckling Stress Under Axial Load

Fig.C8.11a Increase in C_c Due to Burst Pressure, p

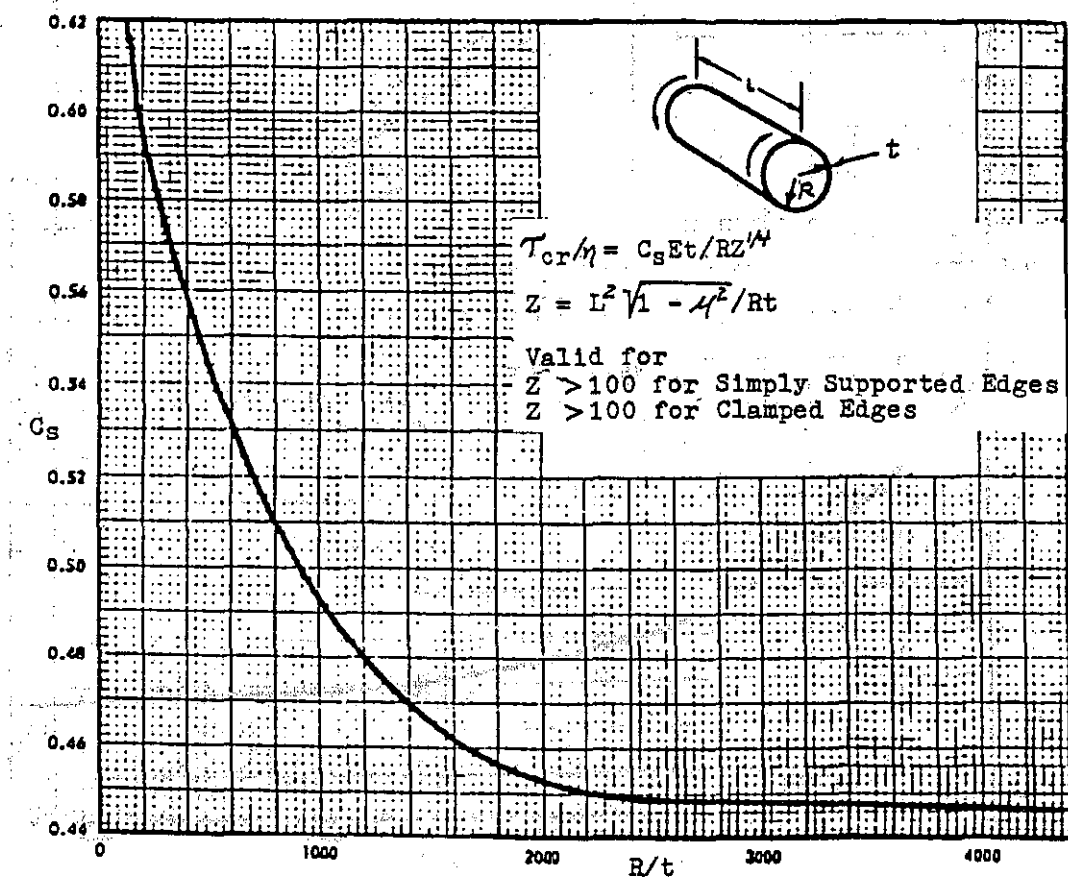
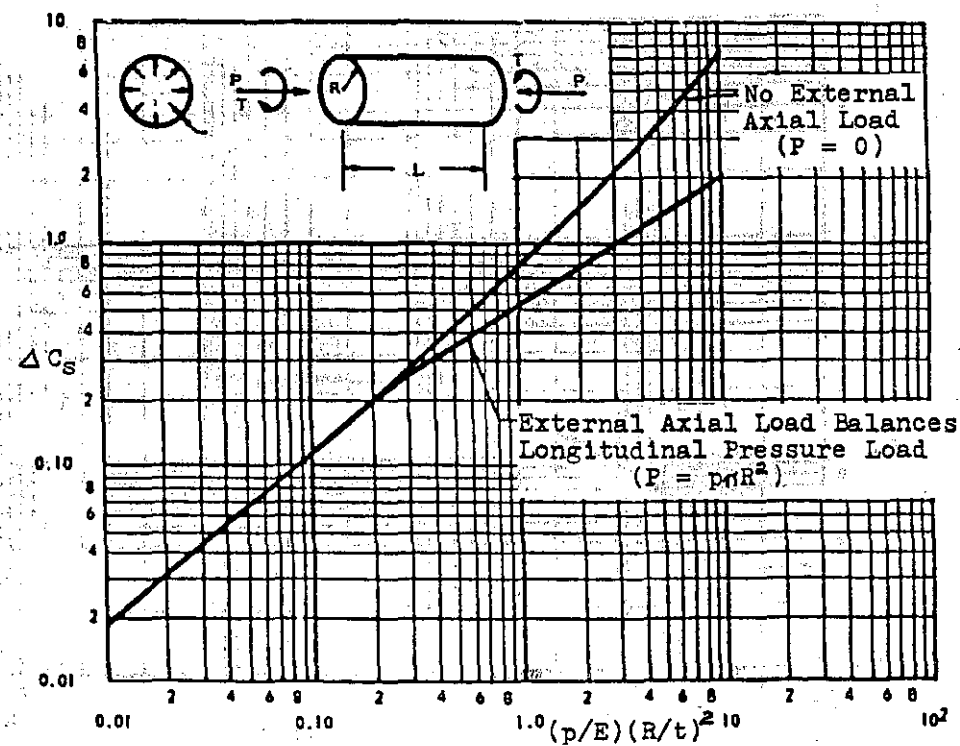


Fig.C8.20a Buckling Due to Torsion

Fig.C8.20b Increase in C_s Due to Burst Pressure, p

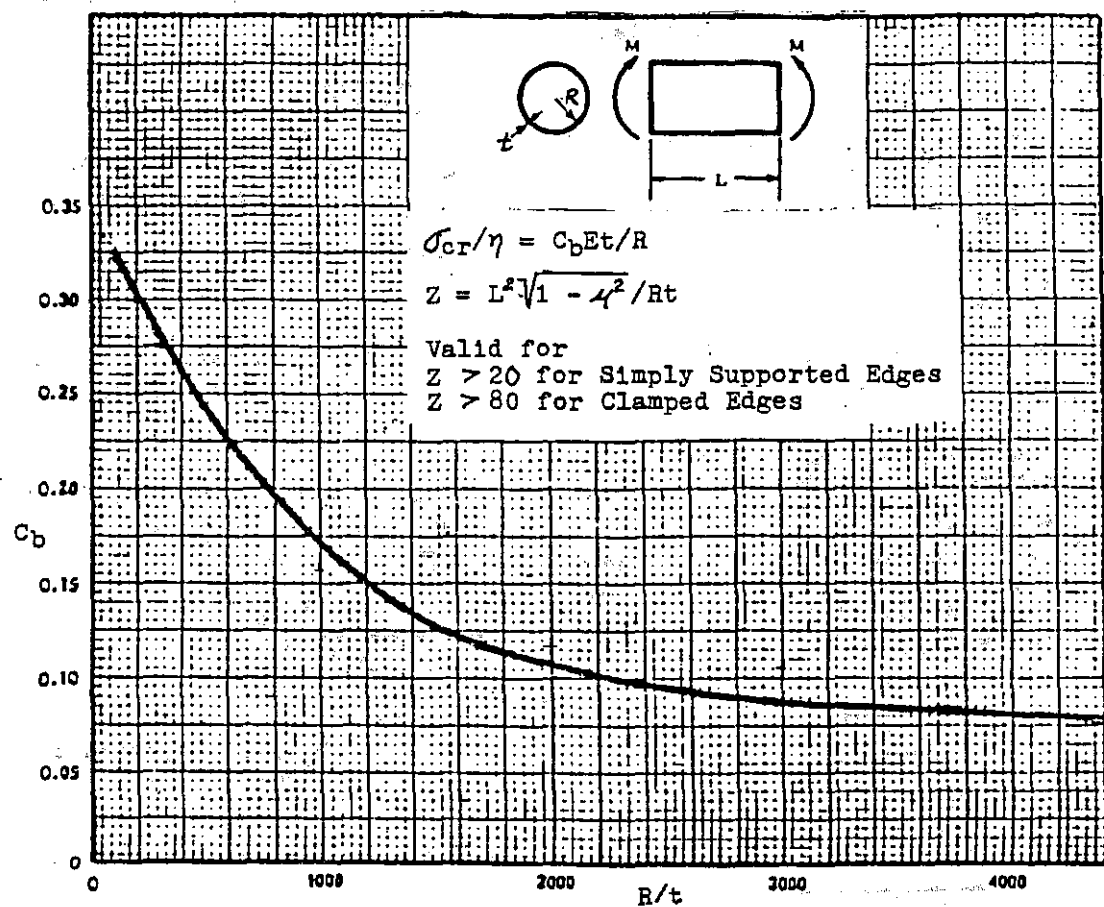
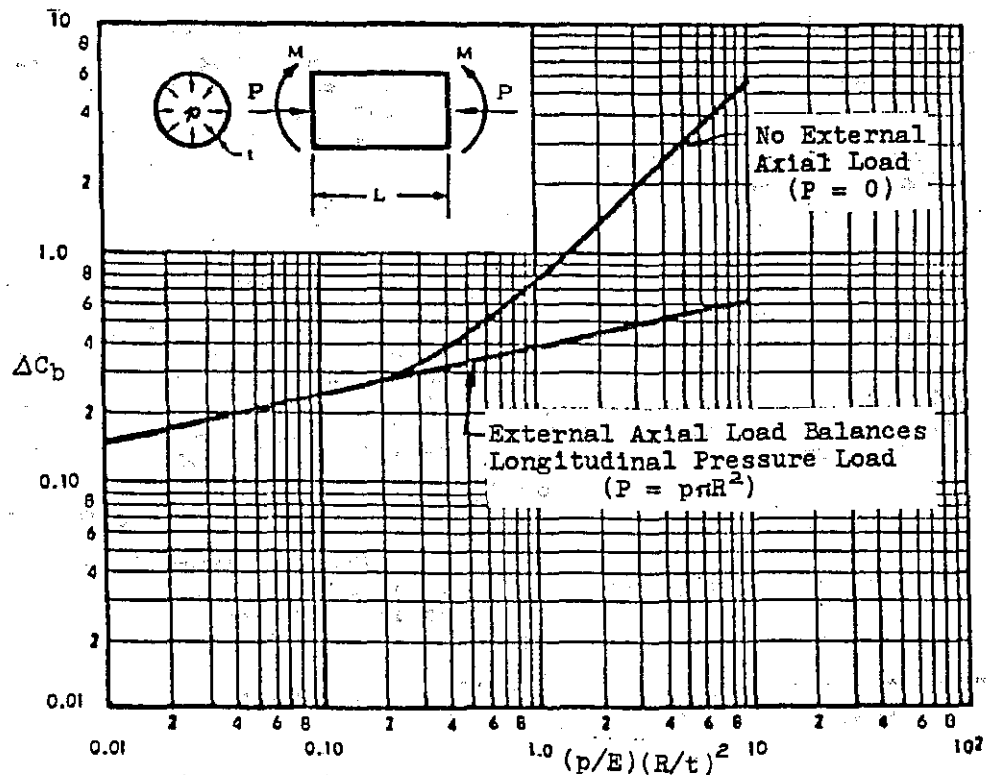


Fig. C8.13a Buckling Stress Under Bending Moment

Fig. C8.14a Increase in C_b Due to Burst Pressure, p

can be calculated directly by formula.

a) When $R_s = 0$

$$M.S. = \frac{2}{R_c + R_p + R_b + \sqrt{(R_c + R_p + R_b)^2 + 4R_{st}}} - 1.0$$

b) When $R_b = 0$

$$M.S. = \frac{2}{R_c + R_p + R_s + \sqrt{(R_c + R_p + R_s)^2 + 4R_{st}}} - 1.0$$

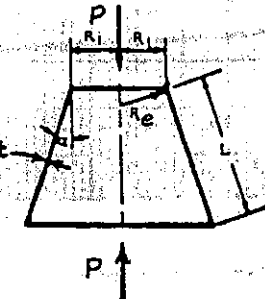
c) When $R_{st} = 0 = R_c = R_p$

$$M.S. = 1/(R_s^3 + R_b^3)^{1/3} - 1.0$$

C8.19a Additional Design Buckling Curves for Thin-Walled Conical Shells

σ_{cr}/γ is calculated per Fig.C8.25a. F_{ccr} is then obtained as for a cylinder in Art.C8.3a. F_{ccr} is at the small end of the conical shell, and

$$P_{cr} = F_{ccr} 2\pi R_1 t \cos\alpha$$



$$\sigma_{cr}/\gamma = C_c E t / R_e \quad R_e = R_1 / \cos\alpha$$

$$Z = L^2 \sqrt{1 - \mu^2} / R_{et}$$

Valid for
 $Z > 25$ for Simply Supported Edges
 $Z > 80$ for Clamped Edges
 $\alpha < 75^\circ$

To obtain C_c enter Fig.C8.8aa with R_e/t

Fig.C8.25a Buckling Stress Under Axial Load

When an internal (burst) pressure, p , is present along with the axial compressive stress, it increases C_c by an amount ΔC_c per Fig.C8.25b, which increases σ_{cr}/γ . F_{ccr} is then obtained as above. The critical axial load is then

$$P_{cr} = F_{ccr} 2\pi R_1 t \cos\alpha + p\pi R_1^2$$

For conical shells subject to bending σ_{cr}/γ is calculated per Fig.C8.26a, and F_{bcr} is then obtained as in Art.C8.3a. F_{bcr} is at the small end of the shell. The bending stress is $f_b = Mc/I$, so

$$Mc = F_{bcr} \pi R_1^2 t \cos\alpha$$

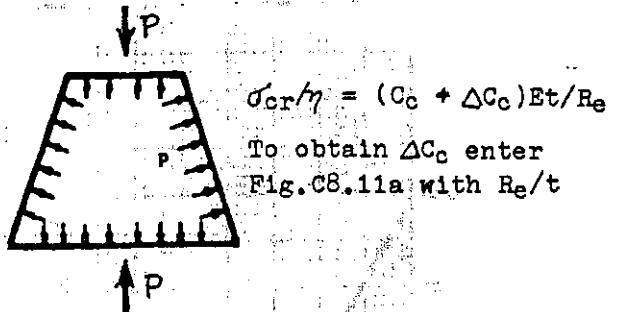
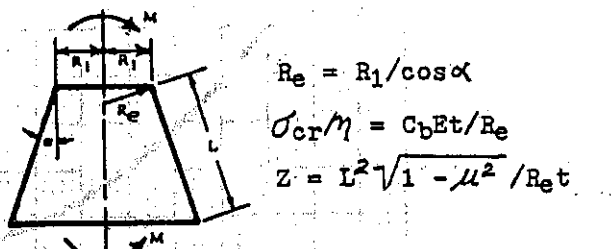


Fig.C8.25b Increase in C_c with Burst Pressure, p



$$R_e = R_1 / \cos\alpha$$

$$\sigma_{cr}/\gamma = C_b E t / R_e$$

$$Z = L^2 \sqrt{1 - \mu^2} / R_{et}$$

Valid for
 $Z > 20$ for Simply Supported Edges
 $Z > 80$ for Clamped Edges
 $\alpha < 60^\circ$

To obtain C_b enter Fig.C8.13a with R_e/t

Fig.C8.26a Buckling Stress Under Bending Moment

When an internal (burst) pressure, p , is present along with the bending moment, it increases C_b by an amount ΔC_b per Fig.C8.26b. This increases σ_{cr}/γ , and F_{bcr} is then obtained, as before, by entering Fig.C8.9 with $(\sigma_{cr}/\gamma)/F_{0.7}$ and obtaining $F_c/F_{0.7}$. F_{bcr} is then calculated as $F_{0.7}(F_c/F_{0.7})$, and

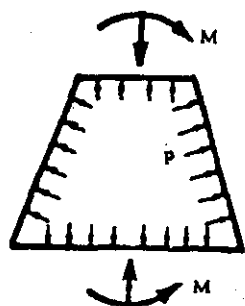
$$Mc = F_{bcr} \pi R_1^2 t \cos\alpha + p\pi R_1^3 / 2$$

For conical shells subject to torsion σ_{cr}/γ is calculated per Fig.C8.27a and F_{scr} is then obtained by entering Fig.C8.19 with $(\sigma_{cr}/\gamma)/F_{0.7}$ and getting $F_s/F_{0.7}$. F_{scr} is then calculated as $F_{0.7}(F_s/F_{0.7})$, and

$$T_{cr} = F_{scr} \pi R_1^2 t$$

When an internal (burst) pressure, p , is also present with torsion stresses the pressure increases F_{ccr} . However there is no data for calculating the increase.

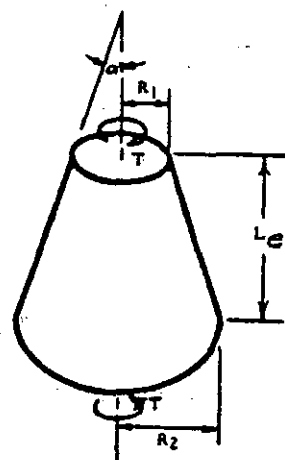
For conical shells subject to hydrostatic (collapse) pressure σ_{cr}/γ is calculated per Fig.C8.28a. F_{ccr} is then obtained by entering Fig.C8.9 with $(\sigma_{cr}/\gamma)/F_{0.7}$, obtaining $F_c/F_{0.7}$ and then



$$\sigma_{cr}/\gamma = (C_b + \Delta C_b)Et/R_e$$

To obtain ΔC_b enter Fig. C8.14a with R_e/t

Fig. C8.26b Increase in C_b Due to Burst Pressure, p



$$\tau_{cr}/\gamma = C_s Et R_e^2 / R_1^2 R_e Z^{1/4}$$

$$R_e = [1 + (1 + R_2/R_1)^5 \sqrt{2} - (1 + R_2/R_1)^5 \sqrt{2}] R_1 \cos \alpha$$

$$Z = L_e^2 \sqrt{1 - \mu^2} / R_{et}$$

Valid for

$Z > 100$ for Simply Supported Edges

$Z > 100$ for Clamped Edges

$\alpha < 60^\circ$

To obtain C_s enter Fig. C8.20a with R_e/t

Fig. C8.27a Buckling Due to Torsion

F_{scr} as $F_{0.7}(F_c/F_{0.7})$. p_{cr} is then

$$p_{cr} = F_{scr} t \cos \alpha / R_2$$

For conical shells subject to a transverse shear, V , the buckling stress is obtained by determining the buckling stress due to torsion and then multiplying this by 1.25. Then, since $f_s = VQ/I_t$ and with f_s being at the neutral axis,

$$V_{cr} = F_{scr} \pi R t / 4$$

where $F_{scr} = 1.25$ times F_{scr} for torsion.

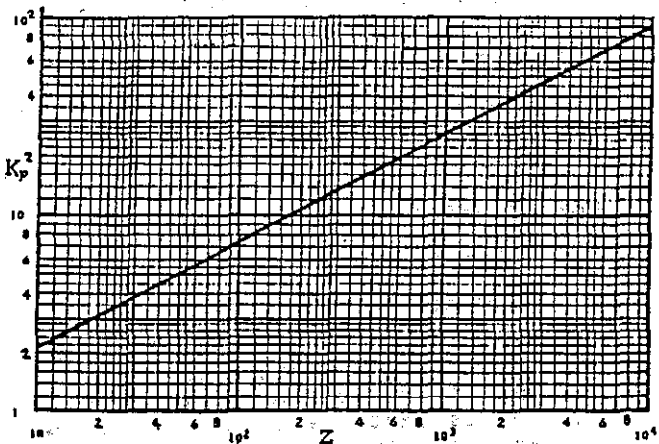
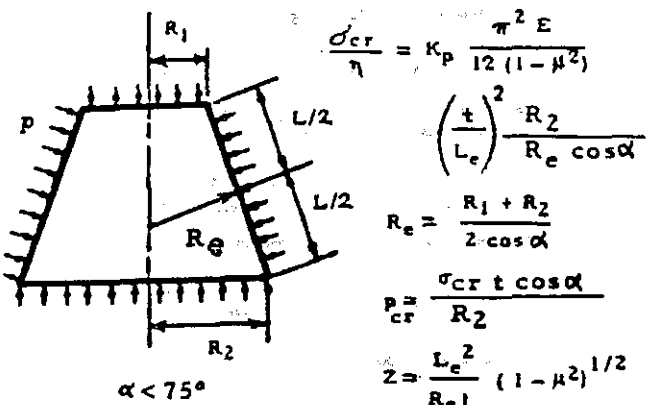


Fig. C8.28a Conical Shell, Collapse Pressure
c8.20 Buckling of Spherical Caps

For a spherical cap subject to a uniform collapse pressure, Fig. C8.29, the buckling stress can be calculated as

$$F_{scr}/\gamma = .175 Et/R$$

F_{scr} is found by entering Fig. C8.9 with $(F_{scr}/\gamma)/F_{0.7}$, obtaining $F_{scr}/F_{0.7}$ and then calculating F_{scr} as $F_{0.7}(F_{scr}/F_{0.7})$. The critical pressure, p_{cr} , is then

$$p_{cr} = F_{scr}^2 t / R$$

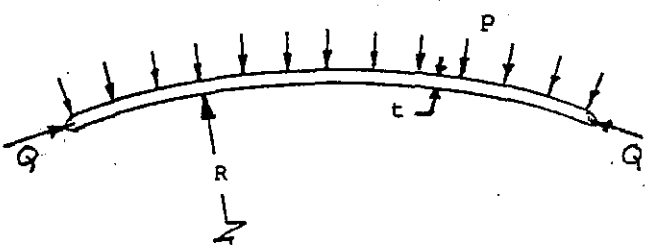


Fig. C8.29 Spherical Cap, Collapse Pressure

NASA CR-912 is recommended to the reader for additional data and discussions not only for shell buckling, but for much other helpful data about shell structures.

D1.2a Economy in Fitting Design

Also see Art.D3.9, items 8 and 12.

D1.3a Fitting Design Loads. Minimum Margins of Safety

Also see Art.C1.13a about design loads and margins of safety.

D1.4a Special or Higher Factors of Safety

Also see Art.C1.13a about design loads and margins of safety.

D1.5a Aircraft Bolts

Unfortunately, Art.D.15 and subsequent articles do not discuss single shear bolted joints. These are widely used in aerospace structures, such as for attaching skins to spar caps, skin splices etc. See Art.D1.28, D1.8aa and D3.5a for helpful information about these cases, and also Art.D1.27.*

D1.6a Aircraft Nuts

Also see Art.D1.27 and Table A46

D1.8aa Bushings

The lug or fitting should be designed so that the required margin of safety will be present if the next size bushing is installed. If no bushing is present, the lug or fitting should be designed to show the required margin if a bushing is installed later on.

D1.12a Lug Strength Analysis Under Transverse Loading

For the case of concentric lugs (Fig.D1.11-a where $e = W/2$) see Art. D1.13a. For the allowable load at 90° (a transverse load) based on test data see Art.D1.13a below.

D1.13a Lug Strength Analysis Under Oblique Loads

For the case of concentric lugs (Fig.D1.11-a where $e = W/2$) Fig.D1.15 can be used to quickly determine the allowable load, P_θ for any angle from 0° to 90° . Only the calculated allowable axial load, P_0 , is needed (Art.D1.11). P_θ is then calculated as

$$P_\theta = P_0(P_\theta/P_0)$$

The curve is based on a great number of tests and with different materials. As shown, the reduction factor varies from 1.0 for $\theta = 0^\circ$ to .75 for $\theta = 90^\circ$. If the lug width increases as in Fig.D1.11-b, the curve gives a conservative allowable load. If it narrows, as with an eye-bolt

type lug, the curve gives an unconservative allowable load.

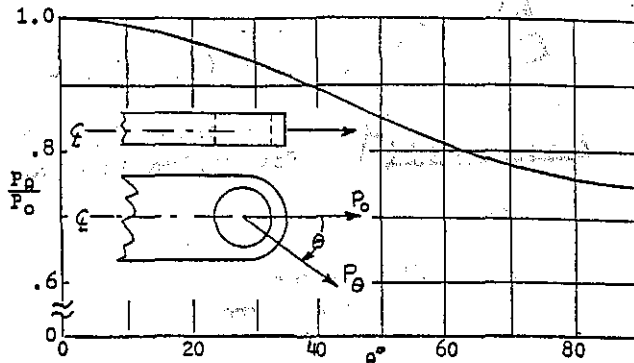


Fig.D1.15a Concentric Lug Oblique Load Strength, P_θ

D1.27a The Importance of Good Clamp-up

It is important that the stress analyst and structural designer have a good understanding of the importance of clamp-up action as to shear joint strength, particularly for single shear joints which are so common in aerospace structures. Previous articles about riveted joints, D1.18 to D1.22, and bolted joints D1.16, have not discussed this important subject. As discussed later, lack of good clamp-up is why blind or countersunk or shaved head rivets and and blind, countersunk, thin head bolts or bolts with soft collars always result in joints having less strength/stiffness than do protruding head rivets or bolts with thick heads and nuts. It is also why the allowable joint loads with these must always be determined by tests rather than by calculations.* The following discussion discusses the reasons for this.

A fastener transferring a shear load in a typical single shear joint is shown in Fig.D1.41. If the fastener does not have a head (i.e., a pin), or otherwise does not clamp the two sheets together, the joint equilibrium and bearing stresses will be like that sketched in Fig.D1.42. The extremely high bearing stresses in the sheets at the faying surfaces will result in early yielding, a permanent set and a greatly reduced joint strength and yield load. Thus the cardinal rule is to never use any headless type pin or a bolt or rivet not providing good clamp-up.

Clamp-Up

When a bucked protruding head rivet or a conventional bolt with a tightened nut is used, the joint equilibrium and the resulting bearing stress distri-

* See p.A10 - A21 for bolted joint allowable data.

* For much such data see p. A10 - A21

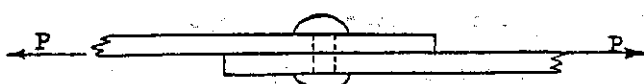


Fig.D1.41 A Single Shear Joint

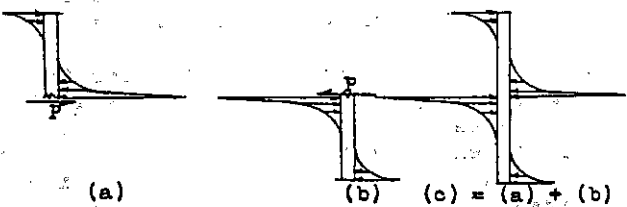


Fig.D1.42 Bearing Stresses Without Clamp-Up

bution are quite different, as shown in Fig.D1.43. The presence of the tight head provides clamp-up and thereby allows the loads Q to be generated and balance the moment due to the bearing stresses.

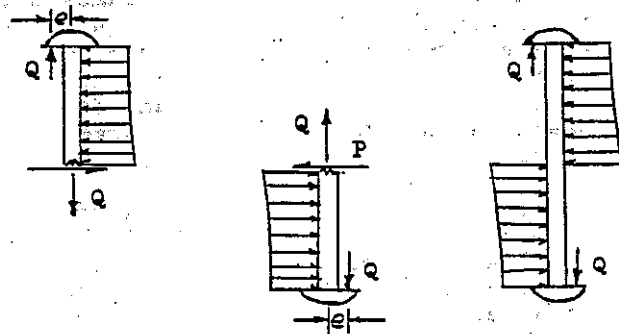


Fig.D1.43 Bearing Stresses With Clamp-Up

Thus there exists

1. A prying load on the fastener heads
2. A tension in the fastener
3. A near uniform bearing stress on the fastener (and sheets)

With good clamp-up the bearing stresses are near uniform, but even a "finger-tight" clamping of a bolt's nut is far better than none (a "loose" nut). Those fasteners, previously discussed, which do not develop as much clamp-up, have less joint strength and stiffness, and their joint allowables must be obtained from tests rather than from calculations. Blind fasteners are the worst in this respect. A steel collar is much better than an aluminum one but is heavier.

Shims (Fillers) Between Sheets in Single Shear Joints

When a shim is present between the fastened sheets, its effect is to increase the loads Q (Fig.D1.43). This results in more bending and tension in the

fastener which can cause less strength and stiffness. When the shim is fairly thin, say less than 10-12% of the fastener diameter, its effect is usually ignored. Otherwise, see Art.D3.5a, Art. D3.5 and Fig.D3.18 as to how to proceed.

D1.23a Riveted Sheet Splice Information *

The following information should be added at the end of "Proper Rivet Size to Use".

Structural joints should be made critical in sheet bearing, not in shear. A bearing critical joint has ductility, whereas a shear critical joint is of a comparatively "brittle" nature. This is because once the fastener begins to shear failure follows quite quickly, but when bearing critical there is considerable deformation within the joint before failure occurs.** This can be seen from the comparison of load-deflection curves for a joint as shown in Fig.D1.44. The joint deflection here is that within the joint, between the upper and lower sheets in the direction of the shear load. A shear critical joint might be desirable when a piece of structure is to be ejected or "blown off", such as the ejection of a nose cone by an explosive charge.

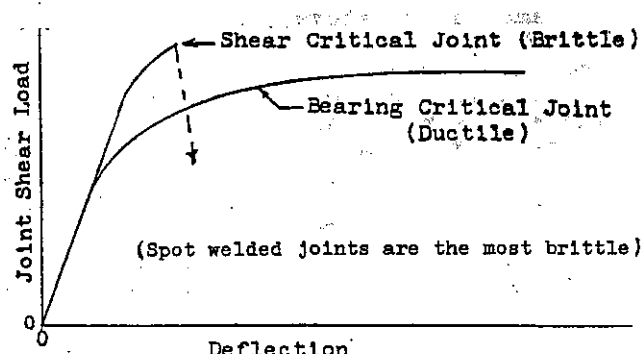


Fig.D1.44 Brittle and Ductile Joints

D1.27 Design and Strength of Threads

The purpose here is to provide helpful information for the design of threads to transmit a given load. Applications are for bolts in tapped holes, bolt-nut combinations and hydraulic cylinder end caps. The general question is how many threads are required. The answer depends upon the shear strength, F_{su} , of the material in which the threads will strip and the cylindrical area which will be sheared. The following assumptions are made for bolt-nut combinations and tapped hole combinations.

* See p.A10 - A21 for riveted joint allowable data.
See p.A10 for fastened sheet edge distances.

** Essentially mandatory for any multifastener pattern installation

1. If the bolt material has a higher strength than the nut material the threads will be stripped from the nut.
2. If the nut material has the higher strength the threads will be stripped from the bolt.
3. If the nut and bolt materials are of equal shear strength the bolt threads will usually be stripped first.

The strength of the combination is calculated for the three above assumptions as follows:

1. Load at which threads strip from nut

$$P_{\text{nut}} = K_n D_b L F_{\text{su}}$$

where

$K_n = .4$ = efficiency of nut threads

D_b = bolt thread major diameter

L = length of thread engagement

F_{su} = Shear strength of nut material

2. Load at which threads strip from bolt

$$P_{\text{bolt}} = K_b D_n L F_{\text{su}}$$

where

$K_b = .4$ = efficiency of bolt threads

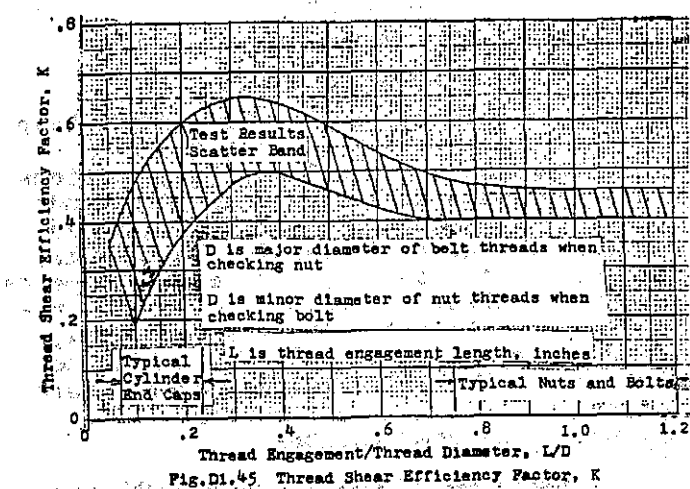
D_n = nut thread minor diameter

L = length of thread engagement

F_{su} = shear strength of bolt material

3. Same as (2) above

The formulas apply for typical bolt-nut combinations or bolts in tapped holes where L is more than $2/3$ of the bolt diameter. For smaller values of L , K will increase slightly, as shown in Fig.D1.45, because of a more uniform thread loading, but such short thread engagement is usually not good practice, since it may not develop the strength of the bolt.



Hydraulic Cylinder End Caps

There are many types of hydraulic cylinders used in aerospace vehicles. In general, the larger their diameters and the thinner their walls the more critical the end cap thread design becomes.

For the end cap to cylinder threads there is a tendency (due to the angle of the threads) for the part with the internal threads to expand (due to hoop tension) and for the part with the external threads to contract (due to hoop compression). This lessens the thread contact area. With quite flexible (thin) parts only the tip portion of the threads may be engaged, and failure will occur at a low percentage of the calculated load, even less than 20% in some cases. In addition to this the cylinder expands under the internal pressure, and this will lessen the thread engagement even more if the threads on the cylinder are internal ones. This is most significant for cylinders having thin walls and large diameters.

In general it is suggested that for cylinder end cap combinations a K factor of .3 be used, and that the design be carefully considered to minimize the relative expansion and contraction of the mating parts. Threads on piston rods, end caps, rod ends and barrels are usually machine cut. Machined threads have a lower fatigue life than do rolled threads, so this should be kept in mind when designing parts which might be fatigue critical in the threaded region.

D3.5a Fillers (and Shims)

As discussed in Art.D3.5, a filler (or shim) between the two sheets of a single shear joint reduces the strength of the fasteners because of the increased prying load. Extending the filler and adding more attachments, as shown in Fig.D3.18, restores the strength, but in many cases this is not feasible or necessary.

Another approach is to determine the reduced joint strength and use this, if it is adequate. The following is a suggested method for doing this for single shear bolted joints. It can be particularly helpful when shims are found to be necessary in manufacturing and salvage procedures.

For a conventional single shear joint having a protruding head bolt with a stiff collar or nut, the allowable load

is calculated as the lesser of a shear failure of the bolt or a bearing failure of the sheet (for all other types of bolts and nuts, or collars, the joint strength must be determined by tests rather than by calculations, as discussed in Art.D1.27a).

Placing a shim between the sheets causes an increased tension and bending moment in the bolt, so there may then be a third type of failure, bending and tension in the bolt. The thicker the shim, the lower the joint allowable shear load, V_o , becomes. The interaction of shear and bending is not critical, so the joint allowable shear load, V_o , is calculated as follows, referring to Fig.D3.19a. Also see Fig.D1.43 for more about fastener equilibrium.

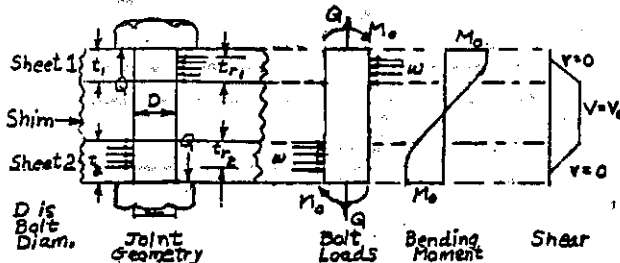


Fig.D3.19a Shimmmed Single Shear Bolted Joint, Loads on Bolt (and Sheets)

The sheet bearing stresses generate a bending moment in the bolt which is, from statics

$$M_o = V_o(t_{s1}/2 + t_{s2}/2 + t_f)/2$$

where t_s is the required thickness of the sheet to develop the applied shear load, V_o , and t_f is the thickness of the filler (shim).

$$t_{s1} = V_o/F_{bru1}D \quad t_{s2} = V_o/F_{bru2}D$$

hence $M_o = V_o^2(1/(2F_{bru1}D) + 1/(2F_{bru2}D) + t_f)/2$

Letting $A = 2D/(1/F_{bru1} + 1/F_{bru2})$
Then $V_o^2/A + V_o t_f - 2M_o = 0$

or, $V_o^2 + V_o t_f A - 2M_o A = 0$

- Solving for V_o (the allowable shear load) and letting M_o be M_B where $M_B = .88 M_B^*$

$$V_o = (-A t_f + \sqrt{(A t_f)^2 + 8 M_B^2})/2$$

- If $V_o > V_B$ use $V_o = V_B$ where V_B is the bolt single shear allowable load

- Calculate $t_{s1} = V_o/F_{bru1}D$ and

* M_B = bolt shank allowable bending moment (Table A45)
and .88 accounts for the tension in the bolt.

calculate $t_{s2} = V_o/F_{bru2}D$

- If $t_{s1} > t_1$ use $t_{s1} = t_1$ and recalculate $V_o = F_{bru1}D t_1$

If $t_{s2} > t_2$ use $t_{s2} = t_2$ and recalculate $V_o = F_{bru2}D t_2$

- Use the smallest of the calculated V_o loads in (1), (2) and (4) above as the allowable shear load, V_o .

For all other fasteners a joint allowable load, V_o , is gotten by assuming it varies inversely with the prying load (moment) on the fastener head. Hence, V_o is the allowable load for no filler (Table 33-44 and MIL HDBK 5) multiplied by $t_s/(t_s + t_f/2)$, where t_s is the average of the two sheet thicknesses.

The above procedures are believed to be reasonable, but they have not been checked by single shear joint tests, which are needed for substantiation.

For riveted joints a similar procedure could be considered, with substantiating tests of single shear joints.

A suggested test specimen for single shear joints is sketched in Fig.D.46.

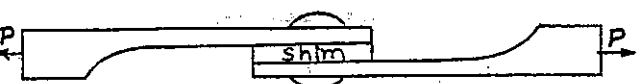


Fig.D.46 Shimmmed Single Shear Test Specimen

D3.7a Special Cases of Beam Design

See Art.A13.11a for additional curved beam discussions and data.

D3.3a Tension Clips

Additional allowable data for several types of such clips is in Fig.A1 - A2.

D1.21a Strength of Rivets Flush Type

See p. A10 - A21 for allowable data

D1.22a Blind Rivets

See p. A10 - A21 for allowable data

D1.7a Bolt Shear, Tension & Bending Strengths

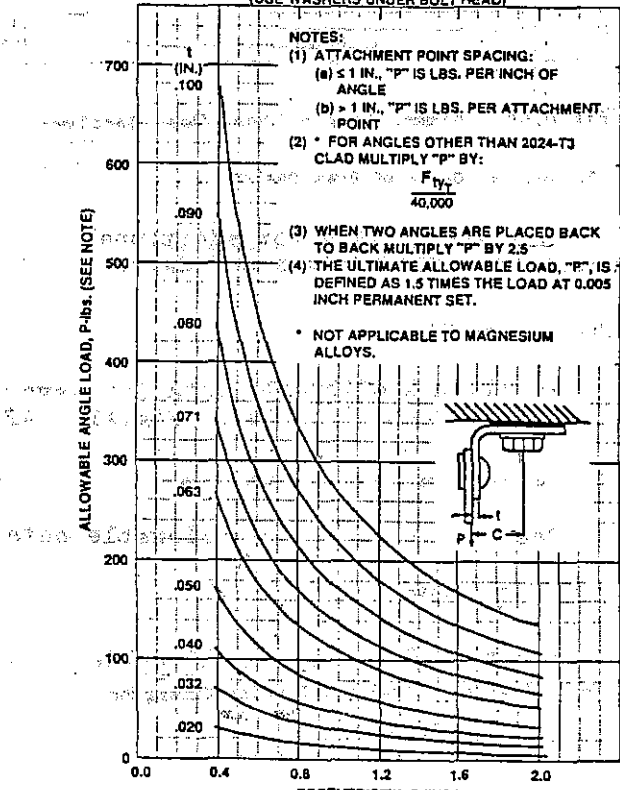
See Table A45

DRAWING CHECKLIST

ITEM	SHEET METAL	MACHINED PARTS	CASTING	CABLE ASSEMBLY	WELDED PARTS
ITEM AND SPECIFICATION REQUIREMENTS	X	X	X	X	X
MATERIAL CALLOUT AND SPECIFICATION	X	X	X	X	X
ADDITIONAL MATERIAL REQUIREMENTS	X	X	X	X	X
QUALIFICATION SPECIFICATION AND CLASSIFICATION	X	X	X	X	X
SHRUBBER	X	X	X	X	X
WELD CALLOUTS	X	X	X	X	X
INSPECTION AND ACCEPTANCE REQUIREMENTS	X	X	X	X	X
RADIOGRAPHIC INSPECTION	X	X	X	X	X
MAGNETIC PARTICLE INSPECTION	X	X	X	X	X
INITIAL TIGHT INSPECTION	X	X	X	X	X
ULTRASONIC INSPECTION	X	X	X	X	X
AUTOMATIC PIGEONHOLE INSPECTION	X	X	X	X	X
TEST SPECIMEN LOCATIONS	X	X	X	X	X
CRITICAL AREAS INDICATED	X	X	X	X	X
PROOF LOAD REQUIREMENTS	X	X	X	X	X
GEOMETRIC AND DETAIL REQUIREMENTS	X	X	X	X	X
MINIMUM EDGE DISTANCE ON TUGS	X	X	X	X	X
MIN. WALL THICKNESS, ANGULARITY & ECCENTRICITY	X	X	X	X	X
FILED RADIUS	X	X	X	X	X
EDGE DISTANCE, CONSISTENT WITH LOAD DIRECTION	X	X	X	X	X
DRAIN DIRECTION REQUIREMENT	X	X	X	X	X
READ AT PARTING LINE, REMOVED	X	X	X	X	X
ADVERSE TOLERANCE, BUILD UP	X	X	X	X	X
FINISH	X	X	X	X	X
PROTECTIVE FINISH	X	X	X	X	X
SURFACE FINISH	X	X	X	X	X
HEAT TREAT REQUIREMENT	X	X	X	X	X
MATERIAL HEAT TREAT	X	X	X	X	X
HEAT TREAT TO OBTAIN PROPER	X	X	X	X	X
MOVE IN ADQUATE HOLE SIZE TO OBTAIN PROPER	X	X	X	X	X
HEAT RESPONSE	X	X	X	X	X
TOUGH MACHINE SECTION, OBTAINABLE PRIOR TO	X	X	X	X	X
HEAT TREAT	X	X	X	X	X
HEAT TREAT AFTER	X	X	X	X	X
(A) SWAGING	X	X	X	X	X
(B) WELDING	X	X	X	X	X
(C) FORMING	X	X	X	X	X
STRESS RELIEVE, AFTER	X	X	X	X	X
FORMING	X	X	X	X	X
WELDING	X	X	X	X	X

FIG.A1 ALLOWABLE TENSION LOADS FOR CLIPS
(FORMED ANGLES)

(USE WASHERS UNDER BOLT HEAD)

SEE FIG.A3 FOR BACK TO BACK ANGLES
ULTIMATE ALLOW. LOAD FOR 2024-T3 CLAD SHEET METAL ANGLES

MARGINS OF SAFETY AND DESIGN CHECKLIST

Margin of Safety

A checklist of minimum margins of safety and items to be considered when designing and analyzing structural joints is presented below.

Margins of Safety (M.S.) for fasteners and joints.

- M.S. = 0.15 on all shear joints at ultimate.
- M.S. = 0.00 on all joints at yield.
- M.S. = 0.50 on all tension joints at ultimate.
- M.S. = 0.15 on lugs.
- M.S. = 0.25 on critical joints (wing pivot, landing gear attach lugs, etc.) as designated by the aircraft design philosophy.

Checklist

The stress analyst should take care not to be limited by the items listed and to utilize good engineering judgment at all times.

- Make joint critical in sheet bearing rather than shear or fastener.
- Specify torque values on pre-loaded bolts and special applications.
- Avoid using rivets (solid and blind) in primary tension applications.
- Hole tolerances and fits to suit the installation.
- Corrosion and dissimilar metals protection (Contact M & P Group).
- Wear and friction qualities of moving parts.
- Excessive bearing stresses in rotating parts.
- Stress raisers in highly stressed areas (threads, grooves, lubrication fittings).
- Local discontinuities and eccentricities.
- Possible strength reductions due to adverse tolerances.
- Minimum thickness of sheet for countersunk holes.
- Effects of deflections.
- Compatibility of strains.
- Stiffness requirements.
- Local deflections (i.e., thin fairings) relative to aerodynamic tolerances.
- Panel flutter on large, thin gauge, flat external panels.
- Fatigue requirements.
- Thermal stresses or strains.
- Reduction in allowable for temperature.
- Proof load of parts per specification requirements (arresting hooks, hydraulic actuators, etc.)

FIG.A2 ALLOWABLE TENSION LOADS FOR CLIPS
(EXTRUDED ANGLES)

(USE WASHERS UNDER BOLT HEAD)

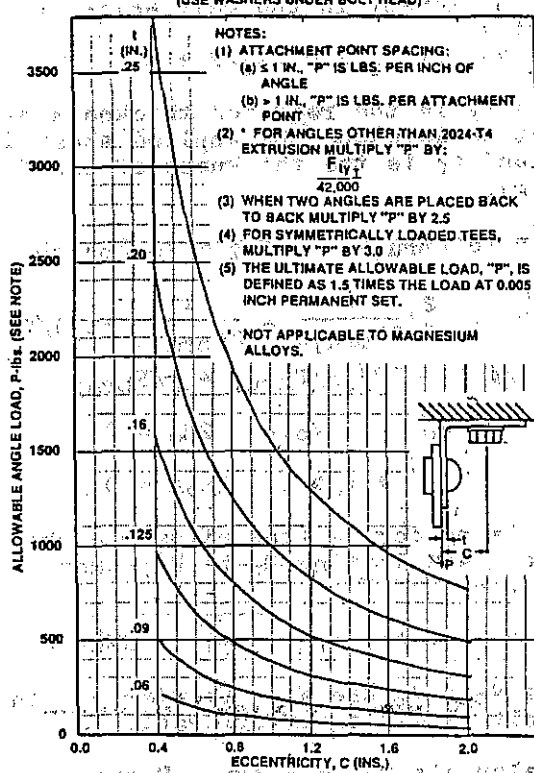
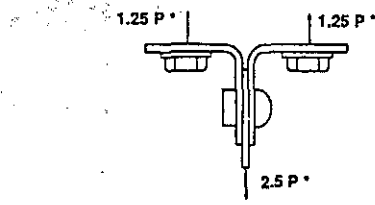
(SEE FIG.A3 FOR BACK TO BACK ANGLES OR TEE SECTIONS)
ULTIMATE ALLOW. LOAD FOR 2024-T4 EXTRUDED ANGLE

FIG.A3 ALLOWABLE LOADS FOR TENSION CLIPS**ALLOWABLE TENSION LOADS**

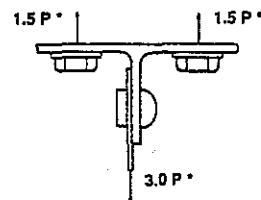
1. SINGLE ANGLES:
 Figures A1 and A2 give the ultimate allowable loads for various gages of 2024-T3 AlClad formed sheet and 2024-T4 extruded angles. Ultimate loads for angles of other heat-treated aluminum alloys, titanium, steel, or any material except magnesium alloys, may be obtained by direct ratioing with the MIL-HDBK-5 transverse yield strength as noted in the figures.

2. BACK TO BACK ANGLES:

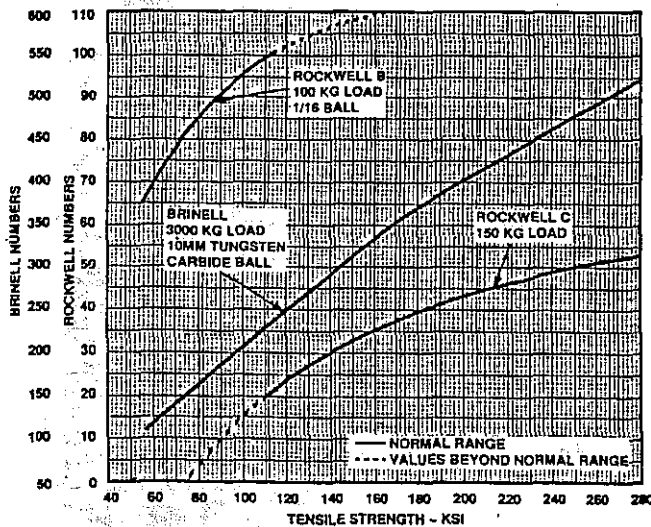
The allowables (and conditions) used for single angles are also used to derive allowables for double angles using the multiplying factors shown below:

**3. TEE SECTIONS:**

When extruded tees are loaded symmetrically in both outstanding flanges, the allowables obtained from FIG.A2 are to-be multiplied by three (3) as shown below.

**FIG.A4 ROCKWELL AND BRINELL HARDNESS DATA**

APPROXIMATE HARDNESS - TENSILE STRENGTH
RELATIONSHIP OF CARBON AND LOW ALLOY STEELS *



* FOR CARBON AND ALLOY STEELS IN ANNEALED, NORMALIZED,
AND QUENCHED-AND-TEMPERED CONDITIONS

TABLE A1 TORQUE RATIO FACTORS FOR TENSION
PRELOAD ON BOLTS

BOLT/NUT MATERIALS	F _u MIN (KSI)	DIAMETER SIZES (IN)	DRY (AS REC'D)*	LUBRICATED (MIL-T-5544)	SPECIFICATION 208-13-233 REF SEE NOTE (2)
			R FACTORS	R FACTORS	
1. STEEL/STEEL (ALLOY OR CRES)	125	3/16 - 5/16 3/8 - 1 1/8	.165 .170	.090 .0731	40 40
2. STEEL/STEEL (ALLOY OR CRES)	160	1/4 - 5/16 3/8 - 1 1/8	.165 .170	.090 .0731	50.67 50.67
3. STEEL/STEEL (ALLOY OR CRES)	180	1/4 - 5/16 3/8 - 1 1/8	.165 .170	.090 .0731	57.0 57.0
4. Ti/STEEL	160	1/4 - 5/16 3/8 - 1 1/8	.180 .190	.090 .085	50.67 50.67

* The "as received" condition may vary from no lubricant ("dry") to various degrees of unknown "light" lubricant such as machine oil. Testing is required for unknown conditions when establishing preload for critical applications.

NOTES:

1. The ratio factors and torque equations are based on selection of a tension type nut having adequate strength to develop the fastener with a proper margin of safety. Tensile strengths for common nut types are presented on TDE A46. Ultimate tensile strengths of threaded fasteners and the thread root areas are presented on TDE A12.
2. The reference stresses shown are the preload tensile stresses for the standard torque values of specification 208-13-233. These were used to develop the R factors using the equation:

$$T = R (d_{nom}) f_u (A_{root}) ; \quad \text{or} \quad T = R (d_{nom}) P_i$$

where: T = torque (in-lbs.)
 d_{nom} = nominal shank diameter
 f_u = desired stress level at thread root
 A_{root} = thread root area of bolt
 P_i = axial tensile preload on bolt

3. This method is not applicable to Hi-Lok collars having controlled torque-off features and various lubricants. See Hi-Lok standards data.

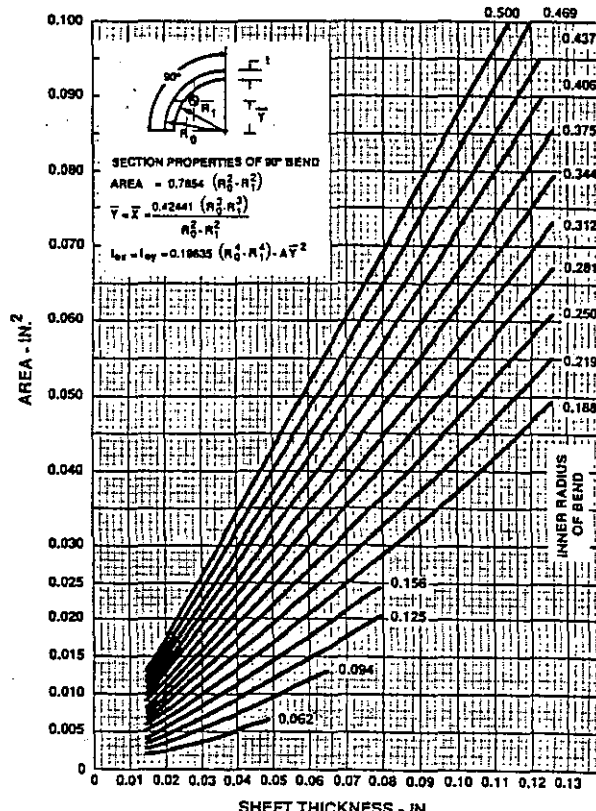
FIG.A5 AREA OF 90° BENDS

FIG. A6 MINIMUM I OF STIFFENERS

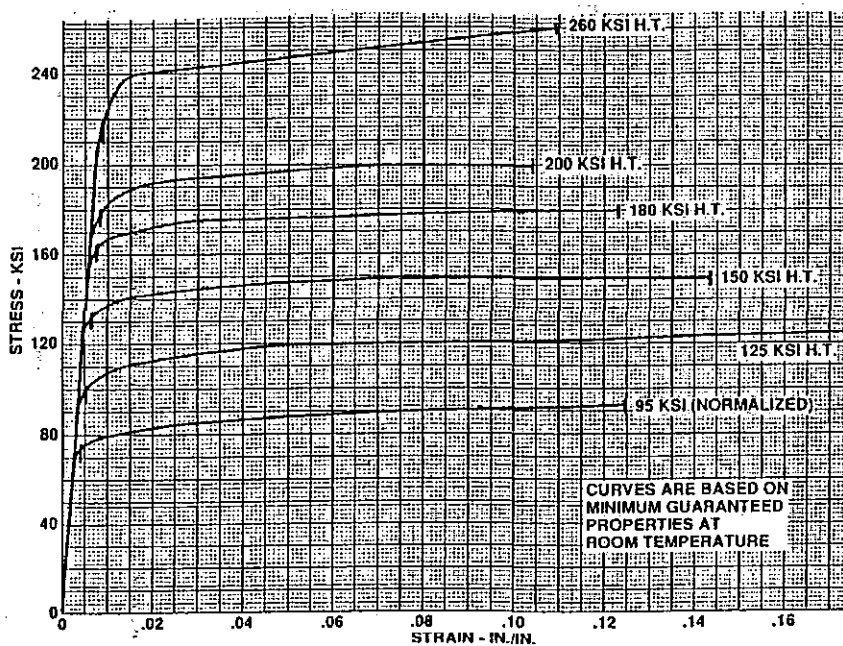


FIG. A7 ALLOY STEEL TENSILE STRESS-STRAIN

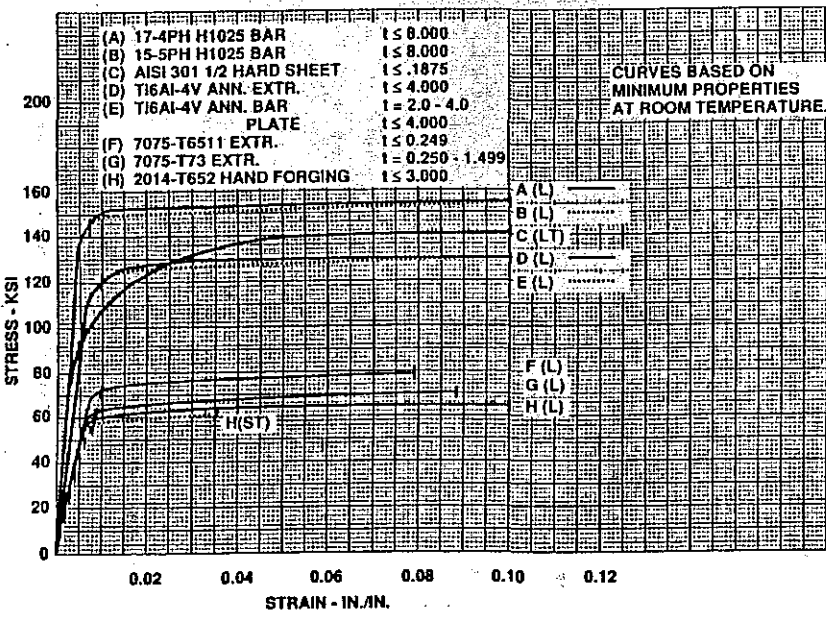


FIG. A9 VARIOUS TENSILE STRESS-STRAIN CURVES

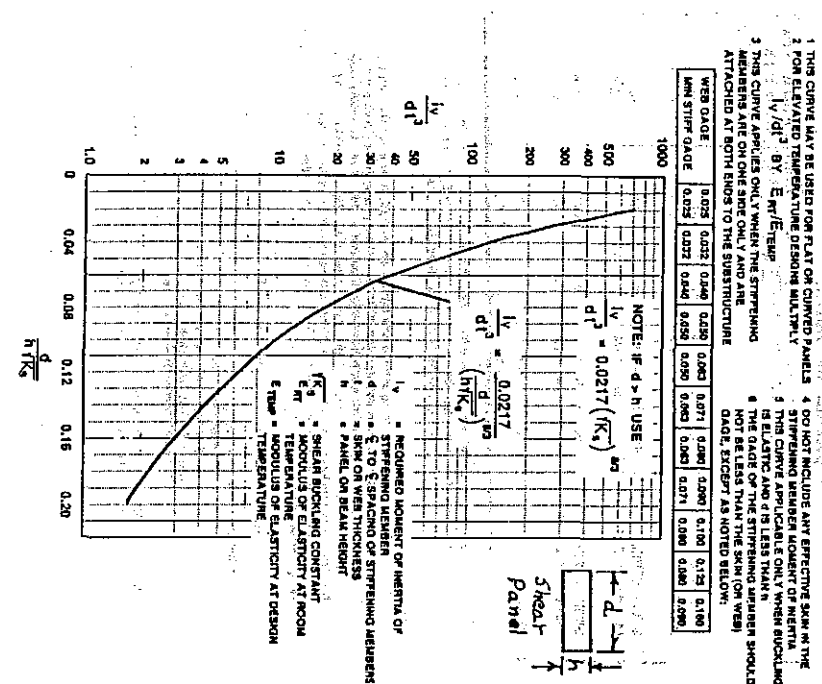


FIG. A8 ALUMINUM TENSILE STRESS-STRAIN CURVES

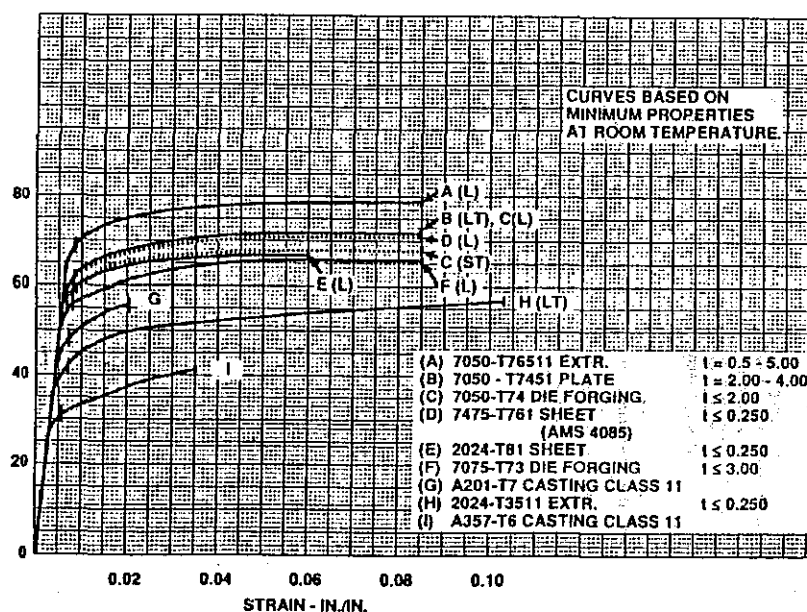


FIG.A10 COMPRESSION BUCKLING CONSTANT FLAT SHEET

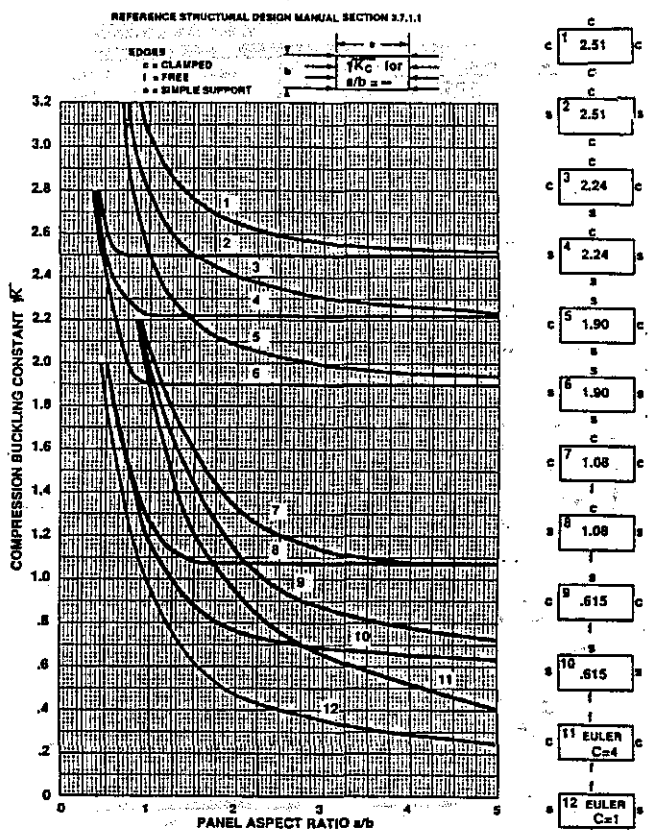


FIG.A12 COMPRESSION BUCKLING CURVES FOR SHEET MATERIAL WITH NO EDGE FREE

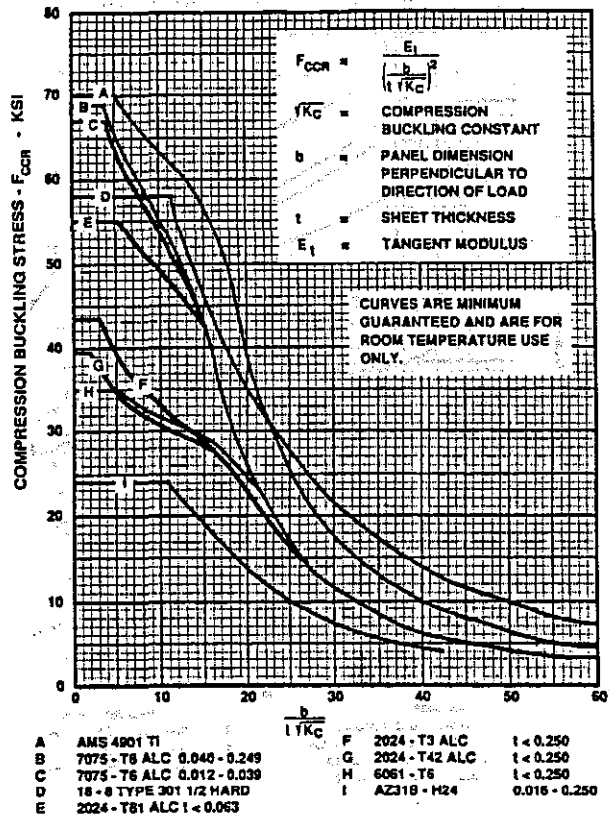


FIG.A11 SHEAR BUCKLING CURVES FOR SHEET MATERIAL

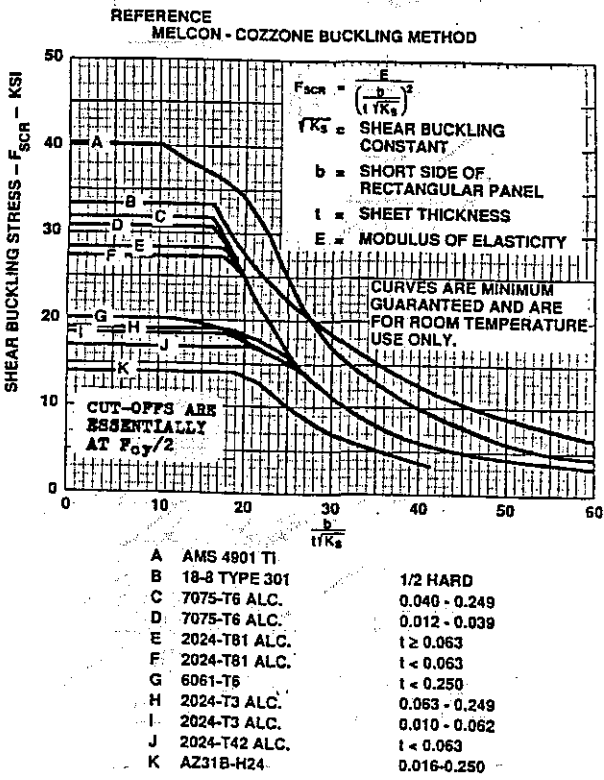
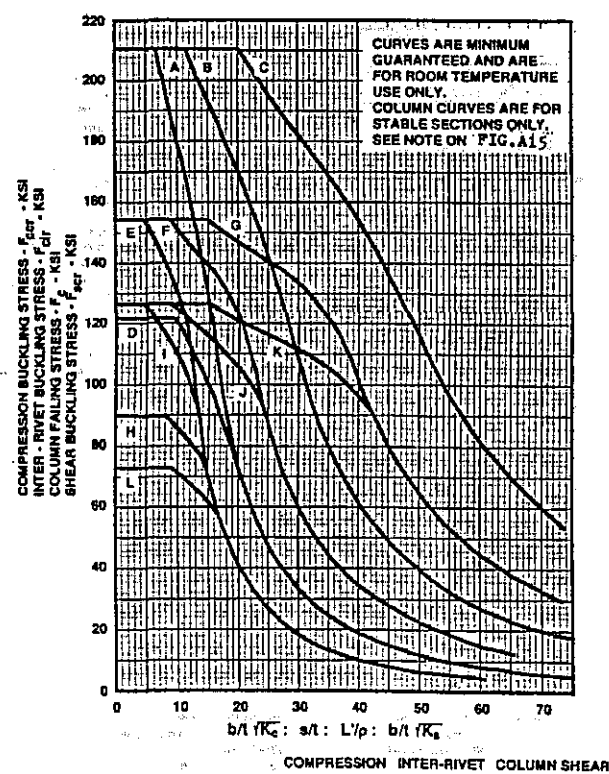


FIG.A13 BUCKLING CURVES FOR TITANIUM AND STEEL



SEE FIG.A13 FOR STEEL & TI

PM 15 - 7 Mo RH950 SHEET A B C D
 Ti - 6 Al - 4 V H.T. SHEET t = 0.184 - 0.250 E F G H
 Ti - 6 Al - 4 V ANN. SHEET I J K L

FIG. A14 COLUMN CURVES FOR SHEET MATERIAL

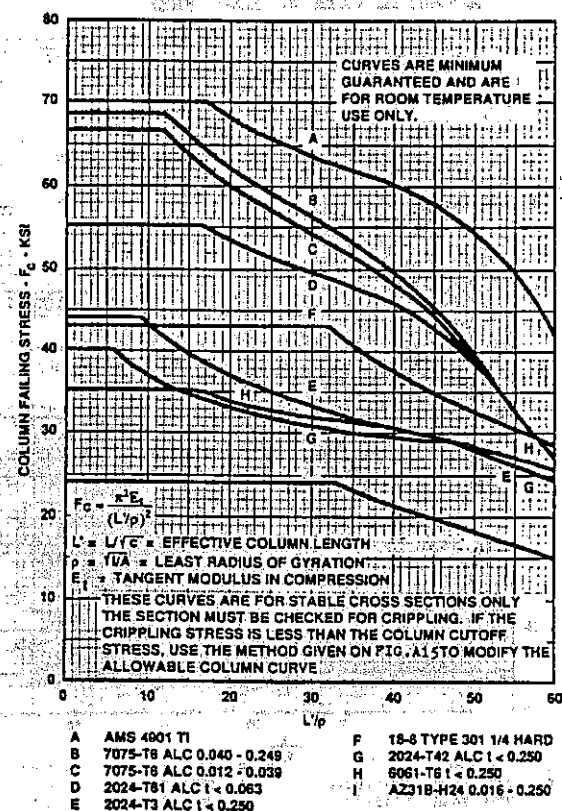


FIG. A16 TITANIUM AND STEEL ALLOY COLUMN CURVES

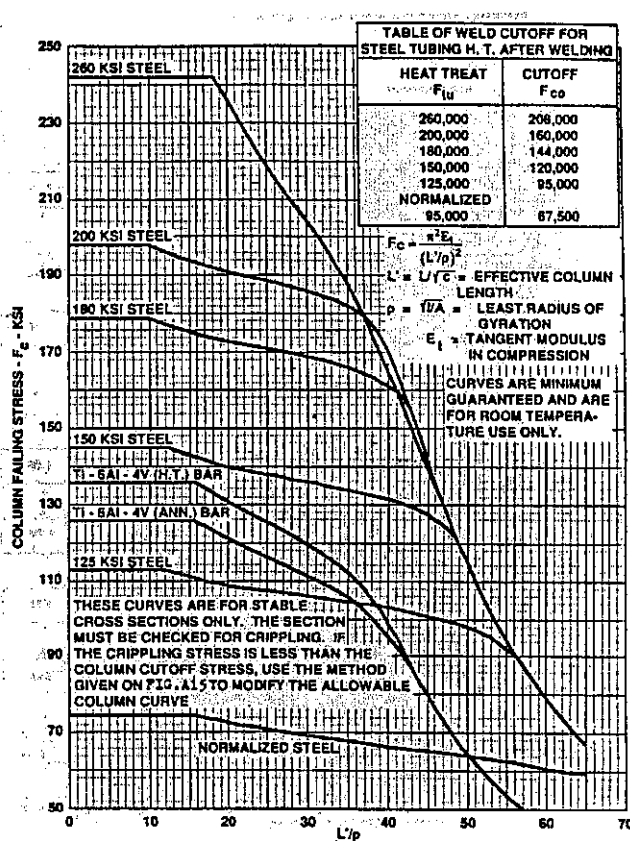


FIG. A15 COLUMN CURVES FOR EXTRUSIONS AND FORGING

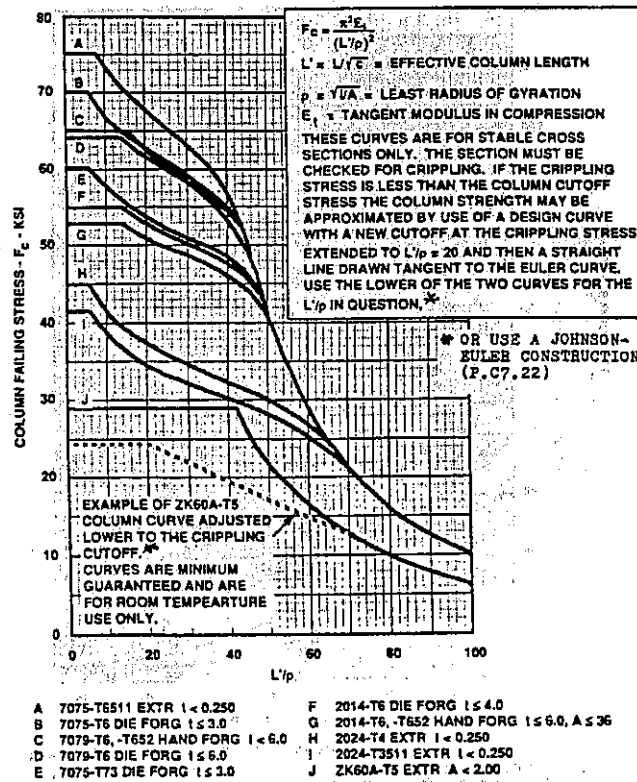
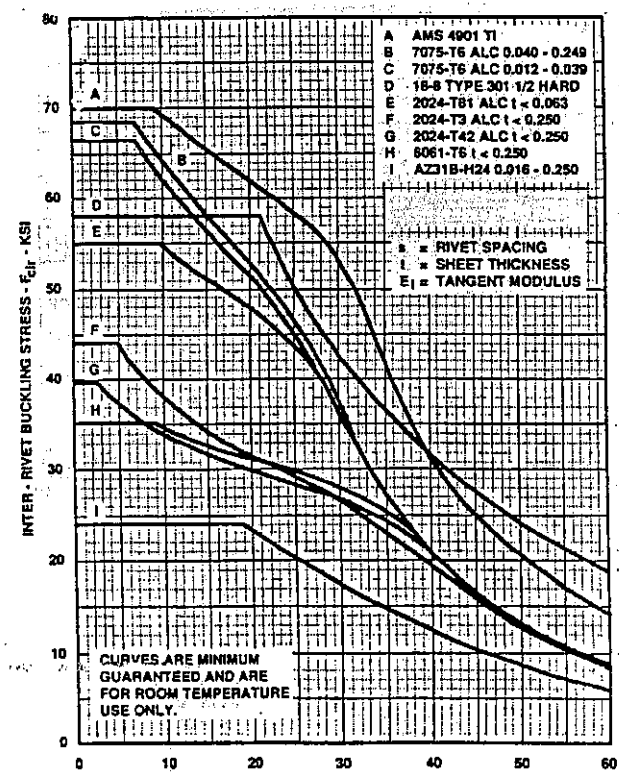


FIG. A17 INTER-RIVET BUCKLING CURVES FOR SHEET MATERIALS



* For c/s, dimpled or spotweld joints multiply S by 1.10.

TABLE A2 MATERIAL PROPERTIES

GENERAL NOTE: Data shown are the most commonly used and thickness ranges are shown in MIL-HDBK-5. Unless specified otherwise, the sizes shown are thickness dimensions.

- (a) L-Longitudinal, T-Transverse, LT-Long Transverse, ST-Short Transverse-grain direction.
- (b) Values in the "A" column are minimum guaranteed properties (either "A" or "S" values). Values in the "B" column are based on probability data (lowest expected in 90% of the material).
- (c) Average modulus of elasticity in tension (E_t) and compression (E_c).
- (d) See SDM Manual (or MIL-HDBK-5) for secondary modulus in compression (E_c -secondary) for clad materials.
- (e) Percent elongation is expressed in terms of the specification "S" values, usually for 2.0 inch gage length on flat specimens and 4D for round specimens. See note (h) or (k) when noted.
- (f) Coefficient of thermal expansion, α , in terms of $\text{In}/\text{In}/^{\circ}\text{F}$ (10^{-6}) and assumed linear for range of 70° to 212°F . For other temperature data see MIL-HDBK-5.
- (g) Consult Materials and Processes Unit in regard to reduced transverse properties for sections of thickness over 6 inches or areas greater than 40 square inches.
- (h) These elongation values are for gage length of 4 times the diameter.
- (i) Hand forgings shall not be used without the specific approval of the Engineering Materials and Process Unit.
- (j) For aluminum castings the data are applicable to special mold, permanent mold or investment mold processes. This data is applicable to strength class number which must be negotiated with the vendor. All of the casting strength data are representative of specimens taken from the castings.
- (k) Elongation value is a minimum for this thickness range. For a specific thickness see MIL-HDBK-5.

- (l) Mechanical properties at the 200 ksi and 260 ksi strength level apply to 4340 material only.
- (m) Reference MIL-HDBK-5 for correlation of thicknesses, diameters, and shapes relative to the materials and heat treat levels shown.

TEMPER DESIGNATIONS

- F As-fabricated wrought material.
- O Annealed, recrystallized wrought material.
- N Normalized.
- T3 Solution heat treated and cold worked by flattening.
- T4 Solution heat treated and naturally aged.
- T42 Solution heat treated by user.
- T6 Solution heat treated and artificially aged.
- T62 Applicable to sheet and plate heat treated and aged by the user.
- T7 Solution heat treated and stabilized.
- T73 Solution heat treated, special aging.
- T74 Solution heat treated, special aging and mech. property differences.
- T81 Solution heat treated, cold worked and artificially aged.

STRESS RELIEF VARIATIONS

- T-51 Stress relieved by stretching (plate, rolled or cold-finished rod and bar).
- T510 Stress relieved by stretching (extruded rod, bar, shapes and tubing).
- T511 Same as T-510 except minor straightening after stretching.
- T-52 Stress relieved by compression.
- T-54 Stress relieved by combined stretching and compression.

FORM	MATERIAL	ROOM TEMPERATURE MATERIAL PROPERTIES - KIPS PER SQUARE INCH (GEN. NOTE)									
		COLD DRAWN	SPEC. THICKNESS	THICKNESS	TEMPER						
		A	B	C	D	E	F	G	H	I	
2024	BARE ALUMINUM ALLOY	0.010-0.128	0.129-0.448	0.449-0.998	1.001-1.500	1.501-2.000	2.001-2.500	2.501-3.000	3.001-4.000	4.001-5.000	5.001-6.000
T3	T31	1.1	1.2	1.3	1.4	1.5	1.6	1.7	1.8	1.9	2.0
T4	T41	1.1	1.2	1.3	1.4	1.5	1.6	1.7	1.8	1.9	2.0
T42	T421	1.1	1.2	1.3	1.4	1.5	1.6	1.7	1.8	1.9	2.0
T6	T61	1.1	1.2	1.3	1.4	1.5	1.6	1.7	1.8	1.9	2.0
T62	T621	1.1	1.2	1.3	1.4	1.5	1.6	1.7	1.8	1.9	2.0
T7	T71	1.1	1.2	1.3	1.4	1.5	1.6	1.7	1.8	1.9	2.0
T73	T731	1.1	1.2	1.3	1.4	1.5	1.6	1.7	1.8	1.9	2.0
T74	T741	1.1	1.2	1.3	1.4	1.5	1.6	1.7	1.8	1.9	2.0
T81	T811	1.1	1.2	1.3	1.4	1.5	1.6	1.7	1.8	1.9	2.0

FORM	MATERIAL	ROOM TEMPERATURE MATERIAL PROPERTIES - KIPS PER SQUARE INCH (GEN. NOTE)									
		COLD DRAWN	SPEC. THICKNESS	THICKNESS	TEMPER						
		A	B	C	D	E	F	G	H	I	
2024	CLAD ALUMINUM ALLOY	0.010-0.128	0.129-0.448	0.449-0.998	1.001-1.500	1.501-2.000	2.001-2.500	2.501-3.000	3.001-4.000	4.001-5.000	5.001-6.000
T3	T31	1.1	1.2	1.3	1.4	1.5	1.6	1.7	1.8	1.9	2.0
T4	T41	1.1	1.2	1.3	1.4	1.5	1.6	1.7	1.8	1.9	2.0
T42	T421	1.1	1.2	1.3	1.4	1.5	1.6	1.7	1.8	1.9	2.0
T6	T61	1.1	1.2	1.3	1.4	1.5	1.6	1.7	1.8	1.9	2.0
T62	T621	1.1	1.2	1.3	1.4	1.5	1.6	1.7	1.8	1.9	2.0
T7	T71	1.1	1.2	1.3	1.4	1.5	1.6	1.7	1.8	1.9	2.0
T73	T731	1.1	1.2	1.3	1.4	1.5	1.6	1.7	1.8	1.9	2.0
T74	T741	1.1	1.2	1.3	1.4	1.5	1.6	1.7	1.8	1.9	2.0
T81	T811	1.1	1.2	1.3	1.4	1.5	1.6	1.7	1.8	1.9	2.0

APPENDIX A ADDITIONAL DESIGN AND ANALYSIS DATA

TABLE A2 MATERIAL PROPERTIES (Con'd)

ROOM TEMPERATURE MATERIAL PROPERTIES - KIPS PER SQUARE INCH (GEN. NOTE)												SPEC									
MATERIAL	FORM	COPPER										SPEC									
		A	B	C	D	E	F	G	H	I	J										
TB1	0.0124-0.039	1	74	71	69	70	71	74	48	143	156	117	122	103	104	38	7	12.0	0.33	QA-A-25072	
ALUMINUM ALLOY	0.0460-0.125	1	73	60	58	70	72	73	47	148	155	150	149	122	123	103	38	8	12.0	0.33	
TB2	0.128-0.249	1	72	60	57	61	61	62	47	148	156	160	121	124	123	103	39	8	12.0	0.33	
TB3	0.250-0.499	1	72	58	59	62	62	63	47	148	156	160	121	124	123	103	39	8	12.0	0.33	
TB4	0.500-1.000	1	72	58	59	61	61	62	43	141	145	149	114	118	103	103	39	8	12.0	0.33	
TB5	1.001-2.000	1	72	58	59	61	61	62	44	145	145	147	117	120	103	103	39	8	12.0	0.33	
TB6	1.501-2.000	1	72	58	59	61	61	62	44	145	145	147	117	120	103	103	39	8	12.0	0.33	
TB7	0.048-0.249	1	72	58	59	61	61	62	44	145	147	147	117	120	103	103	39	8	12.0	0.33	
TB8	0.250-0.499	1	72	58	59	61	61	62	44	145	145	147	117	120	103	103	39	8	12.0	0.33	
TB9	0.500-1.000	1	72	58	59	61	61	62	44	145	145	147	117	120	103	103	39	8	12.0	0.33	
TB10	1.001-2.000	1	72	58	59	61	61	62	44	145	145	147	117	120	103	103	39	8	12.0	0.33	
TB11	1.501-2.000	1	72	58	59	61	61	62	44	145	145	147	117	120	103	103	39	8	12.0	0.33	
TB12	2.001-2.500	1	72	58	59	61	61	62	44	145	145	147	117	120	103	103	39	8	12.0	0.33	
TB13	0.048-0.249	1	71	62	65	66	67	68	44	143	143	143	103	103	103	103	39	8	12.0	0.33	
TB14	0.250-0.499	1	71	62	65	66	67	68	44	143	143	143	103	103	103	103	39	8	12.0	0.33	
TB15	0.500-1.000	1	71	62	65	66	67	68	44	143	143	143	103	103	103	103	39	8	12.0	0.33	
TB16	1.001-2.000	1	71	62	65	66	67	68	44	143	143	143	103	103	103	103	39	8	12.0	0.33	
TB17	1.501-2.000	1	71	62	65	66	67	68	44	143	143	143	103	103	103	103	39	8	12.0	0.33	
TB18	2.001-2.500	1	71	62	65	66	67	68	44	143	143	143	103	103	103	103	39	8	12.0	0.33	
TB19	2.501-3.000	1	71	62	65	66	67	68	44	143	143	143	103	103	103	103	39	8	12.0	0.33	
TB20	3.001-3.500	1	71	62	65	66	67	68	44	143	143	143	103	103	103	103	39	8	12.0	0.33	
TB21	3.501-4.000	1	71	62	65	66	67	68	44	143	143	143	103	103	103	103	39	8	12.0	0.33	
TB22	4.001-4.500	1	71	62	65	66	67	68	44	143	143	143	103	103	103	103	39	8	12.0	0.33	
TB23	4.501-5.000	1	71	62	65	66	67	68	44	143	143	143	103	103	103	103	39	8	12.0	0.33	
TB24	5.001-5.500	1	71	62	65	66	67	68	44	143	143	143	103	103	103	103	39	8	12.0	0.33	
TB25	5.501-6.000	1	71	62	65	66	67	68	44	143	143	143	103	103	103	103	39	8	12.0	0.33	
TB26	6.001-6.500	1	71	62	65	66	67	68	44	143	143	143	103	103	103	103	39	8	12.0	0.33	
TB27	6.501-7.000	1	71	62	65	66	67	68	44	143	143	143	103	103	103	103	39	8	12.0	0.33	
TB28	7.001-7.500	1	71	62	65	66	67	68	44	143	143	143	103	103	103	103	39	8	12.0	0.33	
TB29	7.501-8.000	1	71	62	65	66	67	68	44	143	143	143	103	103	103	103	39	8	12.0	0.33	
TB30	8.001-8.500	1	71	62	65	66	67	68	44	143	143	143	103	103	103	103	39	8	12.0	0.33	
TB31	8.501-9.000	1	71	62	65	66	67	68	44	143	143	143	103	103	103	103	39	8	12.0	0.33	
TB32	9.001-9.500	1	71	62	65	66	67	68	44	143	143	143	103	103	103	103	39	8	12.0	0.33	
TB33	9.501-10.000	1	71	62	65	66	67	68	44	143	143	143	103	103	103	103	39	8	12.0	0.33	
TB34	10.001-10.500	1	71	62	65	66	67	68	44	143	143	143	103	103	103	103	39	8	12.0	0.33	
TB35	10.500-11.000	1	71	62	65	66	67	68	44	143	143	143	103	103	103	103	39	8	12.0	0.33	
TB36	11.001-11.500	1	71	62	65	66	67	68	44	143	143	143	103	103	103	103	39	8	12.0	0.33	
TB37	11.500-12.000	1	71	62	65	66	67	68	44	143	143	143	103	103	103	103	39	8	12.0	0.33	
TB38	12.001-12.500	1	71	62	65	66	67	68	44	143	143	143	103	103	103	103	39	8	12.0	0.33	
TB39	12.500-13.000	1	71	62	65	66	67	68	44	143	143	143	103	103	103	103	39	8	12.0	0.33	
TB40	13.001-13.500	1	71	62	65	66	67	68	44	143	143	143	103	103	103	103	39	8	12.0	0.33	
TB41	13.500-14.000	1	71	62	65	66	67	68	44	143	143	143	103	103	103	103	39	8	12.0	0.33	
TB42	14.001-14.500	1	71	62	65	66	67	68	44	143	143	143	103	103	103	103	39	8	12.0	0.33	
TB43	14.500-15.000	1	71	62	65	66	67	68	44	143	143	143	103	103	103	103	39	8	12.0	0.33	
TB44	15.001-15.500	1	71	62	65	66	67	68	44	143	143	143	103	103	103	103	39	8	12.0	0.33	
TB45	15.500-16.000	1	71	62	65	66	67	68	44	143	143	143	103	103	103	103	39	8	12.0	0.33	
TB46	16.001-16.500	1	71	62	65	66	67	68	44	143	143	143	103	103	103	103	39	8	12.0	0.33	
TB47	16.500-17.000	1	71	62	65	66	67	68	44	143	143	143	103	103	103	103	39	8	12.0	0.33	
TB48	17.001-17.500	1	71	62	65	66	67	68	44	143	143	143	103	103	103	103	39	8	12.0	0.33	
TB49	17.500-18.000	1	71	62	65	66	67	68	44	143	143	143	103	103	103	103	39	8	12.0	0.33	
TB50	18.001-18.500	1	71	62	65	66	67	68	44	143	143	143	103	103	103	103	39	8	12.0	0.33	
TB51	18.500-19.000	1	71	62	65	66	67	68	44	143	143	143	103	103	103	103	39	8	12.0	0.33	
TB52	19.001-19.500	1	71	62	65	66	67	68	44	143	143	143	103	103	103	103	39	8	12.0	0.33	
TB53	19.500-20.000	1	71	62	65	66	67	68	44	143	143	143	103	103	103	103	39	8	12.0	0.33	
TB54	20.001-20.500	1	71	62	65	66	67	68	44	143	143	143	103	103	103	103	39	8	12.0	0.33	
TB55	20.500-21.000	1	71	62	65	66	67	68	44	143	143	143	103	103	103	103	39	8	12.0	0.33	
TB56	21.001-21.500	1	71	62	65	66	67	68	44	143	143	143	103	103	103	103	39	8	12.0	0.33	
TB57	21.500-22.000	1	71	62	65	66	67	68	44	143	143	143	103	103	103	103	39	8	12.0	0.33	
TB58	22.001-22.500	1	71	62	65	66	67	68	44	143	143	143	103	103	103	103	39	8	12.0	0.33	
TB59	22.500-23.000	1	71	62	65	66	67	68	44	143	143	143	103	103	103	103	39	8	12.0	0.33	
TB60	23.001-23.500	1	71	62	65	66	67	68	44</												

APPENDIX A ADDITIONAL DESIGN AND ANALYSIS DATA

A8

TABLE A2 MATERIAL PROPERTIES (Con'd)

ROOM TEMPERATURE MATERIAL PROPERTIES - KIPS PER SQUARE INCH (GEN. NOTE)											
SPEC											
FORM	MATERIAL	CONDITION	STRENGTH (psi)	STRESS (psi)	ELONG. (%)	COEF. EXPANS.	TEMPERATURE (°F)	DEFORMATION (in/in)	SHEDULING (psi)	TESTS (psi)	ENDS (psi)
TUBE	ALUMINUM ALLOY (1)	1001-3.000 A < 256	12	96	10.2 10.4	1.0	0.33	0.0-A-367	AHS 1111	TI COM. EDGE	ML-T-5046
		1.1	50	81	1.0	1.34	0.33	AHS 4320	AND	ANN.	- CP-1
		1.1	50	81	1.0	1.34	0.33	ML-A-2771	TI-A-4-IV	ANN.	ML-T-5046
		1.1	50	81	1.0	1.34	0.33	0.018-2.00	TITANIUM ALLOY	ANN.	COMP. AB-1
		1.1	50	81	1.0	1.34	0.33	0.0015-5.500	TA1050	E1	ML-T-5046
		1.1	50	81	1.0	1.34	0.33	0.018-0.750	STA	E2	COMP. AB-1
		1.1	50	81	1.0	1.34	0.33	0.018-1.000	H1025	E3	ML-T-5046
		1.1	50	81	1.0	1.34	0.33	0.018-0.750	TA1050	E4	ML-T-5046
		1.1	50	81	1.0	1.34	0.33	0.018-1.000	TA1050	E5	ML-T-5046
		1.1	50	81	1.0	1.34	0.33	0.018-0.750	TA1050	E6	ML-T-5046
		1.1	50	81	1.0	1.34	0.33	0.018-1.000	TA1050	E7	ML-T-5046
		1.1	50	81	1.0	1.34	0.33	0.018-0.750	TA1050	E8	ML-T-5046
		1.1	50	81	1.0	1.34	0.33	0.018-1.000	TA1050	E9	ML-T-5046
		1.1	50	81	1.0	1.34	0.33	0.018-0.750	TA1050	E10	ML-T-5046
		1.1	50	81	1.0	1.34	0.33	0.018-1.000	TA1050	E11	ML-T-5046
		1.1	50	81	1.0	1.34	0.33	0.018-0.750	TA1050	E12	ML-T-5046
		1.1	50	81	1.0	1.34	0.33	0.018-1.000	TA1050	E13	ML-T-5046
		1.1	50	81	1.0	1.34	0.33	0.018-0.750	TA1050	E14	ML-T-5046
		1.1	50	81	1.0	1.34	0.33	0.018-1.000	TA1050	E15	ML-T-5046
		1.1	50	81	1.0	1.34	0.33	0.018-0.750	TA1050	E16	ML-T-5046
		1.1	50	81	1.0	1.34	0.33	0.018-1.000	TA1050	E17	ML-T-5046
		1.1	50	81	1.0	1.34	0.33	0.018-0.750	TA1050	E18	ML-T-5046
		1.1	50	81	1.0	1.34	0.33	0.018-1.000	TA1050	E19	ML-T-5046
		1.1	50	81	1.0	1.34	0.33	0.018-0.750	TA1050	E20	ML-T-5046
		1.1	50	81	1.0	1.34	0.33	0.018-1.000	TA1050	E21	ML-T-5046
		1.1	50	81	1.0	1.34	0.33	0.018-0.750	TA1050	E22	ML-T-5046
		1.1	50	81	1.0	1.34	0.33	0.018-1.000	TA1050	E23	ML-T-5046
		1.1	50	81	1.0	1.34	0.33	0.018-0.750	TA1050	E24	ML-T-5046
		1.1	50	81	1.0	1.34	0.33	0.018-1.000	TA1050	E25	ML-T-5046
		1.1	50	81	1.0	1.34	0.33	0.018-0.750	TA1050	E26	ML-T-5046
		1.1	50	81	1.0	1.34	0.33	0.018-1.000	TA1050	E27	ML-T-5046
		1.1	50	81	1.0	1.34	0.33	0.018-0.750	TA1050	E28	ML-T-5046
		1.1	50	81	1.0	1.34	0.33	0.018-1.000	TA1050	E29	ML-T-5046
		1.1	50	81	1.0	1.34	0.33	0.018-0.750	TA1050	E30	ML-T-5046
		1.1	50	81	1.0	1.34	0.33	0.018-1.000	TA1050	E31	ML-T-5046
		1.1	50	81	1.0	1.34	0.33	0.018-0.750	TA1050	E32	ML-T-5046
		1.1	50	81	1.0	1.34	0.33	0.018-1.000	TA1050	E33	ML-T-5046
		1.1	50	81	1.0	1.34	0.33	0.018-0.750	TA1050	E34	ML-T-5046
		1.1	50	81	1.0	1.34	0.33	0.018-1.000	TA1050	E35	ML-T-5046
		1.1	50	81	1.0	1.34	0.33	0.018-0.750	TA1050	E36	ML-T-5046
		1.1	50	81	1.0	1.34	0.33	0.018-1.000	TA1050	E37	ML-T-5046
		1.1	50	81	1.0	1.34	0.33	0.018-0.750	TA1050	E38	ML-T-5046
		1.1	50	81	1.0	1.34	0.33	0.018-1.000	TA1050	E39	ML-T-5046
		1.1	50	81	1.0	1.34	0.33	0.018-0.750	TA1050	E40	ML-T-5046
		1.1	50	81	1.0	1.34	0.33	0.018-1.000	TA1050	E41	ML-T-5046
		1.1	50	81	1.0	1.34	0.33	0.018-0.750	TA1050	E42	ML-T-5046
		1.1	50	81	1.0	1.34	0.33	0.018-1.000	TA1050	E43	ML-T-5046
		1.1	50	81	1.0	1.34	0.33	0.018-0.750	TA1050	E44	ML-T-5046
		1.1	50	81	1.0	1.34	0.33	0.018-1.000	TA1050	E45	ML-T-5046
		1.1	50	81	1.0	1.34	0.33	0.018-0.750	TA1050	E46	ML-T-5046
		1.1	50	81	1.0	1.34	0.33	0.018-1.000	TA1050	E47	ML-T-5046
		1.1	50	81	1.0	1.34	0.33	0.018-0.750	TA1050	E48	ML-T-5046
		1.1	50	81	1.0	1.34	0.33	0.018-1.000	TA1050	E49	ML-T-5046
		1.1	50	81	1.0	1.34	0.33	0.018-0.750	TA1050	E50	ML-T-5046
		1.1	50	81	1.0	1.34	0.33	0.018-1.000	TA1050	E51	ML-T-5046
		1.1	50	81	1.0	1.34	0.33	0.018-0.750	TA1050	E52	ML-T-5046
		1.1	50	81	1.0	1.34	0.33	0.018-1.000	TA1050	E53	ML-T-5046
		1.1	50	81	1.0	1.34	0.33	0.018-0.750	TA1050	E54	ML-T-5046
		1.1	50	81	1.0	1.34	0.33	0.018-1.000	TA1050	E55	ML-T-5046
		1.1	50	81	1.0	1.34	0.33	0.018-0.750	TA1050	E56	ML-T-5046
		1.1	50	81	1.0	1.34	0.33	0.018-1.000	TA1050	E57	ML-T-5046
		1.1	50	81	1.0	1.34	0.33	0.018-0.750	TA1050	E58	ML-T-5046
		1.1	50	81	1.0	1.34	0.33	0.018-1.000	TA1050	E59	ML-T-5046
		1.1	50	81	1.0	1.34	0.33	0.018-0.750	TA1050	E60	ML-T-5046
		1.1	50	81	1.0	1.34	0.33	0.018-1.000	TA1050	E61	ML-T-5046
		1.1	50	81	1.0	1.34	0.33	0.018-0.750	TA1050	E62	ML-T-5046
		1.1	50	81	1.0	1.34	0.33	0.018-1.000	TA1050	E63	ML-T-5046
		1.1	50	81	1.0	1.34	0.33	0.018-0.750	TA1050	E64	ML-T-5046
		1.1	50	81	1.0	1.34	0.33	0.018-1.000	TA1050	E65	ML-T-5046
		1.1	50	81	1.0	1.34	0.33	0.018-0.750	TA1050	E66	ML-T-5046
		1.1	50	81	1.0	1.34	0.33	0.018-1.000	TA1050	E67	ML-T-5046
		1.1	50	81	1.0	1.34	0.33	0.018-0.750	TA1050	E68	ML-T-5046
		1.1	50	81	1.0	1.34	0.33	0.018-1.000	TA1050	E69	ML-T-5046
		1.1	50	81	1.0	1.34	0.33	0.018-0.750	TA1050	E70	ML-T-5046
		1.1	50	81	1.0	1.34	0.33	0.018-1.000	TA1050	E71	ML-T-5046
		1.1	50	81	1.0	1.34	0.33	0.018-0.750	TA1050	E72	ML-T-5046
		1.1	50	81	1.0	1.34	0.33	0.018-1.000	TA1050	E73	ML-T-5046
		1.1	50	81	1.0	1.34	0.33	0.018-0.750	TA1050	E74	ML-T-5046
		1.1	50	81	1.0	1.34	0.33	0.018-1.000	TA1050	E75	ML-T-5046
		1.1	50	81	1.0	1.34	0.33	0.018-0.750	TA1050	E76	ML-T-5046
		1.1	50	81	1.0	1.34	0.33	0.018-1.000	TA1050	E77	ML-T-5046
		1.1	50	81	1.0	1.34	0.33	0.018-0.750	TA1050	E78	ML-T-5046
		1.1	50	81	1.0	1.34	0.33	0.018-1.000	TA1050	E79	ML-T-5046
		1.1	50	81	1.0	1.34	0.33	0.018-0.750	TA1050	E80	ML-T-5046
		1.1	50	81	1.0	1.34	0.33	0.018-1.000	TA1050	E81	ML-T-5046
		1.1	50	81	1.0	1.34	0.33	0.018-0.750	TA1050	E82	ML-T-5046
		1.1	50	81	1.0	1.34	0.33	0.018-1.000	TA1050	E83	ML-T-5046
		1.1	50	81	1.0	1.34	0.33	0.018-0.750	TA1050	E84	ML-T-5046
		1.1	50	81	1.0	1.34	0.33	0.018-1.000	TA1050	E85	ML-T-5046
		1.1	50	81	1.0	1.34	0.33	0.018-0.750	TA1050	E86	ML-T-5046
		1.1	50	81	1.0	1.34	0.33	0.018-1.000	TA1050	E87	ML-T-5046
		1.1	50	81	1.0	1.34	0.33	0.018-0.750	TA1050	E88	ML-T-5046
		1.1	50	81	1.0	1.34	0.33	0.018-1.000	TA1050	E89	ML-T-5046
		1.1	50	81	1.0	1.34	0.33	0.018-0.750	TA1050	E90	ML-T-5046
		1.1	50	81	1.0	1.34	0.33	0.018-1.000	TA1050	E91	ML-T-5046
		1.1	50	81	1.0	1.34	0.33	0.018-0.750	TA1050	E92	ML-T-5046
		1.1	50	81	1.0	1.34	0.33	0.018-1.000	TA1050	E93	ML-T-5046
		1.1	50	81	1.0	1.34	0.33	0.018-0.750	TA1050	E94	ML-T-5046
		1.1	50	81	1.0	1.34	0.33	0.018-1.000	TA1050	E95	ML-T-5046
		1.1	50	81	1.0	1.34	0.33	0.018-0.750	TA1050	E96	ML-T-5046
		1.1	50	8							

TABLE A2. MATERIAL PROPERTIES (Concluded)

TABLE A3 FASTENER COUNTERSUNK HEAD DEPTH (IN.)

SOLID & BLIND RIVETS					
SHEAR HEAD (SH)		FLUSH HEAD (FH)			
CALLOUT	TABLE	TYPE	CALLOUT	TABLE	TYPE
NAS1097(Std)	A*	SOLID RIVET	MS20426(Std)	C*	SOLID RIVET
MS14218	A*	-	MS14219	C*	-
NAS1200	A*	-	CSR902B	C*	-
NAS1739	B	BLIND RIVET	MS20427	D*	-
			CR3242	B*	BLIND RIVET
			MS20601	C*	-
			CR3212	C*	-
			NAS1399	C*	-
			CR4622	C*	-
			NAS1921	C*	-

FASTENER DIAMETER (in.)	A	B	C	D
.179	.029*-.027	.035	.042*-.041	.048
.5/32	.037*-.035	.047	.055*-.053	.061
.3/16	.046*-.044	.063	.070*-.068	.077
.1/4	.061*-.060*	.086	.095*-.090	.103
.5/16	.067		.106*-.104	.115
.3/8	.077		.134*	.144
.7/16				
.1/2				

Applicable head sizes per specification.

FASTENER/JOINT DESIGN PROCEDURES AND DATA

FASTENER/JOINT DESIGN NOTES

GENERAL NOTES

The tables in the fastener section present data necessary to obtain the strengths of the more common fasteners and fastener-sheet combinations. Additional data are presented in MIL-HDBK-5, or the particular "customer" design manual when applicable.

Basic Yield-Ultimate Relation

The basic yield-ultimate relation for fasteners is ultimate = 1.5 x yield. The yield loading is critical if 1.5 x yield strength is < ultimate strength. When this occurs an adjusted ultimate value must be calculated by taking 1.5 x yield load. The joint strength tables have already been adjusted and are identified by an asterisk.

- Note that when calculating the sheet bearing strength for protruding head fasteners (i.e., those listed on page 28) the yield-ultimate relation must be considered. An asterisk (*) is placed on the bearing ratio factors of Table A9 or A10 to indicate yield critical cases.

Static Joint Analysis Data

- Fastener Shear Strength: Obtain from joint strength tables when applicable or from shear strength tables A6 and A7 (for solid rivets), and page 32 for LK-Bolts and threaded fasteners.
- Sheet Bearing Strength: Obtain from joint strength tables when applicable or from calculations when using protruding head fasteners.
- Sheet Strength: Check sheet for net area tension and shear tearout. Also verify adequate edge margins, no knife edge conditions and use of equivalent hole diameters for countersunk sheets.
- Sheet Intervall buckling or wrinkling and effects of temperature on joint strength
- Margins of Safety are shown on page A1

Edge Distance Variations

All of the joint strength tables are applicable to joints having an edge distance (e) of two diameters (2D). When other edge distances are being analyzed, the table values are to be reduced linearly using the bearing allowables (F_{bu} and F_{by}) presented in MIL-HDBK-5 or using factors in Table A9 and for e/D of 1.50 and 2.0.

Tension Applications

Solid or blind rivets and blind bolts are not allowed in primary tension applications. They are allowed in secondary tension cases such as, skins with aerodynamic lift forces or internal pressure, attachment of shear or compression webs, and stringers to frames.

- For secondary tension an effective tensile "pull-thru" allowable of 20% of the ultimate joint strength allowable (at the specific sheet thickness) is considered to be conservative. This approach is recommended for any fastener type except those having shear heads and reduced head features or if specific data has been developed. For NAS 1097 reduced shear head rivets use 10% of the particular ultimate joint strength allowable.

FLUSH HEAD FASTENERS

The joint strength allowables for all flush head fasteners are based on test data. Calculated joint strengths are not permitted.

- When selecting flush head fasteners and sheet thickness, "knife-edge" conditions are not allowed. The recommended design ratio (countersink depth/sheet thickness) is 0.8 for secondary structure and 0.7 for primary structure with reversed loading.
- See Tables A3 and A4 for the countersink depths of common fasteners. Fig. A16 and A17 provide equivalent hole diameters (D_e in countersunk sheet) for several fasteners and head styles. These diameters are used when determining net "hole-out" in sheet material.

PROTRUDING HEAD FASTENERS

The joint strengths for the following fastener types and conditions must be based on test data:

- Any fastener installed in sheet material where t/D is < 0.18.
- Any joint with protruding shear head or reduced head fasteners.
- Any joint with protruding head blind rivets or blind bolts (with either shear or tension type heads).

The joint strength allowables for protruding "tension" head fasteners may be calculated as described below:

- The load per fastener at which fastener shear or sheet bearing type of failure occurs is determined separately and the lower of the two governs the design.
- Shear strengths for prot. hd. solid rivets of any material, except aluminum, are determined directly from Table A6. For protruding solid aluminum rivets (tension types) an effective rivet strength is obtained by multiplying the Table A6 shear values by the reduction factors of Table A7.
- Shear strengths for protruding head Hi-Loks, Lk-Bolts, and threaded fasteners are obtained listed in Table A8.
- Calculate the effective sheet bearing strengths for all protruding head solid rivets by multiplying the Table A8 values by the ratio of allowable bearing stress/100,000 (K values) of Table A9 or A10 for the applicable sheet material.
- Calculate the effective sheet bearing strengths for Hi-Loks, Lk-Bolts and solid threaded types by multiplying the Table A8 values by the ratio factors (K values) in Tables A9 or A10 for the applicable sheet material.

TABLE A4 FASTENER COUNTERSUNK HEAD DEPTH (IN.)

HI-LOKS/LOCKBOLTS/SCREWS/BLINDBOLTS			FLUSH HEAD (FH) OR TENSION (TH)		
CALLOUT	TABLE	TYPE	CALLOUT	TABLE	TYPE
HL11(STD)	E	HI-LOK	HL13(STD)	H	HI-LOK
GPL3SC	F*	LOCKBOLT	GPL8SC	-	LOCKBOLT
GPL2SC	F*	-	NAS1456-62	-	-
NAS1436-42	F*	-	NAS1516-18	-	-
LGPL9SC	G	-	NAS7024-32	J*	(2)
CSR924	F	SWAGED PIN	LGPL4SC	J	(2)
HSR101	E	-	MS90353	K	(1)BLINDBOLT
HSR201	E	-	MS21140	H*	SCREW
NAS1581	F*	SCREW	AN509(STD)	H*	SCREW
NAS1620	H*	-	NAS517	H*	-
NAS1670L	H*	(1)BLINDBOLT	NAS1580	K*	-

FASTENER DIAMETER (in.)	E	F	G	H	I	J(2)	K
1/8	.041/.039	.043/.034	.040	.070/.068*	.074*.073	.051*.049	.072
5/32	.047/.045	.048*.046	.045	.081/.079*	.084*.082	.060*.056	.082*.080
3/16	.061/.059	.063*.060	.059	.109/.105*	.110*.108*	.078*.074	.111*.105
1/4	.068*.066	.070*.067	.066	.135/.133*	.140*.137	.095*.092	.140*.137
5/16	.079*.076	.081*.077	.076	.162/.160*	.168*.165	.111*.110	.167*.165
3/8	.097*.094	.100*	-	.190*.187*	-	-	.185*.183
7/16	.107*.104	.111*	-	.216/.213	-	-	.222*.220

NOTES:

- Blind bolts (H*, I* and K) are intended for shear application and secondary tension.
- Intermediate head. Primary shear and secondary tension applications. (Reference J)
- Applicable head sizes per specification.

Table A3 is located on p.A9

FIG. A18 EQUIVALENT HOLE DIAMETERS (CSK HOLES)

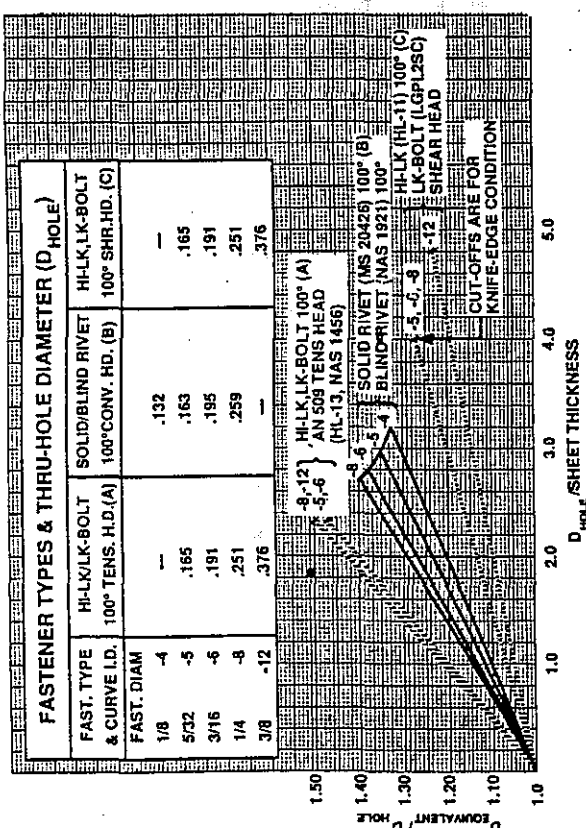


FIG.A19 EQUIVALENT HOLE DIAMETERS (CSK HOLES)

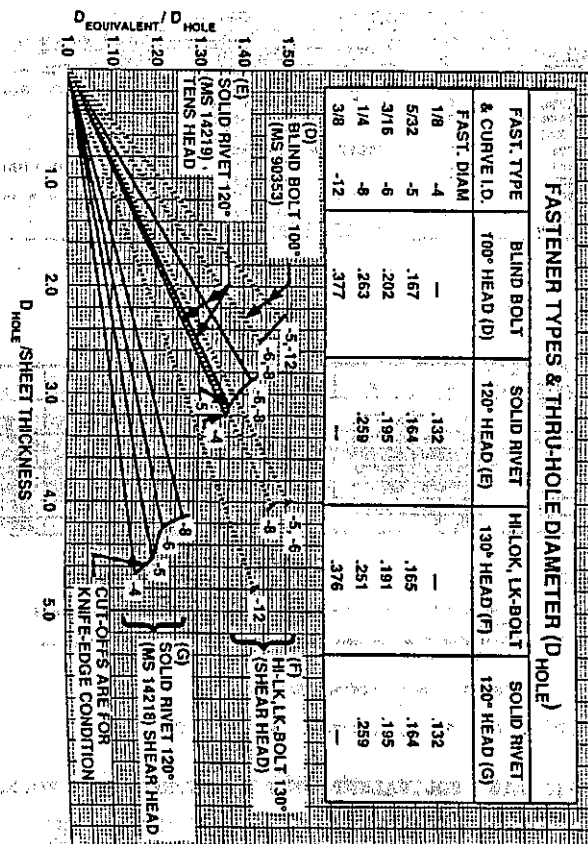


TABLE A5 PROTRUDING HEAD FASTENERS FOR CALCULATED JOINT STRENGTH

Joint strengths for the following fastener types are to be calculated as described BEFORE AND ON THE TABLES LISTED.

PROTRUDING "TENSION" OR UNIVERSAL HEAD STYLES

SOLID RIVETS MS20470 AD & B UNIV. HD. ALUM.
SEE TABLES A6 MS20615M UNIV. HD. MONEL
THRU A10 NAS1198 UNIV. HD. A286
CSR903B UNIV. HD. Ti/Cb

HI-LOK/LK-BOLTS HL-12 HEAD STYLES
SEE TABLES A9
THRU A13 HLT452 HEAD STYLES
LGPL4SP(PULL)/LGPS4SP(STUMP) TYPES
GPL8TP(PULL)/GPS8TP(STUMP) TYPES
NAS1425-32 LOCK-BOLT
NAS1465-72 LOCK-BOLT

BOLTS MS21250
SEE TABLES A9
THRU A13 MS14181
NAS1003
NAS1303 (SERIES)
NAS6203, 6303, 6403, 6703 & 6803 (SERIES)
NAS464

TABLE A6 SOLID RIVET SHEAR STRENGTH

RIVET SIZE, IN.	1/16	3/32	1/8	5/32	3/16	1/4	5/16	3/8	
DRILL NO.	51	41	30	21	11	8	P	W	
NOMINAL HOLE DIAMETER, IN.	0.067	0.095	0.1285	0.159	0.197	0.257	0.323	0.386	
DESIGNATION									
RIVET MATERIAL									
5056-H321 $F_{su} = 28 \text{ ksi}^b$	B	.69	.203	.363	.556	.802	1450	2295	3275
2117-T3 $F_{su} = 30 \text{ ksi}^b$	AD	106	217	388	598	862	1535	2460	3510
2017-T3 $F_{su} = 34 \text{ ksi}^b$	D	120	247	442	875	977	1785	2785	3880
2017-T3 $F_{su} = 38 \text{ ksi}^b$	D	134	275	494	735	1090	1970	3115	4445
2024-T3 $F_{su} = 41 \text{ ksi}^b$	DD	145	296	531	814	1175	2125	3360	4800
7050-T3 $F_{su} = 41 \text{ ksi}^b$	E, KE	145	296	531	814	1175	2125	3360	4800
7050-T731 $F_{su} = 43 \text{ ksi}^b$	E, KE	152	311	556	854	1230	2230	3525	5030
Monei $F_{su} = 49 \text{ ksi}$		173	355	635	973	1405	2540	4015	5735
Ti-Cb $F_{su} = 53 \text{ ksi}$		187	384	687	1050	1520	2750	4340	6200
A-286 $F_{su} = 90 \text{ ksi}$		317	651	1170	1790	2580	4870	7370	10500

a Based on nominal hole diameter specified above.

b Values are for the as driven condition, on a probability basis (B values).

c Undriven S value; driven B value has not been demonstrated.

d Apply shear strength reduction factors: TAB A7, when using protruding head aluminum alloy solid rivets.

TABLE A7. PROTRUDING HEAD RIVET REDUCTION FACTORS

PROTRUDING HEAD ALUM. SOLID RIVET SHEAR STRENGTH REDUCTION FACTORS (3), (4)
(FOR ALUM. RIVETS ONLY) MS20470 HEAD STYLES

DIA OF RIVET	SHEET THICKNESS (in.)							
	1/16	3/32	1/8	5/32	3/16	1/4	5/16	3/8
0.016 SS	0.964							
0.016 DS	0.687							
0.018 SS	0.981	0.912						
0.018 DS	0.744	0.518						
0.020 SS	0.995	0.933						
0.020 DS	0.769	0.585						
0.025 SS	1.000	0.970	0.920					
0.025 DS	0.870	0.708	0.545					
0.032 SS	1.000	0.964	0.925					
0.032 DS	0.941	0.814	0.687	0.560				
0.036 SS	0.989	0.857	0.981	0.948	0.912			
0.036 DS			0.744	0.630	0.518			
0.040 SS	0.992	0.891	0.995	0.964	0.933			
0.040 DS			0.789	0.687	0.585			
0.045 SS	1.000	0.924	0.834	0.744	0.653			
0.050 SS				0.955	0.970	0.920		
0.050 DS				0.951	0.870	0.788	0.545	
0.063 SS					1.000	1.000	0.961	0.922
0.063 DS					0.937	0.872	0.808	0.550
0.071 SS						0.966	0.909	0.979
0.071 DS						0.852	0.737	0.622
0.080 SS							0.995	0.954
0.080 DS							0.992	0.941
0.090 SS							0.989	0.981
0.090 DS							1.000	0.924
0.100 SS							0.992	0.951
0.100 DS							1.000	1.000
0.125 SS							1.000	1.000
0.125 DS							0.992	0.941
0.160 SS								0.992
0.160 DS								1.000
0.190 SS								0.981
0.190 DS								0.939
0.250 SS								1.000
0.250 DS								1.000

NOTES:

1. Sheet thickness is that of the thinnest sheet in single shear and of the middle sheet in double shear.
2. Values listed are for room temperature use only.
3. Values based on tests of aluminum rivets.
4. Do not use this table for monel, Ti, or steel rivets.

TABLE A8 SHEET UNIT BEARING STRENGTH - LBS BASED
ON $F_{br} = 100,000$ PSI FOR PROTRUDING
TENSION HEAD SOLED RIVETS
(MS 20470 AND HEAD STYLES OF TABLE A5)

		Unit Bearing Strength for Rivet Diameter Indicated, lbs							
RIVET SIZE		1/16	3/32	1/8	5/32	3/16	1/4	5/16	3/8
SHEET THICKNESS, IN.	HOLE DIAMETER	0.067	0.096	0.1285	0.159	0.191	0.257	0.323	0.386
	0.012	80	*	*	*	*	*	*	
	0.016	107	*	*	*	*	*	*	
	0.018	121	173	*	*	*	*	*	
	0.020	134	192	*	*	*	*	*	
	0.025	168	240	321	*	*	*	*	
	0.032	214	307	411	509	*	*	*	
	0.036	241	346	462	572	686	*	*	
	0.040	268	384	514	636	764	*	*	
	0.045	302	432	578	716	860	*	*	
	0.050	335	480	642	795	955	1285	*	
	0.063	422	605	810	1002	1203	1619	2035	
	0.071	476	682	912	1129	1356	1825	2293	2741
	0.080	536	758	1028	1272	1526	2056	2584	3068
	0.090	603	864	1156	1431	1719	2313	2907	3474
	0.100	670	960	1285	1590	1910	2570	3230	3860
	0.125	838	1200	1606	1988	2388	3212	4036	4825
	0.160	1072	1536	2056	2544	3056	4112	5168	6176
	0.190	1273	1824	2442	3021	3629	4883	6137	7334
	0.250	1570	2400	3210	3975	4775	6425	8075	9650

- Where D/t is greater than 5.5, tests are required to substantiate yield and ultimate bearing strengths.

NOTES:

1. Design values of sheet bearing strength are obtained by multiplying the bearing strength (lbs) given above by the ratio of design sheet bearing stress + 100,000. Determine values for both yield and ultimate. If $1.5 \times P_{by}$ is less than P_{yu} the joint is yield critical and $P_{bu} = 1.5 \times P_{by}$. Bearing ratios are presented on TABLES A9 AND A10.
 2. Values for rivets are based on hole diameters shown. See TBL A13 for solid shank threaded fasteners/lockbolts.

TABLE A9 BEARING STRENGTH RATIO FACTORS TO BE USED WITH TABLE A8 AND TABLE A13 DATA

MATERIAL	THICKNESS, IN.	"A" OR "S" VALUES		"B" VALUES	
		K(ULTIMATE)	K(YIELD)	K(ULTIMATE)	K(YIELD)
2024-T3	0.010-0.128	.125 #120	.101 #10	#2.0 #1.5	#2.0 #1.5
0.129-0.249	1.31	1.04	.88	.73	1.31
0.250-0.449	1.19	.97	.86	.72	1.22
0.500-1.000	1.17	.95	.86	.72	1.20
1.001-2.000	1.15	.94	.86	.72	1.19
2024-T42	0.010-0.459	1.16*	.93*	.61	.53
0.500-1.000	1.16	.92	.61	.53	—
1.001-2.000	1.14	.90	.61	.53	—
2.001-3.000	1.10	.87	.61	.53	—
2024-T81	0.010-0.249	1.27	1.00	.94	.83
0.250-0.459	1.31	1.02	1.01	.86	1.23
0.500-1.000	1.29	1.00	1.01	.86	1.23
1.001-1.459	1.29	1.00	.99	.85	—
2024-Y3 (CLAD)	0.010-0.052	1.1	.97	.82	.68
0.068-0.128	1.25	1.01	.84	.70	1.27
0.129-0.249	1.27	1.02	.84	.70	1.26
0.250-0.449	1.15	.94	.82	.63	1.13
0.500-1.000	1.13	.92	.82	.69	1.17
1.001-2.000	1.11	.91	.82	.69	1.15
2024-T42 (CLAD)	0.010-0.052	1.00*	.86*	.54	.49
0.068-0.249	1.14*	.90*	.58	.52	1.18*
0.250-0.449	1.14	.90	.58	.52	—
0.500-1.000	1.12	.89	.58	.50	—
1.001-2.000	1.10	.87	.58	.50	—
2024-T81 (CLAD)	0.010-0.052	1.22	1.00	.94	.83
0.250-0.449	1.27	.93	.98	.83	1.29
0.500-1.000	1.23	.95	.98	.83	—

SHEAR STRENGTH OF THREADED/SOLID SHANK FASTENERS

SHEAR STRENGTH OF THREADED/SOLID SHANK FASTENERS

	F _{lu} (MIN)	125 (KSI)	160	180	210	220
	F _{su} (MIN)	75 (KSI)	95	108	125	132
FAST. DIAM. IN.	AREA IN ²	ULTIMATE SINGLE SHEAR STRENGTH, LBS				
3/16	0.188	0.02761	2071	2623	2982	3452
#10	0.190	0.02835	2126	2694	3062	3544
1/4	0.250	0.04909	3682	4660	5300	6140
5/16	0.312	0.0767	5750	7290	8280	9590
3/8	0.375	0.11045	8280	10490	11930	13810
7/16	0.438	0.15033	11270	14280	16240	18790
1/2	0.500	0.19635	14730	18650	21210	24540
9/16	0.562	0.24850	18640	23610	28840	31060
5/8	0.625	0.30680	23010	29150	33130	38356
3/4	0.750	0.44179	33130	42000	47700	55200
7/8	0.875	0.60132	45100	57100	64900	75200
1	1.000	0.78540	58900	74600	84800	98200

NOTES:

- 1.** Shear values above are based on the basic shank diameters shown and are also applicable to solid shank pins, i.e., lockbolts. The values may vary for some fastener types when the procurement specification lists different diameters and material shear strengths (F_{su}).

ULTIMATE VALUES MUST BE BASED ON 1.5 X (YIELD) RATIO SHOWN.
RATIO DATA OBTAINED FROM MIL-HDBK-5E (CHANGE NOTICE 1 AND 2).

TABLE A12 ULTIMATE TENSILE STRENGTH OF THREADED STEEL FASTENERS (MIL-S-8879 ROLLED THREADS)

FASTENER DIAMETER (INCH)	MAXIMUM MINOR AREA (IN ²)	FASTENER TENSILE STRENGTH-KSI			
		160	180	220	
10-32	0.190	0.018602	2 976	3 348	4 090
1/4-28	0.250	0.034241	5 480	6 160	7 530
5/16-24	0.312	0.054905	8 780	9 800	12 080
3/8-24	0.375	0.083679	13 420	15 100	18 450
7/16-20	0.438	0.11323	18 120	20 380	24 910
1/2-20	0.500	0.15358	24 570	27 640	33 790
9/16-18	0.562	0.19502	31 200	35 100	42 900
5/8-18	0.625	0.24700	39 520	44 500	54 300
3/4-18	0.750	0.38082	57 700	64 900	79 400
7/8-14	0.875	0.49327	78 900	88 800	108 500
1-12	1.000	0.64156	102 600	115 500	141 100
1-1/8-12	1.125	0.83129	133 000	149 600	182 900
1-1/4-12	1.250	1.0456	187 300	188 200	230 000
1-3/8-12	1.375	1.2844	205 500	231 200	282 600
1-1/2-12	1.500	1.51477	247 600	278 600	340 500

NOTES:

- Values shown are the fastener capability at the thread root area, using nuts designed to develop the fastener.
- The root area is computed using nominal maximum diameter as published in Tables II and III of MIL-S-8879, Ref. MIL-HDBK-5.
- See FIG. A46 for strength ratings of common nut types.

TABLE A13 SHEET/PLATE UNIT BEARING STRENGTH -- LBS BASED ON $F_{bd} = 100,000 \text{ PSI}$ (PROT. HEAD SOLID SHANK FASTENERS/PINS)

FASTENER EXAMPLES (SEE TABLE A5)

THREADED TYPES: NAS 1303, 6203, 6303, 6403, 6703, 6803, MS21250
HI LOKS; TENSION HEAD STYLES SUCH AS HL 12, HL 452
LOCKBOLTS; TENSION HEAD STYLES NAS 1465-72 AND NAS 1525-32

Unit Bearing Strength of Sheet for Fastener Diameter Indicated, lb												
Fastener Diameter Sheet Thickness	5/32	3/16	1/4	5/16	3/8	7/16	1/2	9/16	5/8	3/4	7/8	1
0.032	500	-	-	-	-	-	-	-	-	-	-	-
0.036	563	575	-	-	-	-	-	-	-	-	-	-
0.040	625	750	-	-	-	-	-	-	-	-	-	-
0.045	704	845	-	-	-	-	-	-	-	-	-	-
0.050	781	940	1,250	-	-	-	-	-	-	-	-	-
0.063	985	1,180	1,575	1,969	-	-	-	-	-	-	-	-
0.071	1,110	1,330	1,775	2,219	2,662	-	-	-	-	-	-	-
0.080	1,250	1,500	2,000	2,500	3,000	3,500	-	-	-	-	-	-
0.090	1,407	1,690	2,250	2,812	3,375	3,938	4,500	-	-	-	-	-
0.100	1,562	1,875	2,500	3,125	3,750	4,375	5,000	-	-	-	-	-
0.125	1,953	2,440	3,125	3,905	4,688	5,469	6,256	7,030	7,812	-	-	-
0.160	2,500	3,000	4,000	5,000	6,000	7,000	8,000	9,000	10,000	12,000	-	-
0.200	3,125	3,750	5,000	6,250	7,500	8,750	10,000	11,250	12,500	15,000	17,500	20,000
0.250	3,916	4,688	6,250	7,812	9,375	10,940	12,500	14,060	15,625	18,750	21,875	25,000
0.312	4,867	5,856	7,800	9,734	11,700	13,870	15,800	17,530	19,500	23,400	27,200	31,200
0.375	5,850	7,050	9,375	11,700	14,060	16,425	18,750	21,075	23,440	28,125	32,810	37,500
0.500	7,800	9,400	12,500	15,600	18,750	21,900	25,000	28,100	31,250	37,500	43,750	50,000
0.625	9,750	11,750	15,625	19,500	23,440	27,375	31,250	35,125	39,062	46,875	54,890	62,500
0.750	11,700	14,100	18,750	23,400	28,125	32,850	37,500	42,150	46,875	54,250	65,825	73,000
0.875	13,650	16,450	21,875	27,300	32,810	38,325	43,750	49,175	56,690	65,825	78,560	87,500
1.000	15,500	18,800	25,000	31,200	37,500	43,800	50,000	56,200	62,500	75,000	87,500	100,000

- * Where D/t is greater than 5.5 tests are required to substantiate yield and ultimate bearing strength.
 1. Sheet bearing strengths are obtained by multiplying the above values (LB) by the ratio of design sheet bearing stress - 100,000. Determine values for both yield and ultimate. If t/t is less than P_{bd}/P_{br} , the joint is yield critical and $P_{bd} = 1.5 \times P_{br}$. Bearing ratios are presented on TABLES A9 AND A10.
 2. Values for solid shank threaded fasteners and pins are based on the nominal diameters shown.

TABLE A14 SOLID RIVETS CSK IN 2024-T42 CLAD

RIVET	SHEET MATL.	ULTIMATE STRENGTH - LB		(2117-T3) FSU = 30 KSI	(2117-T3) FSU = 38 KSI	2024-T3 FSU = 41 KSI	MS2042BD cr	MS2042BD cr
		1/8	3/16					
0	0.032	352	532	—	—	—	—	—
0.040	163	326	506	—	—	—	—	—
0.045	206	340	532	—	—	—	—	—
0.050	216	353	532	—	—	—	—	—
0.063	407	512	717	—	—	—	—	—
0.080	508	526	720	—	—	—	—	—
0.100	610	535	726	—	—	—	—	—
0.125	725	633	833	—	—	—	—	—
0.160	919	814	1014	—	—	—	—	—
0.190	1100	914	1114	—	—	—	—	—
0.250	217	388	596	—	—	—	—	—
SHEAR				753	1093	1370	1180	2120

NOTES:
 1. Values are for room temperature use only.
 2. * Denotes ultimate values based on 1.5 Yield.
 Values that are (underlined) are knife edge condition.
 SEE "PARTNERS FOR ACCOMMODATING RIVET SIZES"

TABLE A15 SOLID SHEAR HEAD RIVETS CSK IN CLAD

ULTIMATE STRENGTH OF NAS1097-E RIVETS COUNTERSUNK IN CLAD ALUMINUM ALLOY (100° SHEAR HEAD)

RIVET	NAS1097-E (FSU = 41 ksi) (7050-T73)						
SHEET MATL.	Clad 2024-T3			Clad 7075-T6			
DIAM. (NOM)	1/8 (0.1285)	5/32 (0.159)	3/16 (0.191)	1/4 (0.257)	1.8 (0.1285)	5/32 (0.159)	3/16 (0.191)
ULTIMATE STRENGTH, LBS⁽²⁾							
0.025	(227)	—	—	—	(278)	—	—
0.032	326	(367)	—	—	354	(441)	—
0.040	437	505	(561)	627	439	547	(661)
0.050	466	679	773	(908)	456	674	823
0.063	485	717	1005	1275	477	700	980
0.071	497	731	1025	1500	490	716	999
0.080	507	747	1045	1750	505	734	1020
0.090	521	765	1065	1840	520	754	1045
0.100	531	781	1085	1870	531	774	1070
0.125	—	814	1135	1835	—	814	1130
0.160	—	—	—	1175	2030	—	—
0.190	—	—	—	2110	—	—	—
0.250	—	—	—	2125	—	—	—
SHEAR	531	814	1175	2125	531	814	1175

- NOTES:
 1. Values are for room temperature use only.
 2. Values that are (underlined) are knife edge condition. See page 21 for recommended sheet thicknesses.

TABLE A16 SOLID SHEAR HEAD RIVETS CSK IN CLAD

ULTIMATE STRENGTH OF MS14218AD RIVETS
COUNTERSUNK IN ALUMINUM (120° SHEAR HEAD)

RIVET SHEET	MS14218AD ($F_{su} = 30 \text{ ksi}$) (2117-T3)					
	CLAD 2024-T3					
	ULTIMATE STRENGTH, LBS (2)					
t / D	5/32	1/8	5/32	3/16	7/32	1/4
0.020	(125)	—	—	—	—	—
0.025	(153)	(212)	—	—	—	—
0.032	186	263	(334)	—	—	—
0.040	216	322	408	(498)	—	—
0.050	217	380	498	609	(740)	(849)
0.063	—	388	568	751	910	1040
0.071	—	—	596	817	1015	1155
0.080	—	—	—	862	1125	1290
0.090	—	—	—	—	1205	1425
0.100	—	—	—	—	1225	1520
0.125	—	—	—	—	—	1555
SHEAR	217	388	596	862	1225	1555

ULTIMATE STRENGTH OF MS14218E RIVETS
COUNTERSUNK IN ALUMINUM (120° SHEAR HEAD)

RIVET SHEET	MS14218E ($F_{su} = 43 \text{ ksi}$) (7050-T73)					
	CLAD 2024-T3					
	ULTIMATE STRENGTH, LBS (2)					
t / D	5/32	3/16	7/32	1/4	9/32	5/16
0.025	—	—	—	—	—	—
0.032	(346)	—	—	—	—	—
0.040	478	(529)	—	—	—	—
0.050	673	732	(806)	—	—	—
0.063	781	1045	1135	(1200)	(1285)	—
0.071	803	1110	1365	1445	1530	(1630)
0.080	827	1140	1565	1735	1835	1930
0.090	854	1175	1605	1990	2200	2320
0.100	—	1205	1645	2030	2525	2725
0.125	—	1230	1740	2140	2650	3205
0.160	—	—	1755	2230	2820	3400
0.190	—	—	—	—	2840	3525
SHEAR	854	1230	1755	2230	2840	3525

NOTES:

- Values are for R.T. use only.
- Values that are underlined are knife-edge condition. See page A10, recommended sheet thicknesses.

TABLE A17 SOLID TENSION HEAD RIVETS CSK IN ALUM.

ULTIMATE STRENGTH OF MS14219E RIVETS
COUNTERSUNK IN ALUMINUM (120° TENSION HEAD)

RIVET SHEET	MS14219E ($F_{su} = 43 \text{ ksi}$) (7050-T73)					
	CLAD 2024-T3					
	ULTIMATE STRENGTH, LBS (2)					
t / D	5/32	3/16	7/32	1/4	9/32	5/16
0.050	(527)	(560)	—	—	—	—
0.063	743	(819)	—	—	—	—
0.071	788	979	(1065)	—	—	—
0.080	834	1105	1280	—	—	—
0.090	854	1185	1520	(1625)	(1715)	—
0.100	—	1230	1605	1890	(2020)	(2120)
0.125	—	—	1755	2145	2580	2965
0.160	—	—	—	2230	2840	3415
0.190	—	—	—	—	—	3525
SHEAR	854	1230	1755	2230	2840	3525

ULTIMATE STRENGTH OF MS14219E RIVETS
COUNTERSUNK IN ALUMINUM (120° TENSION HEAD)

RIVET SHEET	MS14219E ($F_{su} = 43 \text{ ksi}$) (7050-T73)					
	CLAD 7075-T6					
	ULTIMATE STRENGTH, LBS (2)					
t / D	5/32	3/16	7/32	1/4	9/32	5/16
0.040	(563)	—	—	—	—	—
0.050	(704)	(846)	—	—	—	—
0.063	803	(1065)	(1270)	—	—	—
0.071	832	1140	(1435)	(1615)	—	—
0.080	854	1180	1600	(1920)	(2055)	—
0.090	—	1220	1650	(2030)	(2310)	(2575)
0.100	—	1230	1700	2090	(2365)	(2860)
0.125	—	—	1755	2230	2740	3295
0.160	—	—	—	—	2840	3525
SHEAR	854	1230	1755	2230	2840	3525

NOTES:

- Values are for R.T. use only.
- Values that are underlined are knife-edge condition. See page A10, recommended sheet thicknesses.

TABLE A18 SOLID T1-45Cb RIVETS CSK IN ALUMINUM
AND IN T1-6Al-4VULTIMATE STRENGTH OF COUNTERSUNK BRFS-T
RIVETS IN ALUMINUM AND TITANIUM (120° SHEAR HEAD)

RIVET SHEET	BRFS-T ($F_{su} = 53 \text{ ksi}$) (T1-45Cb)					
	CLAD 7075-T6 T1-6Al-4V, ANNEALED					
	ULTIMATE STRENGTH, LBS (2)					
t / D	1/8	5/32	3/16	1/8	5/32	3/16
0.025	(288)	—	—	(400)	—	—
0.032	369	(456)	—	513	(635)	—
0.040	461	572	(684)	564	798	(952)
0.050	577	713	858	602	867	1190
0.063	810	891	1080	650	927	1270
0.071	628	914	1220	680	954	1310
0.080	849	939	1300	687	1005	1360
0.090	671	967	1330	—	1050	1420
0.100	687	996	1370	—	—	1470
0.125	—	1050	1450	—	—	1520
0.160	—	—	1520	687	1050	1520
SHEAR	687	1050	1520	687	1050	1520

ULTIMATE STRENGTH OF COUNTERSUNK CSR902B RIVETS
IN ALUMINUM 2024-T81 CLAD (100° FLUSH HEAD)

RIVET SHEET	CSR902B ($F_{su} = 50 \text{ ksi}$) (T1-45Cb)					
	CLAD 2024-T81					
	ULTIMATE STRENGTH, LBS (2)					
RIVET DIAMETER	3/32	1/8	5/32	3/16		
Sheet Thickness (in.)						
0.020	—	—	—	—	—	—
0.025	—	—	—	—	—	—
0.032	—	—	—	—	—	—
0.040	293	—	(357)	—	—	—
0.050	361	458	(554)	—	—	—
0.063	—	—	648	732	—	—
0.071	—	—	648	910	(942)	—
0.080	—	—	—	994	1172	—
0.090	—	—	—	—	1433	—
RIVET SHEAR	362	548	994	994	1433	—

NOTES:

- Values are for R.T. use only.
- Values that are underlined are for knife-edge condition.
- *Fastener notes for recommended sheet thicknesses.

• Denotes ultimate values based on 1.5 x yield.

ULTIMATE STRENGTH OF 20472 MONEL RIVETS
COUNTERSUNK IN STAINLESS STEEL SHEET (100° HEAD)

RIVET SHEET MATERIAL	AISI 301 - 1/2 HARD					
	AISI 302 ANNEALED					
	ULTIMATE STRENGTH, LBS (2)					
t / D	1/8	5/32	3/16	5/32	3/16	5/32
0.040	(389)	—	(439)	—	(431)	—
0.050	496	(602)	468	—	322	447
0.063	603	612	759	—	595	688
0.071	612	—	855	(1028)	635	741
0.080	612	—	955	1157	615	741
0.090	—	—	1298	—	973	—
0.100	—	—	1400	—	1400	—
0.125	—	—	—	—	635	973
SHEAR	1400	635	973	973	1400	—

NOTES:

- Values are for R.T. use only.
- Values that are underlined are for knife-edge condition.
- * Denotes ultimate values based on 1.5 x yield.

TABLE A20 TENSION STRENGTH OF SOLID ALUM. RIVETS

EFFECTIVE ULTIMATE TENSION STRENGTH OF ALUMINUM
RIVETS IN ALUMINUM SHEET (FOR SECONDARY LOADING)

PROTRUDING HEAD RIVETS

RIVET	MS 20470 AD (2117-T3)			
SHEET	BARE & CLAD 2024-T3, T4, T6, T8X, 7075-T6			
ULTIMATE STRENGTH - LBS				
D	1/8	5/32	3/16	1/4
.020	140			
.025	180	220		
.032	240	260	320	
.040	300	350	420	570
.050	375	430	520	700
.063	416	560	840	850
.071		642	730	970
.080			825	1100
.090			935	1230
.100				1380
.125				1650

FLUSH HEAD RIVETS

RIVET	MS 20425 AD (2117-T3)			
SHEET	BARE & CLAD 2024-T3, T4, T6, T8X, 7075-T6			
ULTIMATE STRENGTH - LBS				
D	1/8	5/32	3/16	1/4
.050	230			
.063	330	360		
.071	375	440	480	
.080		535	590	
.090		578	715	
.100			842	925
.125				1350
.160				1485

TABLE A22 BLIND PROT. HEAD RIVETS IN ALUMINUM

ULTIMATE STRENGTH OF BLIND PROTRUDING HEAD ALUMINUM ALLOY (2017) RIVETS IN ALUMINUM SHEET (1)
(OVERSIZE DIAMETER)

RIVET TYPE	NAS 1758D (F _u = 38 ksl)		
SHEET MATERIAL	CLAD 2024-T3		
RIVET DIAMETER	1/8 (0.144)	5/32 (0.178)	3/16 (0.207)
ULTIMATE STRENGTH, LBS.			
SHEET THICK			
0.020	199		
0.025	278	307	
0.032	373	453	476
0.040	429	577	677
0.050	494	659	810
0.063	583	767	934
0.071	619	830	1011
0.080		906	1097
0.090		935	1185
0.100			1280
RIVET SHEAR	619	935	1260

RIVET TYPE	NAS 1758D (F _u = 38 ksl)		
SHEET MATERIAL	CLAD 7075-T6		
RIVET DIAMETER	1/8 (0.144)	5/32 (0.178)	3/16 (0.207)
ULTIMATE STRENGTH, LBS.			
SHEET THICK			
0.020	252		
0.025	301	384	
0.032	373	469	557
0.040	442	570	676
0.050	508	674	819
0.063	578	777	953
0.071	619	827	1028
0.080		890	1098
0.090		935	1178
0.100			1260
RIVET SHEAR	619	935	1260

NOTES:
1. Values are for room temperature use only.

TABLE A21 BLIND PROT. HEAD RIVETS IN ALUM.

ULTIMATE STRENGTH OF BLIND PROTRUDING HEAD ALUMINUM ALLOY RIVETS IN ALUMINUM SHEET (1)

RIVET TYPE	HAS 1398 B AND C		HAS 1398 D AND E		NAS 1738 B AND C
SHEET MATERIAL	CODE A (F _u = 30 ksl)		CODE B (F _u = 38 ksl)		NAS 1738 D, E, (F _u = 34 ksl)
CLAD 2024-T3 AND HIGHER STRENGTH ALUMINUM ALLOYS					
RIVET DIAMETER	1/8	5/32	3/16	1/4	1/8
HOLE DIAMETER	(0.130)	(0.162)	(0.194)	(0.130)	(0.162)
SHEET THICK					
0.020	167	189	199	187	189
0.025	228	262	290	314	226
0.032	269	364	412	479	364
0.040	337	448	553	670	355
0.050	384	521	662	914	416
0.063	598	781	1145	944	647
0.071				1240	854
0.080				1350	785
0.090					1475
0.100					1550
0.125					1580
RIVET SHEAR	368	598	682	1550	1090

* Denotes ultimate values based on 1.5 x yield.

ULTIMATE STRENGTH OF BLIND PROTRUDING HEAD MONEL RIVETS IN ALUMINUM SHEET (1)

RIVET	NAS 1398 MS, MW AND CODE A (F _u = 55 ksl)		
SHEET	CLAD 7075-T6 & HIGHER ALUM ALLOYS		
ULTIMATE STRENGTH, LBS.			
D	1/8	5/32	3/16
0.020	232	258	
0.025	318	361	394
0.032	404	506	569
0.040	466	624	774
0.050	546	720	922
0.063	647	845	1072
0.071	710	921	1168
0.080		1099	1272
0.090			1387
0.100			1507
0.125			1580
RIVET SHEAR	710	1090	1580

NOTES:
1. Values are for room temperature use only.

TABLE A23 BLIND PROT. HEAD RIVETS IN ALUMINUM

ULTIMATE STRENGTH OF BLIND PROTRUDING HEAD ALUMINUM ALLOY (5056 "CHERRymax") RIVETS IN ALUMINUM SHEET

PART NO.	HEAD STYLE	CLAD	CR2012
H640 STYLE		2024-T3 CLAD	ARH
FASTERNER DIAMETER, IN. (NOMINAL DIAMETER, IN.)	1/8 (0.130)	5/32 (0.162)	3/16 (0.194)
SHEET THICKNESS, IN.			
0.016	102		
0.020	172	202	
0.025	223	267	308
0.032	295	358	517
0.040	334	458	538
0.050	383	520	688
0.063	445	599	768
0.071	470	648	1150
0.080	498	697	892
0.090	530	736	1320
0.100	561	775	1020
0.125	636	873	1135
0.160	664	1001	1300
0.190		1030	1428
0.250		—	1490
0.312		—	2615
FASTENER SHEAR STRENGTH	664	1030	1480

ULTIMATE STRENGTH OF BLIND PROTRUDING HEAD ALUMINUM ALLOY (5056 "CHERRymax") RIVETS IN ALUMINUM SHEET (OVERSIZE DIAMETER)

PART NO.	HEAD STYLE	CLAD	CR243
H640 STYLE		2024-T3 CLAD	ARH
FASTERNER DIAMETER, IN. (NOMINAL DIAMETER, IN.)	1/8 (0.144)	5/32 (0.178)	3/16 (0.207)
SHEET THICKNESS, IN.			
0.016	132		
0.020	206	240	241
0.025	269	317	358
0.032	356	426	485
0.040	423	552	527
0.050	485	659	610
0.063	558	748	830
0.071	589	805	993
0.080	619	867	1065
0.090	652	909	1150
0.100	685	950	1205
0.125	758	1053	1252
0.160	787	1163	1495
0.190		1206	1573
0.250		—	2465
0.312		—	2745
FASTENER SHEAR STRENGTH	814	1245	1685

NOTES:
1. Values are for room temperature use only.

2. * denotes ultimate values based on 1.5 x yield.

3. Preliminary allowable, Cherry Textron testing.

TABLE A24 BLIND PROT. HEAD RIVETS IN ALUMINUM

ULTIMATE STRENGTH OF BLIND PROTRUDING HEAD MONEL RIVETS IN ALUMINUM SHEET

RIVET TYPE	CR4523 ($F_{u0} = 65$ ksi)		
SHEET MATERIAL	CLAD 7075-T6		
RIVET DIAMETER, IN. (NOMINAL HOLE DIAMETER, IN.)	1/8 (0.130)	3/16 (0.194)	1/4 (0.256)
ULTIMATE STRENGTH, LBS.			
SHEET THICKNESS, IN.			
0.020	221	344	
0.025	294	444	
0.032	373	566	500
0.040	475	742	664
0.050	602	940	878
0.063	701	945	1120
0.071	729	1055	1270
0.080	760	1095	1440
0.090	796	1140	1540
0.100	831	1180	1590
0.125	863	1290	1725
0.160		1340	1905
0.190			2125
0.250			3400
RIVET SHEAR STRENGTH	863	1340	1920
			3400

ULTIMATE STRENGTH OF BLIND PROTRUDING HEAD MONEL RIVETS IN ALUMINUM SHEET (OVERSIZE DIAMETER)

RIVET TYPE	NAS 1768M ($F_{u0} = 65$ ksi)		
SHEET MATERIAL	CLAD 7075-T6		
RIVET DIAMETER, IN. (NOMINAL HOLE DIAMETER, IN.)	1/8 (0.144)	5/32 (0.178)	3/16 (0.207)
ULTIMATE STRENGTH, LBS.			
SHEET THICKNESS, IN.			
0.020	245	380	
0.025	322	484	
0.032	444	526	591
0.040	521	687	771
0.050	597	802	934
0.063	697	925	1140
0.071	761	1001	1226
0.080	830	1087	1324
0.090	885	1182	1435
0.100		1280	1547
0.125		1353	1623
RIVET SHEAR	895	1353	1623

NOTES: Values are for room temperature use only.

TABLE A25 BLIND PROT. HEAD RIVETS IN ALUMINUM AND AISI 301

ULTIMATE STRENGTH OF BLIND PROTRUDING HEAD A-286 RIVETS IN ALUMINUM

RIVET TYPE	CR4523 ($F_{u0} = 75$ ksi)		
SHEET MATERIAL	CLAD 7075-T6		
RIVET DIAMETER, IN. (NOMINAL HOLE DIAMETER, IN.)	1/8 (0.130)	5/32 (0.162)	3/16 (0.194)
ULTIMATE STRENGTH, LBS.			
SHEET THICKNESS, IN.			
0.020	237		
0.025	298	367	
0.032	385	478	566
0.040	486	601	714
0.050	610	757	902
0.063	772	958	1145
0.071	856	1080	1290
0.080	903	1220	1455
0.090	956	1340	1645
0.100	995	1405	1830
0.125		1545	2055
0.160			2215
0.190			3570
0.250			3920
RIVET SHEAR STRENGTH	995	1545	2215
			3920

ULTIMATE STRENGTH OF BLIND PROTRUDING HEAD MONEL RIVETS IN STAINLESS STEEL SHEET

RIVET TYPE	NAS 1395 MS OR MW AND NAS 1398 MS OR MW CODE A ($F_{u0} = 55$ ksi)		
SHEET MATERIAL	AISI 301-HALF HARD		
RIVET DIAMETER, IN. (NOMINAL HOLE DIAMETER, IN.)	1/8 (0.130)	5/32 (0.162)	3/16 (0.194)
ULTIMATE STRENGTH, LBS.			
SHEET THICKNESS, IN.			
0.020	378	480	591
0.025	452	584	715
0.032	548	734	894
0.040	594	870	1094
0.050	632	915	1270
0.063	678	971	1235
0.071	705	1009	1380
0.080	710	1048	1428
0.090		1090	1478
0.100			1532
0.125			1580
RIVET SHEAR	710	1090	1590

NOTES: Values are for room temperature use only.

TABLE A26 BLIND CSK RIVETS IN ALUMINUM

ULTIMATE STRENGTH OF BLIND COUNTERSUNK HEAD RIVETS IN CLAD ALUMINUM ALLOYS (100° HEAD) (1)

RIVET TYPE	NAS 1399 B AND NAS 1399 B, CODE A (5058) ($F_{u0} = 30$ ksi)		NAS 1399 D AND NAS 1399 D, CODE A (2017) ($F_{u0} = 36$ ksi)			
SHEET MATERIAL	CLAD 2024-T3 AND HIGHER STRENGTH ALUMINUM ALLOYS					
RIVET DIAMETER (NOMINAL HOLE)	1/8 (0.130)	5/32 (0.162)	3/16 (0.194)	1/8 (0.130)	5/32 (0.162)	3/16 (0.194)
ULTIMATE STRENGTH, LBS.						
SHEET THICKNESS						
0.032						
0.040	(108°)			(108°)		
0.050	171°	(170°)		171°	(170°)	
0.063	266°	273°	(255°)	296°	273°	(255°)
0.071	366°	330°	371°	368°	330°	330°
0.080	388	474°	458°	423	474°	456°
0.090		578	599°	459	594°	590°
0.100		596	740°	494	652	740°
0.125				862		755
0.160						1090
RIVET SHEAR	388	596	862	494	755	1090

RIVET TYPE	NAS 1399 MS OR MW AND NAS 1399 MS OR MW, CODE A ($F_{u0} = 55$ ksi)		
SHEET MATERIAL	CLAD 7075-T6 AND HIGHER STRENGTH ALUMINUM ALLOYS		
RIVET DIAMETER (NOMINAL HOLE)	1/8 (0.130)	5/32 (0.178)	3/16 (0.207)
ULTIMATE STRENGTH, LBS.			
SHEET THICKNESS			
0.032			
0.040	(209°)		
0.050	335°	(327°)	
0.063	467°	530°	(527°)
0.071	557°	654°	677°
0.080	610	784	845°
0.090	636	873	1031°
0.100	662	937	1175
0.125	710	1015	1370
0.160		1090	1505
0.190			1580
RIVET SHEAR	710	1090	1580

NOTES:
1. Values are for room temperature use only.
2. * Denotes ultimate values based on 1.5 x yield.
3. Values that are underlined are knife edge.

TABLE A27 BLIND CSK RIVETS IN ALUMINUM ULTIMATE STRENGTH OF BLIND COUNTERSUNK HEAD RIVETS IN CLAD ALUMINUM 2024-T3 ALLOY (100° HEAD) (1)

RIVET TYPE	NAS 1739 B AND NAS 1739 E ($F_{u0} = 34$ ksi)		
SHEET MATERIAL	CLAD 2024-T3 AND HIGHER		
RIVET DIAMETER, IN. (NOMINAL HOLE DIAMETER, IN.)	1/8 (0.144)	5/32 (0.178)	3/16 (0.207)
ULTIMATE STRENGTH, LBS.			
SHEET THICKNESS, IN.			
0.032			
0.040	(212)		
0.050	266	(326)	
0.063	344	410	
0.071	441	533	(606)
0.080	504	608	696
0.090	554	693	794
0.100		787	900
0.125		837	1015
RIVET SHEAR STRENGTH	554	837	1128

RIVET TYPE	NAS 1769 D ($F_{u0} = 36$ ksi)		
SHEET MATERIAL	CLAD 2024-T3		
RIVET DIAMETER, IN. (NOMINAL HOLE DIAMETER, IN.)	1/8 (0.144)	5/32 (0.178)	3/16 (0.207)
ULTIMATE STRENGTH, LBS.			
SHEET THICKNESS, IN.			
0.032			
0.040	290°		
0.050	361	447°	(470°)
0.063	446	561	675
0.071	502	624	741
0.080	564	700	818
0.090	619	786	921
0.100		871	1020
0.125		935	1260
RIVET SHEAR STRENGTH	619	935	1260

NOTES:
1. Values are for room temperature use only.
2. * Denotes ultimate values based on 1.5 x yield.
3. Values that are underlined are knife edge.

TABLE A28 BLIND CSK RIVETS IN ALUMINUM

ULTIMATE STRENGTH OF BLIND COUNTERSUNK HEAD RIVETS
IN CLAD 7075-T6 ALUMINUM ALLOY (100° HEAD) (1)

RIVET TYPE	NAS 1769 D (F _{u0} = 36 ksi) AOP		
SHEET MATERIAL	2017 SLEEVE, 7075 STEM (F _{u0} = 36 ksi)		
RIVET DIAMETER, IN. (NOMINAL HOLE DIAMETER, IN.)	1/8 (0.144)	5/32 (0.178)	3/16 (0.207)
ULTIMATE STRENGTH, LBS.			
SHEET THICKNESS, IN.			
0.032	(244)		
0.040	(305)		
0.050	382	(470)	
0.063	485	592	(676)
0.071	525	683	773
0.080	569	749	891
0.090	619	811	988
0.100		871	1060
0.125		935	1237
0.160			1260
RIVET SHEAR STRENGTH	619	835	1260

RIVET TYPE	NAS 1769 M (F _{u0} = 55 ksi) AOP		
SHEET MATERIAL	CLAD 7075-T6 (MONEL)		
RIVET DIAMETER, IN. (NOMINAL HOLE DIAMETER, IN.)	1/8 (0.144)	5/32 (0.178)	3/16 (0.207)
ULTIMATE STRENGTH, LBS.			
SHEET THICKNESS, IN.			
0.032	(273)		
0.040	342	(423)	
0.050	455	528	
0.063	653	732	(771)
0.071	686	817	920
0.080	724	1007	1170
0.090	765	1058	1345
0.100	805	1109	1405
0.125	895	1236	1551
0.160		1353	1757
0.190			1823
RIVET SHEAR STRENGTH	895	1353	1823

NOTES:

- Values are for room temperature use only.
- Denotes ultimate values based on 1.5 x yield.
- Values that are (underlined) are knife edge.

TABLE A29 BLIND CSK RIVETS IN ALUMINUM

ULTIMATE STRENGTH OF BLIND COUNTERSUNK HEAD RIVETS
IN CLAD 7075-T6 ALUMINUM (100° HEAD) (1)

RIVET TYPE	NAS 1921 B (F _{u0} = 36 ksi) AOP		
SHEET MATERIAL	CLAD 7075-T6		
RIVET DIAMETER, IN. (NOMINAL HOLE DIAMETER, IN.)	1/8 (0.130)	5/32 (0.162)	3/16 (0.194)
ULTIMATE STRENGTH, LBS.			
SHEET THICKNESS, IN.			
0.032			
0.040	(165)		
0.050	232	(257)	
0.063	313	366	(405)
0.071	360	427	(484)
0.080	416	498	566
0.090	477	571	658
0.100	494	647	748
0.125		755	978
0.160			1090
RIVET SHEAR STRENGTH	495	755	1090

RIVET TYPE	NAS 1921 M (F _{u0} = 75 ksi), MONEL	NAS 1921 C (F _{u0} = 75 ksi), WH
SHEET MATERIAL	CLAD 7075-T6	
RIVET DIAMETER, IN. (NOMINAL HOLE DIAMETER, IN.)	1/8 (0.130)	5/32 (0.162)
ULTIMATE STRENGTH, LBS.		
SHEET THICKNESS, IN.		
0.050	531	
0.063	671	831
0.071	756	938
0.080	854	1061
0.090	911	1194
0.100	939	1328
0.125	1020	1458
0.160	1565	2145
0.190		2260
RIVET SHEAR STRENGTH	1020	1565

NOTES:

- Values are for room temperature use only.
- Denotes ultimate values based on 1.5 x yield.
- Values that are (underlined) are knife edge.

TABLE A30 BLIND CSK RIVETS IN ALUMINUM

ULTIMATE STRENGTH OF BLIND COUNTERSUNK HEAD RIVETS
(CHERRYMAX) IN 2024-T3 ALUMINUM ALLOY (100° HEAD) (1)

RIVET TYPE	CR3212 (F _{u0} = 50 ksi)		
SHEET MATERIAL	CLAD 2024-T3		
RIVET DIAMETER, IN. (NOMINAL HOLE DIAMETER, IN.)	1/8 (0.130)	5/32 (0.162)	3/16 (0.194)
ULTIMATE STRENGTH, LBS.			
SHEET THICKNESS, IN.			
0.032	(152)		
0.040	(219)	(239)	
0.050	302	(341)	(388)
0.063	380	474	(527)
0.071	423	536	(524)
0.080	474	599	(625)
0.090	511	669	810
0.100	548	737	893
0.125	620	852	1085
0.160	654	977	1285
0.190		1007	1304
0.250			2100
0.312			2453
RIVET SHEAR STRENGTH	664	1030	2665

RIVET TYPE	CR3242 (F _{u0} = 55 ksi)		
SHEET MATERIAL	CLAD 2024-T3		
RIVET DIAMETER, IN. (NOMINAL HOLE DIAMETER, IN.)	1/8 (0.144)	5/32 (0.178)	3/16 (0.207)
ULTIMATE STRENGTH, LBS.			
SHEET THICKNESS, IN.			
0.025	(144)		
0.032	(200)	(230)	
0.040	275	(312)	(344)
0.050	349	425	(462)
0.063	445	543	(641)
0.071	514	605	714
0.080	545	701	794
0.090	573	803	911
0.100	600	837	1035
0.125	669	921	1165
0.160	765	1040	1305
0.190	814	1145	1425
0.250		1245	1650
0.312			1685
0.375			2795
RIVET SHEAR STRENGTH	814	1245	1685

NOTES:

- Values are for room temperature use only.
- Denotes ultimate values based on 1.5 x yield.
- Values that are (underlined) are knife edge.

4. Preliminary allowables, Cherry Textron testing.

TABLE A31 BLIND CSK RIVETS IN ALUMINUM

ULTIMATE STRENGTH OF BLIND COUNTERSUNK HEAD RIVETS
IN 7075-T6 ALUMINUM ALLOY (100° HEAD) (1)

RIVET TYPE	CR4522 (F _{u0} = 65 ksi)		
SHEET MATERIAL	CLAD 7075-T6		
RIVET DIAMETER, IN. (NOMINAL HOLE DIAMETER, IN.)	1/8 (0.130)	5/32 (0.162)	3/16 (0.194)
ULTIMATE STRENGTH, LBS.			
SHEET THICKNESS, IN.			
0.050	254		
0.063	519	410	
0.071	681	612	
0.080	754	843	725
0.090	776	1095	1032
0.100	797	1170	1332
0.125	852	1240	1695
0.160	863	1335	1810
0.190		1340	1910
0.250			3105
0.312			3365
RIVET SHEAR STRENGTH	863	1340	3400

RIVET TYPE	CR4622 (F _{u0} = 75 ksi)		
SHEET MATERIAL	CLAD 7075-T6		
RIVET DIAMETER, IN. (NOMINAL HOLE DIAMETER, IN.)	1/8 (0.144)	5/32 (0.178)	3/16 (0.207)
ULTIMATE STRENGTH, LBS.			
SHEET THICKNESS, IN.			
0.050	317		
0.063	576	509	
0.071	734	705	
0.080	913	930	861
0.090	947	1191	1161
0.100	982	1420	1455
0.125	995	1525	2060
0.160			2258
0.190			2215
0.250			3605
RIVET SHEAR STRENGTH	995	1545	3920

NOTES:

- Values are for room temperature use only.

2. Denotes ultimate values based on 1.5 x yield.

TABLE A32 BLIND CSK RIVETS IN AISI 301 SS

ULTIMATE STRENGTH OF BLIND COUNTERSUNK MONEL RIVETS
IN AISI 301 SHEET (100° HEAD) (1)

RIVET TYPE	NAS 1399 MS OR MW AND NAS 1399 MS OR MW, CODE A ($F_{uH} = 55$ ksi)				
	AISI 301 - HALF HARD				
SHEET MATERIAL	1/8 (0.130)	5/32 (0.162)	3/16 (0.194)		
ULTIMATE STRENGTH, LBS.					
SHEET THICKNESS, IN.					
0.032					
0.040	(245 *)				
0.050	363	(380 *)			
0.063	491	569			
0.071	569	668	(744 *)		
0.080	657	776	886		
0.090		898	1032		
0.100		1019	1182		
0.125		1090	1580		
RIVET SHEAR STRENGTH	710	1090	1580		

NOTES:

- Values are for room temperature use only.
- * Denotes ultimate values based on 1.5 x yield.
- Values that are underlined are knife edge.

TABLE A33 BLIND BOLTS CSK IN ALUMINUM

ULTIMATE STRENGTH OF BLIND BOLTS (100° HEAD) IN
ALUMINUM ALLOY (1)

FASTENER TYPE	MS 90353 ($F_{uH} = 112$ ksi)				
	CLAD OR BARE 7075-T6 OR T651				
SHEET MATERIAL	5/32 (0.163)	3/16 (0.198)	1/4 (0.259)	5/16 (0.311)	3/8 (0.373)
ULTIMATE STRENGTH, LBS.					
SHEET THICKNESS					
0.050					
0.063					
0.071		(835 *)			
0.080	1000 *		(1116 *)		
0.090	1181 *	1313 *		(1673 *)	
0.100	1364 *	1538 *		(1880 *)	
0.125	1823 *	2093 *	2460 *	(2790 *)	
0.160	2340	2885 *	3473 *	3885 *	(4275 *)
0.190		3450	4343 *	4935 *	5531 *
0.250			5900	7020 *	8018 *
0.312				8500	10613 *
0.375					12200
FASTENER SHEAR	2340	3450	5900	8500	12200

NOTES:

- Values are for room temperature use only.
- * Denotes ultimate values based on 1.5 x yield.
- Values that are underlined are knife edge.

TABLE A34 BLIND BOLTS CSK IN ALUMINUM

ULTIMATE STRENGTH OF BLIND BOLTS (100° HEAD) IN
CLAD 7075-T6 ALUMINUM (1)

FASTENER TYPE	MS 21140 ($F_{uH} = 95$ ksi)				
	ACQ				
SHEET MATERIAL	CLAD 7075-T6				
FASTENER DIAM, IN. (NOMINAL SHANK DIAM)	5/32 (0.163)	3/16 (0.198)	1/4 (0.259)	5/16 (0.311)	3/8 (0.373)
ULTIMATE STRENGTH, LBS.					
SHEET THICKNESS					
0.050					
0.063					
0.071		(717 *)			
0.080	876 *	(941 *)			
0.090	1053 *	1095 *			
0.100	1229 *	1352 *	(1538 *)		
0.125	1673 *	1890 *	2153 *	(2310 *)	
0.160	1972 *	2640 *	3135 *	3428 *	(3645 *)
0.190		2880 *	3963 *	4448 *	4853 *
0.200			4260 *	4785 *	5285 *
0.250			4868 *	5480 *	7290 *
0.312					9690 *
FASTENER SHEAR	1980	2925	5005	7215	10380

RIVET TYPE

NAS 1670-L

AKV

CLAD 7075-T6

FASTENER TYPE	NAS 1670-L				
	AKV				
SHEET MATERIAL	CLAD 7075-T6				
FASTENER DIAM, IN. (NOMINAL SHANK DIAM)	5/32 (0.163)	3/16 (0.198)	1/4 (0.259)	5/16 (0.311)	3/8 (0.373)
ULTIMATE STRENGTH, LBS.					
SHEET THICKNESS					
0.063					
0.071		(750 *)	(971 *)		
0.080	1067 *	1182 *	(1308 *)		
0.090	1203 *	1412 *	(1590 *)		
0.100	1331 *	1828 *	(1883 *)	(2025 *)	
0.125	1658 *	2010 *	2655 *	(2895 *)	
0.160	1678	2550 *	3375 *	4080 *	(4583 *)
0.190		2620	3983 *	4800 *	(5835 *)
0.250			4500	6000	7530 *
0.312					9420 *
0.375					9750
FASTENER SHEAR	1678	2620	4500	6000	9750

NOTES

- Values are for room temperature use only.
- * Denotes ultimate values based on 1.5 x yield.
- Values that are underlined are knife edge.

TABLE A35 BLIND BOLTS CSK IN ALUMINUM

ULTIMATE STRENGTH OF BLIND BOLTS (100° HD.) IN
CLAD 2024 AND 7075 ALUMINUM (1)

FASTENER TYPE	FF-200					FF-260
	FF-260					
SHEET MATERIAL	CLAD 2024-T42	CLAD 7075-T6	CLAD 2024-T42	CLAD 7075-T6	CLAD 2024-T42	CLAD 7075-T6
ULTIMATE STRENGTH, LBS.						
FASTENER DIAM, IN. (NOMINAL SHANK)	3/16 (0.198)	3/16 (0.198)	1/4 (0.259)	1/4 (0.259)	5/16 (0.311)	5/16 (0.311)
SHEET THICKNESS						
0.032						
0.040						
0.050						
0.063		(1028 *)	(1125 *)			
0.071		1155 *	1285 *			
0.080		1305 *	1538 *			
0.100		1470	1682 *	(1682 *)	(1920 *)	
0.125		1800 *	1960	2070 *	2400 *	(2160 *)
0.160		2160	2200	2550 *	3075 *	2730 *
0.190		2400	2420	3015 *	3705 *	3380 *
0.250		2620	2620	3900 *	4320	4425 *
0.312				4500	4500	5545 *
FASTENER SHEAR	2620	2620	4500	4500	6000	6000

FASTENER TYPE	SSHFA-200					$(F_{uH} = 50$ ksi)
	$(F_{uH} = 50$ ksi)					
SHEET MATERIAL	CLAD 2024-T42	CLAD 7075-T6	CLAD 2024-T42	CLAD 7075-T6	CLAD 2024-T42	CLAD 7075-T6
ULTIMATE STRENGTH, LBS.						
FASTENER DIAM, IN. (NOMINAL SHANK)	3/16 (0.198)	3/16 (0.198)	1/4 (0.259)	1/4 (0.259)	5/16 (0.311)	5/16 (0.311)
SHEET THICKNESS						
0.032						
0.040						
0.050						
0.063						
0.071						
0.080						
0.100						
0.125						
0.160						
0.190						
0.250						
FASTENER SHEAR	1550	1550	1550	2650	2650	2850

NOTES

- Values are for room temperature use only.
- * Denotes ultimate values based on 1.5 x yield.
- Values that are underlined are knife edge.

TABLE A36 BLIND BOLTS CSK IN ALUMINUM

ULTIMATE STRENGTH OF BLIND BOLTS (100° HEAD) IN ALUMINUM ALLOY (1)

FASTENER TYPE	PLT-150 ($F_{su} = 112 \text{ ksi}$) (H-11 Nut and screw, Inconel X-750 or A-286 Sleeve) CLAD 7075-T6			
SHEET MATERIAL	5/32 (0.164)	3/16 (0.190)	1/4 (0.250)	
FASTENER DIAM, IN. (NOMINAL SHANK)	5/32 (0.163)	3/16 (0.188)	1/4 (0.259)	
ULTIMATE STRENGTH, LBS.				
SHEET THICKNESS				
0.050	(801)*			
0.071	923*	(1095)*		
0.080	1058*	1245*		
0.090	1208*	1430*	(1815)*	
0.100	1359*	1613*	(2018)*	
0.125	1853*	2085*	2625*	
0.160	2318*	2865*	3465*	
0.190			4448*	
0.250			5760*	
0.312			8093*	
			10476*	
FASTENER SHEAR	2340	3450	5900	12250

NOTES:

1. Values are for room temperature use only.
2. * Denotes ultimate values based on 1.5 x yield.
3. Values that are underlined are knife edge.

TABLE A38 LOCKBOLTS CSK IN ALUMINUM

ULTIMATE STRENGTH OF 100° FLUSH SHEAR HEAD TI LOCKBOLTS IN ALUMINUM ALLOY (1)

RIVET TYPE	LGPL2SC-V Pin ($F_{su} = 95 \text{ ksi}$), 3SLC-C Collar CLAD 2024-T3			
SHEET MATERIAL	3/16 (0.190)	1/4 (0.250)	5/16 (0.312)	
FASTENER DIAM, IN. (NOMINAL SHANK)	5/32 (0.164)	3/16 (0.190)	1/4 (0.250)	
ULTIMATE STRENGTH, LBS.				
SHEET THICKNESS				
0.050	(835)			
0.063	1180	(1350)		
0.071	1395	1630	(1775)	
0.080	1640	1950	2155*	
0.090	1875	2300	2595*	
0.100	2070*	2650	3035*	
0.125	2340	3420*	4140	
0.160	2655	4000	5460*	
0.190	2694	4355	6085*	
0.250		4660	6965*	
0.312			7290	
0.375			10270	
FASTENER SHEAR	2694	4660	7290	10490

RIVET TYPE	LGPL2SC-V Pin ($F_{su} = 95 \text{ ksi}$), 3SLC-C Collar CLAD 7075-T6			
SHEET MATERIAL	3/16 (0.190)	1/4 (0.250)	5/16 (0.312)	
FASTENER DIAM, IN. (NOMINAL SHANK)	5/32 (0.164)	3/16 (0.190)	1/4 (0.250)	
ULTIMATE STRENGTH, LBS.				
SHEET THICKNESS				
0.050	(1040)			
0.063	1370	(1710)		
0.071	1575	1980	(2345)	
0.080	1805	2280	2715	
0.090	2060	2615	3130	
0.100	2315	2950	3550	
0.125	2590	3790	4605	
0.160	2694	4430	6070	
0.190		4660	6750	
0.250			7290	
0.312			10154	
0.375			10490	
FASTENER SHEAR	2694	4660	7290	10490

NOTES:

1. Values are for room temperature use only.
2. * Denotes ultimate values based on 1.5 x yield.
3. Values that are underlined are knife edge.

TABLE A37 LOCKBOLTS CSK IN ALUMINUM

ULTIMATE STRENGTH OF 100° FLUSH SHEAR HEAD TI LOCKBOLTS IN ALUMINUM ALLOY (1)

FASTENER TYPE	GPL3SC-V Pin, 2SC-3C Collar ($F_{su} = 95 \text{ ksi}$) CLAD 2024-T3			
SHEET MATERIAL	5/32 (0.164)	3/16 (0.190)	1/4 (0.250)	
FASTENER DIAM, IN. (NOMINAL SHANK)	5/32 (0.164)	3/16 (0.190)	1/4 (0.250)	
ULTIMATE STRENGTH, LBS.				
SHEET THICKNESS				
0.050	(838)			
0.063	1255	(1535)		
0.071	1455	1795	(2085)	
0.080	1680	2085	2440	
0.090	1845*	2410	2845	
0.100	1980*	2735	3245	
0.125	2316*	3308*	4270	
0.160	2694	3930*	5243*	
0.190		4463*	5903*	
0.250		4660	7230	
0.312			9113*	
0.375			10490	
FASTENER SHEAR	2694	4660	7290	10490

FASTENER TYPE	GPL3SC-V Pin, 2SC-3C Collar ($F_{su} = 95 \text{ ksi}$) CLAD 7075-T6			
SHEET MATERIAL	5/32 (0.164)	3/16 (0.190)	1/4 (0.250)	
FASTENER DIAM, IN. (NOMINAL SHANK)	5/32 (0.164)	3/16 (0.190)	1/4 (0.250)	
ULTIMATE STRENGTH, LBS.				
SHEET THICKNESS				
0.050	(1105)			
0.063	1500	(1800)		
0.071	1740	2125	(2430)	
0.080	2020	2485	(2865)	
0.090	2200	2885	3365	
0.100	2355	3310	3865	
0.125	2694	3945	5135	
0.160		4660	6245	
0.190			7010	
0.250			8005	
FASTENER SHEAR	2694	4660	7290	10490

NOTES:

1. Values are for room temperature use only.
2. * Denotes ultimate values based on 1.5 x yield.
3. Values that are underlined are knife edge.

TABLE A39 CHERRYBUCK FASTENERS CSK IN ALUMINUM

ULTIMATE STRENGTH OF PROTRUDING SHEAR HEAD TI "CHERRYBUCK" FASTENERS IN ALUMINUM ALLOY (1)

FASTENER TYPE	CSR 925 ($F_{su} = 95 \text{ ksi}$) CLAD 2024-T3			
FASTENER DIAMETER (NOMINAL SHANK)	5/32 (0.164)	3/16 (0.190)	1/4 (0.250)	
ULTIMATE STRENGTH, LBS.				
SHEET THICKNESS				
0.050	807			
0.063	1020	1180		
0.071	1150	1335		
0.080	1300	1505	1870	
0.090	1465	1695	2220	
0.100	1630	1885	2470	
0.125	2007	2360	3095	
0.160		2694	3975	
0.190			4660	
FASTENER SHEAR	2007	2694	4660	

FASTENER TYPE	CSR 925 ($F_{su} = 95 \text{ ksi}$) CLAD 7075-T6			
FASTENER DIAMETER (NOMINAL SHANK)	5/32 (0.164)	3/16 (0.190)	1/4 (0.250)	
ULTIMATE STRENGTH, LBS.				
SHEET THICKNESS				
0.050	995			
0.063	1227	1442		
0.071	1371	1607		
0.080	1532	1792	2415	
0.090	1711	2001	2688	
0.100	1890	2205	2960	
0.125	2007	2694	3641	
0.160			4595	
0.190			4660	
FASTENER SHEAR	2007	2694	4660	

NOTES:

1. Values are for room temperature use only.

APPENDIX A ADDITIONAL DESIGN AND ANALYSIS DATA

A20

TABLE A40 CHERRYBUCK FASTENERS CSK IN ALUMINUM

ULTIMATE STRENGTH OF 100° FLUSH SHEAR HEAD TI
"CHERRYBUCK" FASTENERS IN ALUMINUM ALLOY (1)

FASTENER TYPE	CSR 924 ($F_{su} = 95$ ksi)			AMC
SHEET MATERIAL	CLAD 2024-T3			
FASTENER DIAMETER (NOMINAL SHANK)	5/32 (0.164)	3/16 (0.190)	1/4 (0.250)	5/16 (0.312)
ULTIMATE STRENGTH, LBS.				
SHEET THICKNESS				
0.050	737			
0.063	1019	1118		
0.071	1152	1319		
0.080	1260	1509	1837	
0.090	1350	1664	2168	
0.100	1440	1767	2500	
0.125	1665	2028	2969	
0.160	1982	2394	3450	
0.190		2694	3853	
0.250			4660	
FASTENER SHEAR	2007	2694	4660	

FASTENER TYPE	CSR 924 ($F_{su} = 95$ ksi)			AMC
SHEET MATERIAL	CLAD 7075-T6			
FASTENER DIAMETER (NOMINAL SHANK)	5/32 (0.164)	3/16 (0.190)	1/4 (0.250)	5/16 (0.312)
ULTIMATE STRENGTH, LBS.				
SHEET THICKNESS				
0.050	941			
0.063	1207	1393		
0.071	1385	1588		
0.080	1557	1779	2281	
0.090	1775	2050	2594	
0.100	1876	2263	2919	
0.125	1950	2542	3765	
0.160	2007	2660	4387	
0.190		2694	4525	
0.250			4660	
FASTENER SHEAR	2007	2694	4660	

NOTES:

1. Values are for room temperature use only.

2. * Denotes ultimate values based on 1.5 x yield...

TABLE A41 HI-LOK FASTENERS IN ALUMINUM

ULTIMATE STRENGTH OF 100° FLUSH SHEAR HEAD TI HI-LOK
IN CLAD 7075-T6 ALUMINUM (1)

FASTENER TYPE	HL 11 PIN ($F_{su} = 95$ ksi), HL 70 COLLAR			
SHEET MATERIAL	CLAD 7075-T6			
FASTENER DIAMETER (NOMINAL SHANK)	5/32 (0.164)	3/16 (0.190)	1/4 (0.250)	5/16 (0.312)
ULTIMATE STRENGTH, LBS.				
SHEET THICKNESS, IN.				
0.040	(734)	(837)		
0.050	941	1083	(1341)	
0.063	1207	1393	(1762)	(2170)
0.071	1385	1588	2012	2463
0.080	1557	1779	2281	2823
0.090	1775	2050	2594	3193
0.100	1876	2263	2919	3631
0.125	1950	2542	3765	4594
0.160	2007	2660	3970	5890
0.190		2694	4165	6105
0.250			4530	6580
0.312			4660	7050
0.375				7290
FASTENER SHEAR	2007	2694	4660	7290

ULTIMATE STRENGTH OF PROTRUDING SHEAR HEAD ALLOY STEEL
HI-LOK IN CLAD 7075-T6 ALUMINUM (1)

FASTENER TYPE	HL 18 PIN ($F_{su} = 95$ ksi), HL 70 COLLAR			
SHEET MATERIAL	CLAD 7075-T6			
FASTENER DIAMETER (NOMINAL SHANK)	5/32 (0.164)	3/16 (0.190)	1/4 (0.250)	5/16 (0.312)
ULTIMATE STRENGTH, LBS.				
SHEET THICKNESS, IN.				
0.050	1078			
0.063	1353	1559		
0.071	1520	1776		
0.080	1718	1957	2593	
0.090	1890	2224	2937	
0.100	1930	2473	3250	4050
0.125	2007	2580	4063	5075
0.160		2694	4450	6509
0.190			4620	6880
0.250			4660	7290
FASTENER SHEAR	2007	2694	4660	7290

NOTES:

1. Values are for room temperature use only.

2. * Denotes ultimate values based on 1.5 x yield...

TABLE A42 HI-LOK FASTENERS CSK IN ALUMINUM

ULTIMATE STRENGTH OF 100° FLUSH SHEAR HEAD ALLOY STEEL
HI-LOKS IN CLAD 7075-T6 ALUMINUM (1)

FASTENER TYPE	HL 18 PIN ($F_{su} = 95$ ksi), HL 70 COLLAR			
SHEET MATERIAL	CLAD 7075-T6			
FASTENER DIAMETER (NOMINAL SHANK)	5/32 (0.164)	3/16 (0.190)	1/4 (0.250)	5/16 (0.312)
ULTIMATE STRENGTH, LBS.				
SHEET THICKNESS				
0.050	968			
0.063	1251	1408		
0.071	1400	1606		
0.080	1595	1823	2344	
0.090	1815	2050	2675	
0.100	1903	2300	3000	3660
0.125	2005	2570	3781	4885
0.160			2694	4420
0.190			4625	6832
0.250			4660	7290
FASTENER SHEAR	2007	2694	4660	7290

NOTES

1. Values are for room temperature use only.

2. Values that are (underlined) are knife edge.

TABLE A43 THREADED FASTENERS CSK IN ALUMINUM

ULTIMATE STRENGTH OF 100° FLUSH SHEAR HEAD (SS, PH13-8MO-H1000)
FASTENERS IN Ti-6Al-4V ALLOY (1)

FASTENER TYPE	PBF 11 ($F_{su} = 125$ ksi)			
SHEET MATERIAL	ANNEALED Ti-6Al-4V			
FASTENER DIAMETER (NOMINAL SHANK)	5/32 (0.164)	3/16 (0.250)	3/8 (0.375)	1/2 (0.500)
ULTIMATE STRENGTH, LBS.				
SHEET THICKNESS, IN.				
0.040	(1535)			
0.050	1963			
0.063	2528	(3656)		
0.071	2640	4213		
0.080		4813	(6820)	
0.090		5438	7618	
0.100		6140	8775	(11250)
0.125		11264	11264	14575
0.160			13810	19250
0.190				23200
0.200				24540
FASTENER STRENGTH	2640	6140	13810	24540

ULTIMATE STRENGTH OF 100° FLUSH HEAD ALLOY STEEL
NAS 1620 (SERIES) FASTENERS IN CLAD 7075-T6 ALUMINUM (1)

FASTENER TYPE	NAS 1620 ($F_{su} = 95$ ksi)			
SHEET MATERIAL	CLAD 7075-T6			
FASTENER DIAMETER (NOMINAL SHANK)	3/16 (0.190)	1/4 (0.250)	5/16 (0.312)	3/8 (0.375)
ULTIMATE STRENGTH, LBS.				
SHEET THICKNESS, IN.				
0.080	(1553)			
0.090	1748			
0.100	1920	(2573)		
0.125	2340	3195	(3285)	
0.160	2690	3975	4350	
0.190		4590	5160	6180
0.250			4650	6675
0.312				8130
0.375				9945
RIVET SHEAR STRENGTH	2690	4650	7300	10500

NOTES:

1. Values are for room temperature use only.

2. * Denotes ultimate values based on 1.5 x yield.

3. Values that are (underlined) are knife edge.

APPENDIX A ADDITIONAL DESIGN AND ANALYSIS DATA

TABLE A44 SLEEVE BOLTS CSK IN ALUMINUM

FASTENER TYPE SHEET MATERIAL	MIL-B-8831/4 ($F_{uK} = 198 \text{ ksi}$)				
	CLAD 2024-T3	5/16" (0.3695)	3/8" (0.4350)	7/16" (0.5022)	1/2" (0.5735)
ULTIMATE STRENGTH, LBS.					
SHEET THICKNESS					
0.100	2175				
0.125	2720	3450	4205		
0.160	3290	4415	5380	6335	7315
0.190		5240	6300	7525	8685
0.250		5480	7045	9895	11425
0.312		5655	8185	11095	14260
0.375		5670	8385	11345	14845
0.500			8760	11865	15445
0.625				12285	16045
0.750					20440
0.875					21225
1.000					21805
FASTENER SHEAR	3290	5670	8760	12640	17100
					22250

FASTENER TYPE SHEET MATERIAL	MIL-B-8831/4 ($F_{uK} = 198 \text{ ksi}$)				
	CLAD 7075-T6	5/16" (0.3695)	3/8" (0.4350)	7/16" (0.5022)	1/2" (0.5735)
ULTIMATE STRENGTH, LBS.					
SHEET THICKNESS					
0.100	2585				
0.125	3205	4100	5035		
0.160	3290	5205	6385	7560	8790
0.190		5670	7535	8925	10360
0.250			8760	11840	13495
0.312				12395	16195
0.375				12640	16625
0.500				17100	21265
FASTENER SHEAR	3290	5670	8760	12640	17100
					22250

NOTES:

- Values are for room temperature use only.
- Fasteners installed in interference levels of 0.0025-0.006 in.
- See MIL-B-8831/4 for nominal hole diameters.

TABLE A46 NUT AND COLLAR ALLOWABLE TENSILE LOADS

THREAD SIZE (IN.)	CASTILLATED (SHR)	CASTILLATED (REG.)	MS 1105	MS 1144	HL 70	HL 70	MS 1105	MS 1144	(S. ALGIN)	HL 70	MS 21043	MS 21045	MS 21046	MS 20500	KPN 509	KPN 526	(S. ALGIN)
1/8-32	120	2040	3000	4080	4800	5600	6500	7000	7500	8700	10100	13500	12100	11450	10000	2300	2750
1/4-28	3250	3700	5250	6500	7000	8000	8500	9000	9500	10500	12500	14500	13500	12100	11450	10000	2300
5/16-24	5620	6500	7500	8700	9500	10500	11450	12100	13500	14500	15300	16500	15000	13500	12100	10000	2300
3/8-24	7716-20	8000	9250	10500	11800	13000	14500	15000	16500	17000	18000	19500	18000	16500	15000	13000	2300
7/16-20	112-20	12500	13250	14500	15000	16500	17000	18000	19000	20000	21100	22500	21000	19000	17000	15000	2300
9/16-18	15050	17050	18000	19000	20000	21000	22000	23000	24000	25000	26000	27000	25000	23000	21000	19000	2300
5/8-18																	

NOTES:
1. The room temperature static load ratings above are not design allowances. They are based on the specification standards and are to be used as guideline data to aid in nut selection.

TABLE A45 STEEL BOLT/SCREW BENDING MOMENTS

ULTIMATE ALLOWABLE SHANK BENDING MOMENTS FOR STEEL BOLTS AND SCREWS (ROOM TEMPERATURE)

F_{uK} ksi	125	160	180	220
F_p ksi	103	142	163	180
F_{p0} ksi	197	250	294	346
SECTION MODULUS (IN ³) (IN ³)				
DIAMETER (INCH)	0.190	0.250	0.312	0.375
	133	302	590	1020
	397	776	881	1340
	531	1040	1790	1820
	.000673	.001534	.002996	.00518
	.001534	.01227	.01747	.02387
	.002996	.04142	.04430	.04687
	.00518	.04245	.04330	.04587
	.01227	.04430	.04687	.04817

NOTES:
1. CRES steel is recommended when subjected to appreciable bending.
2. The use of bolts with an $F_{uK} > 180$ ksi requires approval by Structural Integrity.
3. The use of bolts and screws having a 0.190 inch diameter or less is not recommended for bending applications.

TYPE AND LOADING	LOCATION OF LOAD FROM SUPPORT	LOAD, LBS.	LBS/IN.	LBS/IN.²	LBS/IN.³	LBS/IN.⁴	LBS/IN.⁵	LBS/IN.⁶	LBS/IN.⁷	LBS/IN.⁸	LBS/IN.⁹	LBS/IN.¹⁰	LBS/IN.¹¹	LBS/IN.¹²	LBS/IN.¹³	LBS/IN.¹⁴	LBS/IN.¹⁵	LBS/IN.¹⁶	LBS/IN.¹⁷	LBS/IN.¹⁸	LBS/IN.¹⁹	LBS/IN.²⁰	LBS/IN.²¹	LBS/IN.²²	LBS/IN.²³	LBS/IN.²⁴	LBS/IN.²⁵	LBS/IN.²⁶	LBS/IN.²⁷	LBS/IN.²⁸	LBS/IN.²⁹	LBS/IN.³⁰	LBS/IN.³¹	LBS/IN.³²	LBS/IN.³³	LBS/IN.³⁴	LBS/IN.³⁵	LBS/IN.³⁶	LBS/IN.³⁷	LBS/IN.³⁸	LBS/IN.³⁹	LBS/IN.⁴⁰	LBS/IN.⁴¹	LBS/IN.⁴²	LBS/IN.⁴³	LBS/IN.⁴⁴	LBS/IN.⁴⁵	LBS/IN.⁴⁶	LBS/IN.⁴⁷	LBS/IN.⁴⁸	LBS/IN.⁴⁹	LBS/IN.⁵⁰	LBS/IN.⁵¹	LBS/IN.⁵²	LBS/IN.⁵³	LBS/IN.⁵⁴	LBS/IN.⁵⁵	LBS/IN.⁵⁶	LBS/IN.⁵⁷	LBS/IN.⁵⁸	LBS/IN.⁵⁹	LBS/IN.⁶⁰	LBS/IN.⁶¹	LBS/IN.⁶²	LBS/IN.⁶³	LBS/IN.⁶⁴	LBS/IN.⁶⁵	LBS/IN.⁶⁶	LBS/IN.⁶⁷	LBS/IN.⁶⁸	LBS/IN.⁶⁹	LBS/IN.⁷⁰	LBS/IN.⁷¹	LBS/IN.⁷²	LBS/IN.⁷³	LBS/IN.⁷⁴	LBS/IN.⁷⁵	LBS/IN.⁷⁶	LBS/IN.⁷⁷	LBS/IN.⁷⁸	LBS/IN.⁷⁹	LBS/IN.⁸⁰	LBS/IN.⁸¹	LBS/IN.⁸²	LBS/IN.⁸³	LBS/IN.⁸⁴	LBS/IN.⁸⁵	LBS/IN.⁸⁶	LBS/IN.⁸⁷	LBS/IN.⁸⁸	LBS/IN.⁸⁹	LBS/IN.⁹⁰	LBS/IN.⁹¹	LBS/IN.⁹²	LBS/IN.⁹³	LBS/IN.⁹⁴	LBS/IN.⁹⁵	LBS/IN.⁹⁶	LBS/IN.⁹⁷	LBS/IN.⁹⁸	LBS/IN.⁹⁹	LBS/IN.¹⁰⁰	LBS/IN.¹⁰¹	LBS/IN.¹⁰²	LBS/IN.¹⁰³	LBS/IN.¹⁰⁴	LBS/IN.¹⁰⁵	LBS/IN.¹⁰⁶	LBS/IN.¹⁰⁷	LBS/IN.¹⁰⁸	LBS/IN.¹⁰⁹	LBS/IN.¹¹⁰	LBS/IN.¹¹¹	LBS/IN.¹¹²	LBS/IN.¹¹³	LBS/IN.¹¹⁴	LBS/IN.¹¹⁵	LBS/IN.¹¹⁶	LBS/IN.¹¹⁷	LBS/IN.¹¹⁸	LBS/IN.¹¹⁹	LBS/IN.¹²⁰	LBS/IN.¹²¹	LBS/IN.¹²²	LBS/IN.¹²³	LBS/IN.¹²⁴	LBS/IN.¹²⁵	LBS/IN.¹²⁶	LBS/IN.¹²⁷	LBS/IN.¹²⁸	LBS/IN.¹²⁹	LBS/IN.¹³⁰	LBS/IN.¹³¹	LBS/IN.¹³²	LBS/IN.¹³³	LBS/IN.¹³⁴	LBS/IN.¹³⁵	LBS/IN.¹³⁶	LBS/IN.¹³⁷	LBS/IN.¹³⁸	LBS/IN.¹³⁹	LBS/IN.¹⁴⁰	LBS/IN.¹⁴¹	LBS/IN.¹⁴²	LBS/IN.¹⁴³	LBS/IN.¹⁴⁴	LBS/IN.¹⁴⁵	LBS/IN.¹⁴⁶	LBS/IN.¹⁴⁷	LBS/IN.¹⁴⁸	LBS/IN.¹⁴⁹	LBS/IN.¹⁵⁰	LBS/IN.¹⁵¹	LBS/IN.¹⁵²	LBS/IN.¹⁵³	LBS/IN.¹⁵⁴	LBS/IN.¹⁵⁵	LBS/IN.¹⁵⁶	LBS/IN.¹⁵⁷	LBS/IN.¹⁵⁸	LBS/IN.¹⁵⁹	LBS/IN.¹⁶⁰	LBS/IN.¹⁶¹	LBS/IN.¹⁶²	LBS/IN.¹⁶³	LBS/IN.¹⁶⁴	LBS/IN.¹⁶⁵	LBS/IN.¹⁶⁶	LBS/IN.¹⁶⁷	LBS/IN.¹⁶⁸	LBS/IN.¹⁶⁹	LBS/IN.¹⁷⁰	LBS/IN.¹⁷¹	LBS/IN.¹⁷²	LBS/IN.¹⁷³	LBS/IN.¹⁷⁴	LBS/IN.¹⁷⁵	LBS/IN.¹⁷⁶	LBS/IN.¹⁷⁷	LBS/IN.¹⁷⁸	LBS/IN.¹⁷⁹	LBS/IN.¹⁸⁰	LBS/IN.¹⁸¹	LBS/IN.¹⁸²	LBS/IN.¹⁸³	LBS/IN.¹⁸⁴	LBS/IN.¹⁸⁵	LBS/IN.¹⁸⁶	LBS/IN.¹⁸⁷	LBS/IN.¹⁸⁸	LBS/IN.¹⁸⁹	LBS/IN.¹⁹⁰	LBS/IN.¹⁹¹	LBS/IN.¹⁹²	LBS/IN.¹⁹³	LBS/IN.¹⁹⁴	LBS/IN.¹⁹⁵	LBS/IN.¹⁹⁶	LBS/IN.¹⁹⁷	LBS/IN.¹⁹⁸	LBS/IN.¹⁹⁹	LBS/IN.²⁰⁰	LBS/IN.²⁰¹	LBS/IN.²⁰²	LBS/IN.²⁰³	LBS/IN.²⁰⁴	LBS/IN.²⁰⁵	LBS/IN.²⁰⁶	LBS/IN.²⁰⁷	LBS/IN.²⁰⁸	LBS/IN.²⁰⁹	LBS/IN.²¹⁰	LBS/IN.²¹¹	LBS/IN.²¹²	LBS/IN.²¹³	LBS/IN.²¹⁴	LBS/IN.²¹⁵	LBS/IN.²¹⁶	LBS/IN.²¹⁷	LBS/IN.²¹⁸	LBS/IN.²¹⁹	LBS/IN.²²⁰	LBS/IN.²²¹	LBS/IN.²²²	LBS/IN.²²³	LBS/IN.²²⁴	LBS/IN.²²⁵	LBS/IN.²²⁶	LBS/IN.²²⁷	LBS/IN.²²⁸	LBS/IN.²²⁹	LBS/IN.²³⁰	LBS/IN.²³¹	LBS/IN.²³²	LBS/IN.²³³	LBS/IN.²³⁴	LBS/IN.²³⁵	LBS/IN.²³⁶	LBS/IN.²³⁷	LBS/IN.²³⁸	LBS/IN.²³⁹	LBS/IN.²⁴⁰	LBS/IN.²⁴¹	LBS/IN.²⁴²	LBS/IN.²⁴³	LBS/IN.²⁴⁴	LBS/IN.²⁴⁵	LBS/IN.²⁴⁶	LBS/IN.²⁴⁷	LBS/IN.²⁴⁸	LBS/IN.²⁴⁹	LBS/IN.²⁵⁰	LBS/IN.²⁵¹	LBS/IN.²⁵²	LBS/IN.²⁵³	LBS/IN.²⁵⁴	LBS/IN.²⁵⁵	LBS/IN.²⁵⁶	LBS/IN.²⁵⁷

Following is an alternative analysis to that presented in Chapter A9. It is based upon the minimum energy principal instead of upon deflections as in Art.A9.2

A loaded bulkhead or frame, in a fuselage for example, is supported by the fuselage skin panels as in Fig.B1, which shows the general (but uncommon) case of an unsymmetrical bulkhead. The applied loads consist of the loads, Q , and the reacting shear flows, q (determined by VQ/I and $T/2A$ per Art.A20.3-A20.10). To determine the internal loads in the bulkhead it is "cut" at the top, and the unknown internal loads M_o , V_o and P_o there are shown acting on the left side of the cut ('on segment 1) in Fig.B1(b). Opposite loads act on the right side of the cut (on segment 20). M_o , V_o and P_o are redundant loads and are positive for the directions shown. x and y are the moment arms for the forces V_o and P_o respectively, positive as shown. The bulkhead is then divided into a large number, N , of segments of length ΔS , at least twenty. The segments are usually of the same length.

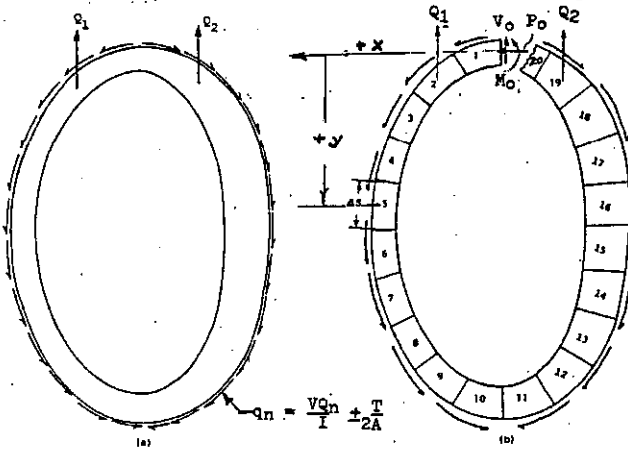


Fig.B1 Unsymmetrical Frame Analysis Data

The bending moment in each segment, n , is
 $M_n = M_{Qn} + M_{qn} + M_o + V_o x_n + P_o y_n \dots\dots\dots(1)$

where M_n is at the center of the segment. The moment of the shear flows, q , about each segment's center is calculated as shown on p.A19.19. Positive moments produce compression in the segments outer flange. The bending energy in each segment will be

$$U_n = M_n^2 \Delta S_n / 2 E_n I_n$$

and the total energy in the frame will be

$$U = \sum_{n=1}^{N} (M_{Qn} + M_{qn} + V_o x_n + P_o y_n)^2 \frac{\Delta S_n}{2 E_n I_n} \dots\dots\dots(2)$$

where M_{Qn} is $M_{Qn} + M_{qn}$.

* Bulkheads are relatively highly loaded and sturdy frames. For very light frames also see Fig.C9.13a.

The values of M_o , V_o and P_o must be such that U is a minimum. Therefore

$$\frac{\partial U}{\partial M_o} = 0; \frac{\partial U}{\partial V_o} = 0 \text{ and } \frac{\partial U}{\partial P_o} = 0$$

Differentiating (2) as indicated yields the three simultaneous equations

$$\sum_{n=1}^{N} (M_{Qn} + M_{qn} + V_o x_n + P_o y_n) \frac{\Delta S_n}{E_n I_n} = 0 \dots\dots\dots(3)$$

$$\sum_{n=1}^{N} (M_{Qn} + M_{qn} + V_o x_n + P_o y_n) \frac{\Delta S_n x_n}{E_n I_n} = 0 \dots\dots\dots(4)$$

$$\sum_{n=1}^{N} (M_{Qn} + M_{qn} + V_o x_n + P_o y_n) \frac{\Delta S_n y_n}{E_n I_n} = 0 \dots\dots\dots(5)$$

All terms in the equations are known except the redundants and these are found by solving the three equations. The final values of M at the center of each segment are then calculated using Eq.(1).

The analysis is most easily carried out by using a tabular form (Table B1), and this is illustrated for the bulkhead shown in Fig.B2. The values of M_{Qn} , q_n , $\Delta S_n/E_n I_n$, x and y for the bulkhead are shown in Columns 3, 2, 4, and 5 respectively of Table B1. The final bending moments are shown in Col. 14. The values of V and P at the center of the segments would be calculated as noted in Col. 16 and 17 of Table B1 (by statics).

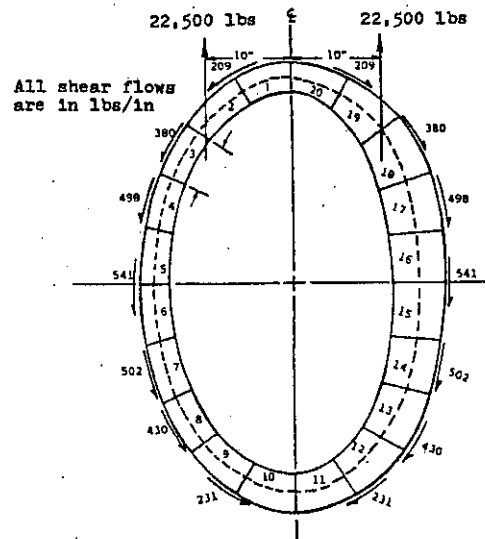


Fig.B2 Unsymmetrical Frame Analysis Data
Symmetrical Frame and Symmetrical Loads

For this case, due to symmetry, $V_o = 0$ so only Eq.(3) and (5) apply, and it is only necessary to use one-half of the frame. This procedure is illustrated for the frame of Fig.B2 assuming that its right side is the same as its left side. Table B2 shows

Table B1 Unsymmetrical Frame Analysis

①	②	③	④	⑤	⑥	⑦	⑧	⑨	⑩	⑪	⑫	⑬	⑭	⑮	⑯
Segment	$\Delta S/EI$	M_{Q_n}	y	r	$M_{Q_n} \Delta S$	ΔS_x	ΔS_y	$M_{Q_n} \Delta S$	ΔS_x	ΔS_{xy}	$M_{Q_n} \Delta S_y$	ΔS_y^2	M_{final}	Axial Load	Shear Load
	I/Lb-In	Lb-In	In.	In.	$(3) \times (2)$	$(2) \times (4)$	$(2) \times (5)$	$(4) \times (6)$	$(2) \times (4)$	$(2) \times (4) \times (5)$	$(6) \times (5)$	$(2) \times (5)$	$(3) + M_o + V_o \times (4)$	$P_o \times (5)$	
1	.900	0	3.0	.7	0	2.70	.63	6 x 4	0	8.10	1.89	0	.44	-21,649	This is the component for the axial load but using the parallel to the neutral axis component.
2	.900	2,700	8.8	3.9	2,430	7.92	3.51	21,384	69.70	36.89	9,477	13.69	-38,854	Same as for the axial load but using the component parallel to the neutral axis.	
3	.900	70,900	12.5	9.0	63,810	11.25	8.10	797,625	140.63	101.25	574,290	72.90	-1,516		
4	.900	138,200	14.9	14.7	124,381	13.41	13.23	1,853,262	199.80	197.13	1,828,386	194.48	31,565		
5	.900	177,600	15.8	20.5	159,841	14.22	18.45	2,525,472	224.68	291.51	3,276,720	378.23	36,384		
6	.900	209,200	16.8	26.6	188,280	14.22	23.94	2,974,824	224.68	378.25	5,008,248	636.81	31,763		
7	.900	250,300	14.9	33.1	225,270	13.41	29.79	3,356,523	199.81	443.87	7,456,437	986.05	34,406		
8	.900	259,700	12.5	38.4	233,730	11.25	34.56	2,921,025	140.63	432.00	8,975,232	1,322.1	12,708		
9	.900	250,800	8.8	43.2	225,720	7.92	38.88	1,986,335	69.70	342.14	9,751,104	1,679.6	-24,118		
10	.900	240,300	3.0	46.1	216,270	2.70	41.49	648,810	8.10	124.47	9,970,047	1,912.7	-50,934		
11	1,154	240,300	-3.0	46.0	277,308	-3.46	53.08	-831,918	10.38	-159.25	12,756,076	2,441.9	-49,406		
12	1,598	248,100	-8.2	43.0	396,464	-13.10	68.71	-3,251,005	107.45	-563.45	17,047,952	2,954.7	-22,981		
13	1,864	246,400	-11.6	38.3	459,290	-21.62	71.39	-5,327,764	250.82	-828.14	17,590,807	2,734.3	3,757		
14	2,130	231,100	-13.4	33.2	492,243	-28.54	70.72	-6,595,056	382.46	-947.69	16,342,468	2,347.8	19,021		
15	2,308	191,100	-14.3	26.5	441,059	-33.00	61.39	-6,307,143	471.98	-877.92	11,732,169	1,633.0	18,352		
16	2,308	157,100	-14.3	20.5	382,588	-33.00	47.31	-5,184,980	471.98	-676.59	7,433,013	989.9	20,574		
17	2,130	109,800	-13.4	14.8	233,235	-28.54	31.52	-3,125,349	382.46	-422.42	3,451,978	466.5	6,680		
18	1,864	75,700	-11.6	9.1	141,105	-21.62	16.96	-1,636,818	250.82	-196.76	1,284,056	154.3	6,446		
19	1,598	4,800	-8.2	3.9	7,361	-13.10	6.23	-50,278	107.45	-61.10	28,669	24.3	-34,306		
20	1,154	0	-3.0	.7	0	-3.46	.81	0	10.38	-2.42	0	0	.6	-20,714	

$$\Sigma = 27,108$$

$$\Sigma M_o g = M_o + M_g$$

* When ΔS or EI is constant over the frame it can be considered to be unity for Column (2). For this example E and ΔS are constant and are taken as being 1.0.

$$\Sigma (6) + M_o \Sigma (2) + V_o \Sigma (7) + P_o \Sigma (8) = 0$$

$$\Sigma (3) + M_o \Sigma (7) + V_o \Sigma (10) + P_o \Sigma (11) = 0$$

$$\Sigma (12) + M_o \Sigma (8) + V_o \Sigma (11) + P_o \Sigma (13) = 0$$

$$\text{Solve for } M_o, V_o, \text{ & } P_o$$

$$M_o = -17025$$

$$V_o = -185.8$$

$$P_o = -5938$$

Table B2 Symmetrical Frame with Symmetrical Applied Loads

①	②	③	④	⑤	⑥	⑦	⑧	⑨	⑩	⑪	⑫	⑬	⑭	⑮	⑯
Segment	$\Delta S/EI$	M_{Q_n}	y	r	$M_{Q_n} \Delta S$	ΔS_y	$M_{Q_n} \Delta S_y$	ΔS_y^2	M_{final}	$(3) + M_o + P_o \times (4)$	Axial Load	Shear Load			
	Given	Given	Given	Given	$(3) \times (2)$	$(2) \times (4)$	$(3) \times (5)$	$(2) \times (4)^2$							
1	1	0	.7	0	.7	0	0	0	-24,907						
2	1	2,700	3.9	2,700	3.9	11,000	15.2	-41,063							
3	1	70,900	9.0	70,900	9.0	638,000	81.0	-2,197							
4	1	138,200	14.7	138,200	14.7	2,032,000	216.1	30,794							
5	1	177,600	20.5	177,600	20.5	3,841,000	420.3	36,016							
6	1	209,200	26.6	209,200	26.6	5,585,000	707.6	31,870							
7	1	250,300	33.1	250,300	33.1	8,285,000	1,095.6	34,446							
8	1	259,700	38.4	259,200	38.4	9,972,000	1,474.6	12,634							
9	1	260,800	43.2	260,800	43.2	10,835,000	1,866.2	-24,551							
10	1	240,300	46.1	240,300	46.1	11,076,000	2,105.2	-52,140							

$$\Sigma = 10 \quad \Sigma = 1,599,700 \quad \Sigma = 236.2 \quad \Sigma = 52,057,000 \quad \Sigma = 8,001.8$$

$$\Sigma (5) + M_o \Sigma (2) + P_o \Sigma (6) = 0 \quad 1,599,700 + 10 M_o + 236.2 P_o = 0$$

$$\Sigma (7) + M_o \Sigma (6) + P_o \Sigma (8) = 0 \quad 52,057,000 + 236.2 M_o + 8,001 P_o = 0$$

Symmetrical Frame and Unsymmetrical Loads

This case could be analyzed as was done for Fig.B2, using Table B1, but an easier procedure is as follows, which uses only one-half of the frame (segments 1-10).

An unsymmetrical loading can be resolved into a symmetrical loading and an antisymmetrical one, as shown in Fig.B3. An antisymmetrical loading is one which when rotated 180° and the load directions reversed will give the original loading. The final internal loads are found by determining those due to the antisymmetrical and then adding these to those due to the

These are obtained from Eq.(2) (with $V_o=0$) by differentiating it with respect to M_o and to P_o .

$$\sum_{n=1}^N (M_{Q_n} + M_o + P_o y_n) \frac{\Delta S}{E I_n} = 0$$

$$\sum_{n=1}^N (M_{Q_n} + M_o + P_o y_n) \frac{\Delta S y_n}{E I_n} = 0$$

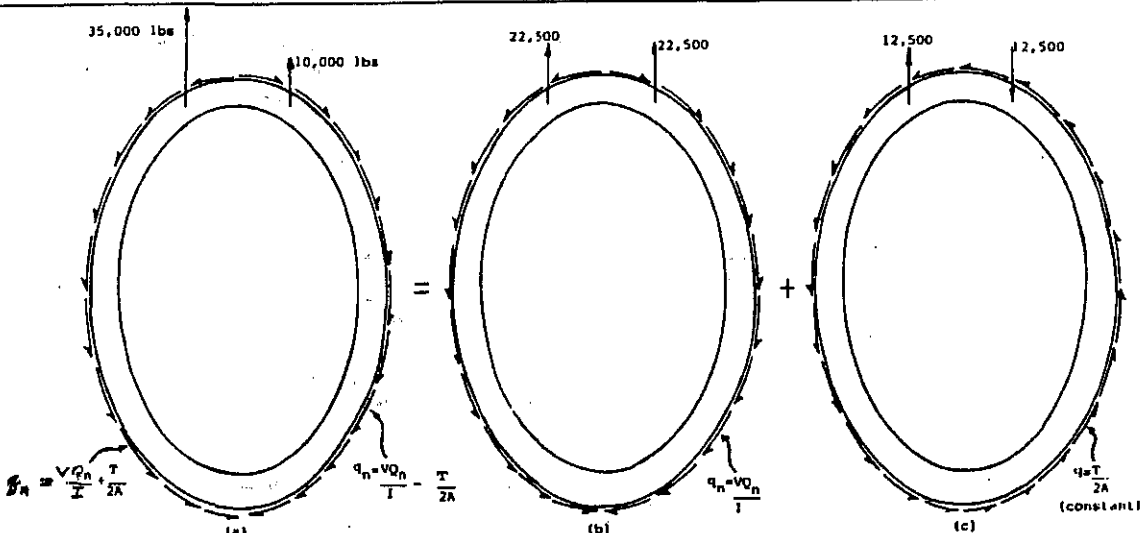


Fig. B3 Resolving Unsymmetrical Loads

Fig.B3 Resolving Unsymmetrical Loads

symmetrical ones. The antisymmetrical loads will add to the symmetrical ones on one-half of the frame and subtract from those on the other half, to give the final internal loads.

To illustrate this procedure assume that the frame in Fig. B3 is the same as that in the previous example (in Table B2). The symmetrical loads will be the same as in Table B2. Those due to the antisymmetrical loading are found as follows. Due to geometric symmetry and loading asymmetry M_0 and P_0 are zero, so the only redundant is V_0 . Therefore, the only equation is Eq. (4) with $M_0 = 0$ and $P_0 = 0$, or

$$\sum_{n=1}^{N_s} (M_{Qn} + M_{qn} + V_{oxn}) \Delta S_n x_n / E_n I_n = 0 \quad (6)$$

This is solved for V_0 , and the final antisymmetrical loads are obtained for each segment by using the terms in the parentheses of Eq. (6). These antisymmetrical

loads are determined as shown in Table B3. The final internal bending moments are shown in Table B4, Col.8. It is seen that the asymmetrical loads add to the symmetrical ones on the left side and subtract from them on the right side.

Two-Lobe Frame

Such a frame is shown in Fig. B4. For an unsymmetrical frame there are six redundants as shown, hence there would be six simultaneous equations, derived in the same manner as was done for the previous bulkhead. Aside from this the procedure is the same as before. For the more common symmetrical frame V_o and V_a are zero, so there would be only four equations for a symmetrical loading involving M_o , P_o , M_a and P_a . For an asymmetrical loading there would be only two simultaneous equations involving V_o and V_a , since M_o ,

Table B3 Symmetrical Frame with Antisymmetrical Applied Loads

(1)	(2)	(3)	(4)	(5)	(6)	(7)	(8)	(9)
Segment	$\frac{\Delta S}{EI}$	$M_{Q,q}$	x	$M_{Q,q} \Delta S x$	$\frac{\Delta S x^2}{EI}$	M_{final}	Axial Load	Shear Load
	Data	Data	Data	$(2) \times (3) \times (4)$	$(2) \times (4)^2$	$(3) + V_o \times (4)$		
1	1	445	3.0	1,300	9.0	-15,131	This is the component parallel to the neutral axis of the vector sum of all loads from the "cut" to the segment center, including V_o .	Same as for the axial load but using the component normal to the neutral axis at the segment center.
2	1	1,197	8.8	10,500	77.4	-44,493		
3	1	37,509	12.5	468,900	156.3	-27,391		
4	1	70,851	14.9	1,055,700	222.0	-6,510		
5	1	85,916	15.8	1,357,500	249.6	3,882		
6	1	94,598	15.8	1,494,600	249.6	12,564		
7	1	99,671	14.9	1,485,100	222.0	22,310		
8	1	85,216	12.5	1,065,200	156.3	20,316		
9	1	52,122	8.8	458,700	77.4	6,432		
10	1	6,539	3.0	19,600	9.0	-9,037		

$$\Sigma \text{ (5)} + V_o \Sigma \text{ (6)} = 0 \quad 7,417,100 + 1,428.6 V_o = 0 \quad V_o = -5,192$$

Table B4 Symmetrical Frame with Unsymmetrical Applied Loads

①	②	③	④	⑤	⑥	⑦	⑧	⑨	⑩
Segment	M_{sym} in-lbs	Axial _{sym} lbs	Shear _{sym} lbs	M_{asym} in-lbs	Axial _{asym} lbs	Shear _{asym} lbs	M_{unsym} in-lbs (2) + (5)	Axial _{unsym} lbs (3) + (6)	Shear _{unsym} lbs (4) + (7)
1	-24,907	This is the component parallel to the neutral axis of the vector sum of all loads from the "cut" to the segment center, including P_o .	Same as for the axial load but using the component normal to the neutral axis at the segment center.	-15,131	This is the component parallel to the neutral axis of the vector sum of all loads from the "cut" to the segment center, including V_o .	Same as for the axial load but using the component normal to the neutral axis at the segment center.	-40,038	This is the component parallel to the neutral axis of the vector sum of all loads from the "cut" to the segment center, including P_o and V_o .	Same as for the axial load but using the component normal to the neutral axis at the segment center.
2	-41,063			-44,493			-85,556		
3	-2,197			-27,391			-29,588		
4	30,794			-6,510			24,284		
5	36,016			3,882			39,898		
6	31,670			12,564			44,234		
7	34,466			22,310			56,776		
8	12,634			20,316			32,950		
9	-24,551			6,432			-18,119		
10	-52,140			-9,037			-61,177		
11	-52,140			9,037			-43,103		
12	-24,551			-6,432			-30,983		
13	12,634			-20,316			-7,682		
14	34,466			-22,310			12,156		
15	21,670			-12,564			19,106		
16	36,016			-3,882			32,134		
17	30,794			6,510			37,304		
18	-2,197			27,391			25,194		
19	-41,063			44,493			3,430		
20	-24,907			15,131			-9,776		

P_o , M_o and V_o are zero. If the cross-beam were pinned at its ends M_o and V_o would be zero, so the above six equations would become only four, the four equations would become only three and the two equations would become only one.

Calculations and Data

In all of the preceding calculation tables (and also in Table A9.5, Col.8) the most laborious effort is calculating the values of the applicable shear flow moments, M_q , and of the concentrated applied loads, M_o , about each segment's center. This is done starting with segment one and proceeding counterclockwise (M_q can be calculated per p.A19.19 or per p.A9.12). Once these moments are calculated and entered in Col.3 the remaining calculations are routine so they can also be programmed for calculation by computer or suitable calculators. In Col.3 and elsewhere positive moments produce compression in the outer flange. Positive values of x and y and of M_o , V_o and P_o are as shown in Fig.B1.

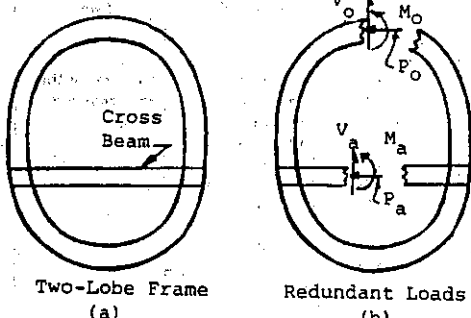


Fig. B4 Two-Lobe Frame

Inner Flange Lateral Supports

Unlike the outer flanges, the inner flange of a frame is not usually supported against buckling by skin panels. Therefore lateral supports of some type are needed when the flange compressive loads are significant. The support spacing must be such that lateral buckling will not occur. The supports are usually tubes (struts) or intercostals as in Fig.B5.

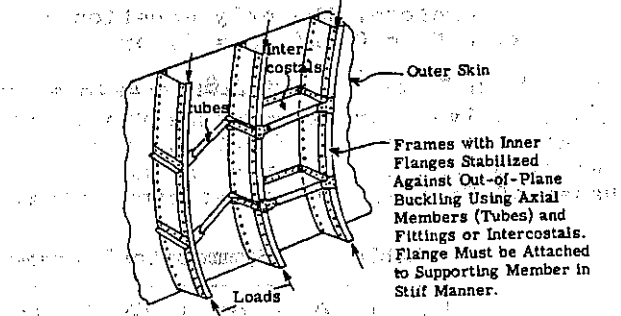


Fig. B5 Inner Flange Lateral Supports

Circular Frames of Uniform EI

When these are supported by skin panels as in previous analyses, data is available in Ref.15 of p.A21 for a more direct solution (using the "Wise Coefficients", from Jour. Aero Sciences, Sept.'39) The data can also be used when any self-equilibrating loads (no supporting skins) are present, by superposition of the applied and reacting load cases. The data is of graphical form, giving the internal moments, axial and shear loads for applied normal, tangential and moment loadings.

Accuracy of Analyses

Since the previous analyses do not include the stiffnesses of the structure adjacent to the bulkheads (skin panels, stringers and adjacent frames) the results are approximate and usually conservative for the bulkhead, but unconservative for the other structure. A discussion of this with examples is available in "The Analysis of Structures", N.J.Hoff, John Wiley and Sons. A more accurate analysis requires an involved finite element analysis which models all of the structure. However, the previous analyses are commonly used, and the results can also be used to size the frame for a finite element model.

Arches

Arches are beams with significant curvature, as in Fig.B6. They can be analyzed in the same manner as previously illustrated for frames. The internal loads depend upon the end fixities, so the analyses are as follows. Also see Art. A13.11a

Both Ends Fixed

This case is shown in Fig.B6, the redundants being taken at the right end, O. The applied loads, Q, can be in any direction. The arch is like a half-frame. The internal loads are determined in Table B5. The segment EI values may be uniform or varied. Table B5 is the same as Table B2 except that x and y are interchanged since the arch is shown in a horizontal position, and there are no shear flows, q.

For a symmetrical arch, loads, reactions and an even number of segments only $\frac{1}{2}$ of the arch is needed for the analysis with segment 5 fixed at its left end. $P_o = \sum Q_y / 2$ so only the first 2 equations are used with the P_o terms omitted. Loads in 6-10 are same as 5-1.*

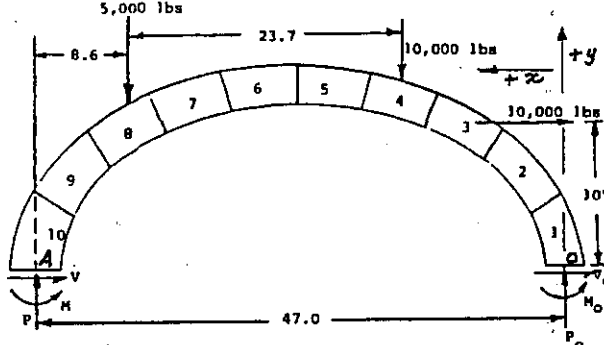


Fig.B6 Arch with Both Ends Fixed

One End Fixed and One End Pinned.

This is as shown in Fig.B7, there being only the two redundants V_o and P_o at the right end, so only two simultaneous equations are involved. These are

$$\Sigma (12) + V_o \Sigma (13) + P_o \Sigma (11) = 0$$

$$\Sigma (9) + V_o \Sigma (11) + P_o \Sigma (10) = 0$$

Therefore, Table B5 would be used except that Col. 7 and 8 and their sums are eliminated.

* With pinned ends $M_o = 0$, so only the first equation applies with the P_o and M_o terms omitted.

Table B5 Arch with Both Ends Fixed

①	②	③	④	⑤	⑥	⑦	⑧	⑨	⑩	⑪	⑫	⑬	⑭	⑮	⑯
Segment	$\frac{\Delta S}{EI}$	$M_{Q,x}$	x	y	M_Q	$\frac{\Delta S}{EI} x$	$\frac{\Delta S}{EI} y$	M_Q	$\frac{\Delta S}{EI} x^2$	$\frac{\Delta S}{EI} xy$	M_Q	$\frac{\Delta S}{EI} y^2$	M_{final}	Axial Load	Shear Load
1 lb-in	in-lbs	in	in	in	(3) x (2)	(2) x (4)	(2) x (5)	(4) x (6)	(2) x (4) ²	(2) x (4) x (5)	(8) x (6)	(3) x (5) ²	(3) + $M_o + V_o x (5)$ + $P_o x (4)$		
1	1.0	0	.7	3.0	0	.7	3.0	0	.49	2.1	0	9.0	24,666		
2	1.0	0	3.9	8.8	0	3.9	8.8	0	15.21	34.32	0	77.44	-32,829		
3	1.0	25,000	9.0	12.5	25,000	9.0	12.5	225,000	81.0	112.50	312,500	156.25	-17,669		
4	1.0	49,000	14.7	14.9	49,000	14.7	14.9	720,300	218.09	219.03	730,100	222.01	20,937		
5	1.0	0	20.5	15.8	0	20.5	15.8	0	420.25	323.90	0	249.64	9,552		
6	1.0	-61,000	26.6	15.8	-61,000	26.6	15.8	-1,622,600	707.56	420.28	-963,800	249.64	2,078		
7	1.0	-135,000	33.1	14.9	-135,000	33.1	14.9	-4,468,600	1,095.61	493.19	-2,011,500	222.01	-1,607		
8	1.0	-212,000	38.4	12.5	-212,000	38.4	12.5	-8,140,800	1,474.66	480.00	-2,660,000	156.25	3,310		
9	1.0	-321,000	43.2	8.8	-321,000	43.2	8.8	-13,867,200	1,856.24	380.16	-2,874,800	77.44	-8,890		
10	1.0	-422,500	46.1	3.0	-422,500	46.1	3.0	-19,477,250	2,125.21	138.30	-1,287,500	9.0	541		

$$\Sigma = 10.0$$

$$\Sigma = 1,077,500 \quad 236.2 \quad 110.0 \quad -46,631,050 \quad 8,002,22 \quad 2,603.8 \quad -8,675,000 \quad 1,428.7$$

$$M_o = M_{Q,y} + M_{Q,z}$$

* When ΔS or EI is constant over the frame it can be considered to be unity for column (2). For this example all of these are constant.

$$\left. \begin{aligned} \Sigma (6) + M_o \Sigma (3) + V_o \Sigma (8) + P_o \Sigma (7) &= 0 \\ \Sigma (12) + M_o \Sigma (8) + V_o \Sigma (13) + P_o \Sigma (11) &= 0 \\ \Sigma (9) + M_o \Sigma (7) + V_o \Sigma (11) + P_o \Sigma (10) &= 0 \end{aligned} \right\} \begin{aligned} M_o &= 62,787 \\ V_o &= -14,754 \\ P_o &= 5,774.8 \end{aligned}$$

This is the component parallel to the neutral axis of the vector sum of all loads from the "cut" to the segment center, including P_o and V_o .

APPENDIX B BULKHEADS, FRAMES, ARCHES AND BENTS

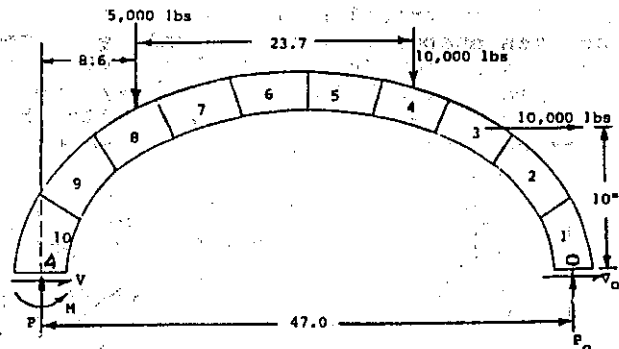


Fig. B7 Arch, One End Fixed, One Pinned

inated, the sum of Col. 6 is not needed, M_0 is zero and only the above two equations are used to determine V_o and P_o . Proceeding as in the above manner the final internal loads are as shown in Table B6 ($V_o = -11,173$ and $P_o = 94,633$)

Table B6 One End Fixed and One End Pinned

Segment	M_a $\textcircled{3} + V_o \times \textcircled{5}$ $\textcircled{3} + P_o \times \textcircled{4}$	Axial Load	Shear Load
1	-26,901		
2	-61,435	This is the component parallel to the neutral axis of the vector sum of all loads from the "cut" to the segment center, including P_o and V_o .	Same as for the axial load but using the component normal to the neutral axis at the segment center.
3	-29,519		
4	21,602		
5	17,433		
6	14,160		
7	11,730		
8	11,707		
9	-10,519		
10	-19,759		

One End Fixed and One End on Rollers

For this case, Fig. B8, there is only the redundant P_o at the right end, so the only minimum energy equation is, referring to Table B7,

$$\Sigma \textcircled{5} + P_o \Sigma \textcircled{6} = 0$$

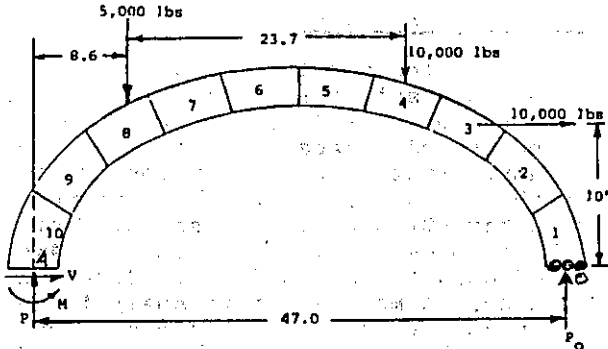


Fig. B8 Arch, One End Fixed, One Rollers

The final loads are determined using Table B7.

Both Ends Pinned

This case is shown in Fig. B9. Since V_o passes through point A, P_o can be calculated directly as $P_o = \sum M_A / L$ leaving V_o as the only redundant. It is determined from the minimum energy equation, referring to Table B8,

$$\Sigma \textcircled{5} + V_o \Sigma \textcircled{6} = 0$$

The final internal loads are determined using Table B8, as shown,

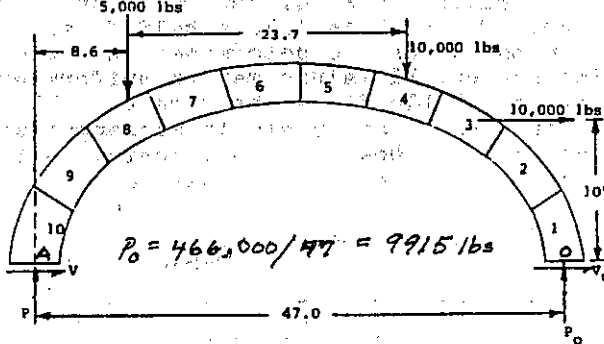


Fig. B9 Arch with Both Ends Pinned

Table B7 Arch with One End Fixed and One on Rollers

①	②	③	④	⑤	⑥	⑦	⑧	⑨
Segment	ΔS EI	M_Q Data	x Data	$M_Q \Delta S x$ $\textcircled{2} \times \textcircled{3} \times \textcircled{4}$	$\Delta S x^2$ EI	M_{load} $\textcircled{3} + P_o \times \textcircled{4}$	Axial Load	Shear Load
	Data	Data	Data	$\textcircled{2} \times \textcircled{3} \times \textcircled{4}$	$\textcircled{2} \times \textcircled{4}^2$			
1	1.0	0	.7	0	.5	4,078		
2	1.0	0	3.9	0	15.2	22,725		
3	1.0	25,000	9.0	225,000	81.0	77,443		
4	1.0	49,000	14.7	720,000	216.1	134,657		
5	1.0	0	20.5	0	420.3	119,453		
6	1.0	-61,000	26.6	-1,622,600	707.6	93,998		
7	1.0	-135,000	33.1	-4,468,500	1,095.6	57,874		
8	1.0	-212,000	38.4	-8,140,800	1,474.6	11,757		
9	1.0	-321,000	43.2	-13,867,200	1,866.2	-69,274		
10	1.0	-422,500	46.1	-19,477,250	2,125.2	-153,875		

$$\Sigma = -46,631,050$$

$$8,002.3 \quad \Sigma \textcircled{5} + P_o \times \Sigma \textcircled{6} = 0$$

$$P_o = 5,827 \text{ lbs}$$

Table B8 Arch with Both Ends Pinned

(1)	(2)	(3)	(4)	(5)	(6)	(7)	(8)	(9)
Seg. ment	$\frac{\Delta S}{EI}$	M_{Q,P_0}^* Data	y Data	$M_{Q,P_0} \frac{\Delta S_y}{EI}$ $\frac{(3) \times (3) \times (4)}{EI}$	$\frac{\Delta S_y^2}{EI}$ $\frac{(2) \times (4)^2}{EI}$	M_{final} $\frac{(3) + V_o \times (4)}{EI}$	Axial Load	Shear Load
1	1.0	6,940	3.0	20,820	9.0	-29,057		
2	1.0	38,699	8.8	340,551	77.4	-66,892		
3	1.0	114,235	12.5	1,427,938	156.3	-3,575		
4	1.0	194,751	14.9	2,901,790	222.0	15,966		
5	1.0	203,258	15.8	3,211,476	249.6	13,764		
6	1.0	202,739	15.8	3,203,276	249.6	13,155		
7	1.0	193,187	14.9	2,878,486	222.0	14,402		
8	1.0	168,736	12.5	2,109,200	156.3	18,749		
9	1.0	107,328	8.8	944,486	77.4	1,737		
10	1.0	34,582	3.0	103,746	9.0	-1,415		

 $* M_Q + M_{P_0}$ $\Sigma M = 17,141,769$ $1,428.6$ $\Sigma (5) + V_o \Sigma (6) = 0$ $V_o = -11,999 \text{ lbs}$ One End Pinned and One End on Rollers

This case is statically determinate since $P_o = \sum M_A / L$, so the moments at all segments can be calculated directly. For the previous applied loads

$$P_o = 466,000 / 47 = 9,915 \text{ lbs}$$

which is the same as for the previous case.

Bents*

Examples of these are shown in Fig. B10. The same discussions and tables presented for arches also apply for these.

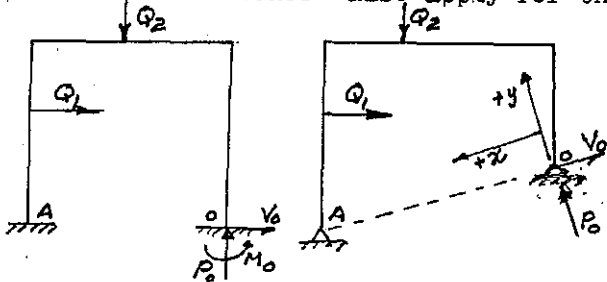


Fig. B10 Bents*

The discussions and calculation tables for arches and bents enable one to quickly proceed with the determination of their internal loads. All one needs to do is to enter the applicable data in Col. 1 through 4 (or 5) and then carry out the calculations as indicated in the tables. The same also applies for bulkheads and frames. Stress analyses can then be performed for the structures.

Accuracy of Analyses

For the usual "sturdy" arches (and bents) the calculated final bending moments are suitable for engineering design purposes, even though they are not "exact".

* Does not account for side-sway effects, see Art. A1.11 and the reference below. For axial load effects and buckling of bents, see Engineering Column Analysis by W.F. McCombs, published by Datatec, 2106 Siesta Dr., Dallas, Tx 75224.

since the effects of curvature of the arch were not considered. There is no analytical way to include these effects**. The following successive approximation procedure can be used to see if deflections matter.

1) Use the final bending moments from the arch analysis as the moments in Table C3.3 and calculate the deflections. These moments are at the segment centers, but they must be at the segment ends in Table C3.3. Therefore, plot the moments versus distance along the arch, draw a curve through them and then obtain the moments at the ends of the segments for Table C3.3.

2) The calculated deflections are at the segment ends, so they must be found at the segment centers in the manner described above. The deflections are normal to the arch neutral axis, positive deflections being outward (or "up"). This gives a new shape for the arch and the applied load locations. Recalculate the arches final moments for this new geometry. If they are not significantly different from the original ones they are used for design purposes.

3) If the recalculated final moments are significantly different, successively repeat (1) and (2) until they are not so.*

It is for relatively long and slender arches that the deflections are most likely to be significant. The following rough guide can be used to see if a deflection analysis is needed (see "Advanced Structural Analysis", Borg & Gennaro, D. Van Nostrand Co.). Calculate the following factor, F. If F is less than 3 a deflection analysis is probably necessary.

$$F = CP_{cr}/P$$

** Successively increasing deflections indicate instability

P_{cr} is the buckling load assuming the arch to be a pin-ended column whose length is the arc length of the arch. For pinned ends $C = 4$ and for fixed ends $C = 8$. For a uniform EI $P_{cr} = \pi^2 EI / L^2$. For a non-uniform EI P_{cr} is per Art.C2.6a - C2.6b. P is the average compressive load in the arch

Carrying out (1) above for the pin-ended arch of Fig.B9 and Table B8, where ΔS is 6.1" and L is 61", assuming EI is 16×10^6 the deflections at the segment centers (using Table C3.3) are found to be

Seg.	1	2	3	4	5	6	7	8	9	10
Def.	.08	.22	.15	.05	-.06	-.12	-.16	-.16	-.10	-.03

These deflections are so small that they would cause a very minor change in the arches shape, and its resulting effects on the final moments would be inconsequential if (2) were carried out (the arch in Fig. B9 is therefore a "sturdy" one). Also, for this case F is much larger than 3, which indicates no deflection analysis is needed (as the deflection calculations also showed).

Buckling of Arches and Bents*

Some arches and bents and their applied loadings are such that no bending is present, but there is considerable axial stress. For such cases the allowable loading is the buckling load for the member. When there is also some bending present it is magnified by the "beam-column effect". The buckling normally occurs as a "sidesway", as shown for two typical cases in Fig.B11, (a) being a circular arch and (b) being a bent,



Fig.B11 Buckling of an Arch and a Bent

The buckling of arches and bents is discussed in the book of Art.A18.27a.** For a few cases such as the following, the critical value of the loading can be determined by formulas and related data.

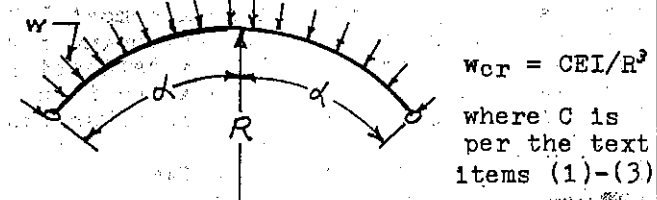


Fig.B12 Uniform Circular Arch and Uniform Radial Distributed Loading

* For additional discussions and other cases see "Theory of Elastic Stability", Timoshenko and Gere, McGraw-Hill Book Co.

** To detect instability (p.27 footnote) there must be some nonsymmetry in the arch or in the load. If not, add a small lateral load, about 5% of the total load, at the center of the arch.

- 1) For pinned ends $C = (\pi^2/\alpha^2) - 1.0$
- 2) For fixed ends $C = k^2 - 1.0$ where k is the value satisfying the equation $k \tan \alpha \cot k\alpha = 1.0$
- 3) For fixed ends or pinned ends having a center pin, C is obtained from Table B9.

Table B9 Circular Arch with a Center Pin

α	Fixed Ends	Pinned Ends
15	162	108
30	40.2	27.6
45	17.4	12.0
60	10.2	6.75
75	6.56	4.32
90	4.61	3.30

For a uniform parabolic arch and loading as in Fig.B13

$$w_{cr} = CEI/L^3$$

C is per Table B10

Fig.B13

Table B10 Parabolic Arch (Fig.B13) Data

h/L	No Pins	1 Pin	2 Pins	3 Pins
.1	60.7	33.8	28.5	22.5
.2	101	59	45.5	39.6
.3	115	82	46.5	46.5
.4	111	96	43.9	43.9
.5	97.4	91	36.4	36.4
.6	83.8	80	30.5	30.5
.8	59.1	59.1	20.0	20.0
1.0	43.7	43.7	14.1	14.1

For a catenary arch see Table B11.

Table B11 Catenary Arch with a Center Pin

h/L	Fixed Ends	Pinned Ends
.1	59.4	28.4
.2	96.4	43.2
.3	112	41.9
.4	92.3	35.4
.5	80.7	27.4
1.0	27.8	7.06

* Same load and formula as in Fig.B13

For a very shallow arch, Fig.B14, buckling can occur as a "snap-through" movement as shown by the broken line and is due to shortening caused by compression.



Fig.B14 Very Shallow Uniform Arch

When there are several loads express them in terms of only one, Q , as shown. The critical value of Q is defined by the equation

$$\delta/e = 1 + \sqrt{4(1-m)^3/27m^2}$$

where δ = deflection at center of arch and e is written in terms of Q (or of w if only w is present)

$$m = 4I/Ae^2 \quad (A = \text{cross-sectional area})$$

The above equation is solved to get the critical value of Q (or of w if only w is present).

When $m \geq 1.0$ this type of buckling cannot occur, but the general type (sidesway) can.

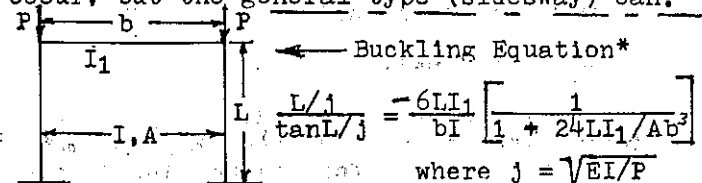


Fig.B15 Special Case of Bent Buckling

Solve by successive trials for P . When $P = P_c$ the equation will be satisfied. Also applies within a very few percent for any P (b and L) loads having a total of $2P$, may be unsymmetric.

For pinned ends the equation is $(L/j)\tanL/j = 6I_L/T_b$ and the above comments apply

Effect of Column End Support Stiffness

When the lateral end supports for a column are significantly flexible, this can reduce the allowable axial load to be below the buckling load, as follows. For the pinned case the allowable axial load due to support stiffness is in Fig. B16 (see the book of Art. A18.27a for a derivation).

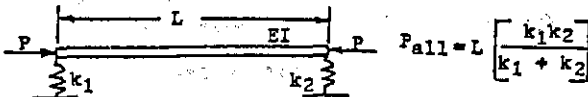


Fig. B16 Effect of End Support Stiffness

When $k_1 = \infty$ (simple support) $P_{all} = k_2 L$ and vice-versa if $k_2 = \infty$. For the column itself the allowable load is $\pi^2 EI/L^2$. Therefore, minimum values of k_1 and k_2 needed to provide adequate support are given by

$$k_1 k_2 / (k_1 + k_2) = \pi^2 EI / L^3$$

If less than this, P_{cr} cannot be reached but P_{all} may be adequate for the actual load, P .

For any multispan column the ability of flexible supports to provide simple support for a given axial load, P , can be checked using the formula in Fig. B16 with successive calculations from end A to end E as in Fig. B17. This is discussed and illustrated in the above mentioned book and also in NACA TN 871. Pinned joints are assumed.

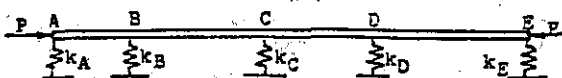


Fig. B17 Multispan Column Flexible Supports

Structural Requirements for Secondary Structure and Operating Devices

Troubles for these items are caused by a lack of strength or insufficient stiffness and usually show up during proof testing or during service.* Some suggestions for avoiding such troubles are as follows.

1. All devices must maintain full strength at limit loading. Therefore, the effects of limit deflection, whether due to limit load on the device or to limit load on other parts of the structure, must be checked. All operating devices must function properly at deflections due to limit loading.

2. For areas of engagement of locking devices where retention depends upon bearing pressure between two parts, keep the bearing stresses below 10,000 psi and/or provide for .25" misalignment on assembly.

3. As to location and direction of loads, assume them to be anywhere within a 30° cone centered on the computed direction. When the load direction is based on a properly oriented machined fitting face assume a 10° mis-

* And are then very expensive, both dollar and time-wise, to fix.

alignment to exist. For analysis of back-up structure, assume the most adverse position of load, e.g., at the tip end of lugs (which is universal practice in gear tooth design). Where strength depends on a dead-center mechanism, provide both strength and mechanical advantage from the operating standpoint to take care of a 10° misalignment either way.

4. Design limit switch brackets and installations to deflect a maximum of .03" under a 100 lb load in the direction of switch actuation and to have no permanent set under a load of 100 lbs in any direction.

5. Design external power plug receptacle installations for a limit load of 1500 lbs along the plug axis and, simultaneously, 500 lbs normal to the plug axis in any direction and at the largest moment arm which the plug permits. External power plugs are subject to rough and careless handling.

6. Gaps provided to prevent secondary structure from loading up must be checked for adequacy against gap closure due to structural load and/or temperature deflections.

7. Provide adequate hinges and warp for doors to remain closed and sealed under proof loads and, where applicable, design the hinges for superposition of proof loads and warp loads.

8. The structural analysis of control surfaces hinged to primary structure must include the effects of the deflections of the supporting structure. This also applies to power or control system shafting. See examples in the book of Art. A18.27a.

9. When control surface skin panels are allowed to buckle, the secondary loads due to tension field action must be considered. Otherwise these loads may cause either a failure or excessive deformation, particularly for thin trailing edges (see p.67).

It is recognized that procedures (2) through (5) may run into difficulties, inconsistencies and designs which, when installed properly, will be considerably over strength. The design penalty may seem to be large in the layout stage, but actually it is only a small fraction of the cost, dollar and time-wise, of making the changes at any later date, particularly in the field. The weight penalty is more than justified in terms of increased reliability.

Adding material to a structure never reduces its strength but can reduce its life. With a redundant ductile structure (and joints, Fig. D1.44) the redundant loads can be assumed, the member loads calculated and the structure will deform to this load distribution prior to strength failure. This does not apply to structural life, however, or to no yielding at limit load.

There are two main cases of axial load transfer, by shear, between members which require detailed analyses. These cases are the installations of doublers and splices.

Splices

Splices involving the transfer of load, by shear, from one member to another should be kept as short as possible. For example, when two "skins" are spliced together an ideal splice would involve only a single line of fasteners, but two or three lines may sometimes be needed.

Doublers

Doublers are relatively long members installed on a "base" member, such as on a wing-skin for example, for various purposes such as the following.

a) Strength

- 1) To strengthen an existing structure
- 2) To salvage a damaged area
- 3) To strengthen an axially loaded member having a hole or a cut-out or a non-structural door.

b) Fatigue Life

- 1) To increase the life of an existing design in a fatigue critical region.
- 2) To properly salvage a damaged structure for an adequate service life.
- 3) To salvage a "fatigue damaged" structure where fatigue damage has been accumulating too rapidly in a particular vehicle or group of vehicles

c) Reinforcement for additional stiffness purposes which must include a consideration of possible fatigue life limitation due to the installation.

d) Any member attached to an axially loaded base structure will act as a local

doubler picking up axial load, so a check on a possible harmful effect on fatigue life at the fasteners may be necessary.

- e) The effect of ending an axial member, such as a stringer, on a skin or sheet material. This may be desirable from a manufacturing or salvage standpoint, but its effect on fatigue life must be considered or investigated.

The main effort in analyzing doublers or splices is the determination of the loads in the attachments. Once these are known the loads and stresses in the members are known and can be evaluated as to strength or fatigue life or stiffness.

Figure B18 shows a comparison of the fastener (and member) loads in a doubler and in a long (undesirable) splice. Note that the loads are largest in the end fasteners, so the members must be designed and "tailored" to reduce this "peaking" of loads. The fastener load distribution also depends upon the spring constants of the fastener joints (determined experimentally).

A discussion of the analyses and design of doublers and splices is beyond the scope of this book. However, a detailed and practical discussion of the subject is available in the Air Force Flight Dynamics Laboratory Report AFFDL-TR-67-184, January 1968, "Analytical Design Methods for Aircraft Structural Joints" which contains numerous examples. It also accounts for fastener hole clearance or "slop" and loadings into the plastic range of the joints. The report is over 187 pages and will enable the reader to obtain a good understanding of the subject and its many applications, and is available at some libraries. A copy, with corrections and added comments, is also available from W.F. McCombs, 2106 Siesta Dr., Dallas, TX 75224, \$19.95 plus \$3.00 shipping. The reader is encouraged to consult the report.*

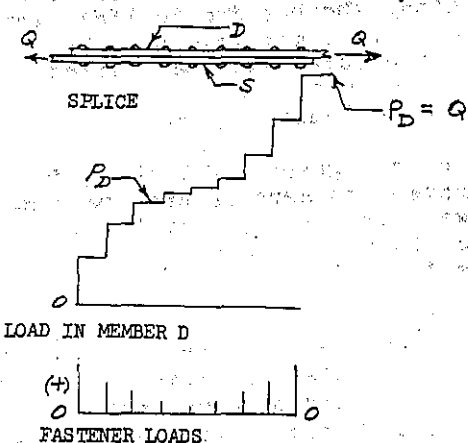
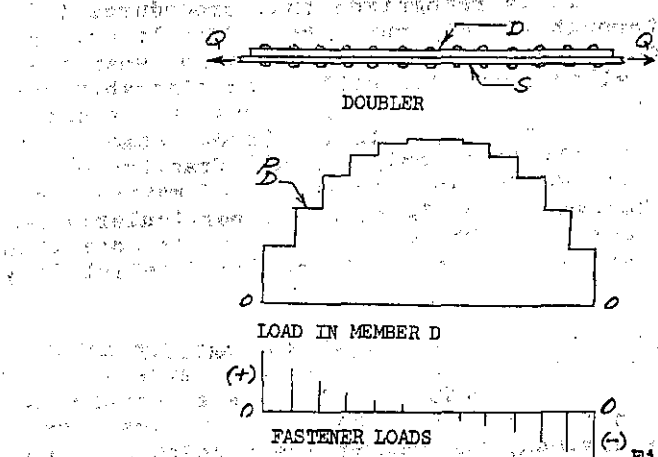


Fig. B18

* Being the only such comprehensive report available, it should be included in any structures library.

APPENDIX B JOGGLED FLANGES AND RIGID JOINT TRUSS BUCKLING ANALYSIS B11

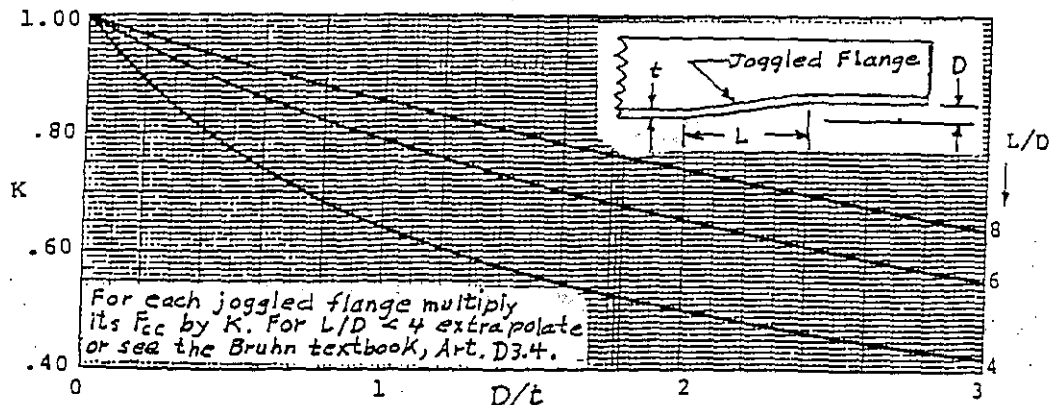


Fig.C7.45 Crippling Stress (F_{cc}) Reduction Factor for Aluminum Flanges

Calculating the Critical (Buckling) Value for a Rigid Joint Truss's Loading

The critical (buckling) loading for the truss (all members deforming in bending) is found by a successive trial procedure as follows.

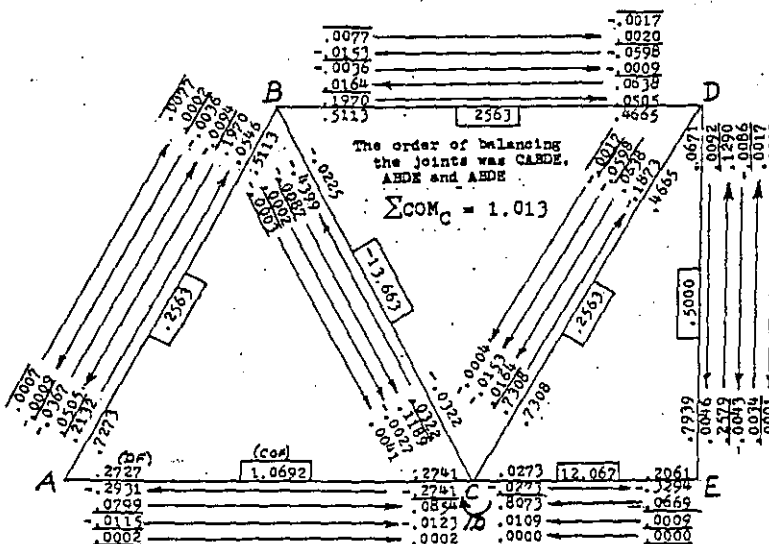
1. For the applied loading determine the member loads assuming pin joints. Factor the applied loads to cause a load of about 1.6 times the buckling load in the first member that would fail, assuming pin joints. Then determine the COF and DF for all members, for rigid joints.
2. Apply a unit couple at the joint, N, whose members have the largest compression loads and carry out the moment distribution procedure until all joints have been balanced and the balancing moments carried back to the joint N.
3. Do not rebalance N but again rebalance all other joints (in the same sequence as before) carrying the balancing moments back to N.
4. Repeat until the moments carried back to N are negligible, usually 2-3 sets of balancing.
5. If the sum of the moments carried back to N, ΣCOM_N , is < 1.0 the loading is less than critical. If more than 1.0 it is above the critical load.
6. Repeat the above with another loading, successively, until $\Sigma COM_N = 1.0$ (or, say, between .99 and 1.01) and that is the critical loading.

The procedure is illustrated below for the truss of Fig.A11.92 where, after several successive trials, it is found that for an applied load of 12,377 lbs $\Sigma COM_C = 1.013$, so that is, essentially, the critical load (for a load of 12,360 lbs $\Sigma COM_C = 1.00$).

As discussed in Art.11.15b and Table A11.6, the failing load will be less than the buckling load because of beam-column failure. Usually it will be at about 90% of the buckling load, but only a successive trials analysis as in Art. A11.15a will give the M.S..

The COF and SC values used to obtain SF and DF values were calculated using the formulas on p.3.

Gusset plates can considerably increase the critical loading and the failing loading. The analyses are as before, but the SC and COF values are different. These are available in Ref.14 and in "The Analysis of Structures", Hoff, N.J., and on p. B/2-13.



Assuming pin joints to determine the axial loads is quite reasonable, although the joint secondary bending moments do change these slightly. Actually the assumption is conservative, the final bending moments always being smaller (see "Moment Distribution", Gere, James M., Van Nostrand Co.).

In Table A11.4 cross-sections are square. At the end of item 6, p.4 add: "Then see Art.A5.31a".

At the bottom of p.4 add the following: "If the applied loading is above the critical value, the successive carry over moments will diverge. To calculate the critical (buckling) loading value see P/B11, inside the rear cover. Rigid joint strength is usually over 60% more than is predicted by a pin joint stress analysis."

The failing load for the truss is 11,088 lbs, failure occurring in member CE as a beam-column, 3.6" from C ($M=48$ in-lbs). This is 89.6% of the above buckling load and is obtained by successive trials using the procedure of Art.A11.15a.

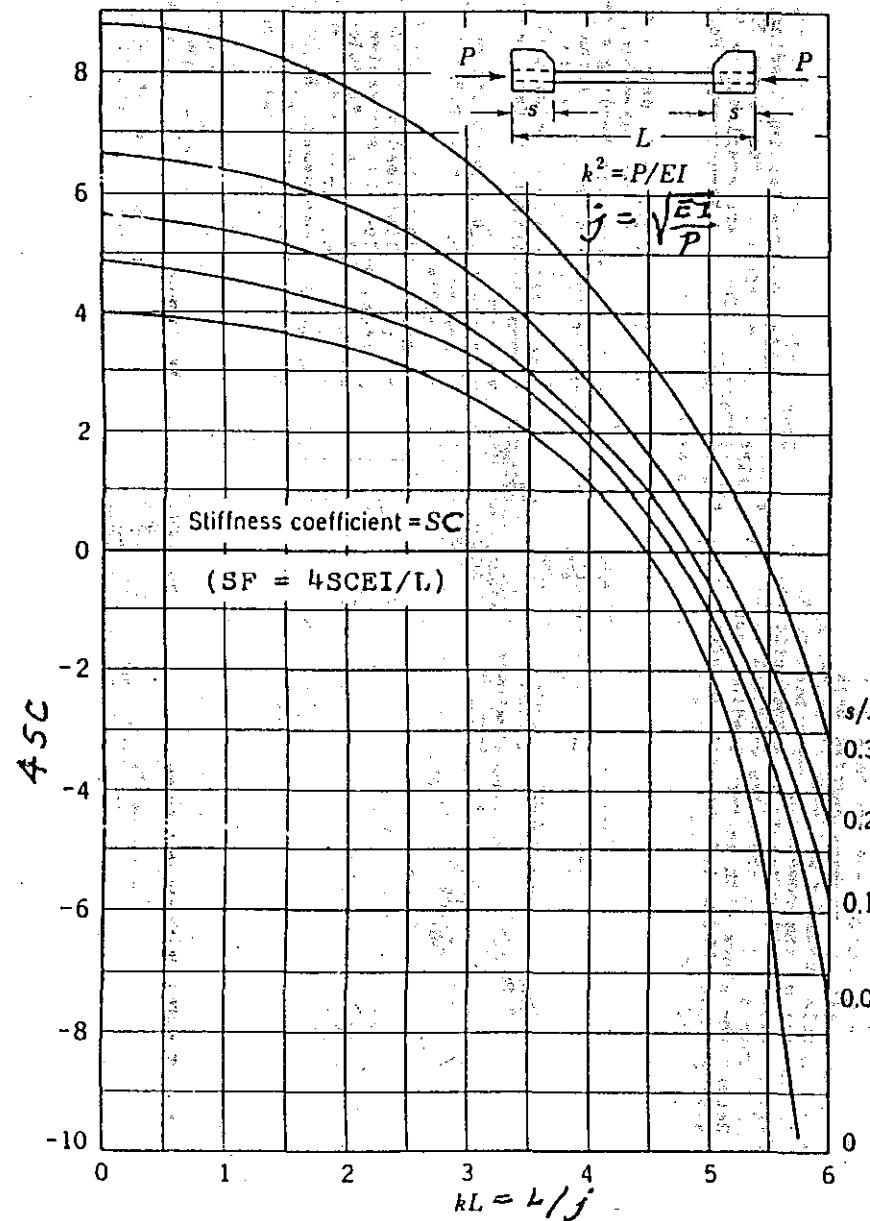


Fig. 2.4.9. Stiffness coefficients for compression bars with gusset plates.
From author's paper in ASCE Transactions, #2454

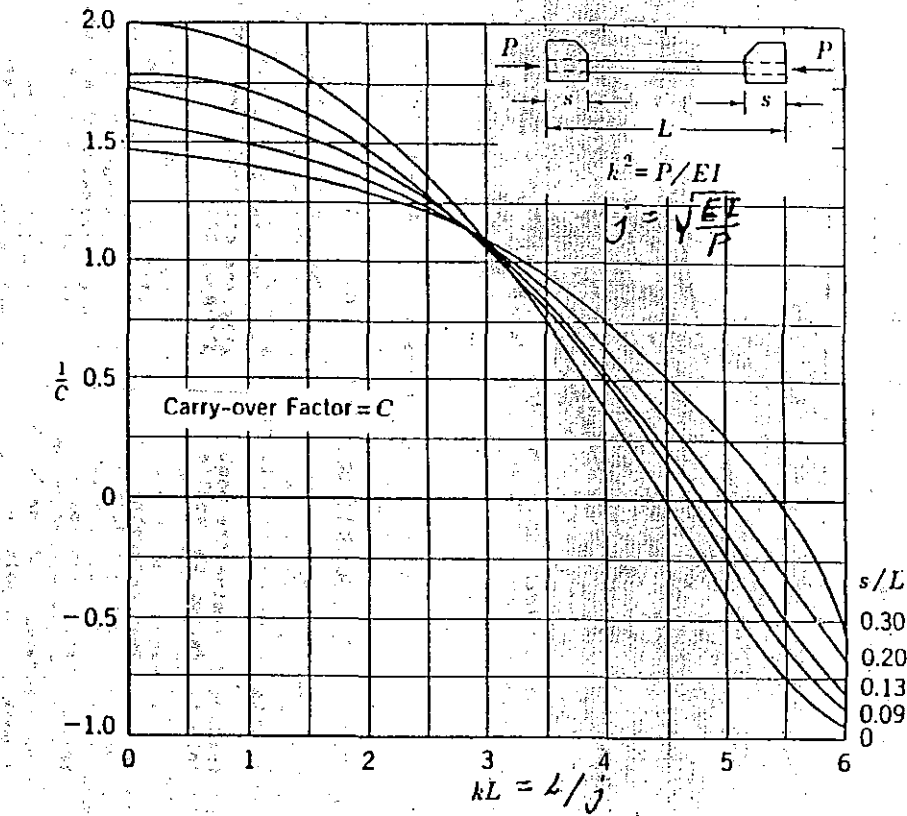


Fig. 2.4.10. Carry-over factors for compression bars with gusset plates.
From author's paper in ASCE Transactions #2454

For more accuracy enlarge the region between $kL = 4.2$ and 5.7 2 or 3 times

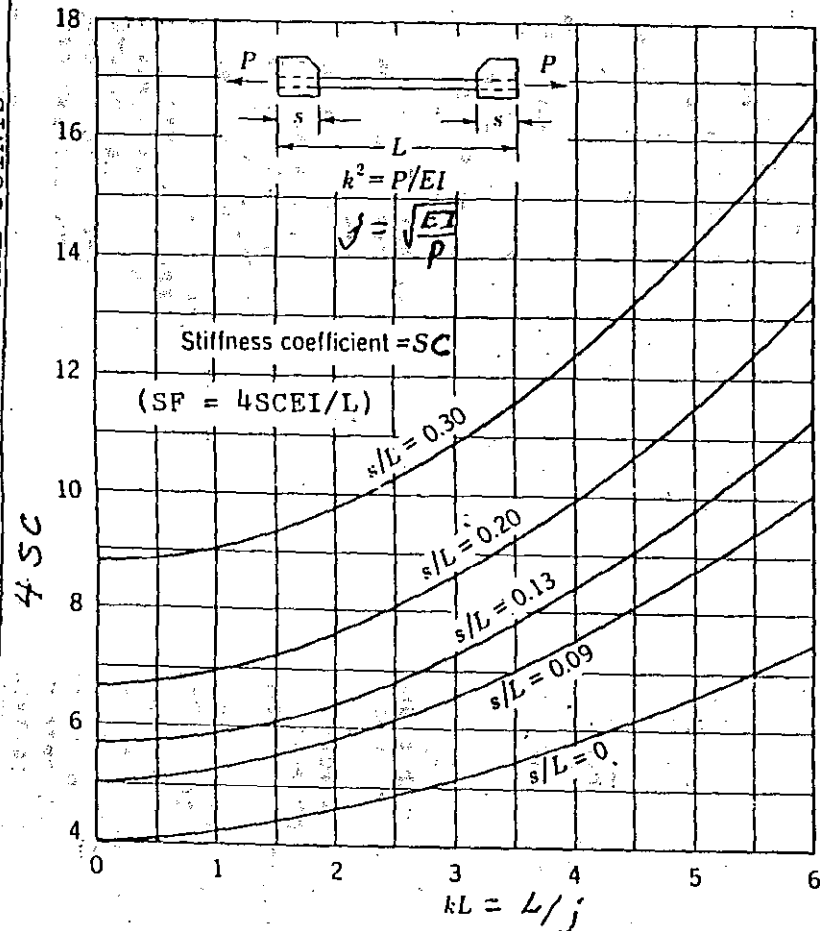


Fig. 2.4.11. Stiffness coefficients for tension bars with gusset plates.
 From author's paper in *ASCE Transactions*, #2454

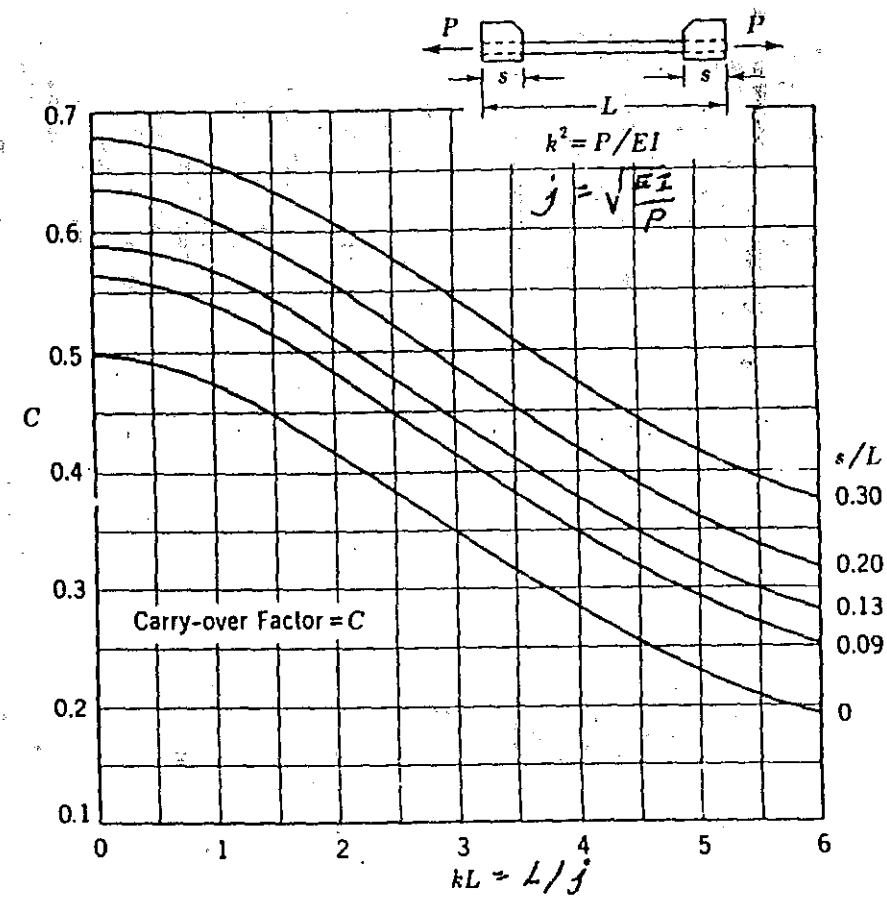


Fig. 2.4.12. Carry-over factors for tension bars with gusset plates.
 From author's paper in *ASCE Transactions*, #2454

INDEX

- Arch Analysis B5
 Beam deflections 1, A21
 Beam formulas A21
 Beam-columns
 analyses 34, 39
 allowable stresses 38
 approximate formula 1, 37
 calculating P_{cr} 36
 carry-over factor 3
 deflections 1, 35
 equivalent loads 37
 formulas 8
 initially bent 37
 margin of safety 38, 39
 numerical analysis 3, 34-36
 other considerations 37
 varying EI 34
 Bolts 74
 Bolt strengths 77, A21
 Bent Analysis B7
 Bushings 74
 Bulkhead Analysis B1
 Carry-over factor 3
 Clamp-up importance 74-75
 Columns
 buckling data 23-29, B9
 design curves 12, A4-A5
 effective modulus 25
 end friction effects 30
 initially bent 21
 instability criteria 15
 non-dimensional curves 24
 one end free 12
 shear effect on buckling 14
 stepped 16
 torsional buckling 7, 44-46
 two-span 15
 moving (mechanisms) 30
 multispan 14
 numerical analysis 17
 varying EI 17
 Combined stresses 11
 Crippling 41-44
 Curved beams 6
 Doublers B10
 Design check list A1
 Diagonal tension
 stringer system 51-60
 longeron system 60-66
 flat web holes 49-50

 Effective modulus of elasticity 25

 Factors of safety 8, 74
 Fastener/joint design guides A10
 Fastener / joint design data A10-A21
 Fillers, effects on joints 76
 Fittings
 design 74
 margins of safety 9, 74, A1
 factors of safety 74
 Fixed end moments 4
 Frame stiffness criteria 47

 Frame Analysis B1
 Flexible lateral supports 23, 26, 29, B9
 Interaction equations 10
 Gusset plate data B12-13
 Joint strengths A10 - 21
 Joints, brittle and ductile 75
 Joggled flanges 42, B11
 Lugs, oblique loads 74
 Lugs, transverse loads 74

 Margins of safety 9,10, 38,39, A1
 true 10
 apparent 10
 Material properties 8, A6-A9
 Moment distribution 1, 3, 15
 Monocoque shell buckling
 cylindrical shells 67-71
 conical shells 72-77
 spherical end caps 73

 Numerical analyses
 columns 17-21
 beam-columns 34-36
 Nuts 74
 Nut/collar tension strength A21
 Operating devices B9
 Preload torque factors for bolts A2
 Plastic bending 1, 31
 residual stresses 33
 shear stresses 32
 Plastic torsion 1, 38
 Plate buckling
 shear 39
 bending, one edge free 40
 Principal stresses 11
 Proportional limit stress 38

 Rib crushing loads 8
 Rivet design 50
 Rockwell/Brinell hardness data A2
 Secondary structure B9
 Shear stresses in plastic range 32
 Sheet buckling (see plate buckling)
 Shims (see fillers)
 Sign convention 3, 19
 Stiffener minimum I A2
 Stiffness coefficient 3
 Stiffness factor 3
 Stress-strain curves A3
 Successive trial solutions 10, 23, 39
 Splices B10

 Tangent modulus 1, 24, 25
 Tension clip strengths 77, A1-A2
 Thread design/strength 75-76
 Thick-web beam analysis 47
 Tolerances, allowable 11
 Torsional buckling 44-46
 Truss analysis 1, 3-5, B11
 Tension field (see diagonal tension)

 Yield stress bending modulus 33

INDEX FOR THE BRUHN TEXTBOOK

The current (1973) textbook has no Index. Following is an updated index for that edition.

Accelerated Motion of	
Rigid Airplane	A4.8
Aircraft Bolts	D1.2
Aircraft Nuts	D1.2
Aircraft Wing Sections - Types	A19.1
Aircraft Wing Structure - Truss Type	A2.14
Air Forces on Wing	A4.4
Allowable Stresses (and Interactions)	C11.36
Analysis of Frame with Pinned Supports	A9.16
Angle Method	C7.1
Application of Matrix Methods to Various Structures	A7.23
Applied Load	A4.1
Axis of Symmetry	A9.4
Beaded Webs	C10.16
Beam Design - Special Cases	D3.10
Beam Fixed End Moments by Method of Area Moments	A7.32
Beam Rivet Design	C10.8
Beam Shear and Bending Moment	A5.1
Beams - Forces at a Section	A5.7
Beams - Moment Diagrams	A5.6
Beams with Non-Parallel Flanges	C11.9
Beams - Shear and Moment Diagrams	A5.2
Beams - Statically Determinate & Indeterminate	A5.1
Bending and Compression of Columns	A18.1
Bending Moments - Elastic Center Method	A9.1
Bending of Rectangular Plates	A18.13
Bending Strength - Basic Approach	C3.1
Bending Strength - Example Problems	C3.4
Bending Strength of Round Tubes	C4.15
Bending Strength - Solid Round Bar	C3.1
Bending Stresses	A13.1
Bending Stresses - Curved Beams	A13.15
Bending Stresses - Elastic Range	A13.13
Bending Stresses - Non- homogeneous Sections	A13.11
Bending Stresses About Principal Axes	A13.2
Bending of Thin Plates	A18.10
Bolt Bending Strength	D1.9
Bolt & Lug Strength Analysis Methods	D1.5
Bolt Shear, Tension & Bending Strengths	D1.3
Boundary Conditions	A24.8
Box Beams Analysis	A22.5
Brazing	D2.4
Buckling Coefficient	C5.1
Buckling of Flat Panels with Dissimilar Faces	C12.25
Buckling of Flat Sheets under Combined Loads	C5.6
Buckling of Rectangular Plates	A18.20
Buckling of Stiffened Flat Sheets under Longitudinal Compression	C6.4
Buckling under Bending Loads	C5.6
Buckling under Shear Loads	C5.6
Buckling under Transverse Shear	C8.14
Carry Over Factor	A11.4
Castigliano's Theorem	A7.5
Centroids - Center of Gravity	A3.1
Cladding Reduction Factors	C5.5
Column Analogy Method	A10.1
Column Curves - Non- Dimensional	C2.2
Column Curves - Solution	C2.13
Column End Restraint	C2.1
Column Formulas	C4.2
Column Strength	C7.21
Column Strength with Known End Restraining Moment	C2.16
Combined Axial and Trans- verse Loads - General Action	A5.21
Combined Bending and Compression	C4.22
Combined Bending and Flexural Shear	C3.10
Combined Bending and Tension	C4.23
Combined Bending and Tension or Compression of Thin Plates	A18.17
Combined Bending & Torsion	C4.23
Combined Stress Equations	C1.2
Compatibility Equations	A24.7
Complex Bending - Symmetrical Section	C3.9
Compressive Buckling Stress for Flanged Elements	C6.1
Conical Shells - Buckling Strength	C8.22
Constant Shear Flow Webs	A14.10
Constant Shear Flow Webs - Single Cell - 2 Flange Beam	A15.3
Constant Shear Flow Webs - Single Cell - 3 Flange Beam	A15.5
Continuous Structures - Curved Members	A11.31
Continuous Structures - Variable Moment of Inertia	A11.15
Core Shear	C12.26
Correction for Cladding	C7.4
Corrugated Core Sandwich Failure Modes	C12.27
Cozzone Procedure	C3.2
Creep of Materials	B1.8
Creep Pattern	B1.12
Crippling Stresses Calculations	C7.7
Critical Shear Stress	C11.16
Crystallization Theory	C13.7
Cumulative Damage Theory	C13.26
Curved Beams	A5.8
Curved Sheet Panels - Buckling Stress	C9.1
Curved Web Systems	C11.29
Cut-Outs in Webs or Skin Panels	D3.7
Deflection Limitations in Plate Analyses	A17.4
Deflections by Elastic Weights	A7.27
Deflections by Moment Areas	A7.30
Deflections for Thermal Strains	A7.17
Deflections by Virtual Work	A7.9
Delta Wing Example Problem	A23.1
Design for Compression	C4.2
Design Conditions and Design Weights	A5.12
Design Flight Requirements for Airplane	A4.6
Design Loads	A4.1
Design for Tension	C4.1
Differential Equation of Deflection Surface	A18.12
Discontinuities	A20.15
Distribution of Loads to Sheet Panels	A21.2
Ductility	B1.5
Dummy Unit Loads	A8.6
Dynamic Effect of Air Forces	A4.13
Effect of Axial Load on Moment Distribution	A11.22
Effective Sheet Widths	C7.10
Elastic Buckling Strength of Flat Sheet in Compression	C5.1
Elastic - Inelastic Action	B1.5
Elastic Lateral Support Columns	C2.17
Elastic Stability of Column	A17.2
Elastic Strain Energy	C1.6
Elasticity and Thermo- elasticity - One-Dimensional Problems	A26.1
Elasticity and Thermo- elasticity - Two-Dimensional Equations	A25.1
Electric Arc Welding	D2.2
End Bay Effects	C11.23
End Moments for Continuous Frameworks	A11.10
Equations of Static Equilibrium	A2.1
Equilibrium Equations	A24.2
Failure of Columns by Compression	A18.4
Failure Modes in Curved Honeycomb Panels	C12.20
Failure of Structures	B1.1
Fatigue Analysis - Statistical Distribution	C13.7
Fatigue and Fail-Safe Design	C13.35
Fatigue of Materials	B1.14
Fatigue S-N Curves	C13.43
Fillers	D3.5
Fitting Design	D1.1
Fixed End Moments	A11.3
Fixed End Moments Due to Support Deflections	A11.9
Fixity Coefficients	C2.1
Flange Design	C10.1
Flange Design Stresses	C10.2
Flange Discontinuities	C10.7
Flange Loads	C11.8
Flange Strength (Crippling)	C10.4
Flat Sheet Web with Vertical Stiffeners	C10.1
Flexural Shear Flow Distribution	A15.24
Flexural Shear Flow - Symmetrical Beam Section	A14.5
Flexural Shear Stress	A14.1
Flight Structures - Required Strength	C1.7
Forces on Airplane in Flight	A4.4
Formulation of Plane Stress Problem	A25.5
Frames with Joint Displacements	A12.8
Frames with One Axis of Symmetry	A10.2
Frames with Unknown Joint Deflections	A11.17
Frames with Unknown Joint Displacement	A12.8
Fuselage - Balance Diagram	A5.13
Fuselage - Basic Structure	A20.1
Fuselage - Example Problem Solutions	A20.9
Fuselage Frames	A21.17
Fuselage Shears and Moments	A5.12
Fuselage Shears and Moments for Landing Conditions	A5.18
Fuselage Stress Methods	A20.3
Fuselage - Ultimate Bending Strength	A20.6
Gas Welding	D2.1
General Organization of Aircraft Co.	A1.1
General Types of Loading	B1.1
Gerard Method	C7.2
Gust Load Factors	A4.6
Gust Loads	C13.27

INDEX FOR THE BRUHN TEXTBOOK - Continued

Honeycomb Flat Panel	
Failure Modes	C12.8
Impact Loading	B1.15
Impact, Testing Methods	B1.15
Inelastic Buckling	A18.6
Inelastic Buckling Strength	
of Flat Sheet in Compression	C5.3
Inelastic Buckling of Thin Sheets	A18.23
Inertia Forces	A4.2
Inertia Loads Due to Angular Acceleration	A5.18
Inertia Loads Due to Unit 100,000 in. lbs. Pitching Moment	A5.19
Initial Stresses	A8.13
Internal Shear Flow Systems	A5.6
Inter-Rivet Buckling Stress	C7.12
Joggled Members	D3.4
Johnson-Euler Equation	C7.22
Joints - Method of	A2.10
Landing Gear Units - Calculating Reactions & Loads on Members	A2.23
Landing Impact Loads	C13.26
Large Deflections in Plates	A17.6
Limit Loads	A4.1
Load Factors	A4.5
Loaded Continuous Beam with Yielding Supports	A12.5
Longeron Type System	C11.41
Maneuver Loads	C13.27
Mass Moments of Inertia	A3.2
Matrices - Element Stiffness	A23.3
MATRIX Methods in Deflections	A7.18
Matrix Methods - Stress Problems	A8.16
Maximum Shear Stresses for Simple Cross-Sections	A14.5
Membrane Action in Thin Plates	A17.5
Membrane Analogy	A6.3
Membrane Equations of Equilibrium	A16.1
Metallic Materials	B2.1
Method of Displacements	A23.3
Method of Joints - Trusses	A2.10
Method of Moments - Trusses	A2.11
Method of Shears - Trusses	A2.12
Methods of Column Failure	C2.1
Modulus of Rupture	C3.3
Modulus of Rupture Stress	C4.15
Modulus Theory	A18.6
Mohr's Circle	C1.3
Moment Distribution Method	A11.1
Moment of Inertia - Strength of Columns	C1.1
Moments for Combinations of Various Load Systems	A5.22
Moments of Inertia - Airplane	A3.8
Moments of Inertia - Centroids	A3.1
Monocoque Circular Cylinders	
Buckling under External Pressure	C8.11
Monocoque Circular Cylinders	
Buckling under Pure Bending	C8.7
Monocoque Circular Cylinders	
Problems for Finding Buckling Strength	C8.17
Monocoque Cylinders - Buckling under Axial Compression	C8.1
Monocoque Cylinders - Buckling under Axial Load and Internal Pressure	C8.3
NACA Method	C11.14
Needham Method	C7.1
Neutral Axis Location	A13.1
Neutral Axis Method	A13.3
Octahedral Shear Stress	
Theory	C1.8
Parallel Axis Theorem	A3.1
Physical Action of Wing Section	
Plane Strain	A25.7
Plane Stress	A25.1
Plate Bending Analysis	A17.3
Plate Bending Equations	A17.1
Poisson's Ratio	B1.7
Practical Wing Section	
Application	A19.24
Pressure Vessels - Applications	A16.2
Pressurized Cabin Stress	
Analysis	A16.6
Principal Axes	A3.10
Principal Strains	C1.5
Principle of Superposition	A8.1
Product of Inertia	A3.9
Radius of Gyration	A3.1
Ramberg-Osgood Equation	C2.2
Redundant Problem Deflection Calculations by Matrix Methods	A8.27
Redundant Reactions by Least Work	A8.2
Redundant Stress Calculations	A8.27
Redundant Stresses by Least Work	A8.3
Redundant Structures with Members Subjected to Loadings	A8.11
Relation - Shear and Bending Moment	A5.4
Restraint Produced by Lips and Bulbs	C7.6
Rib Loads from Discontinuities	A21.11
Rib - Multiple Stringer Beam	A21.9
Rib - Single Cell Beam	A21.6
Rib - Three Stringer Beam	A21.7
Rivet Design	C11.18
Rivet Loads	C11.7
Riveted Connections	DI.14
Rivets in Tension	DI.25
Sandwich Construction and Design	C12.1
Sandwich Structural Properties	C12.4
Sandwich Structures Design	C12.33
Secant Modulus	B1.5
Secondary Bending Moments in Trusses	A11.28
Section of Maximum Bending Moment	A5.4
Section Properties	A3.2
Shear Center	A14.1
Shear Center Location	
Neutral Axis Method	A14.15
Shear Center of Single Cell - Three Flange Beam	A15.6
Shear Center of Single Cell - Two Flange Beam	A15.4
Shear Clips	D3.1
Shear Flow in Cellular Beams	A15.24
Shear Flow - Multiple Cells	A15.16
Shear Flow in Tapered Sheet Panel	A15.27
Shear Lag Influences	A19.24
Shear Loads	C11.5
Shear Stresses & Shear Center - Beam Sections	A14.6
Shear Stresses - Unsymmetrical Beam Sections	A14.8
Shearing Stresses from Principal Stresses	C1.1
Shearing Stresses - Right Angles	C1.1
Sheet-Stiffener Panels - Falling Strength	C7.15
Sheet Wrinkling Failure	C7.15
Single Bolt Fitting	D1.4
Single Cell Beam - Symmetrical about One Axis	A15.1
Single Cell - Multiple Flange - One Axis of Symmetry	A15.7
Single Cell - Unsymmetrical - Multiple Flange	A15.8
Single Spar - Cantilever Wing - Metal Covered	A19.10
Slope Deflection - Hinged End	A12.3
Slope Deflection Method	A12.1
Spot Welding	D2.7
Static Compression Stress - Strain Diagram	B1.4
Static Tension Stress - Strain Diagram	B1.2
Statically Determinate Coplanar Structures and Loadings	A2.7
Statically Determinate and Indeterminate Structures	A2.4
Statically Indeterminate Frames - Joint Rotation	A12.7
Statically Indeterminate Problem	A8.1
Stepped Column - Strength	C2.14
Stiffened Cylindrical Structures - Ultimate Strength	C9.8
Stiffness & Carry-over Factors for Curved Members	A11.30
Stiffness Factor	A11.4
Strain - Displacement Relations	A24.5
Strain Energy	A7.1
Strain Energy of Plates Due to Edge Compression and Bending	A18.19
Strain Energy in Pure Bending of Plates	A18.12
Streamline Tubing - Strength	C4.12
Strength Checking and Design - Problems	C4.5
Strength of Round Tubes under Combined Loadings	C4.22
Stress Analysis Formulas	C11.15
Stress Analysis of Thin Skin - Multiple Stringer Cantilever Wing	A19.10
Stress Concentration Factors	C13.2
Stress Distribution & Angle of Twist for 2-Cell Thin-Wall Closed Section	A6.7
Stress-Strain Curve	B1.7
Stress-Strain Relations	A24.6
Stresses around Panel Cutout	A22.1
Stresses in Uprights	C11.17
Stringer Systems in Diagonal Tension	C11.32
Structural Design Philosophy	C1.6
Structural Fittings	A2.2
Structural Skin Panel Details	D3.12
Structures with Curved Members	A11.29
Successive Approximation Method for Multiple Cell Beams	A15.24
Symbols for Reacting Fitting Units	A2.3
Symmetria Sections - External Shear Loads	A14.2
Tangent Modulus	B1.5
Tangent-Modulus Theory	A18.8
Taxi Loads	C13.26
Tension Clips	D3.2
Tension-Field Beam Action	C11.1
Tension-Field Beam Formulas	C11.2
Theorem of Castigliano	A7.5
Theorem of Complementary Energy	A7.5

INDEX FOR THE BRUHN TEXTBOOK - Continued

Theorem of Least Work	A8.2	Torsional Strength of Round Tubes	C4.17	Unit Analysis for Fuselage Shears and Moments	A5.15
Theorems of Virtual Work and Minimum Potential Energy	A7.5	Torsional Stresses in Multiple-Cell Thin-Walled Tubes	A8.8	Unsymmetrical Frame	A9.2
Thermal Deflections by Matrix Methods	A8.39	Transmission of Power by Cylindrical Shaft	A8.2	Unsymmetrical Frames or Rings	A10.4
Thermal Stresses	A8.14	Triaxial Stresses	C1.5	Unsymmetrical Frames using Principal Axes	A9.18
Thermal Stresses	A8.33	Truss Deflection by Method of Elastic Weights	A7.33	Unsymmetrical Structures	A9.13
Thermoelasticity - Three- Dimensional Equations	A24.1	Truss Structures	A2.9		
Thin Walled Shells	A16.5	Trusses with Double Redundancy	A8.10	Velocity - Load Factor Diagram	A4.7
Three Cell - Multiple Flange Beam - Symmetrical about One Axis	A15.15	Trusses with Multiple Redundancy	A8.11	Wagner Equations	C11.4
Three Flange - Single Cell Wing	A19.5	Trusses with Single Redundancy	A8.7	Web Bending & Shear Stresses	C10.5
Torsion - Circular Sections	A6.1	Tubing Design Facts	C4.5	Web Design	C11.18
Torsion - Effect of End Restraint	A6.16	Two-Dimensional Problems	A26.5	Web Splices	C10.10
Torsion - Non-circular Sections	A6.3	Two-Cell Multiple Flange Beam - One Axis of Symmetry	A15.11	Web Strength, Stable Webs	C10.5
Torsion Open Sections	A6.4	Type of Wing Ribs	A21.1	Webs with Round Lightening Holes	C10.17
Torsion of Thin-Walled Cylinder having Closed Type Stiffeners	A6.15	Ultimate Strength in Combined Bending & Flexural Shear	C4.25	Wing Analysis Problems	A19.2
Torsion Thin Walled Sections	A6.5	Ultimate Strength in Combined Compression, Bending, Flexural Shear & Torsion	C4.26	Wing Arrangements	A19.1
Torsional Moments - Beams	A5.9	Ultimate Strength in Combined Compression, Bending & Torsion	C4.24	Wing Effective Section	A19.12
Torsional Modulus of Rupture	C4.17	Ultimate Strength in Combined Tension, Torsion and Internal Pressure p in psi	C4.26	Wing Internal Stresses	A23.9
Torsional Shear Flow in Multiple Cell Beams by Method of Successive Corrections	A6.10	Uniform Stress Condition	C1.1	Wing Shear and Bending Analysis	A19.14
Torsional Shear Stresses in Multiple-Cell Thin-Wall Closed Section - Distribution	A6.7			Wing Shear and Bending Moments	A5.9

ADDITIONAL TOPICS IN THE BRUHN TEXTBOOK

Beams of Multispan	A11.5	Frame Stiffness Criteria	C9.11	Redundant Structure, Deflection Calculations	A8.9
Beam-Columns	A5.21	Flanges, Bent	D3.11	Rivet/Joint Edge Distance	D1.18
Beam-Column Example	C4.22	Flange Supports	D3.11	Rivet/Joint Shear Strength	D1.20
Beam-Column Formulas	A5.23	Flexural Shear Stress in the Plastic Range	C3.10	Rivet/Joint Tension Strength	D1.28
Beam End Bay Effects	C11.13	Inertia Forces	A4.2		
Buckling of Composite Shapes	C6.1	Interaction Curves	C4.22	Sheet Buckling	C5.1
Centroid Formulas	A3.2	Interaction Curves	C5.8	Shims, See Fillers	D3.5
Column, Elastic Supports	C2.9	Loads, Static	A4.12	Spotwelds	D3.13
Columns, Stepped	G2.10	Loads, Dynamic	A4.12	Statics	A2.1
Columns, Tapered	C2.10	Lug Strength	D1.5	Structural Detail Design Guides	D3.14
Curved Beams	D3.10	Material Properties	B1.10	Structures Department Organization	A1.1
Diagonal Tension, Shell Analysis	C11.29	Multispan Beam Analysis	A11.5	Tension Field Shell Analysis	C11.29
Dummy Unit Load Method	A7.9	Nuts	D1.2	Virtual Loads	A7.9
Effective Sheet Widths	A20.3	Plastic Bending	C3.1	Virtual Work	A7.14
Elastic Weights	A7.27	Plate Buckling	C5.1	V-n Diagrams	A4.8
Factors of Safety	D1.1	Plastic Torsion	C4.20	Welding	D2.1
Fatigue Problem Areas	C13.27	Product of Inertia	A3.9	Wrinkling Failure of Sheet	C7.15
Fatigue Residual Stress Effect	C13.13	Properties of Sections	A3.1		
Fatigue Testing Machines	C13.7	Recessed Shear Panels	D3.13		
Fillers, Joint Strength Effects	D3.5				

ADDITIONAL TOPICS ARE ALSO IN THE SUPPLEMENT'S INDEX, PAGE II